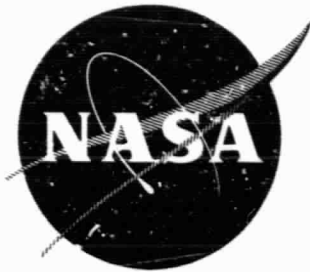


General Disclaimer

One or more of the Following Statements may affect this Document

- This document has been reproduced from the best copy furnished by the organizational source. It is being released in the interest of making available as much information as possible.
- This document may contain data, which exceeds the sheet parameters. It was furnished in this condition by the organizational source and is the best copy available.
- This document may contain tone-on-tone or color graphs, charts and/or pictures, which have been reproduced in black and white.
- This document is paginated as submitted by the original source.
- Portions of this document are not fully legible due to the historical nature of some of the material. However, it is the best reproduction available from the original submission.

NASA CR-54571 50
SEPTEMBER 1968
Allison EDR 5863



Single-Stage Experimental Evaluation of Boundary Layer Bleed Techniques for High Lift Stator Blades

III—Data and Performance of Unslotted 0.75 Hub Diffusion Factor Stator

Prepared for

NATIONAL AERONAUTICS AND SPACE ADMINISTRATION

1
N69-27272
(ACCESSION NUMBER)
155
(PAGE(S))
1
(CODE)
15
(CATEGORY)
EAST-14-54571
(NASA CR OR TMX OR AD NUMBER)



Allison Division • General Motors

Indianapolis, Indiana

NOTICE

This report was prepared as an account of Government sponsored work. Neither the United States, nor the National Aeronautics and Space Administration (NASA), nor any person acting on behalf of NASA:

- A. Makes any warranty or representation, expressed or implied, with respect to the accuracy, completeness, or usefulness of the information contained in this report, or that the use of any information, apparatus, method, or process disclosed in this report may not infringe privately owned rights; or
- B. Assumes any liabilities with respect to the use of, or for damages resulting from the use of any information, apparatus, method or process disclosed in this report.

As used above, "person acting on behalf of NASA" includes any employee or contractor of NASA, or employee of such contractor, to the extent that such employee or contractor of NASA, or employee of such contractor prepares, disseminates, or provides access to, any information pursuant to his employment or contract with NASA, or his employment with such contractor.

Requests for copies of this report should be referred to

National Aeronautics and Space Administration
Scientific and Technical Information Facility
P.O. Box 33
College Park, Maryland 20740

NASA CR 54571
SEPTEMBER 1968
Allis n EDR 5863



**Single-Stage Experimental Evaluation of
Boundary Layer Bleed Techniques
for High Lift Stator Blades**

**III—Data and Performance of
Unslotted 0.75 Hub Diffusion Factor Stator**

by

G. Seren and R. H. Carmody

Prepared for
NATIONAL AERONAUTICS AND SPACE ADMINISTRATION

Contract NAS3-7900

Technical Management
NASA-Lewis Research Center
Cleveland, Ohio

Lewis Project Manager: William L. Beede
Lewis Research Advisor: L. Joseph Herrig

Allison Division • General Motors
Indianapolis, Indiana

PRECEDING PAGE BLANK NOT FILMED.

ABSTRACT

The test described in this report is part of an overall program to establish experimentally the extent to which it is feasible to increase compressor stator loading and stall-free flow margin by employing suction surface boundary layer bleed techniques. The unslotted stator vanes in this test are used with the objective of providing a basis of comparison for the blade suction surface boundary layer control using blowing and bleed techniques. During this test, the only attempt to control the flow in the boundary layer was done by means of varying hub and case wall bleeds. A secondary objective of this test was to obtain blade element data for design use.

In this test, overall and blade element performance of a row of 0.75 diffusion factor unslotted stator vanes was measured with varying wall bleed rates for boundary layer control. In addition, the vane static pressure distribution was obtained at three radial locations and for three different wall bleed rates at design speed. Overall and blade element performance was also obtained for the rotor and compared to data previously obtained for this rotor without stator vanes. Preliminary discussion of test results and correlations of data are presented.

PRECEDING PAGE BLANK NOT FILMED.

TABLE OF CONTENTS

	<u>Page</u>
Summary	1
Introduction	3
Symbols	4
Apparatus and Procedures	6
Test Facility	6
Compressor Test Rig	6
Blading	7
Instrumentation	7
Determination of Annulus Wall Bleed Flow for Stator Vane	
Tests	9
Hysteresis Test	10
Overall and Blade Element Performance Data	10
Data Reduction	10
Presentation of Results	12
Overall Performance of Flow Generation Rotor and Stage	12
Blade Element Performance	12
Discussion of Results	14
Overall Performance	14
Flow Generation Rotor	14
Complete Stage	15
Annulus Wall Bleed for Stator Test	15
Hysteresis and Rotating Stall Results—Complete	
Stage	16
Blade Element Performance	16
Rotor	17
Stator	18
Stator Static Pressure Distributions	19
Concluding Remarks	21
References	22
Appendix—Performance Equations	23

LIST OF ILLUSTRATIONS

<u>Figure</u>	<u>Title</u>	<u>Page</u>
1	Compressor test facility	26
2	Layout of compressor test rig	27
3	Test rig flow path	28
4	Circumferential location of instrumentation viewed downstream	29
5	Radial location of streamlines for instrumentation positions	30
6	Schematics of survey instrumentation	31
7	Unslotted stator vane static pressure tap locations at 10, 50, and 90% streamlines	33
8	Flow generation rotor overall performance in stage test—pressure ratio	34
9	Flow generation rotor overall performance in stage test—adiabatic efficiency	35
10	Stage overall performance—pressure ratio	36
11	Stage overall performance—adiabatic efficiency	37
12	Rotor blade element performance at optimum wall bleed—stage test	38
13	Rotor blade element performance for 100% design speed with varying wall bleed rates—stage test	43
14	Radial variation of rotor blade element performance with optimum wall bleed	48
15	Radial variation of rotor blade element performance with mean wall bleed	49
16	Radial variation of rotor blade element performance with minimum wall bleed	50
17	Rotor out radial mass flux distribution at design speed with varying wall bleed rates	51
18	Rotor loss parameter versus diffusion factor	52
19	Stator blade element performance with optimum wall bleed	53
20	Stator blade element performance for 100% design speed with varying wall bleed rates	58
21	Variation of wall bleed flows with stage pressure ratio	63
22	Radial variation of 0.75 D _f stator blade element performance with optimum wall bleed	64
23	Radial variation of 0.75 D _f stator blade element performance with mean wall bleed	65
24	Radial variation of 0.75 D _f stator blade element performance with minimum wall bleed	66
25	Stator loss parameter versus diffusion factor	67
26	Stator static pressure distribution at 60% speed with optimum wall bleed	68
27	Stator static pressure distribution at 80% speed with optimum wall bleed	73

<u>Figure</u>	<u>Title</u>	<u>Page</u>
28	Stator static pressure distribution at 90% speed with optimum wall bleed	78
29	Stator static pressure distribution at 100% speed with optimum wall bleed	83
30	Stator static pressure distribution at 100% speed with mean wall bleed	88
31	Stator static pressure distribution at 100% speed with minimum wall bleed	92
32	Stator static pressure distribution at 110% speed with optimum wall bleed	96
33	Stator wake surveys with optimum wall bleed	102
34	Stator wake surveys with mean wall bleed	107
35	Stator wake surveys with minimum wall bleed	109
36	Variation in stator wake at 10 and 90% streamlines from tip during wall bleed optimization	111

LIST OF TABLES

<u>Table</u>	<u>Title</u>	<u>Page</u>
I	Blade and vane geometry summary	112
II	Rotor incidence at minimum and maximum flow for flow generation rotor and complete stage	113
III	Rotating stall results for complete stage test	114
IV	Blade element performance for complete stage	115

SINGLE-STAGE EXPERIMENTAL EVALUATION OF BOUNDARY LAYER BLEED TECHNIQUES FOR HIGH LIFT STATOR BLADES

III. DATA AND PERFORMANCE OF UNSLOTTED 0.75 HUB DIFFUSION FACTOR STATOR

By

G. Seren and R. H. Carmody
Allison Division, GM

SUMMARY

To establish the feasibility of increasing compressor stator loading and stall-free flow margin by the use of boundary layer blowing and bleed techniques and to determine the extent to which such concepts may be employed, a series of investigations were made of a single-stage compressor provided with single- and double-slotted blowing stator rows and single- and triple-slotted bleed stator rows. These stators were designed with NACA 65-series airfoils and with hub diffusion factors of 0.65 and 0.75. The results of tests performed with 0.65 hub diffusion factor single-slotted blowing and bleed stators and the single- and double-slotted 0.75 hub diffusion factor blowing stators were discussed in previous reports. This report presents the results of an investigation with an unslotted stator which was carried out to provide data which could be used for evaluating the performance improvements of the blowing and bleed stators. This stator was also designed with NACA 65-series airfoils and had a hub diffusion factor of 0.75 as did the single- and double-slotted blowing stators (References 1 and 2). To ensure an attached stator end wall boundary layer and to minimize secondary flows, annulus wall bleeding was employed, starting from a point upstream of the stator leading edge and extending to a point downstream of the stator trailing edge. During these tests the rates of wall annulus bleed were varied to evaluate the effects of compressor wall boundary layer control on performance and stator blade element data. For this purpose, an optimized bleed rate and two reduced bleed rates were used. The flow into this stator row during the test was generated by the same state-of-the-art flow generation rotor as used for the tests reported in References 1 and 2.

Overall performance of the rotor and inlet guide vanes was evaluated separately for this stage test. Compared with rotor design values of 1.37 pressure ratio, 88.2 lb/sec inlet flow, and 88.8% overall adiabatic efficiency, at the design pressure ratio the corrected inlet flow was 95.0 lb/sec and the adiabatic efficiency was 93%. The overall rotor performance remained essentially unchanged while the wall bleed rates were varied. In general, this performance agreed well with the flow generation rotor performance without

stators reported in Reference 1. The stage exceeded its design requirements on both pressure ratio and efficiency at design flow. Overall performance for the complete stage with optimum wall bleed was found to have a pressure ratio of 1.315 and adiabatic efficiency of 84.0% at the 95.0 lb/sec airflow corresponding to the flow generation rotor design pressure ratio. The overall performance obtained for the mean and minimum wall bleed rates was 1.325 pressure ratio and 83.5% adiabatic efficiency and 1.333 pressure ratio and 83.0% adiabatic efficiency, respectively. Stage design values are 1.35 pressure ratio and 84.9% adiabatic efficiency at 88.2 lb/sec flow rate.

Blade element performance was obtained for the rotor blade and stator vane row. Experimental values are presented in terms of diffusion factor, deviation angle, and loss coefficient as a function of incidence for various annulus heights, with rotative speed as a parameter. Minimum loss values are determined and compared with the NACA loss parameter versus diffusion factor correlation curves. Radial variations of experimental rotor and stator blade element parameters near their design inlet flow conditions are also compared with the design values for all three of the annulus wall bleed rates employed.

Surface pressure distributions and wake surveys were obtained for the stator. A hysteresis test with acquisition of rotating stall characteristics was also obtained at 60% corrected speed for the complete stage. Hysteresis effects for the stage were observed while recovering from stall. Onset of stall was found to be abrupt at all speeds with stall cells first appearing in the hub region.

The 0.75 hub diffusion factor stator performance met or exceeded the design flow turning values at the end walls. The total pressure losses were higher than design at these loadings. Blade element performance loss correlations for these stators with suction at the end wall generally were below an extension of the existing NACA correlations at the mean and hub regions, but fell above these NACA correlations in the tip region.

Suction surface static pressure distributions along the mean line indicated a boundary layer separation at 55 to 65% chord at incidence angles greater than design. The hub and tip static pressure distributions appeared to be extremely erratic, indicating a possible separation at about 40 to 50% chord throughout the entire range of tests. There was, however, some indication of reattachment and the observed losses were much lower than would be expected under conditions of severe flow separation.

INTRODUCTION

Advanced airbreathing propulsion systems require lightweight compact compressors capable of high levels of performance. These compressors should have a broad range of operation and a large stall margin. High reliability and relative insensitivity to inlet flow distortion are generally required for all compressors. In meeting the more demanding compressor design requirements, compromises must be made that are strongly dependent on the particular application. New applications are steadily increasing the range of requirements which the compressor must meet.

Compressor technology has been advanced continuously by extending, among other parameters, the usable rotational speeds; increasing stage loadings or diffusion factors; and reducing stage length through the use of high blade aspect ratios. Whereas further advancements can be made through optimizations and improved combinations of these parameters, severe aerodynamic limitations such as increasing losses and decreased stall margin are being encountered. Significant advancements in compressor technology require the application of advanced concepts in terms of improved blading for high flow Mach numbers and application of high lift devices to extend the stall-free flow range for compressor rotors and stators. Advanced concepts in these areas may result in sizable reductions in the number of compressor stages and in improved performance.

Airfoils designed to provide high lift experience steep blade surface pressure gradients which become steeper as angle of incidence is increased. As a result, the suction surface boundary layer separates and high total pressure losses and a decrease in stall-free flow margin result. To some extent, however, separation of the suction surface boundary layer can be delayed by energizing it with high energy air. In view of these considerations, an experimental single-stage compressor rig was designed and constructed to test high loaded stators using internal blowing and boundary layer suction concepts to reduce losses and improve stall-free flow margin.

The objectives of this program are to establish experimentally the feasibility of increasing blade loading and stall-free flow margin by stator boundary layer bleed and blowing and to determine the extent to which these may be employed. A secondary objective is to obtain blade element data for design use. The stator designs were to be representative of those for middle and latter stages of highly loaded axial-flow compressors. Stator inlet flow was to be generated by a state-of-the-art flow generation rotor. This report presents the test results for the unslotted 0.75 hub diffusion factor stator. Test results of single- and double-slotted 0.75 hub diffusion factor blowing stators are presented in References 1 and 2, respectively. The performances of these stators are compared with the performance of the unslotted stators in this report. Reference 1 also includes a presentation of the flow generation

rotor performance without stators. The performance characteristics of the 0.65 hub diffusion factor blowing and bleed stators are presented, respectively, in References 3 and 4. The design characteristics of the stators that are employed in the series of tests for the evaluation of boundary layer bleed techniques are presented in Reference 5.

SYMBOLS

A_a	Annulus area, ft^2
c	Airfoil chord, in.
D_f	Diffusion factor
g	Gravitational constant, $32.2 \text{ ft-lb}_m/\text{lb}_f \cdot \text{sec}^2$
H	Hysteresis loop data point
i	Incidence angle based on mean camber line, degrees
M	Mach number
n	Number of blades per row
N	Rotational speed, rpm
P_t	Total pressure, psia
p	Static pressure, psia
q	Dynamic pressure, psia
R	Radius, in.
\mathcal{R}	Gas constant, $53.35 \text{ lb}_f \cdot \text{ft}/\text{lb}_m \cdot {}^\circ\text{R}$
R_c	Pressure ratio
S	Airfoil surface pressure coefficient, Equation (A13)
T_t	Total temperature, ${}^\circ\text{R}$
t	Static temperature, ${}^\circ\text{R}$
t/c	Thickness-to-chord ratio

V Air velocity, ft/sec
W_a Compressor airflow, lb_m/sec
W_{BL} Annulus wall bleed flow, lb_m/sec
x Distance from blade leading edge, in.

Greek

β Air angle measured from axial direction, degrees
 γ Ratio of specific heats
 γ° Blade chord angle, degrees
 δ Ratio of total pressure to standard sea level pressure of 14.7 psia
 δ° Deviation angle, degrees
 Δ Incremental value
 η Efficiency
 θ Ratio of total temperature to standard sea level temperature of 518.6°R
 κ Blade metal angle measured from axial direction, degrees
 ρ Density, lb_m/ft³
 σ Blade row solidity
 ϕ Camber angle, degrees
 ω Angular velocity of rotor, radians/sec
 $\bar{\omega}$ Total pressure loss coefficient
 $\frac{\bar{\omega} \cos \beta}{2 \sigma}$ Loss parameter

Subscripts

0 Guide vane inlet
1 Rotor inlet

2 Stator inlet or rotor exit

3 Stator exit

θ Tangential direction

ad Adiabatic

m Mean or 50% streamline

ma Mass averaged

z Axial direction

Superscripts

' Relative value, rotor property

APPARATUS AND PROCEDURES

TEST FACILITY

A general arrangement of the test facility is shown in Figure 1. Air enters the test compressor after passing through the test facility filter house, an inlet duct, plenum, and bellmouth and is exhausted to the atmosphere through a diffuser. Provisions exist for maintaining compressor inlet pressures above or below atmospheric if necessary.

Two power units can be used simultaneously to drive the test compressor. One is a T56 power turbine with combustors which burn fuel mixed with high pressure air from test facility compressors; the other is a complete T56 power section. The two units are coupled by a primary gearbox whose output shaft drives a secondary gearbox which in turn drives the test compressor. Test compressor speed is controlled by throttling the turbine air supply with a hydraulically-operated valve and by independent fuel controls for each unit.

COMPRESSOR TEST RIG

The mechanical arrangement of the test compressor is shown in Figure 2. It consists of a cylindrical inlet section, the test compressor section, and an exhaust diffuser. The single-stage rotor is supported on two bearings whose housings are linked by a vertically-split compressor case. The compressor case houses the inlet guide vanes, the rotor tip abradable coating, the stator vanes, and the case and hub bleed manifolds. The abradable coating on the

compressor cases over the rotor blade tip permits low running clearances between the blade tips and the case. The rotor is designed with an interference fit such that the rotor blade tip will run into the abradable coating at design speed. Radial growth due to centrifugal force and temperature expansion is considered. Nominal design clearances for this rotor are -0.0025 in. at 100% speed and -0.0045 in. at 110% speed. Nominal static clearance is 0.0075 in. The design of the rig allows the rapid exchange of inlet guide vanes, if necessary, without dismantling the remainder of the compressor, and the exchange of stator vanes without disassembly of the entire test rig.

Airflow rate and pressure ratio are varied by throttle plates located in the exhaust diffuser. The throttles are linked by a ring and operated by a common actuator.

Provision is made in the rig for bleeding the wall boundary layers at stator tip and hub. This is accomplished by fabricating the stator flow passage walls from perforated sheet metal. Manifolds behind the perforated metal surfaces are connected by multiple tubes to separate vacuum headers for tip and hub wall bleeds.

BLADING

The design of the stator vanes, rotor blades, and design inlet guide vanes is described in detail in Reference 5. Selected types of airfoil sections are: (1) 63-006-series for the inlet guide vanes, (2) double circular arc for the rotor blades, and (3) 65-series thickness distribution with circular arc meanline for the stator vanes. For convenience, however, the principal geometric details of these components are repeated in Table I.

INSTRUMENTATION

Instrumentation was provided to obtain blade element performance for the rotor and stator row and to measure overall performance. The locations of instrumentation planes are shown in Figure 3; Figure 4 shows schematically the circumferential location of the instruments installed at each plane. The radial element locations at each plane were selected along streamlines passing through the 10, 30, 50, 70, and 90% annulus height stations from the tip at the stator inlet measurement plane. The streamline locations are shown schematically in Figure 5. Dimensioned sketches of the probes used are shown in Figure 6. Instrumentation was distributed so as to minimize area blockages and prevent immersion in upstream instrument wakes. Except at the inlet guide vane exit station, duplicate instrumentation was distributed so as to average out any inlet guide vane effects.

Compressor Inlet Conditions

Weight flow was measured with an ASME thin plate orifice located in each branch of the triple inlet header. Six total pressure probes and two 6-element temperature rakes were located in the cylindrical section approximately three feet upstream of the test compressor inlet for measurement of inlet total pressure and temperature. See Figure 4a. Inlet static pressure was measured at the same axial station by two static taps in the inlet wall.

Rotor Inlet—Station 1

Four approximately equally spaced static pressure taps were located on both the inner and outer walls as shown in Figure 4b. An 8-degree wedge static pressure traverse probe was also installed to measure the radial static pressure distribution. Three radial traverse combination total pressure and yaw angle probes were used to measure the distribution of these parameters across the annulus. Total temperature was obtained from plenum thermocouples.

Stator Inlet or Rotor Exit—Station 2

Four approximately equally spaced static pressure taps were located on both the inner and outer walls, and the radial distribution of static pressure was measured by two 8-degree wedge static pressure traverse probes as shown in Figure 4c. Three radial traverse combination probes were installed at this station to measure the radial distribution of total pressure, total temperature, and flow angle.

Stator Exit—Station 3

Four approximately equally spaced static pressure taps were located on both inner and outer walls and two 8-degree wedge static pressure traverse probes were installed for measurement of the radial static pressure distribution as shown in Figure 4d. One traverse combination total pressure, total temperature, and yaw probe was installed primarily to measure flow angle. A 16-element total pressure circumferential rake, shown in Figure 6d, was installed at this station to measure discharge total pressure and stator vane wake. This rake spanned 1.08 vane spaces at the 10% streamline and 1.43 vane spaces at the 90% streamline. Total temperature was measured by four 5-element radial rakes. Inner and outer wall boundary layers were surveyed by fixed 5-element total pressure probes. All taps, probes, and radial rakes were located on extensions of mid-channel streamlines.

Special Instrumentation

In addition to the instrumentation enumerated for blade element and overall performance, the following special instrumentation was installed.

At the rotor exit, two fixed and one traverse hot wire anemometers were installed to signal the onset of compressor stall and to provide rotating stall data. Shaft whip was monitored by means of a whip pickup mounted in the plane of the rotor blades, and strain gages were mounted on eight rotor blades to monitor blade stresses.

The 10, 50, and 90% streamline sections of the unslotted stator vanes were each provided with 12 suction surface and 7 pressure surface static pressure taps as indicated in Figure 7. The 19 static pressure taps for each streamline section were distributed among 4 vanes.

DETERMINATION OF ANNULUS WALL BLEED FLOW FOR STATOR VANE TESTS

With the compressor operating at design speed and stage pressure ratio, the circumferential total pressure rake at the stator exit was set at the streamline station 10% from the tip. Hub and tip wall bleeds were set at a nominal flow of less than 1% of compressor flow. The stator wake pattern at this bleed flow was noted, and the tip wall bleed was then increased until no further improvement in wake pattern was visually observed on a manometer bank. This bleed flow rate was defined as the "optimum" bleed rate. One limiting consideration set as a reasonable upper value, however, was to extract no more than 2.5% of compressor inlet flow per wall at design conditions.

The circumferential rake was then set at the streamline station 90% from the tip. The tip wall bleed flow rate was reset at its original low value, and the procedure described was repeated for the hub bleed.

After hub and outer wall bleed flows had been optimized, the circumferential rake was moved to the mean position. Hub and outer wall bleeds were varied simultaneously in increments from the original nominal flow rate to optimum flow. The effects on the stator wake at mean depth were studied to check that optimum hub and tip wall bleeds coincided with an optimum wake at mid-span. The valve settings for the optimum bleed flow rate were left unchanged for all subsequent speed and flow conditions, except in the case where the wall bleed was varied to compare the effect of various bleed rates on overall and blade element performance. The hub and tip bleed rates were then set at the minimum wall bleed flow as limited by a condition of no back pressure on the perforated wall material and overall performance and blade element data were obtained for design speed. A similar investigation of overall performance and blade element data was also made with a mean bleed flow which was approximately half-way between the optimum and minimum bleed flow rates.

HYSERESIS TEST

The following method was employed to determine the characteristics of this stage at entry into and when recovering from stall. With corrected speed set at 60%, the throttle was closed until stall cells were indicated by the three hot-wire anemometers (two of which were at the 10% and one at the 90% station from the tip) thus signalling the onset of stall. The first hysteresis point data recording was made prior to the onset of stall. At this near stalled condition, a partial data recording, which consisted of data required for air-flow and pressure ratio calculation, was obtained.

The throttle was then closed further in steps, following the onset of stall, and partial data recordings were made at intermediate points before stage pressure ratio levelled off at a lower pressure ratio and a fourth partial data recording was obtained. The throttle was then gradually opened in steps and three other partial recordings, two at intermediate points and one very close to the stall point, were made before indications of stall, as signalled by the hot-wire anemometers, just disappeared. At this point an eighth short data cycle was recorded.

Rotor blade stresses were monitored continuously during the hysteresis test to ensure that excessive vibratory stresses were not encountered.

OVERALL AND BLADE ELEMENT PERFORMANCE DATA

Overall and blade element performance data were obtained at a sufficient number of points per speed line to define rotor or stage performance between maximum flow and stall. The stage stall point is defined as the onset of a steady stall cell indication on the hot-wire anemometers. Performance at design speed was obtained for the minimum and mean wall bleed rates as well as the optimum wall bleed rate. The near-stall test points were taken as close to the rotating stall condition as could be set without actually being in rotating stall. This type of near-stall setting permitted a full data point recording. At each full data point, fixed and traverse pressure and temperature data were recorded at five radial locations corresponding to streamlines passing through the 10, 30, 50, 70, and 90% span stations at the stator inlet measurement plane.

DATA REDUCTION

Overall performance and blade element data reduction is accomplished in one program. A second program is used to calculate pressure coefficients for the stator vanes.

In the first program, raw data from the test stand is read in and printed. The program converts wedge probe static pressure transducer readings to inches of mercury absolute and applies a Mach number correction. All yaw units are converted to degrees. Data recording system corrections, wire

calibrations, and Mach number corrections are applied to all temperatures. Pressures recorded on the data recording system are corrected to standard inlet total pressure. The corrected data is then printed.

Circumferential arithmetic averages of total pressures, static pressures, total temperatures, and yaw angles are calculated and printed. Individual data readings were compared with the averages to validate the data. Any individual reading which differs from its respective average by more than the prescribed deviation (0.5 in. Hg for pressures, 3° for yaw angles, 1.5, 2, and 3°R, respectively, for reference, inlet, and all other temperatures), is not used in the final calculations. Mass-averaged values required for performance calculations are determined using the averaged and validated data.

The program provides a choice of two radial distributions of static pressure: (1) the distributions measured by the wedge probes and (2) a linear distribution across the flow annulus calculated from the arithmetically-averaged hub and case wall static pressure taps. Overall and blade element performances are calculated and printed using the two static pressure distributions mentioned. If a continuity check at any data measurement station is not satisfied within 5%, a simple radial equilibrium solution is provided to give an indication of the problem.

Overall performance values are calculated for the inlet guide vane and rotor and for the complete stage. The following operations were performed to determine these values.

At the inlet plenum station, two total temperatures are arithmetically averaged at each radial station. Mass flow is integrated radially, assuming that averaged wall static pressure exists over the entire cross section. Total pressures and temperatures are then mass averaged. Behind the rotor, wall static pressures are arithmetically averaged circumferentially and all total pressures and total temperatures are arithmetically averaged circumferentially at each radial station. Mass flow is radially integrated and total pressures and temperatures are radially mass averaged.

At the stator exit, four total temperatures are arithmetically averaged circumferentially at each radial station. Incremental mass flow is computed using an arithmetic average of the circumferential rake total pressure readings spanning a stator vane passage at each radial station. A radial integration is made for weight flow. For performance calculations, the total pressures at each radial station are mass averaged circumferentially and the total pressures and temperatures are mass averaged radially. The overall pressure ratio and efficiencies are obtained using the radially mass averaged values of total pressure and temperature.

The calculation of performance variables, as programmed in the data reduction programs, is delineated in the Appendix.

PRESENTATION OF RESULTS

Experimental results obtained in the test program are summarized herein in detail for the unslotted 0.75 hub diffusion factor stator vane with flow generation rotor with the design inlet guide vane set. The reduced data presented were based on a linear static pressure distribution across the annulus at each axial survey station rather than on the static wedge survey values. Comparison of results using both linear and wedge static data (Reference 1) showed that, when the wedge data were considered reliable, differences in reduced data were small; there was a tendency, however, for the wedge static data to be erratic for some test points. Use of the linear static data gives a consistent basis for comparison over the test range and with the data from other tests.

OVERALL PERFORMANCE OF FLOW GENERATION ROTOR AND STAGE

Overall pressure ratio and adiabatic efficiency are each plotted versus corrected inlet flow with corrected speed as a parameter. These are presented in Figures 8 and 9 for the flow generation rotor during this stage test, and Figures 10 and 11 for the stage.

To indicate whether the rotor or the unslotted stator caused the stage to choke or stall, rotor incidence range is summarized in Table II for the flow generation rotor test of Reference 1 and the flow generation rotor of the unslotted 0.75 D_f stator stage test.

Stage rotating stall characteristics at the stall points and hysteresis points are summarized in Table III.

BLADE ELEMENT PERFORMANCE

Rotor blade and stator vane blade element characteristics were computed at the five streamline positions previously defined. The blade element characteristics chosen to present the detailed performance of each blade row are as follows.

Blade element parameter

- Incidence angle, i or i'
- Total pressure loss coefficient, $\bar{\omega}$ or $\bar{\omega}'$
- Diffusion factor, D_f
- Deviation angle, δ°
- Inlet flow angle, β or β'
- Flow turning, $\Delta\beta$ or $\Delta\beta'$
- Inlet axial velocity, V_z
- Inlet Mach number, M or M'

Rotor blade element data are plotted as a function of incidence with corrected speed as a parameter for each of the streamline stations. The blade element data obtained during the stage test are shown in Figure 12 for the points run at optimum wall bleed and Figure 13 for the points run at design speed with optimum, mean, and minimum wall bleed. For comparison and to aid the analysis of the rotor blade performance, blade element data for the rotor blade, with optimum, mean, and minimum wall bleed, are plotted versus percent annulus height in Figures 14 through 16 for the flow providing the best approximation of the design incidence angle at design speed. Design values are also plotted for comparison. Mass flux distribution out of the rotor corresponding to the design flow rate is plotted and compared with the design flow distribution in Figure 17. Rotor blade element performance is evaluated, in Figure 18, by comparing the loss parameter versus diffusion factor at the 10, 50, and 90% streamline stations from the tip with the NACA correlation curve in Reference 6.

Stator vane blade element data are also plotted as a function of incidence angle with corrected speed as a parameter for each streamline station. The blade element data for the unslotted stator run at optimum wall bleed are plotted in Figure 19. The stator blade element data for the design speed with optimum, mean, and minimum wall bleeds are presented in Figure 20. The annulus wall bleed rates plotted against stage pressure ratio are presented in Figure 21. Blade element data of the unslotted stator vane, for conditions nearest to the design incidence angle, with optimum, mean, and minimum wall bleed, are plotted against the percent annulus height in Figures 22 through 24, respectively, to aid stator vane performance analysis and comparison of the effect of varying the annulus wall bleed rates. Stator vane blade element performance is also evaluated in Figure 25 where the loss parameter versus diffusion factor for 10, 50, and 90% streamline stations from tip is compared with the NACA correlation curve in Reference 6.

The pressure distributions along the 10, 50, and 90% streamlines from the tip of the unslotted stator suction and pressure surfaces are presented in Figures 26 through 32.

Selected stator wakes are plotted in Figure 33 to show the variation of stator wakes with Mach number at fixed incidence angle, and also to show the effect of incidence angle at a fixed Mach number, at optimum wall bleed. The selected stator wakes, plotted in Figure 34, at mean wall bleed, and in Figure 35, at minimum wall bleed are used to show the effects of wall bleed in addition to the Mach number and incidence angle variations. The variation of the stator wake during wall bleed optimization, at the design pressure ratio, is presented in Figure 36.

To enable compressor designers to evaluate and apply the results of this test, detailed summaries of vector diagrams, blade element characteristics, and losses at each streamline station are provided in Table IV.

DISCUSSION OF RESULTS

The method of presentation using the overall and blade element parameter for evaluating the performance has been described in detail. Since the figures and tables are self-explanatory, only general observations are made.

OVERALL PERFORMANCE

Flow Generation Rotor

The design point pressure ratio and efficiency are 1.37 and 88.8%, respectively, at a design flow rate of 88.2 lb/sec with the design inlet guide vanes. Flow generation rotor pressure ratio and adiabatic efficiency measured during the test with the stator are given in Figures 8 and 9. At the design equivalent rotor speed, maximum efficiency was 96.8% with corresponding pressure ratio of 1.44 and flow rate of 90.5 lb/sec. At the design pressure ratio of 1.37 the flow rate was 7.7% higher than design, at 95.0 lb/sec with an adiabatic efficiency of 93%.

The pressure ratio results are in good agreement with the rotor test results without stator vanes (Figure 10 of Reference 1). When the maximum value of the rotor adiabatic efficiencies are examined at a 100% corrected speed, however, a value of 96.8% is obtained from the results of the stage test, Figure 9, as opposed to 92.5% from the flow generation rotor test without stator vanes (Figure 11 of Reference 1) both at the same measured airflow rate. This apparent discrepancy is the result of a reduction in the average total temperature across the stator due to bleeding the inner and outer walls of the stator passage and the method used to compute the efficiency (See Equation (A2) in the Appendix). The mass averaged total temperature at the stator exit is, in general, lower with wall bleed than without. This reflects in a higher rotor efficiency. Figure 9 then indicates the trend in efficiency due to bleed rather than absolute level. The rotor pressure ratio observed with the reduced wall bleeds was similar to that observed with optimum wall bleed.

A prime concern during the design phase of the flow generation rotor, discussed in Reference 1, was that sufficient flow range would be available to avoid excessive limitations on the stator operating range by the rotor. In this report, Table II gives a summary of rotor incidence angles near stall and maximum flow, at hub, mean, and tip streamlines. The stall incidence angles correspond to the minimum flow rate due to either rotor or stator stall. The choke incidence angles correspond to the maximum flow rate due either to rotor choke, stator choke, or facility pressure loss limitations. Rotor incidence angle differences at stall observed between the stator test and the flow generation rotor test of Reference 1 are small, and the stage stall may be primarily due to rotor stall. The comparison of incidence angles at maximum flow indicates that the stator limited the maximum flow at 60 and 80% corrected speed. At 100% corrected speed, the approximately equal rotor incidence angles for both

tests indicate that the rotor or stator is choking at nearly the same flow or the facility pressure loss was controlling. The flow at the hub may, however, be limited by the stator hub choking prior to the mean and tip regions. It is believed that the facility exit duct pressure loss is controlling at these relatively low pressure ratios with high flow rate conditions.

Complete Stage

The overall stage pressure ratio and adiabatic efficiency are shown in Figures 10 and 11, respectively. During these tests only the design inlet guide vanes were employed.

Stage design values for the pressure ratio and adiabatic efficiency are 1.35 and 85.5%, respectively, at a design flow rate of 88.2 lb/sec. At the design equivalent rotor speed, a maximum stage adiabatic efficiency of 87.9% was obtained with a pressure ratio of 1.392 and a flow rate of 90.5 lb/sec. At the flow generation rotor condition of 95.0 lb/sec corrected flow rate the stage pressure ratio was 1.315 and adiabatic efficiency was 84.0%. At this corrected flow rate the values obtained for the pressure ratio and efficiency of the stators with mean and minimum wall bleed rates were 1.325 and 83.5%, and 1.333 and 83%, respectively. For simplicity, the calculated stage adiabatic efficiency, presented herein, is not penalized by the case and hub wall bleed flows. Inasmuch as the rotor loading is not compatible with the stator loading, the stage efficiency is of secondary interest.

The stator is designed to remove all of the tangential whirl imparted by the rotor and the inlet guide vane. This tangential whirl if produced by the rotor alone would give the equivalent of a 1.66:1 pressure ratio level at the stator inlet. Maintaining the same average pressure recovery in the stator of 0.986, a 1.5- to 2.0-point increase in overall stage efficiency would be realized.

Annulus Wall Bleed for Stator Test

Annulus wall bleed over the stator row at tip and hub surface was defined at 100% corrected speed and rotor pressure ratio of 1.37 by visually monitoring the circumferential rake and boundary layer total pressure rakes at tip and hub. Except at very low wall bleed flows of about 0.5%, where stator wakes were still relatively large, the boundary layer total pressure rakes indicated an attached boundary layer. That is, total pressures increased away from the wall. Once the wall boundary layer attached, additional wall bleed essentially affected only the end regions. Optimum wall bleed was selected as the condition where increased bleed did not result in improvement of the stator wake. The bleed valves were held fixed at this setting for all testing defined as optimum bleed flow rate. The wall bleed rate was later varied, at design speed, to determine the influence of the wall bleed on the overall performance and blade element data. The wall bleed flow was first adjusted to its minimum allowable value then to a rate corresponding to approximately half the flow between optimum and minimum values.

The tip and hub wall bleed rates experienced throughout this test with the fixed bleed line valve settings are summarized in Figure 21. The minimum and mean wall bleed rates at design speed are also indicated in Figure 21.

Hysteresis and Rotating Stall Results—Complete Stage

This test was made to determine whether the stall of this stage was gradual or abrupt, and whether the stall would disappear and the stage recover smoothly. The onset of rotating stall at each corrected speed was indicated by the hot wire anemometer located at the 90% streamline. Rotor stall first appeared at the hub and was abrupt at all speeds. The stall zone then progressed to the tip of the rotor with only a slight increase in back pressure.

At 60% corrected speed, an eight-point hysteresis loop test was conducted. The pressure ratio-flow rate points are shown in Figure 10. A hysteresis effect, in terms of pressure ratio and flow rate, was observed from measurements defining the path from point H₁ to H₈.

The maximum transient blade stresses encountered during the hysteresis test were 16,700 psi. There were indications, from the frequent recurrence of stress peaks, that these maximum transient stresses prevailed for a significant period during the hysteresis test. These blade stresses were considered to be at a potentially damaging level. Their magnitudes were appreciably higher than the prescribed stress limit which was 11,250 psi.

Rotative speed, frequency, and number of stall zones are summarized in Table III. Following the onset of stall, a stall zone was recorded in the hub and in the tip regions. The rotative speeds of the cells in both span regions ranged from 27 to 47% rotor speed in the direction of rotation. Multiple stall cells at the tip and hub were recorded during rotating stall tests at design speed. In deep stall, rotative speed was approximately 44% rotor speed in the direction of rotation and the frequency was 110 cps. High rotor blade transient stresses prevented radial traversing of the hot wire probe. It appears, however, that the stall zone extended across the blade span.

BLADE ELEMENT PERFORMANCE

As reported in Reference 1, an extensive study of the inlet guide vanes was made both at design and off-design conditions. Investigation into the possible persistence of the inlet guide vane wakes through the rotor, at the design flow rate condition, indicated the attenuation of these wakes before entering the stator rows. In view of these results, repeated study of inlet guide vane flow for each test was found unnecessary.

Rotor

Figure 12 is a summary of diffusion factor, deviation angle, and loss coefficient data throughout the rotor operating range for the complete stage test at optimum wall bleed. Data at design speed and at all three wall bleed rates are compared in Figure 13. In general, the measured loss coefficients are found to be lower than the design values in the vicinity of the 0° design incidence angle at the 10, 30, 50 and 70% streamline stations and about equal to design values at the 90% streamline station for all the speeds tested using the optimized wall bleed. There were no significant changes in rotor losses as the wall bleed rates were reduced.

Primary rotor blade element performance for the double circular arc blade during the stator test is shown in Figures 14, 15, and 16 for the optimum, mean, and minimum wall bleeds, respectively. Rotor blade measured data for both the flow generation rotor and the complete stage tests operating near the design incidence angle at corrected speed are compared with the design values. The selection of measured data was based on the best agreement with the design incidence angle values since the rotor exceeded its design airflow rate at design pressure ratio. In general, the values obtained for the deviation angles were lower than design and those of the diffusion factor were higher than design.

Values of deviation angle and diffusion factor, differing significantly from the design values, were also evidenced in Reference 1. The lower than design deviation angles result in an effective overcambering of the rotor blades, producing an excessive amount of work on the flow. The combination of higher work input and lower axial exit velocity results in the higher than design values of the diffusion factors.

The radial distribution of mass flux at the rotor outlet for the flow generation rotor and the complete stage test is compared with design values in Figure 17. A flow shift to the tip is indicated, experimentally, with respect to the design distribution. This can be attributed to the low deviation angles in the tip region of the rotor. An additional mass flow shift was observed between the measured test values of the flow generation rotor test, Reference 1, and the 0.75 hub diffusion factor stator test.

Rotor loss parameter data at the 10, 50, and 90% streamlines are shown in Figure 18. When they could be defined, minimum loss coefficient values are indicated in Figure 18 as filled symbols. The minimum values are selected at the data point nearest to the minimum value of the curve drawn through data points in Figure 12. Minimum loss data for the tip region or 10% streamline are found to lie on the lower band of the data scatter (Reference 6). The minimum loss data for the mid-span and hub region are found to agree well with the NACA correlation curves in the test diffusion factor range.

Stator

Figure 19 presents diffusion factor, deviation angle, and loss coefficient over the entire test operating range for the 10, 30, 50, 70, and 90% streamline stations. The measured values of deviation angle are appreciably lower than design values. The tip losses are appreciably higher than the design values. A study of Figure 19 also indicates that the choke or minimum incidence angle limit may not be clearly defined except at the 90% streamline. Further study also shows, however, that the loss coefficient versus incidence angle curve is quite flat over a wide range except at the 70 and 90% streamline height. The lowest hub losses were obtained with the optimum wall bleed rates as shown in Figure 20. The losses at the tip were quite scattered and no firm conclusion could be drawn with respect to the effect of wall bleed rate on tip losses.

The radial variations of blade element data for the stator, at a point where the values of the incidence angle provided the best approximation to design incidence, is compared with the design values in Figures 22 through 24 for the optimum, mean, and minimum wall bleeds, respectively. Inlet axial velocity and incidence angle plots indicate a mass flow shift to the tip with respect to the design value. Other significant results, shown in Figures 22 through 24, are that flow turning was greater than expected or deviation angles much less than designed for over the entire span of the blade and particularly so at the tip. The apparent turning and deviation angles, particularly at the hub and tip, differ greatly from design values, and this margin of difference increases with decreasing wall bleed flow rates. The effect of the varying wall bleed is displayed more prominently at the hub and becomes even more significant as stall incidence is approached. The deviation angles obtained with optimum and mean wall bleed at the hub and tip are considerably less than the design values. The margin between measured and design values increased with decreasing wall bleed flow. This deviation angle result agrees with the measured deviation angles for the single- and double-slotted 0.75 diffusion factor stator of References 1 and 2. Measured losses, in general, were found to be greater than the design values.

Minimum loss coefficient points obtained from Figures 19 and 20 are compared with an extension of the NACA loss parameter versus diffusion factor correlation curves (Reference 6) in Figure 25 for the 10, 50, and 90% streamlines from the tip. The minimum loss coefficient points for the stator for the 10% streamline are generally greater than the values on an extension of the NACA correlation. The data for the 50% streamline agree favorably with the extension of NACA correlation curves with minimum values generally less than the values of the curve.

Typical stator wake distributions are shown in Figures 33 through 35. Selected cases nearest to -3° incidence which show the increasing wake pressure depressions as inlet Mach number increases are given in Figures

33a through 33c, 33e and 33i for optimum wall bleed. The effects of incidence angle at inlet Mach number near 0.7 are illustrated in Figures 33d through 33h for optimum wall bleed, Figures 34a through 34d for mean wall bleed, and Figures 35a through 35d for minimum wall bleed. The wake surveys at high positive incidence angles, in Figures 33h and 33j, with optimum wall bleed flow show low total pressure peaks at the hub, indicated by the rake elements 6 and 7. The wakes presented in Figures 34d, for the mean wall bleed, and Figure 35d, for the minimum wall bleed, show a similar behavior at the hub region.

Wake survey data was recorded during the wall bleed optimization runs at the design stage pressure ratio of 1.35 and 100% corrected speed. The effect of reduced stator losses with increasing wall bleed rate is shown in Figure 36. It is evident in Figure 34 and from the wake surveys at design speed that increased wall bleed reduced the end wall region flow disturbance and stator losses, particularly at the hub. Higher wall bleed rates above the 30.2 and 30 in. H₂O orifice pressure differential at tip and hub, respectively, had little effect on increasing wake total pressure at these depth locations. A comparison of the tip and hub wakes during optimization also indicates that the hub total pressure losses are reduced more effectively by the wall bleeds while the improvements at the tip are less marked. This indicates that a system where the hub and tip wall bleeds are controlled independently may be desirable to further improve stator wakes by means of wall bleeds.

Stator Static Pressure Distributions

Suction surface static pressure distributions along the meanline for the stator indicate the presence of boundary layer separation at 55 to 65% chord for incidence angles greater than the design incidence angle at all the wall bleeds, as shown in Figures 26 through 32. The determination of the apparent boundary layer separation is based on the study of the static pressure distribution along the 50% streamline. The reason for this choice is the difficulty experienced in analyzing the 10 and 90% streamlines for separation. These streamlines are greatly influenced by the secondary flow and end wall effects to varying degrees, depending on the bleed rates applied at the annulus walls. The pressure distributions along 10 and 90% streamlines indicate possible existence of separation further upstream along the suction surface.

The apparent separation point was observed to move upstream as the incidence angle was increased. In cases of high stator incidence angle, some of the static pressure distributions indicate almost totally detached flow at the hub. These cases also indicate separation at the tip occurring further upstream than it appears where the incidence angles are smaller.

The 10% and 90% streamline pressure distributions obtained for high incidence angles at a 110% design speed, in Figures 32e and 32f, indicate separation occurring almost at the leading edge for the hub and tip while it is retarded to about 50% chord along the 50% streamline. Some of the operating conditions indicate the existence of reattachment of the boundary layer. These observed changes in the static pressure distribution may be attributed to the existence of wall bleeds. The similarity in the pressure distributions obtained with varying wall bleed rates made it difficult to determine the direct effects the bleed technique had on the surface pressure distributions.

CONCLUDING REMARKS

Discussion of the experimental results has been based on the work completed to date. Analysis of the data indicates the following points.

1. The overall performance of the flow generation rotor agreed favorably with the results of the rotor without stator vanes in Reference 1. The stage exceeded its design requirements on both pressure ratio and efficiency. The rotor overall performance was not affected by the variations in the wall bleeds. The stage overall performance showed little change in pressure ratio but a drop in efficiency with decreasing wall bleed flow was noted.
2. A hysteresis effect was observed in terms of pressure ratio and mass flow rate at 60% design speed. Stall point tests indicated abrupt stall at all speeds. During the hysteresis tests at 60% speed and the stall point tests above 60% speed, rotor blade stresses frequently exceeded the prescribed stress limit which was 11,250 psi. The maximum stress values, during the hysteresis tests, were 16,700 psi.
3. The wall bleed technique provided a means of controlling the boundary layer flow and reducing losses. Losses were reduced, more effectively at the hub than at the tip, by increasing wall bleed flow rates.
4. The blade surface static pressure distributions along the meanline gave evidence of possible flow separation at 55 to 65% chord, for angles greater than the design incidence angle. The apparent separation point was detected further upstream at the 10 and 90% annulus height locations. Flow turning and pressure loss levels did not indicate severe flow separation on the vane suction surface. Also, there was some indication of flow reattachment.
5. The 0.75 hub diffusion factor stator performance met or exceeded the design flow turning values at the end walls. The total pressure losses were higher than design at these loadings. Blade element performance loss correlations for these stators with suction at the end wall generally were below an extension of the existing NACA correlations at the mean and hub regions, but fell above these NACA correlations in the tip region.

REFERENCES

1. Miller, M. L. and Beck, T. E. Single-Stage Experimental Evaluation of Boundary Layer Blowing Techniques for High Lift Stator Blades, II—Data and Performance of Flow Generation Rotor and Single-Slotted 0.75 Hub Diffusion Factor Stator. NASA CR-54565, Allison Division, GM, EDR 5691, February 1968.
2. Carmody, R. H. and Seren, G. Single-Stage Experimental Evaluation of Boundary Layer Blowing Techniques for High Lift Stator Blades, IV—Data and Performance of Double-Slotted 0.75 Hub Diffusion Factor Stator. NASA CR-54567, Allison Division, GM, EDR 5861, August 1968.
3. Miller, M. L. and Seren, G. Single-Stage Experimental Evaluation of Boundary Layer Blowing Techniques for High Lift Stator Blades, III—Data and Performance of Flow Generation Rotor and Single-Slotted 0.65 Hub Diffusion Factor Stator. NASA CR-54566, Allison Division, GM, EDR 5759, June 1968.
4. Seren, G. and Carmody, R. H. Single-Stage Experimental Evaluation of Boundary Layer Bleed Techniques for High Lift Stator Blades, II—Data and Performance of Single-Slotted 0.65 Hub Diffusion Factor Stator. NASA CR-54570, Allison Division, GM, EDR 5862, August 1968.
5. Chapman, D. C. and Miller, M. L. Single-Stage Experimental Evaluation of Boundary Layer Bleed Techniques for High Lift Stator Blades, I—Compressor Design. NASA CR-54569, Allison Division, GM, EDR 5636, February 1968.
6. Aerodynamic Design of Axial Flow Compressors. NACA SP-36, 1965.

APPENDIX

PERFORMANCE EQUATIONS

The following overall and blade element performance parameters were calculated for the analysis of test data and the evaluation of the unslotted stator performance.

WEIGHT FLOW

Overall performance is presented as a function of corrected weight flow, defined as

$$\frac{W_a \sqrt{\theta}}{\delta} \quad (A1)$$

ADIABATIC EFFICIENCY

Adiabatic efficiency for the inlet guide vane and rotor combination is

$$\eta_{ad2} = \frac{\left(\frac{P_{t2, ma}}{P_{t0}} \right)^{(\gamma-1)/\gamma} - 1}{\frac{T_{t3, ma}}{T_{t0}} - 1} \quad (A2)$$

and for the guide vane, rotor, and stator is

$$\eta_{ad3} = \frac{\left(\frac{P_{t3, ma}}{P_{t0}} \right)^{(\gamma-1)/\gamma} - 1}{\frac{T_{t3, ma}}{T_{t0}} - 1} \quad (A3)$$

DIFFUSION FACTOR

For the rotor, diffusion factor is defined as

$$D_{f2} = 1 - \frac{V'_2}{V'_1} + \frac{V'_{\theta_2} - V'_{\theta_1}}{2 \sigma V'_1} \quad (A4)$$

and for the stator as

$$D_{f3} = 1 - \frac{V_3}{V_2} + \frac{V_{\theta 2} - V_{\theta 3}}{2 \sigma V_2} \quad (A5)$$

These quantities are calculated using the appropriate velocity triangle values previously computed by the program.

DEVIATION ANGLE

Rotor blade deviation is defined as

$$\delta_2^o = \beta_2' - \kappa_2' \quad (A6)$$

and stator deviation as

$$\delta_3^o = \beta_3' - \kappa_3 \quad (A7)$$

where κ_2' is the rotor blade exit metal angle based on the mean camber line for a double-circular arc airfoil and κ_3 is the stator vane exit metal angle based on the circular arc camber line for the 65-series airfoil.

INCIDENCE ANGLE

Rotor blade incidence is defined as

$$i_1' = \beta_1' - \kappa_1' \quad (A8)$$

and stator incidence as

$$i_2 = \beta_2 - \kappa_2 \quad (A9)$$

where κ_1' is the rotor blade inlet metal angle based on the mean camber line for a double-circular arc airfoil and κ_2 is the stator vane inlet metal angle based on the circular arc camber line.

TOTAL PRESSURE LOSS COEFFICIENT

Total pressure loss coefficient for the rotor is defined as

$$\frac{\omega'}{\omega} = \frac{\left[1 + \frac{\gamma-1}{2} \frac{(\omega R_2)^2}{\gamma g \Delta T_{t1}} \left(1 - \frac{R_1^2}{R_2^2} \right) \right]^{\gamma/(\gamma-1)} \left[1 - \frac{P_{t2}/P_{t1}}{(T_{t2}/T_{t1})^{\gamma/(\gamma-1)}} \right]}{1 - \left[1 + \frac{\gamma-1}{2} (M_1')^2 \right]^{-\gamma/(\gamma-1)}} \quad (A10)$$

and for the inlet guide vanes as

$$\bar{\omega} = \frac{1 - \frac{P_{t_1}}{P_{t_0}}}{1 - \left[1 + \frac{\gamma-1}{2} (M_0)^2 \right] - \gamma/(\gamma-1)} \quad (A11)$$

and stator as

$$\bar{\omega} = \frac{1 - \frac{P_{t_3}}{P_{t_2}}}{1 - \left[1 + \frac{\gamma-1}{2} (M_2)^2 \right] - \gamma/(\gamma-1)} \quad (A12)$$

PRESSURE COEFFICIENT

Pressure coefficient (S) is defined by

$$S = \frac{P_{t_2} - p}{q_2} \quad (A13)$$

where:

P_{t_2} = total pressure at stator inlet

p = static pressure at a given point on the vane surface

$q_2 = \frac{\gamma p_2 M_2^2}{2}$ = dynamic pressure at stator inlet

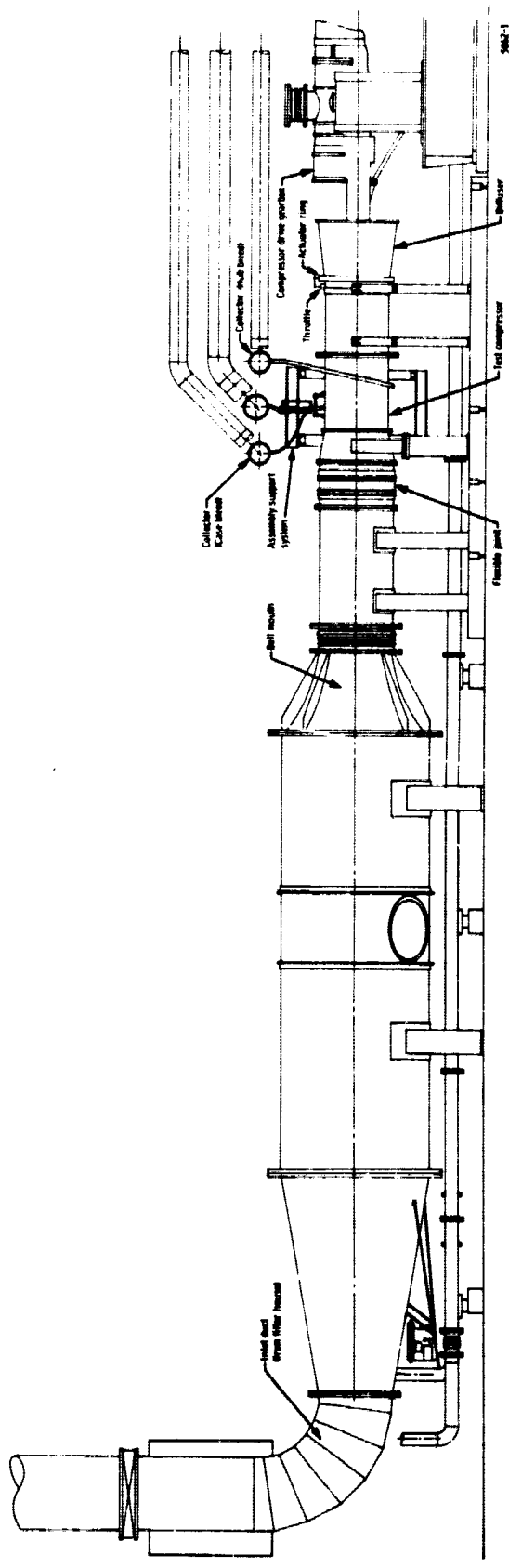


Figure 1. Compressor test facility.

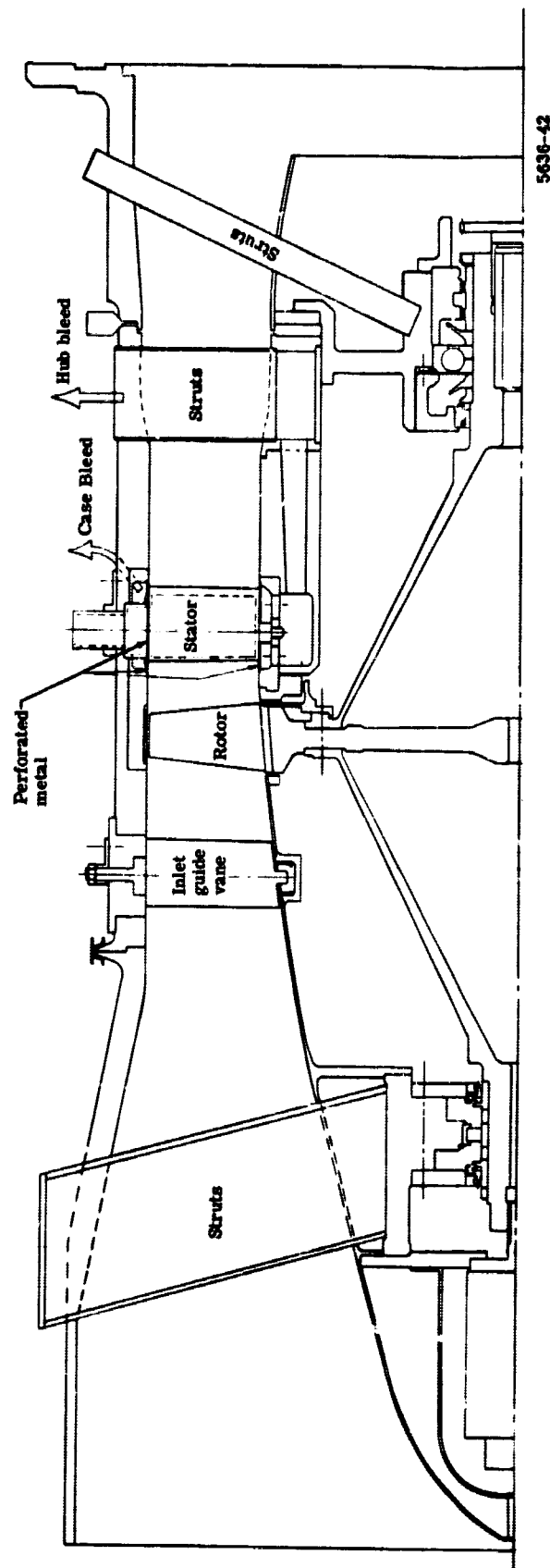


Figure 2. Layout of compressor test rig.

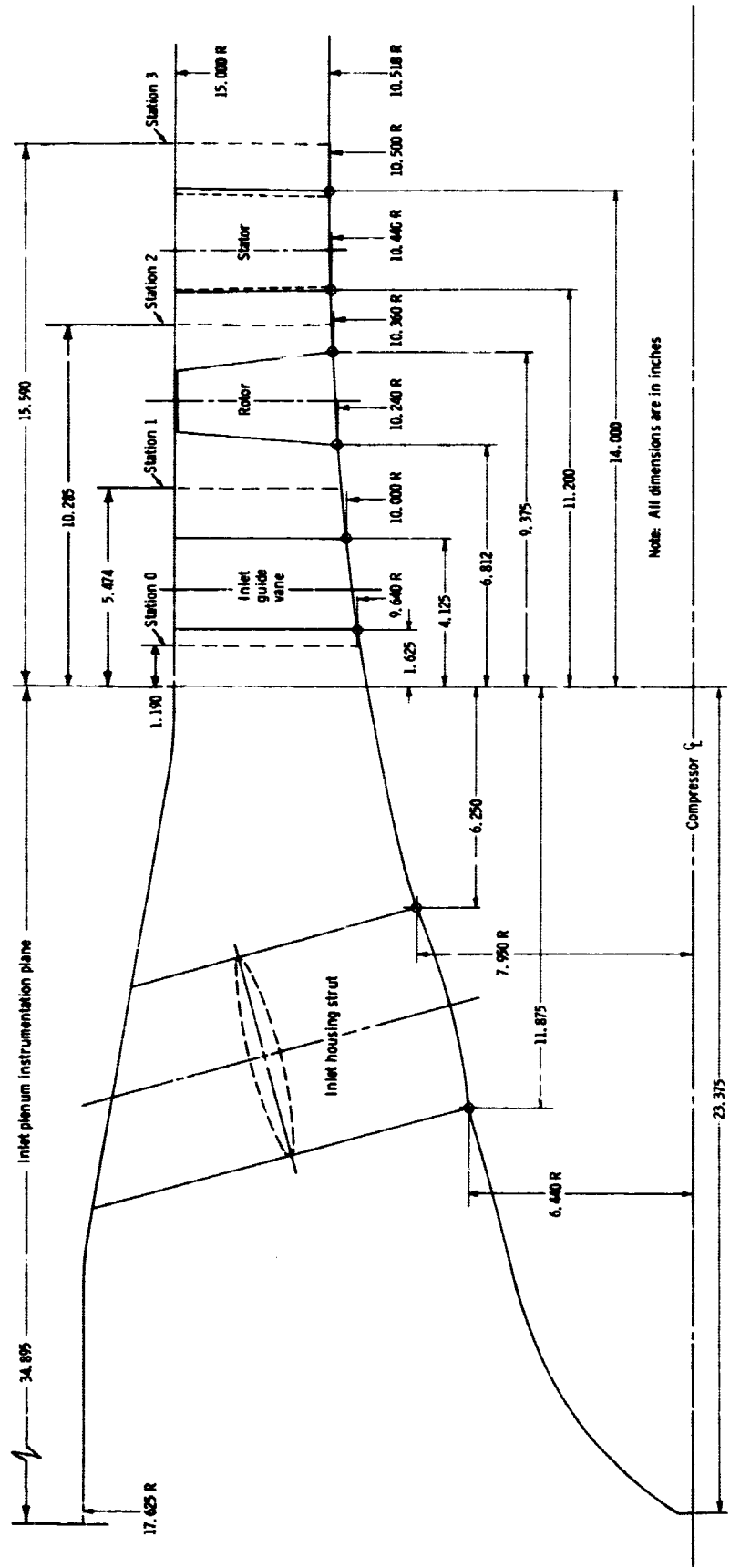


Figure 3. Test rig flow path.

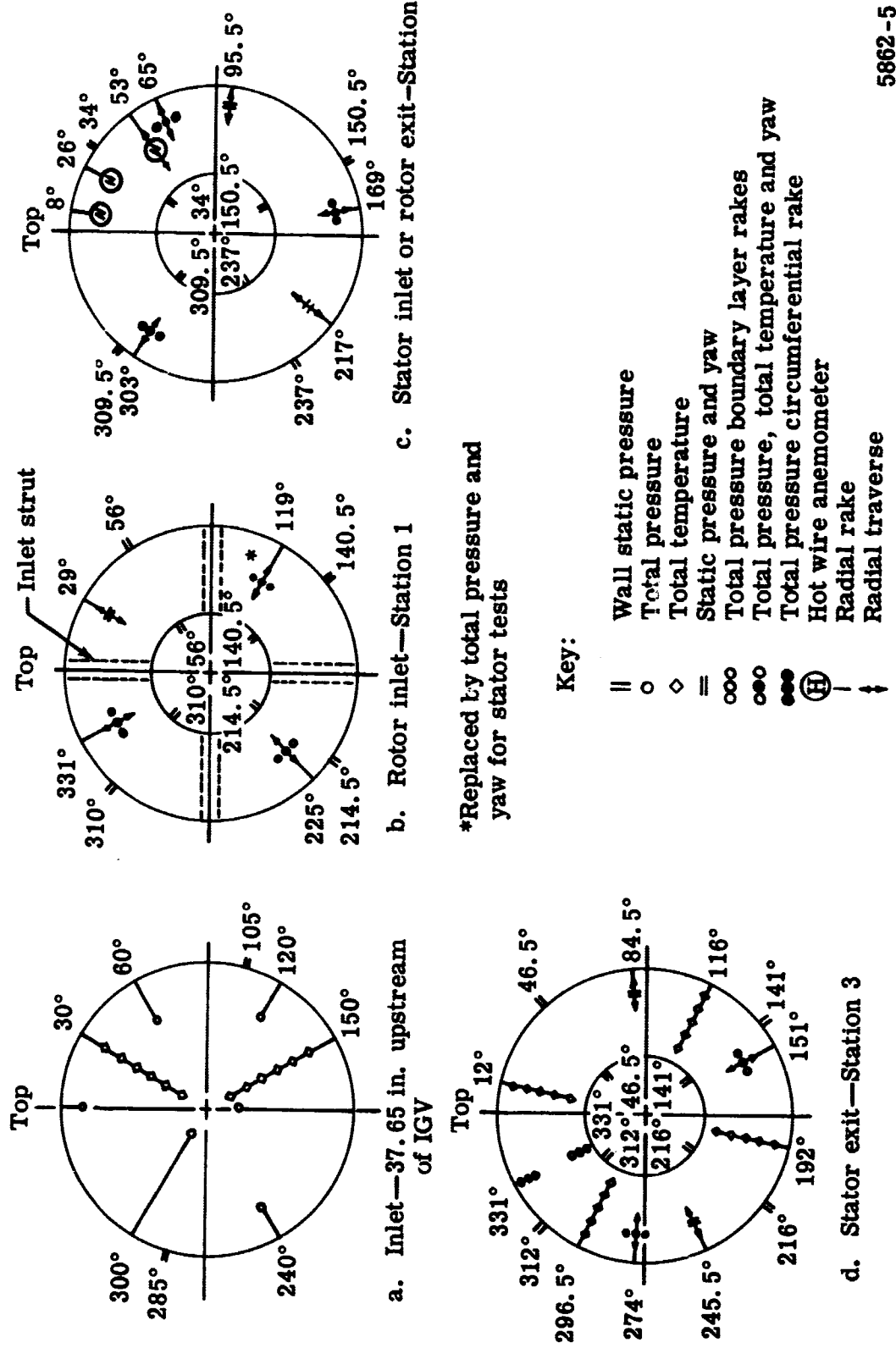


Figure 4. Circumferential location of instrumentation viewed downstream.

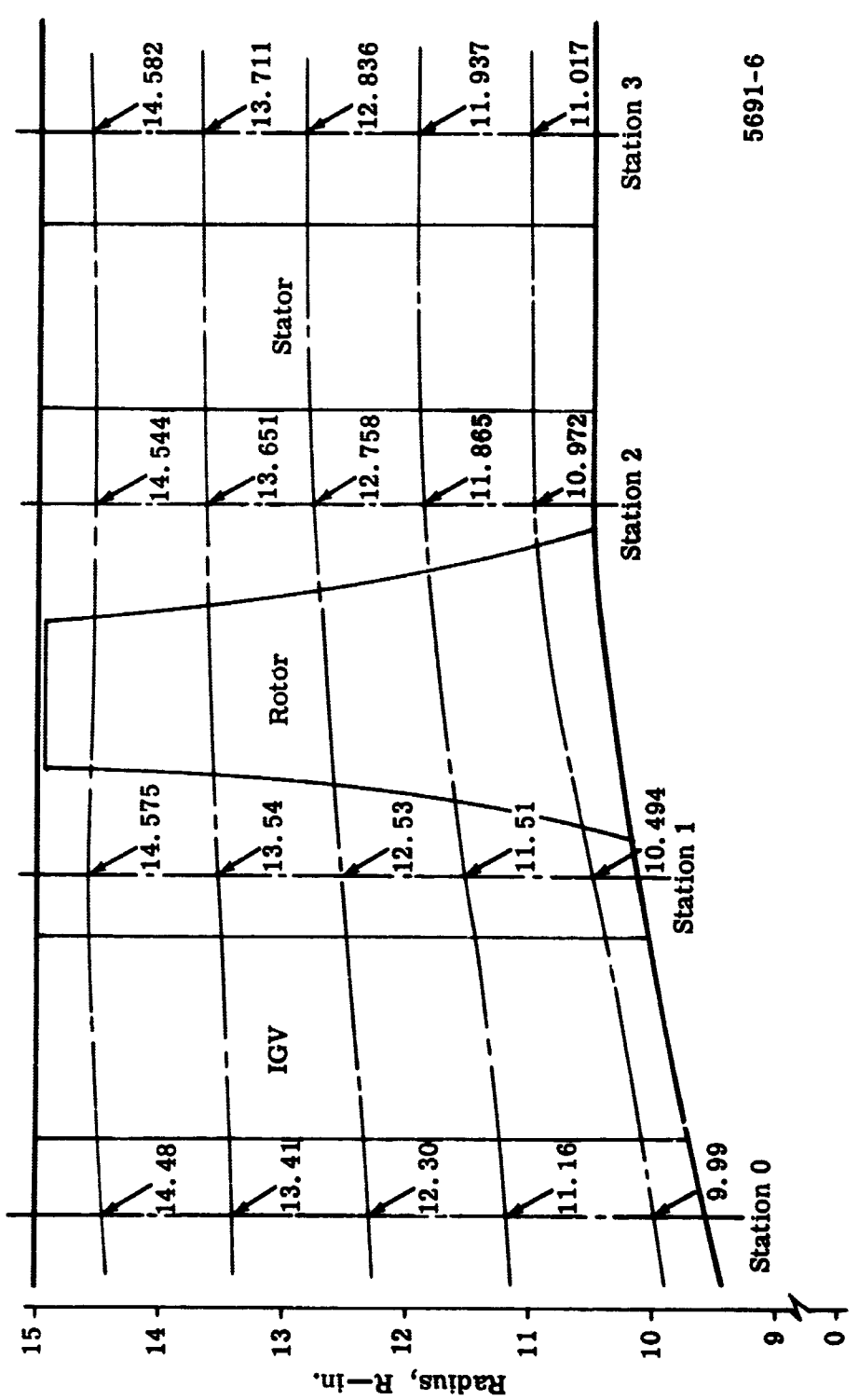


Figure 5. Radial location of streamlines for instrumentation positions.

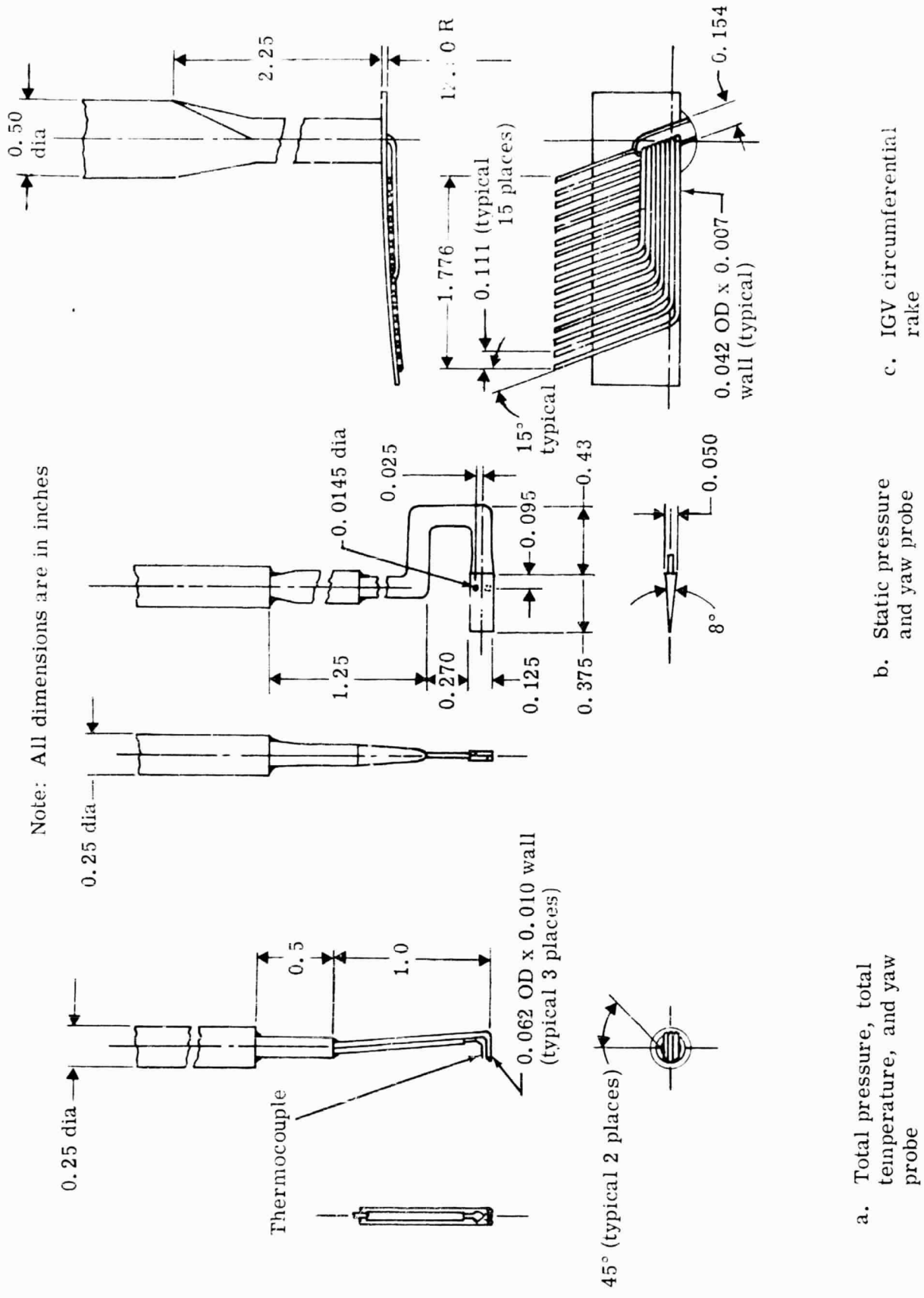


Figure 6. Schematics of survey instrumentation.

Note: All dimensions are in inches

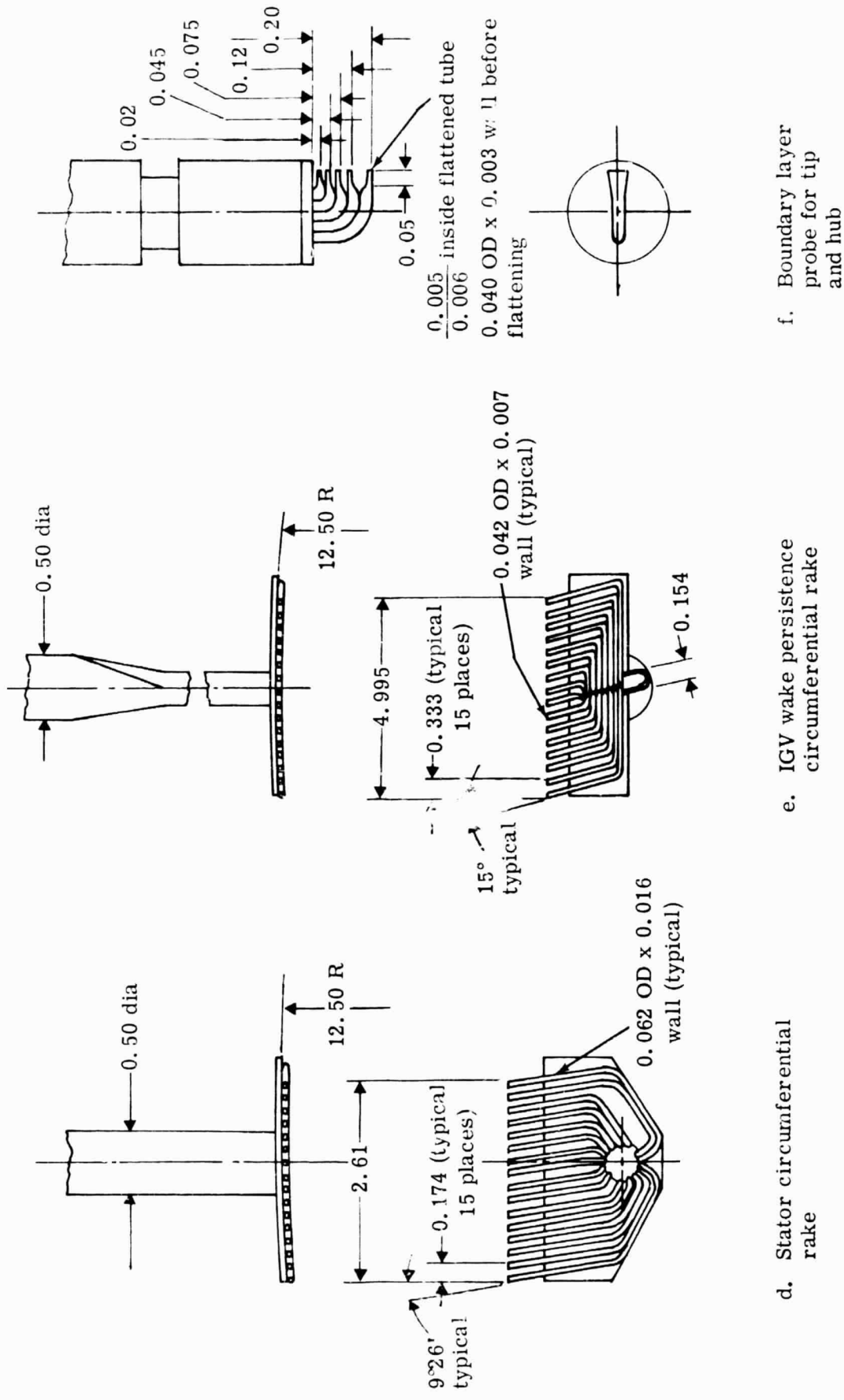
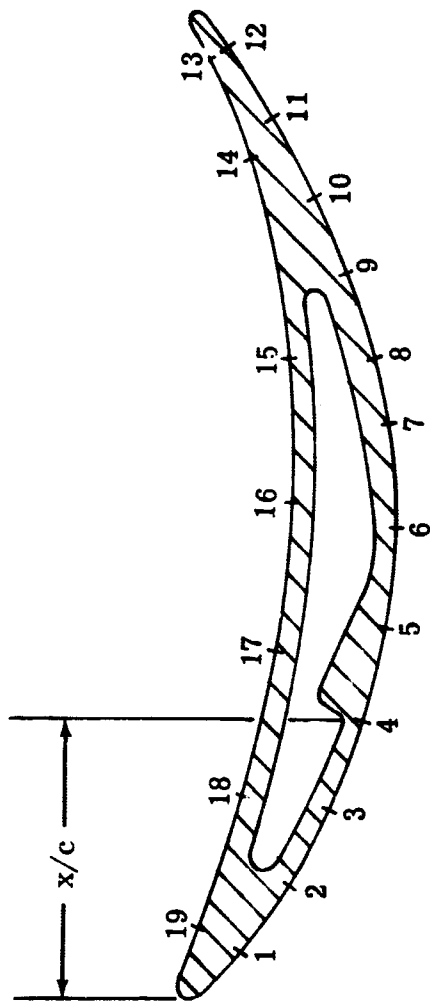


Figure 6. Schematics of survey instrumentation.



Tap	1	2	3	4	5	6	7	8	9	10	11	12
x/c-%	4.98	11.62	19.59	28.22	38.18	48.14	58.43	65.07	73.37	81.34	88.98	96.61
Vane No.	1	2	3	4	1	2	3	4	1	2	3	4

Tap	13	14	15	16	17	18	19
x/c-%	94.29	84.66	65.41	50.46	35.52	20.92	6.64
Vane No.	1	2	3	4	1	2	3

5863-8

Figure 7. Unslotted stator vane static pressure tap locations at 10, 50, and 90% streamlines.

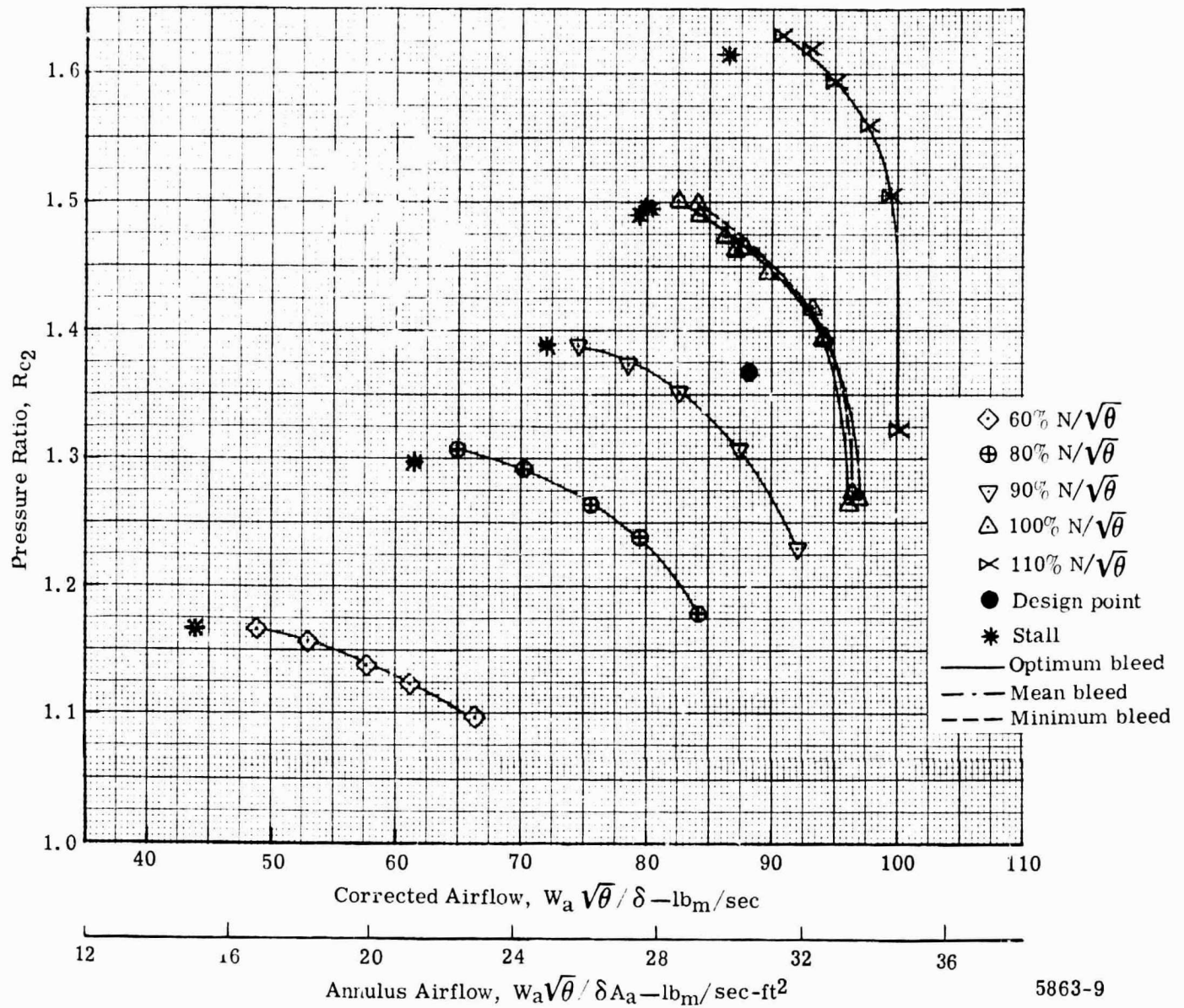


Figure 8. Flow generation rotor overall performance in stage test—pressure ratio.

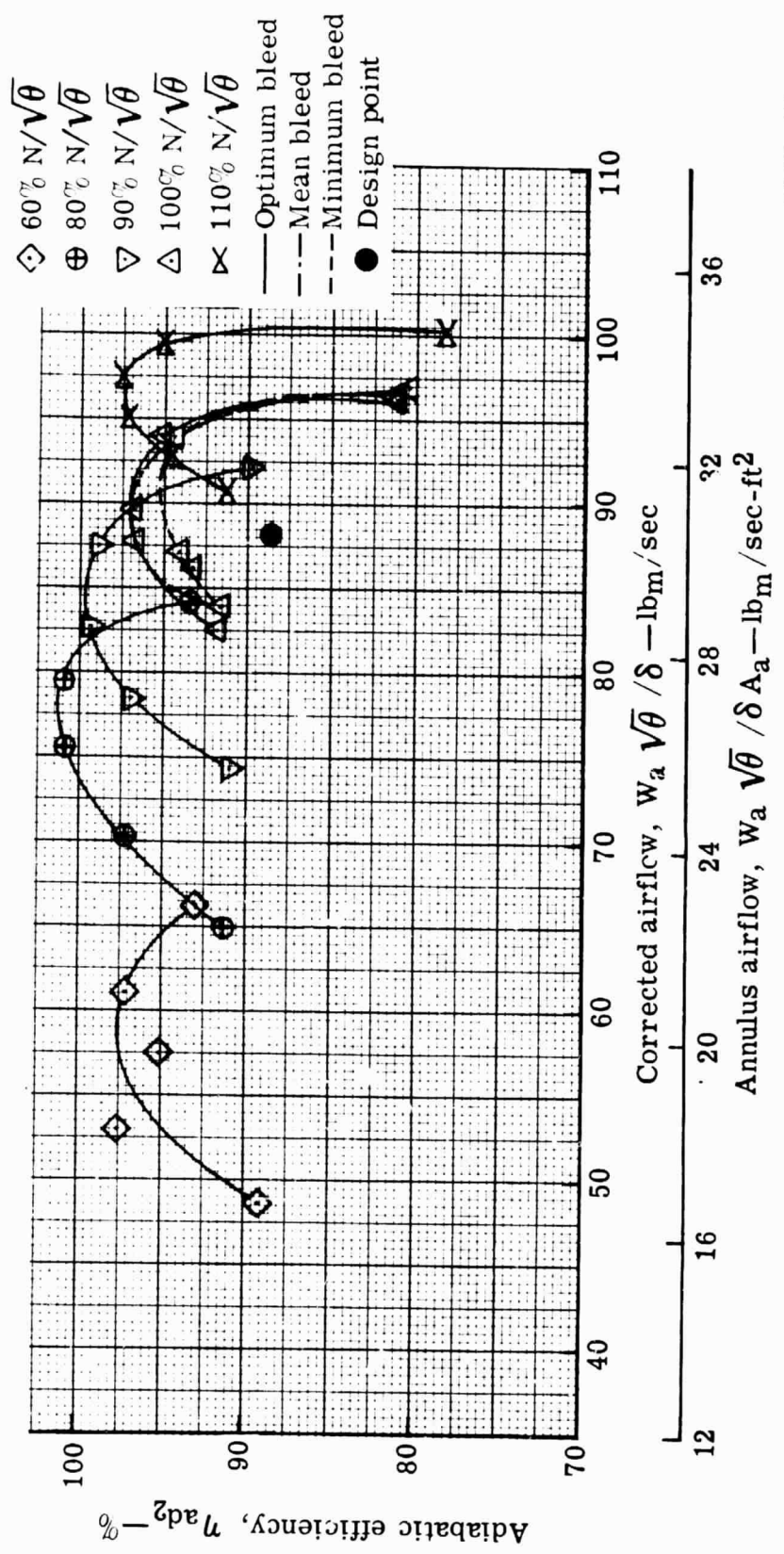


Figure 9. Flow generation rotor overall performance in stage test—adiabatic efficiency.

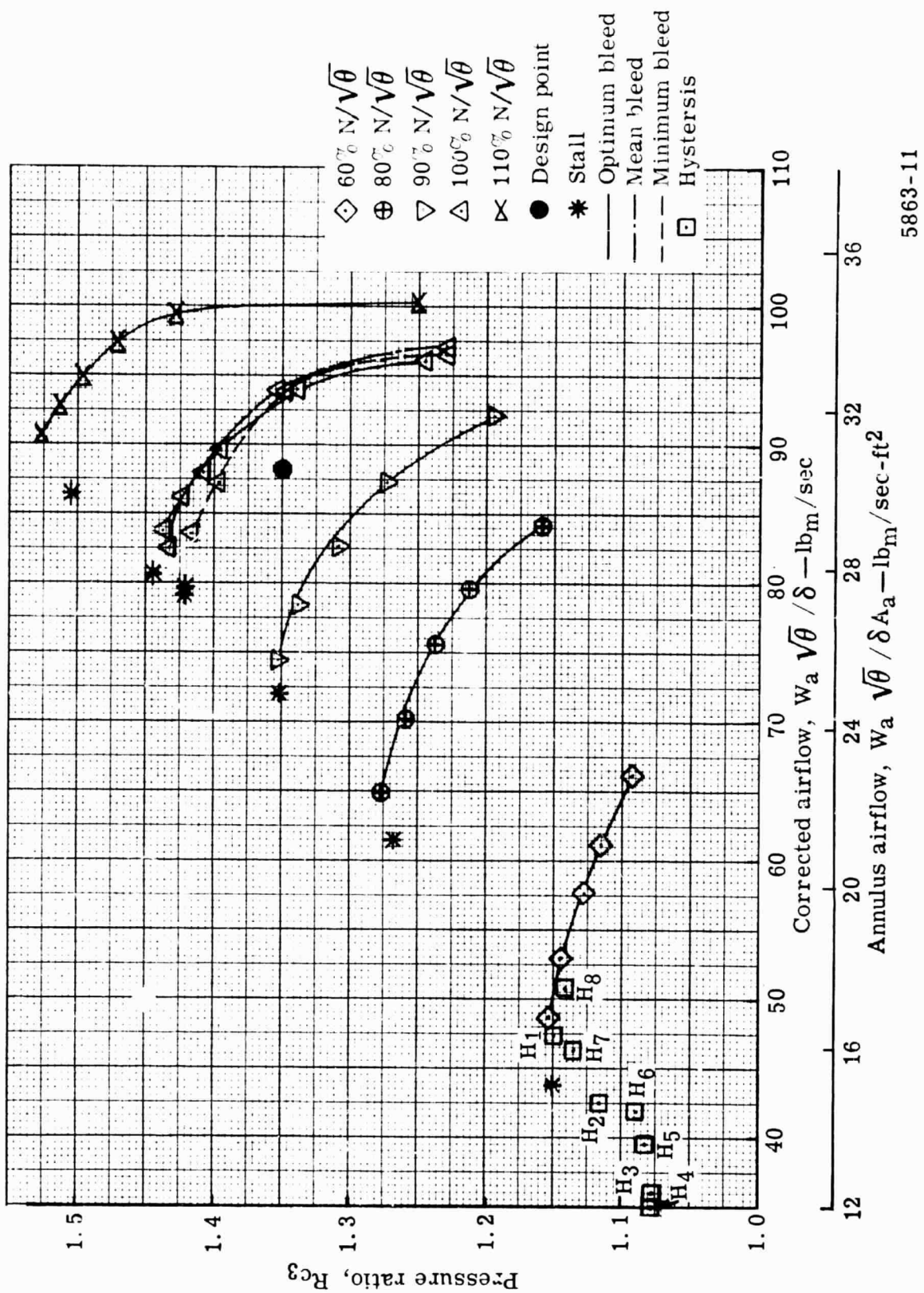


Figure 10. Stage overall performance—pressure ratio.

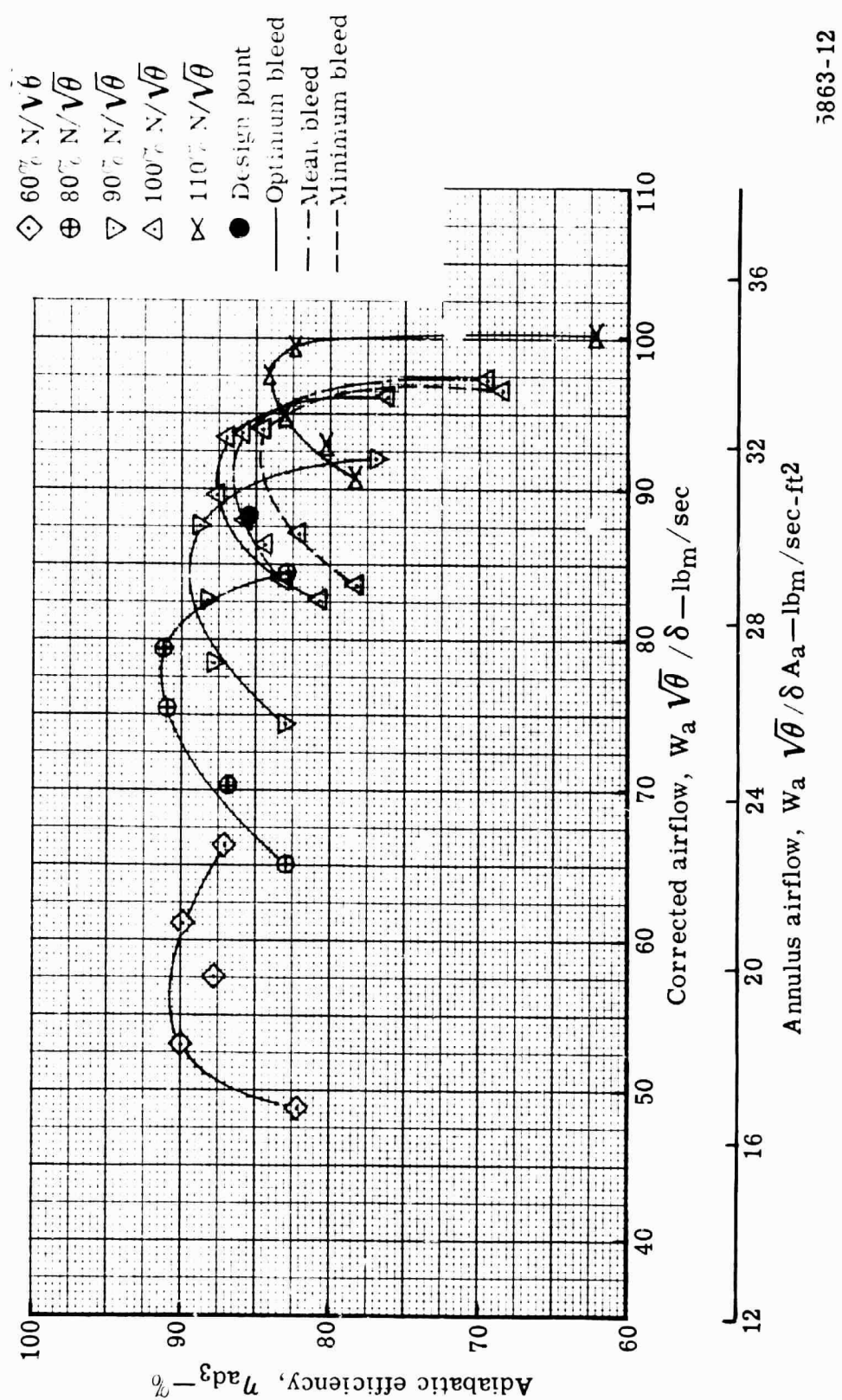
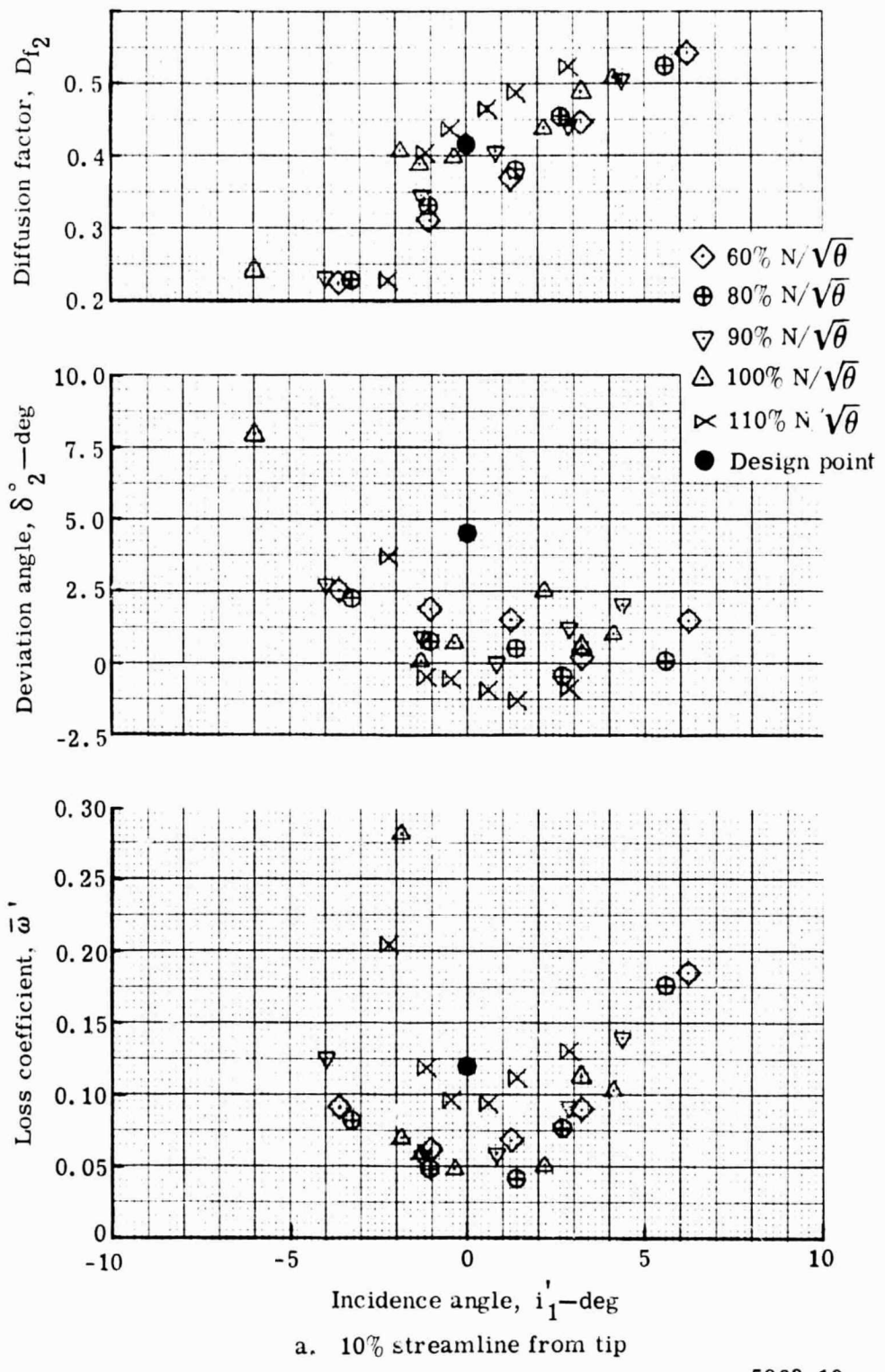
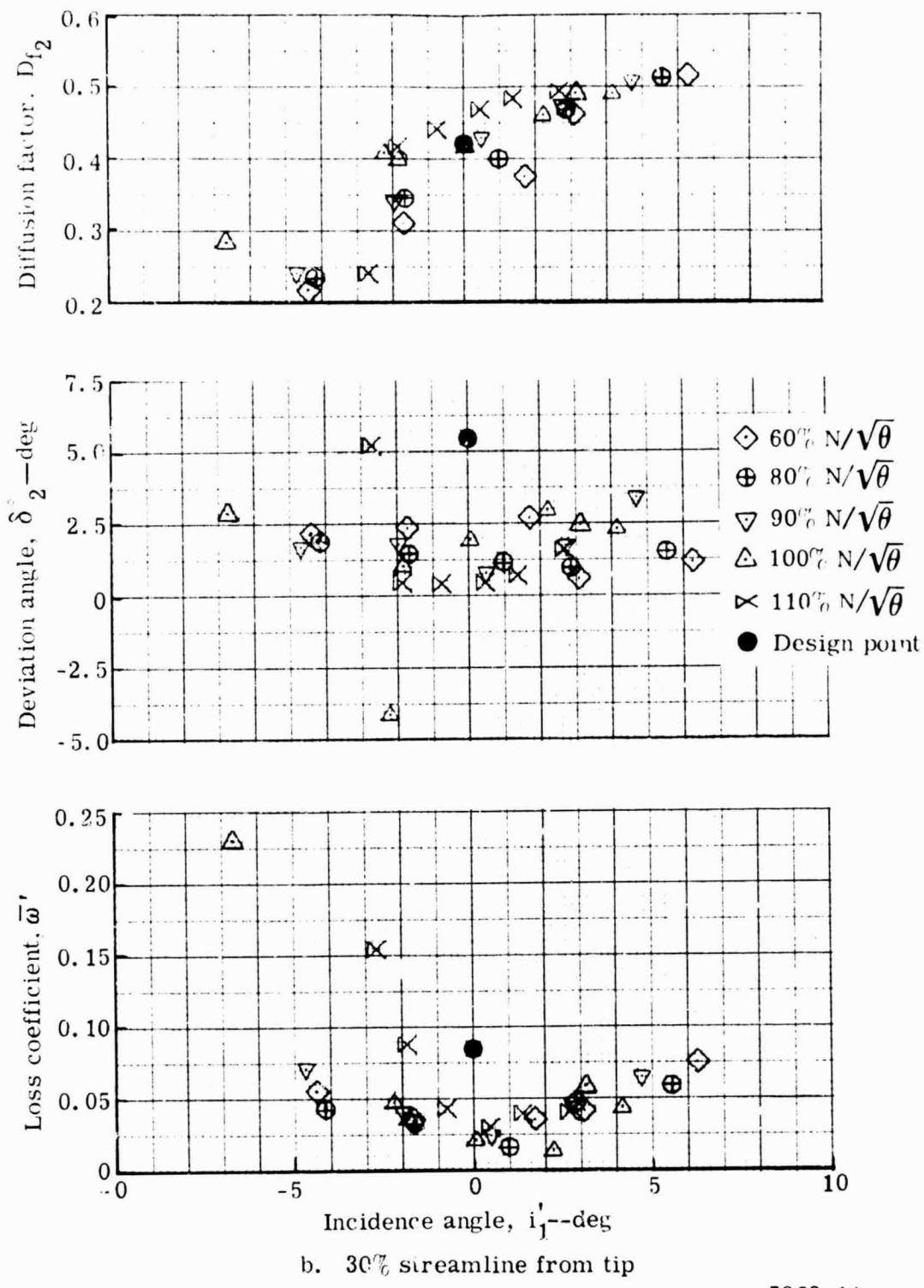


Figure 11. Stage overall performance—adiabatic efficiency.



5863-13

Figure 12. Rotor blade element performance at optimum wall bleed—stage test.



5863-14

Figure 12. Rotor blade element performance at optimum wall bleed—stage test.

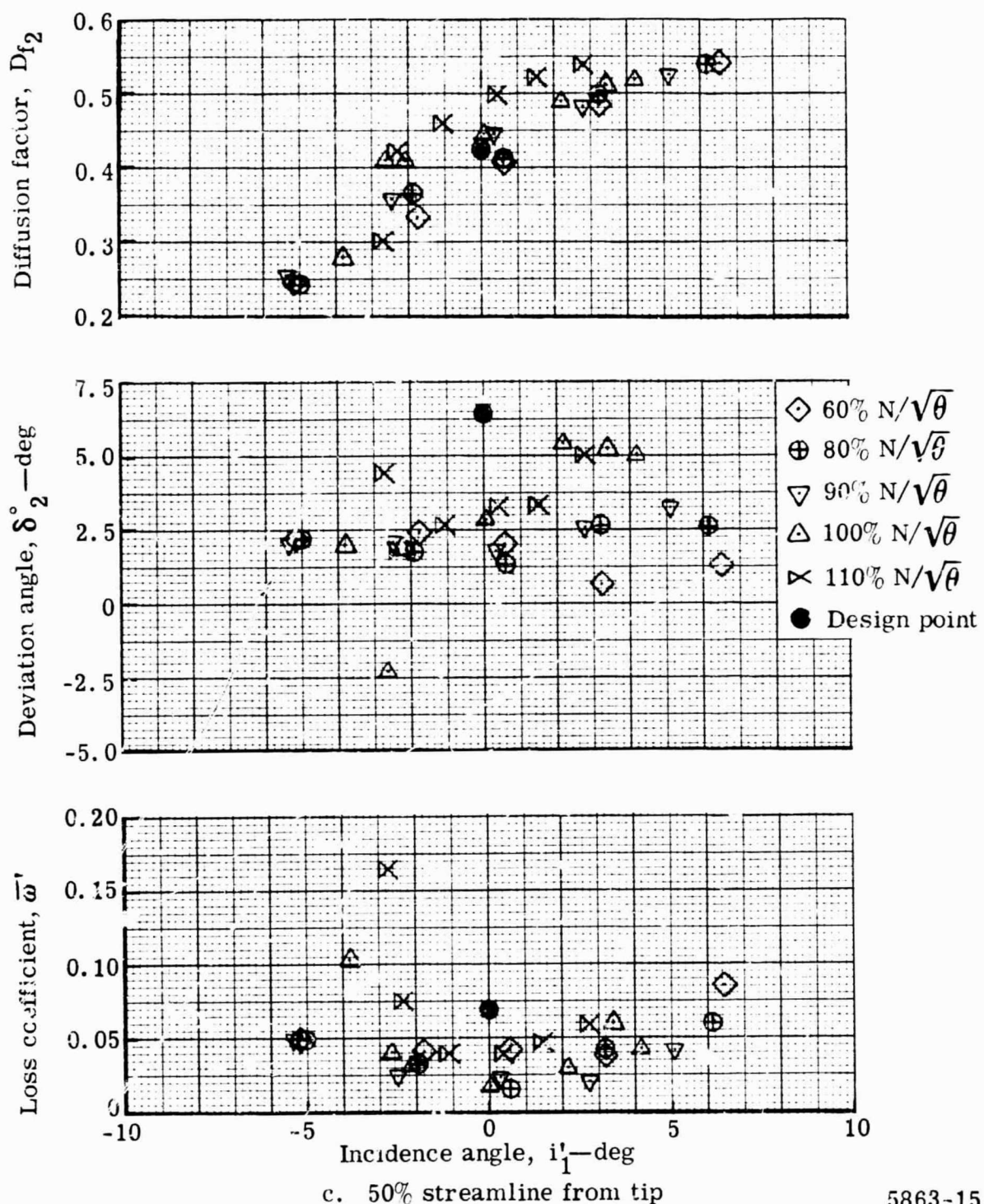
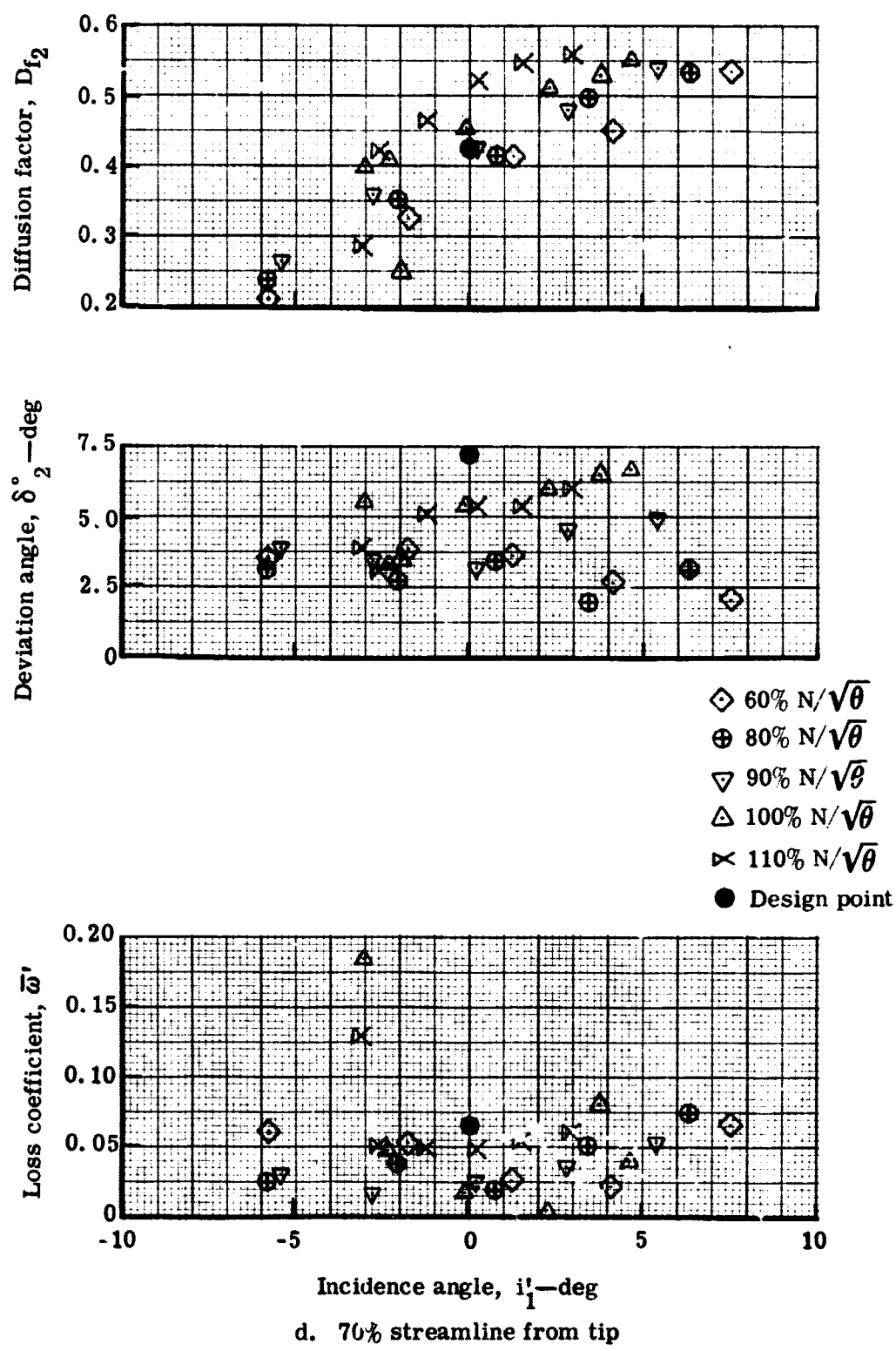


Figure 12. Rotor blade element performance at optimum wall bleed—stage test.



5863-16

Figure 12. Rotor blade element performance at optimum wall bleed—stage test.

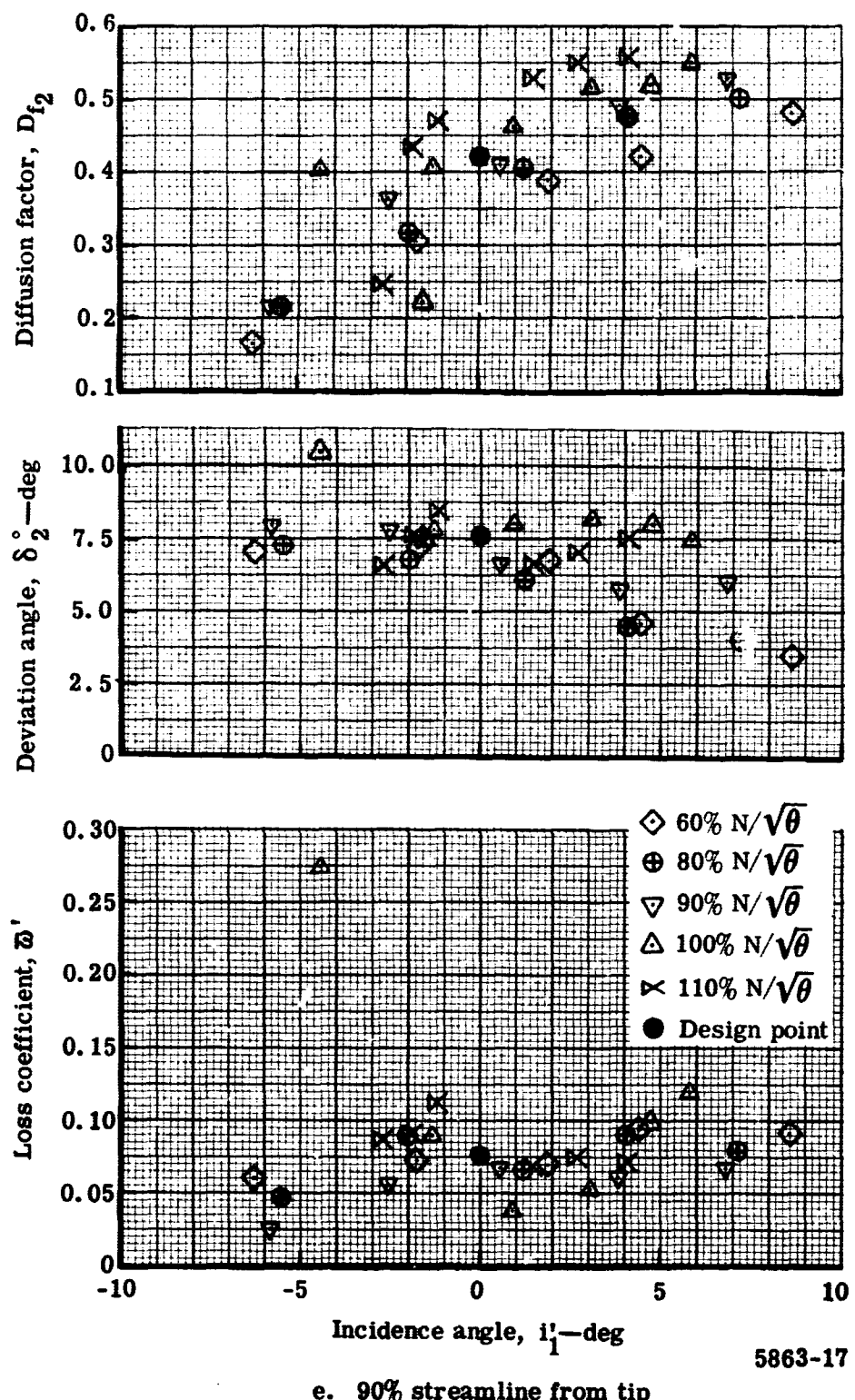


Figure 12. Rotor blade element performance at optimum wall bleed—stage test.

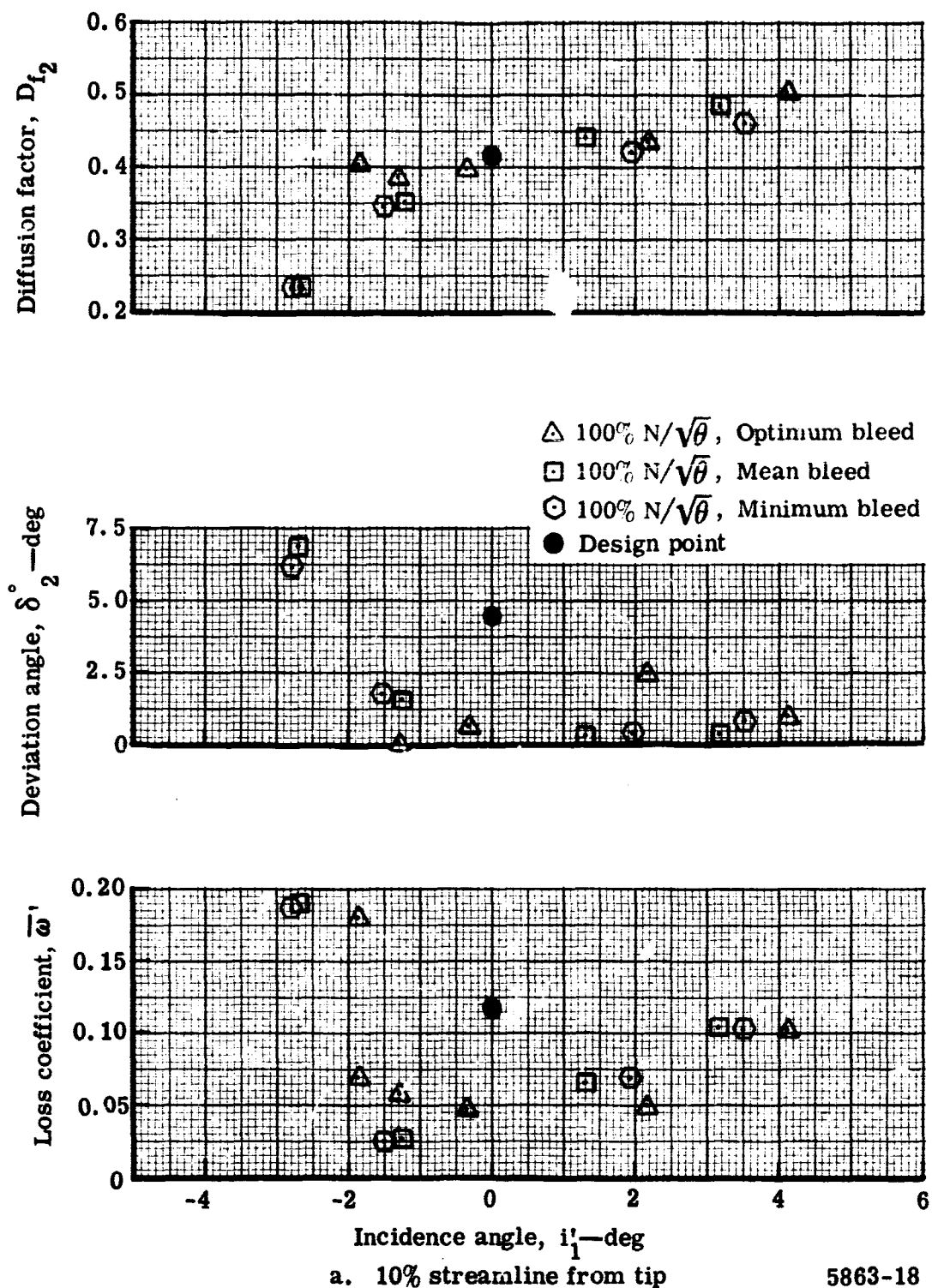


Figure 13. Rotor blade element performance for 100% design speed with varying wall bleed rates—stage test.

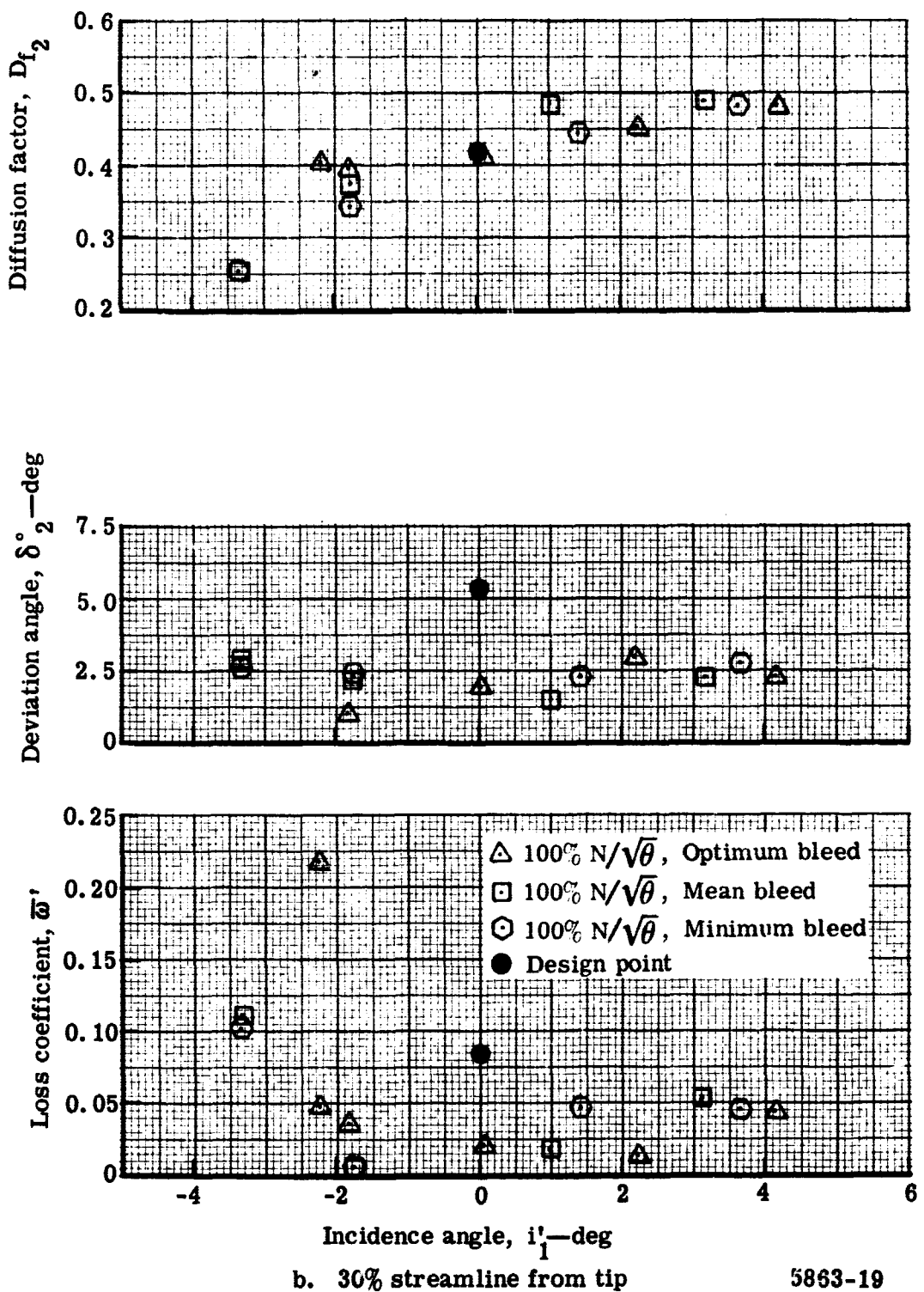


Figure 13. Rotor blade element performance for 100% design speed with varying wall bleed rates—stage test.

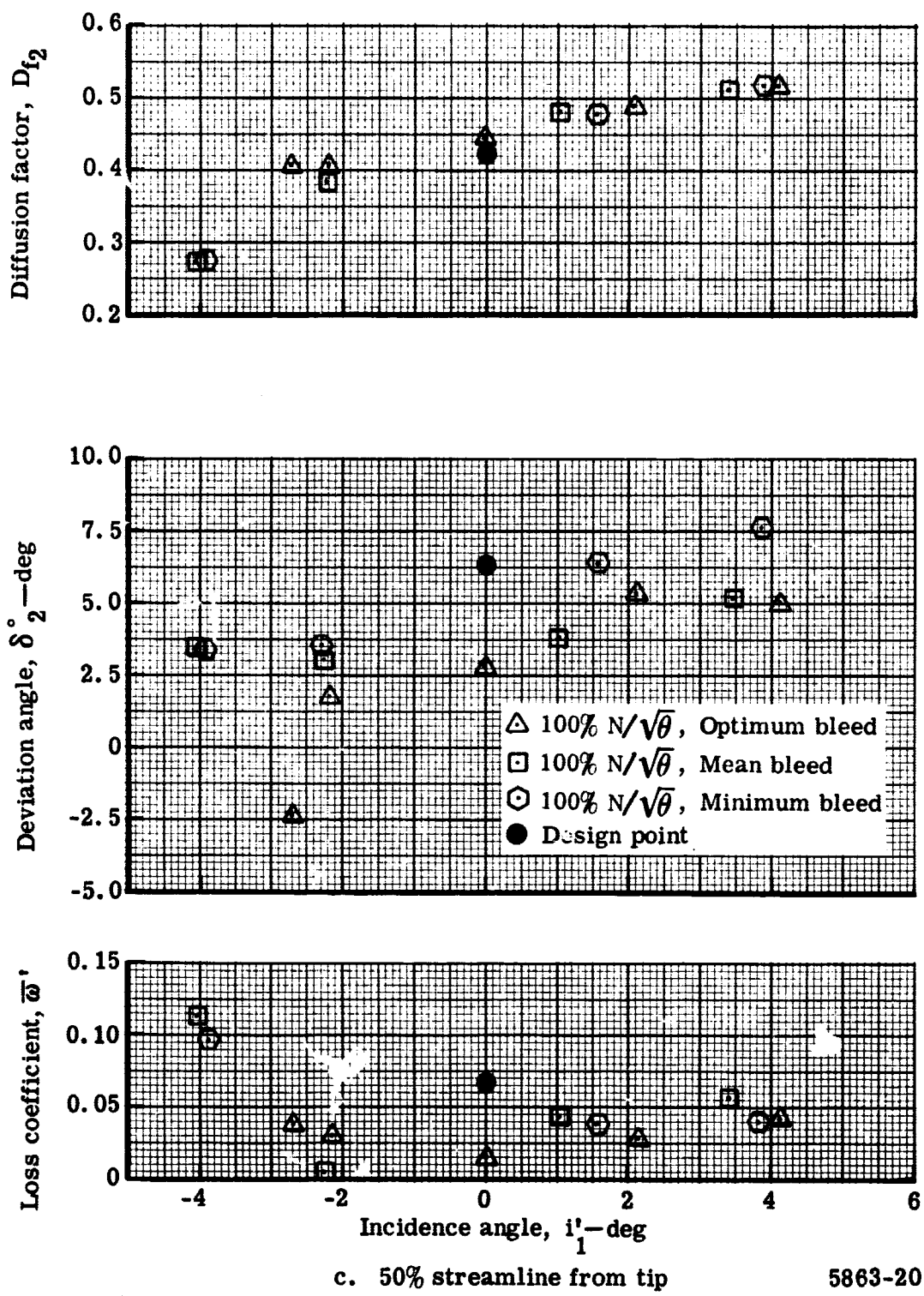


Figure 13. Rotor blade element performance for 100% design speed with varying wall bleed rates—stage test.

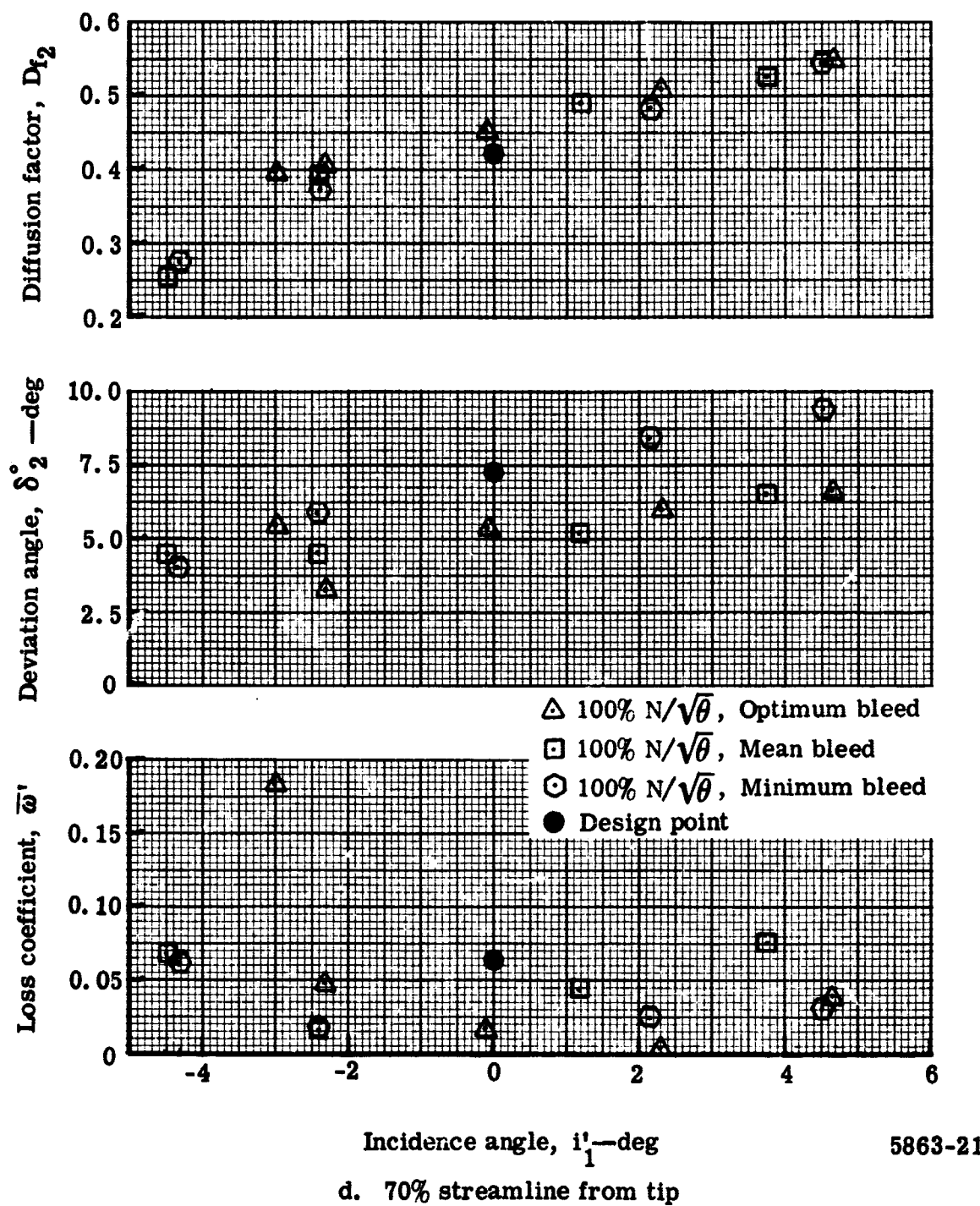


Figure 13. Rotor blade element performance for 100% design speed with varying wall bleed rates—stage test.

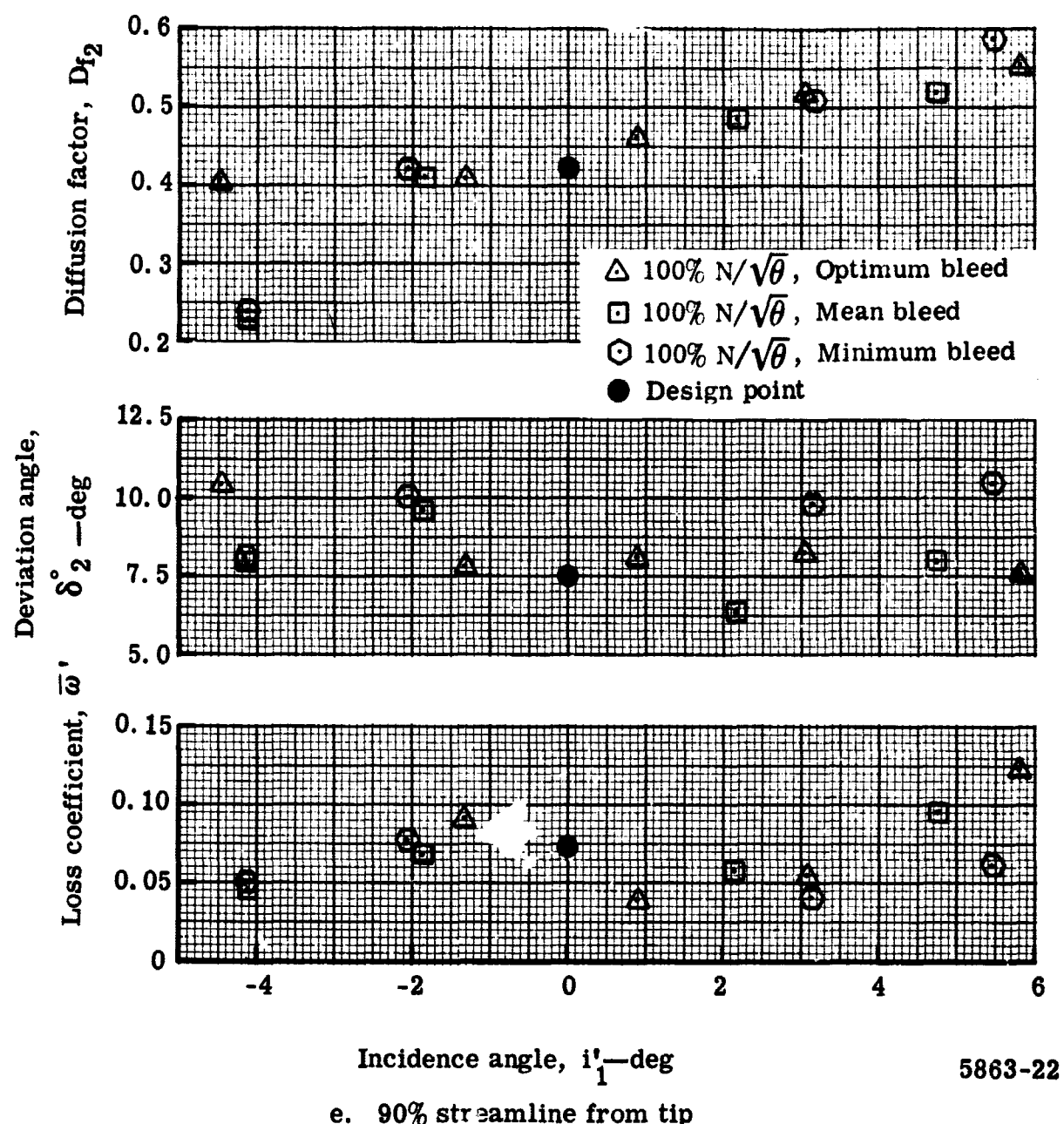


Figure 13. Rotor blade element performance for 100% design speed with varying wall bleed rates—stage test.

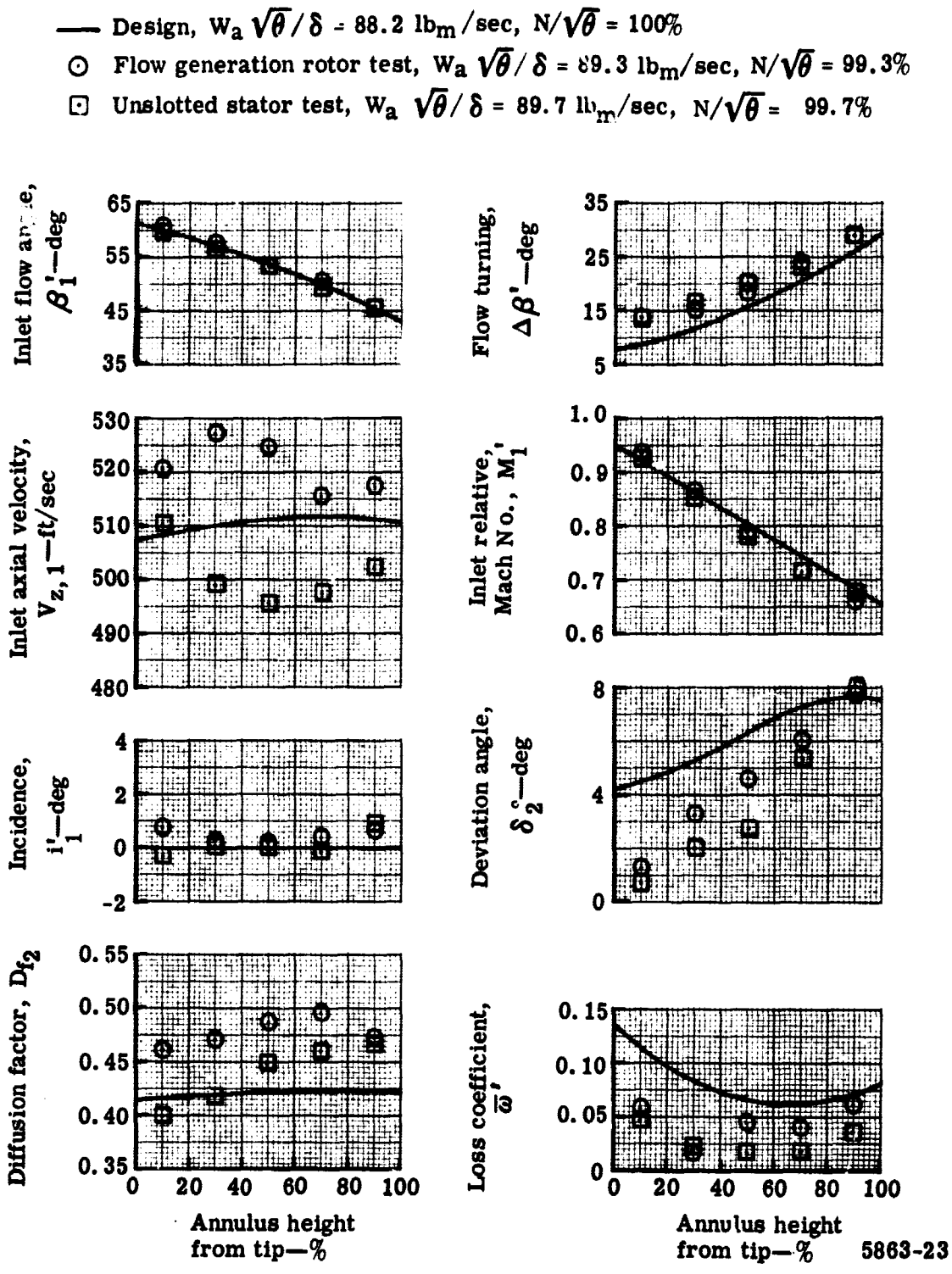


Figure 14. Radial variation of rotor blade element performance with optimum wall bleed.

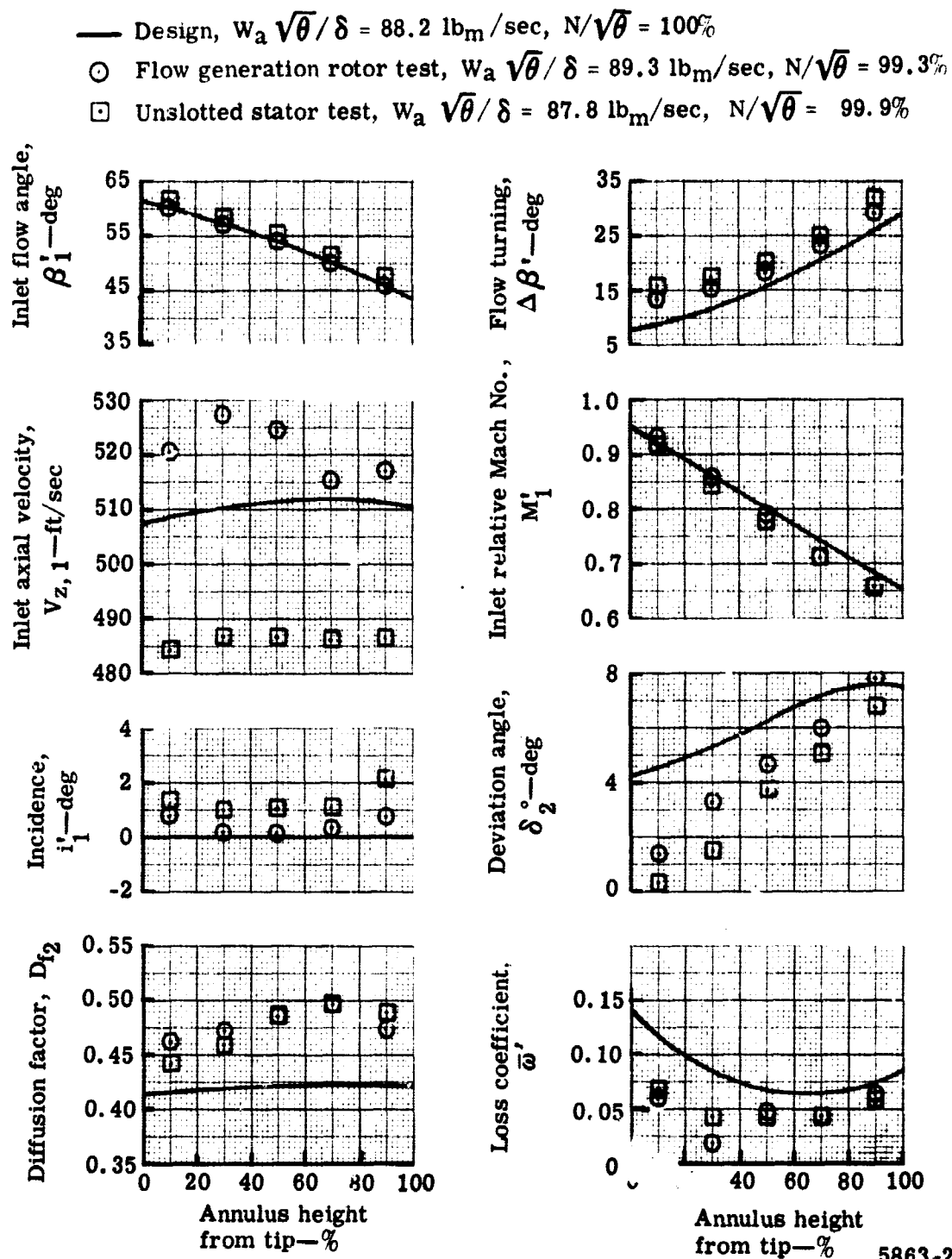
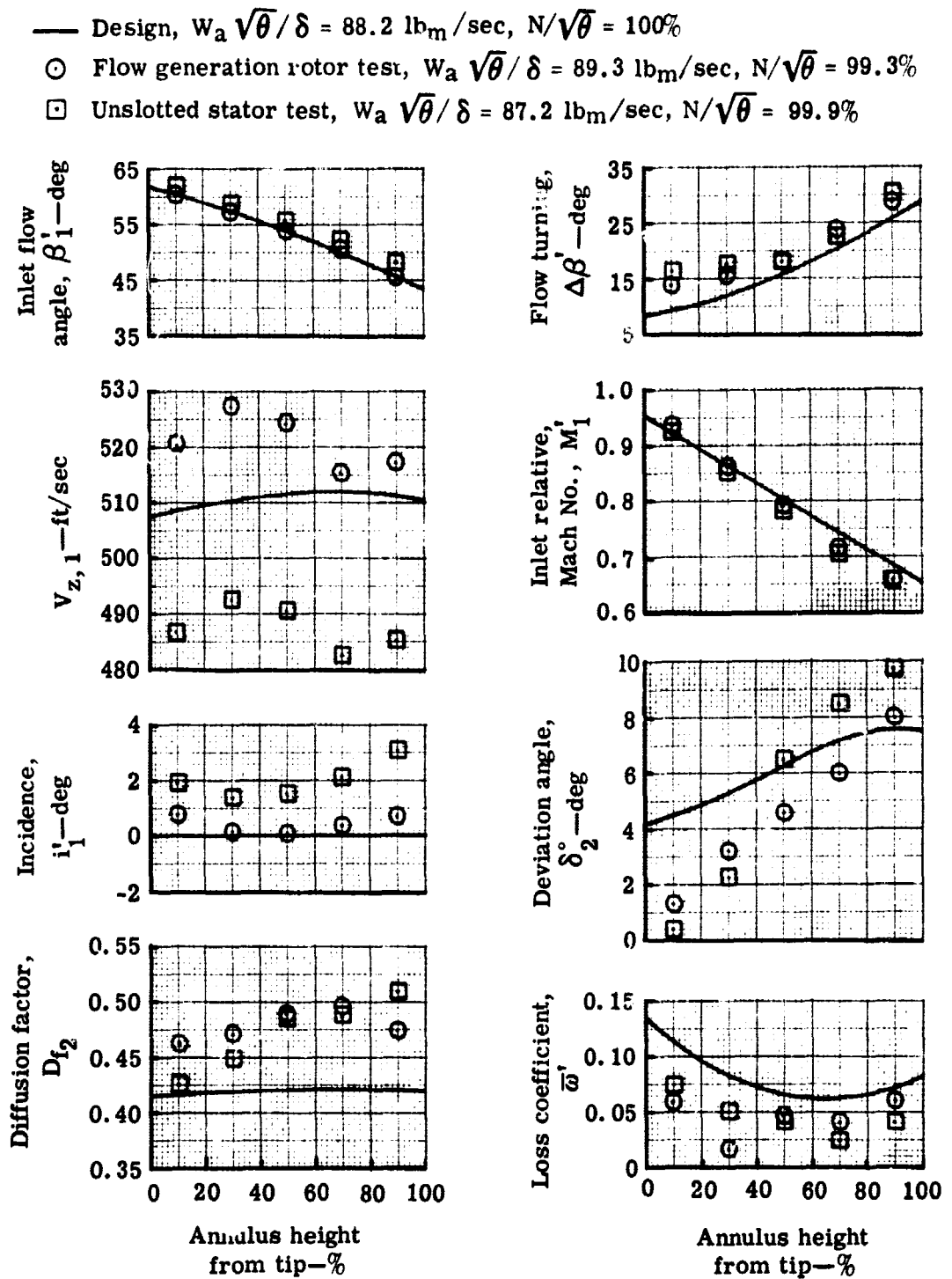


Figure 15. Radial variation of rotor blade element performance with mean wall bleed.



5863-25

Figure 16. Radial variation of rotor blade element performance with minimum wall bleed.

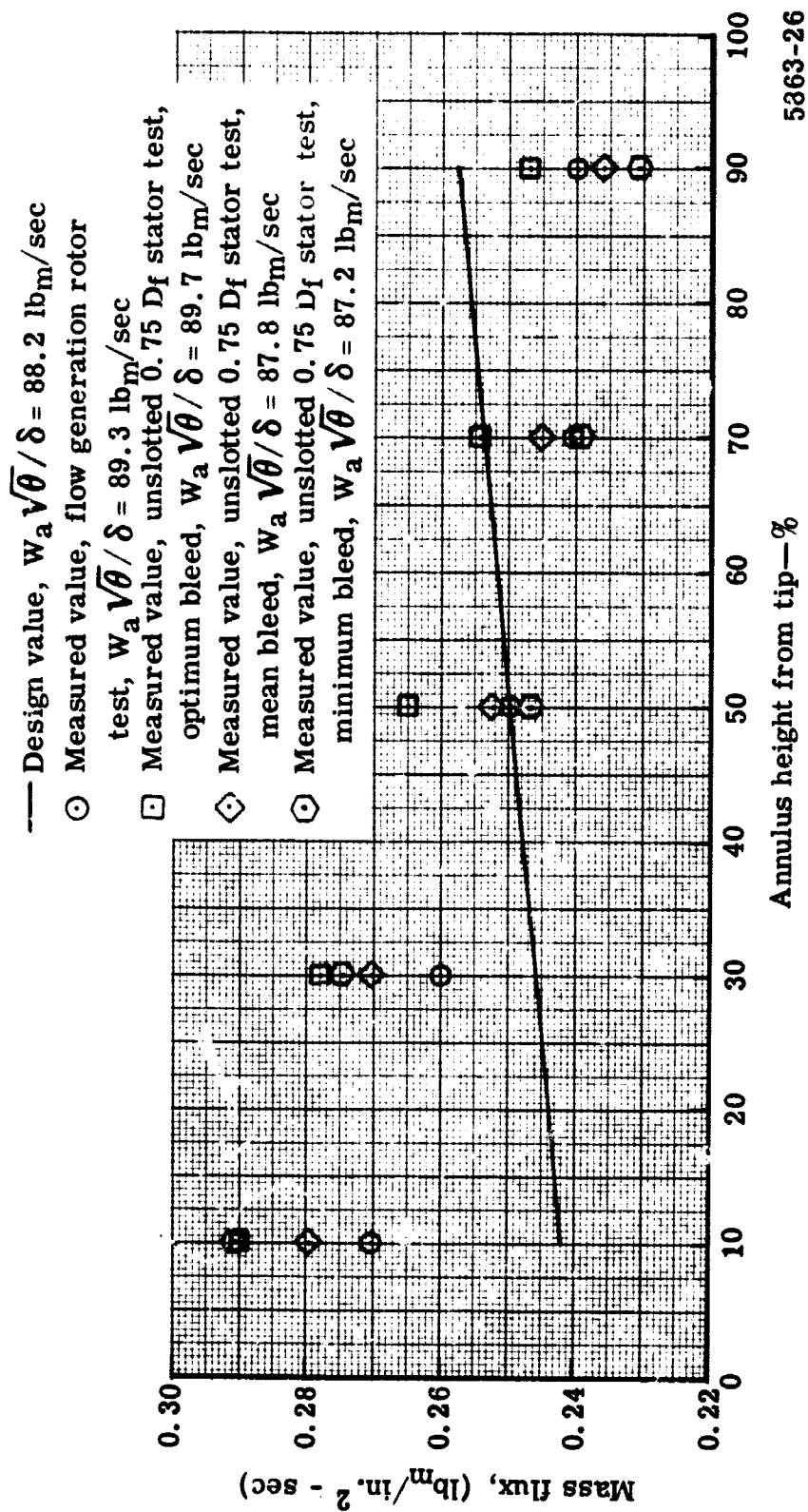


Figure 17. Rotor out radial mass flux distribution at design speed with varying wall bleed rates.

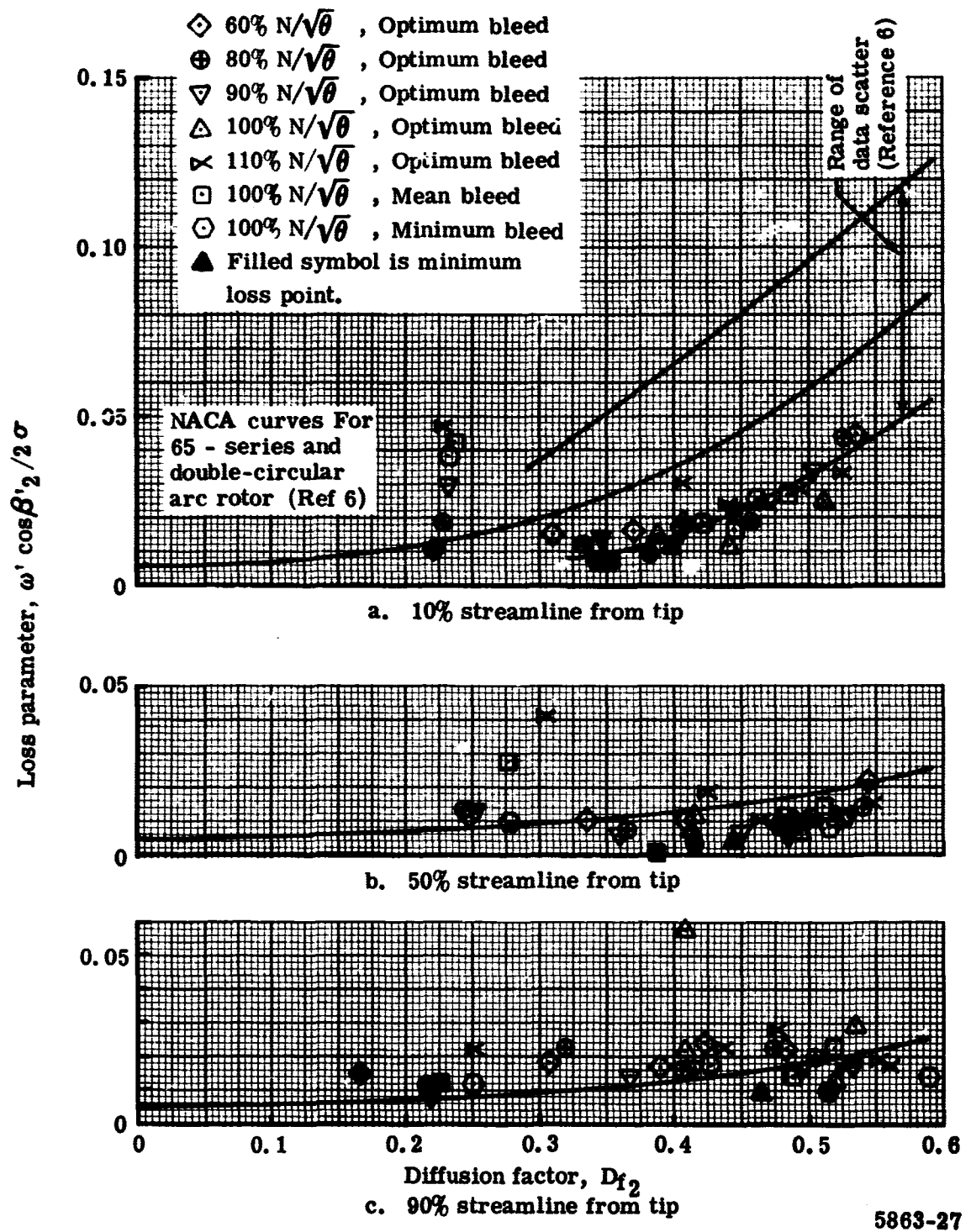


Figure 18. Rotor loss parameter versus diffusion factor.

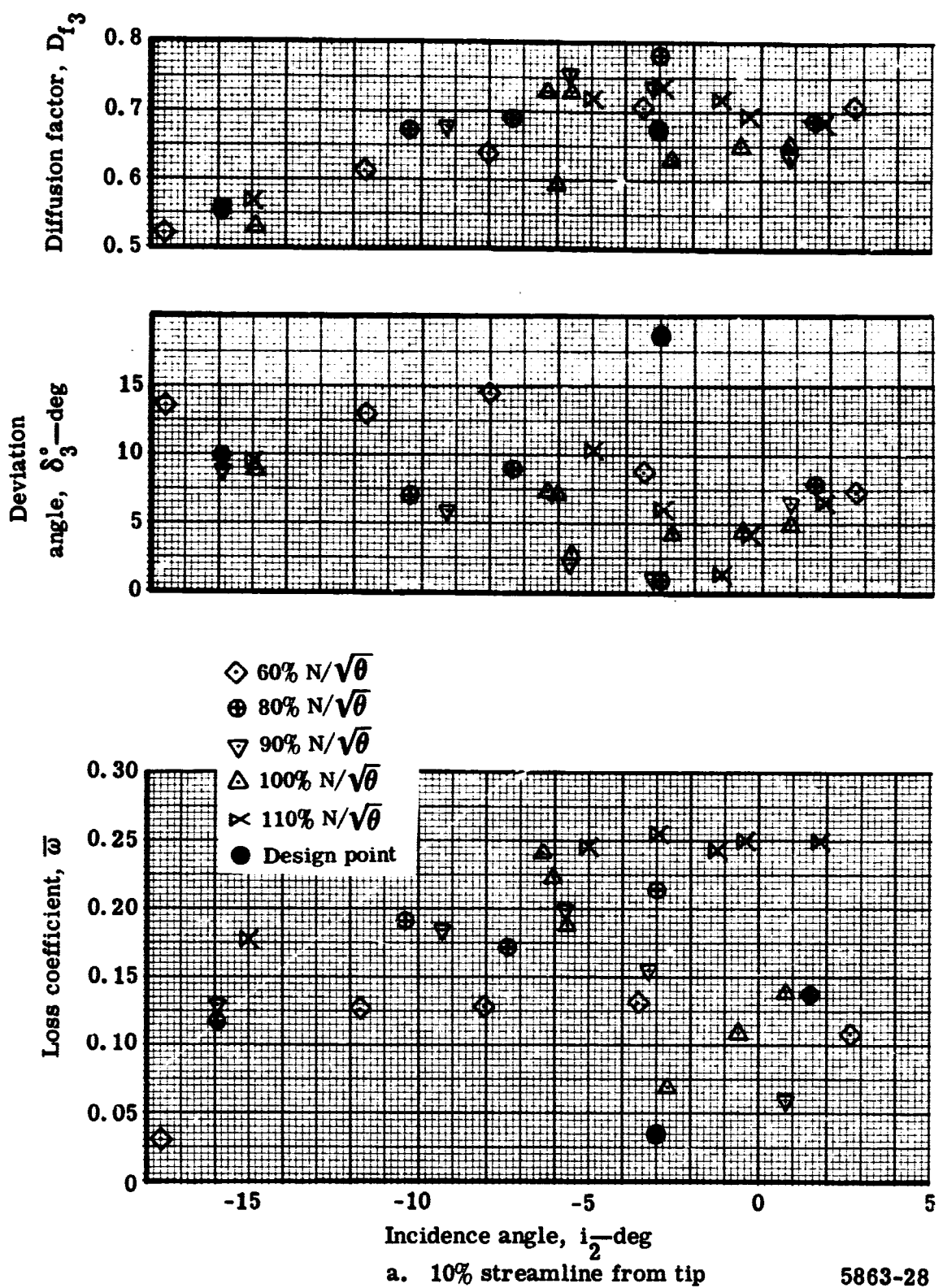


Figure 19. Stator blade element performance with optimum wall bleed.

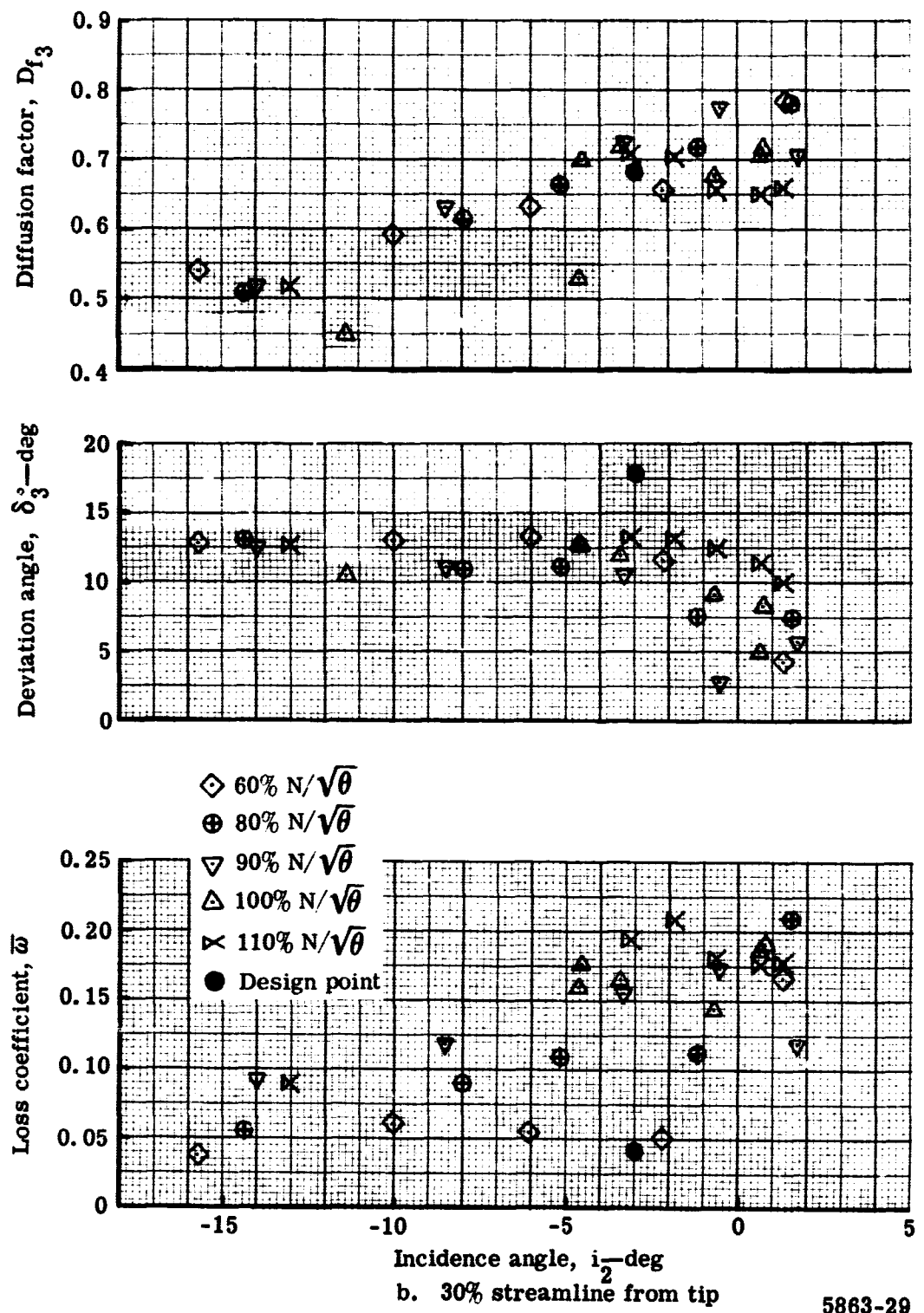


Figure 19. Stator blade element performance with optimum wall bleed.

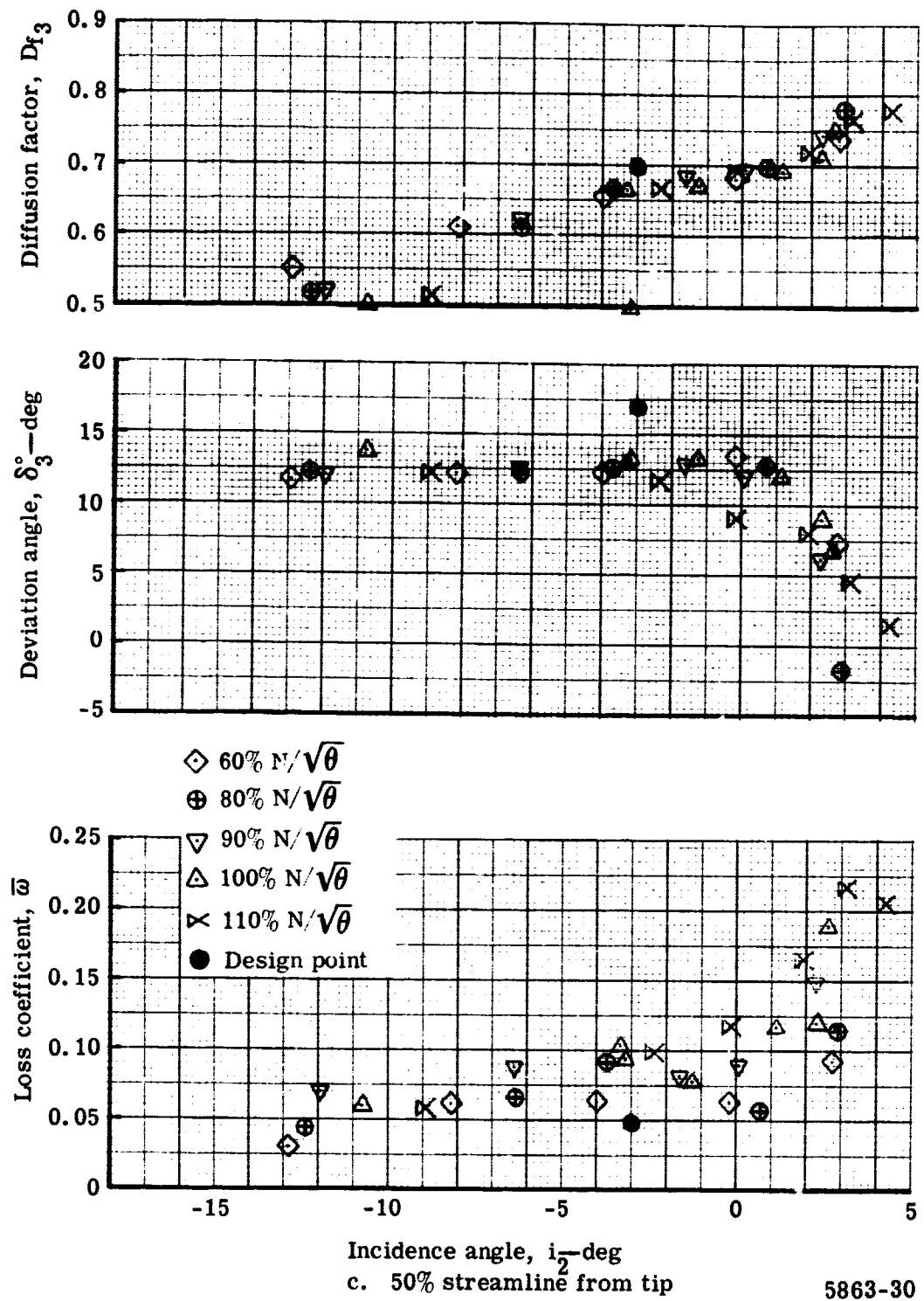


Figure 19. Stator blade element performance with optimum wall bleed.

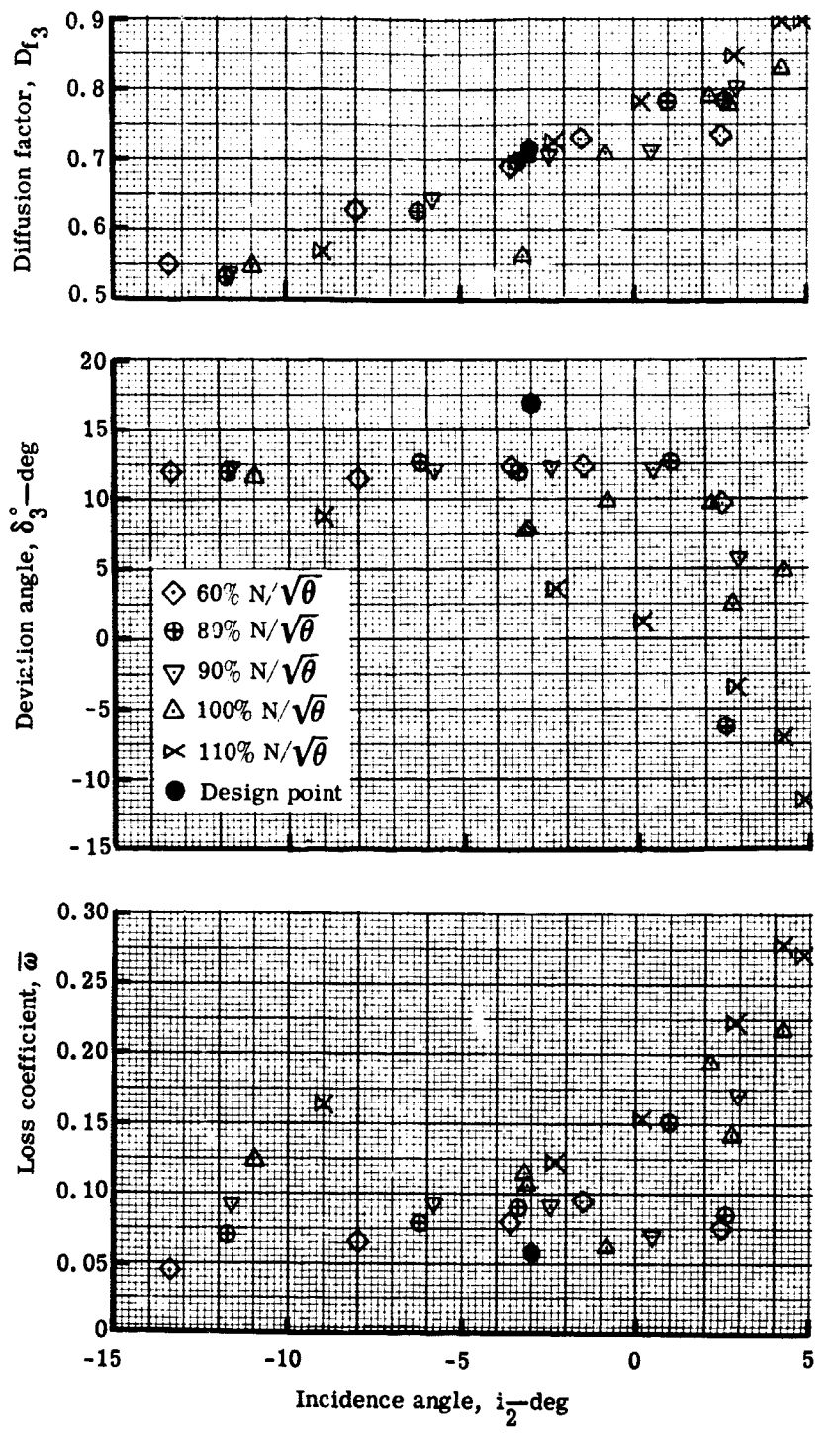
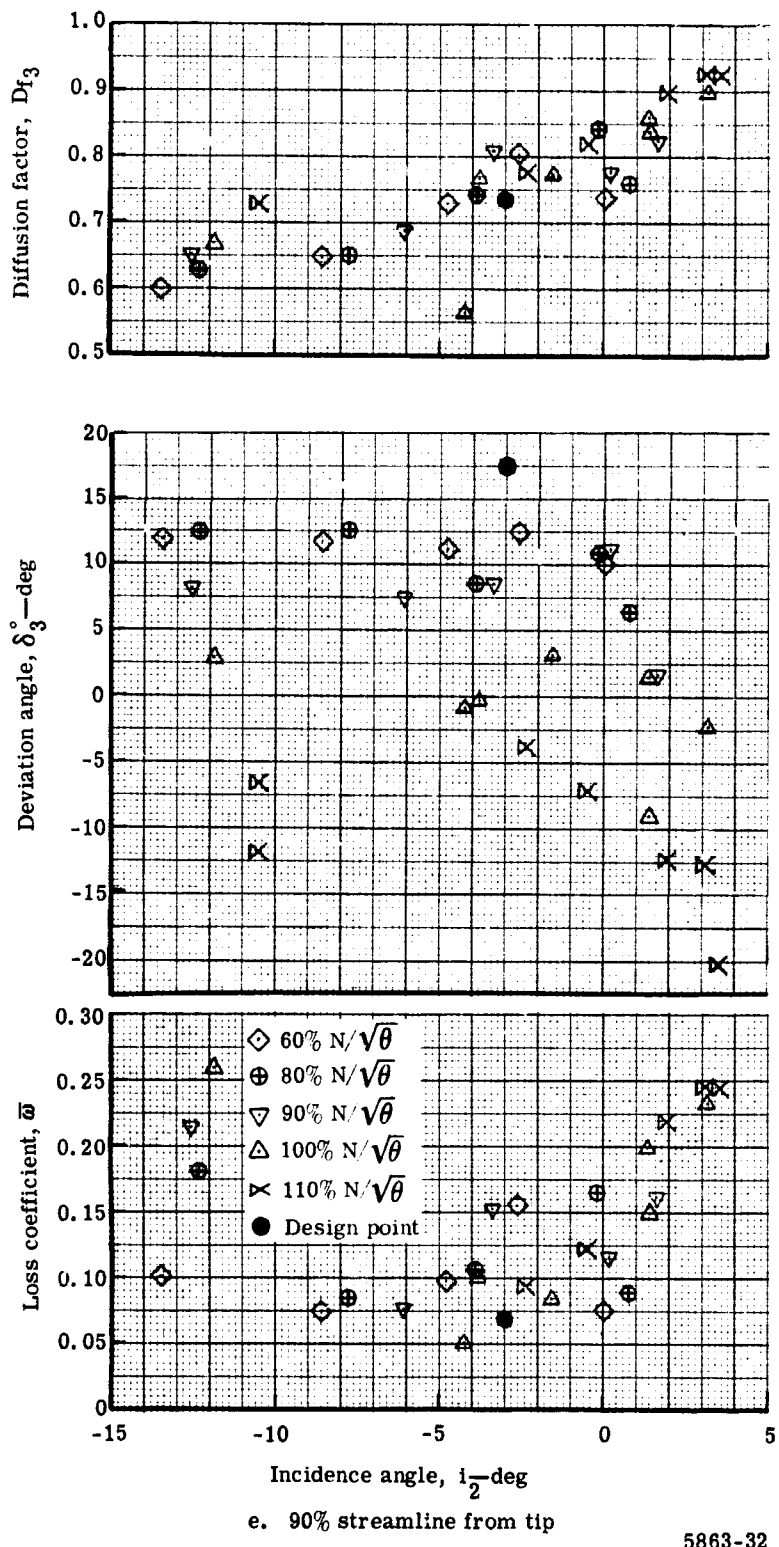


Figure 19. Stator blade element performance with optimum wall bleed.



5863-32

Figure 19. Stator blade element performance with optimum wall bleed.

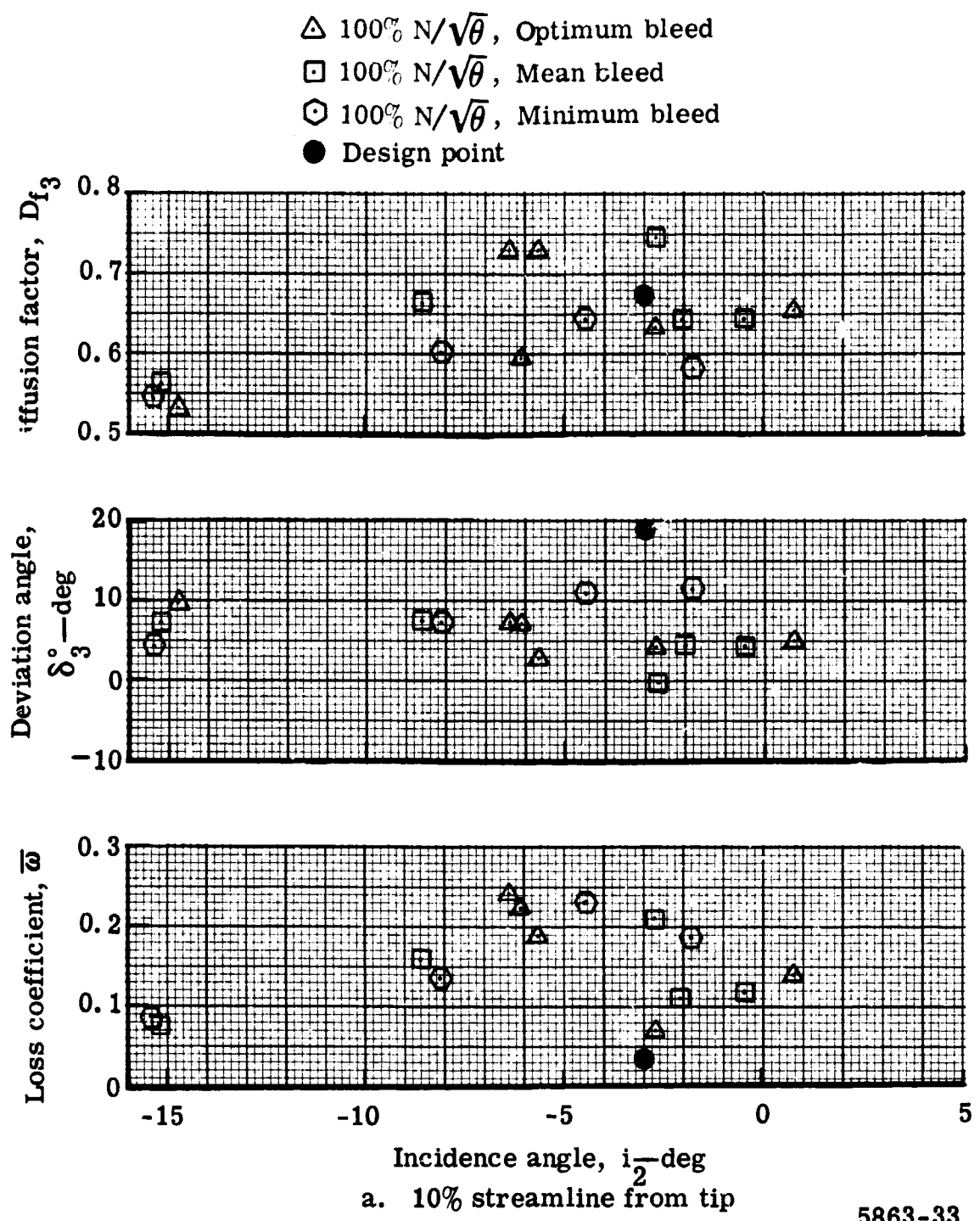


Figure 20. Stator blade element performance for 100% design speed with varying wall bleed rates.

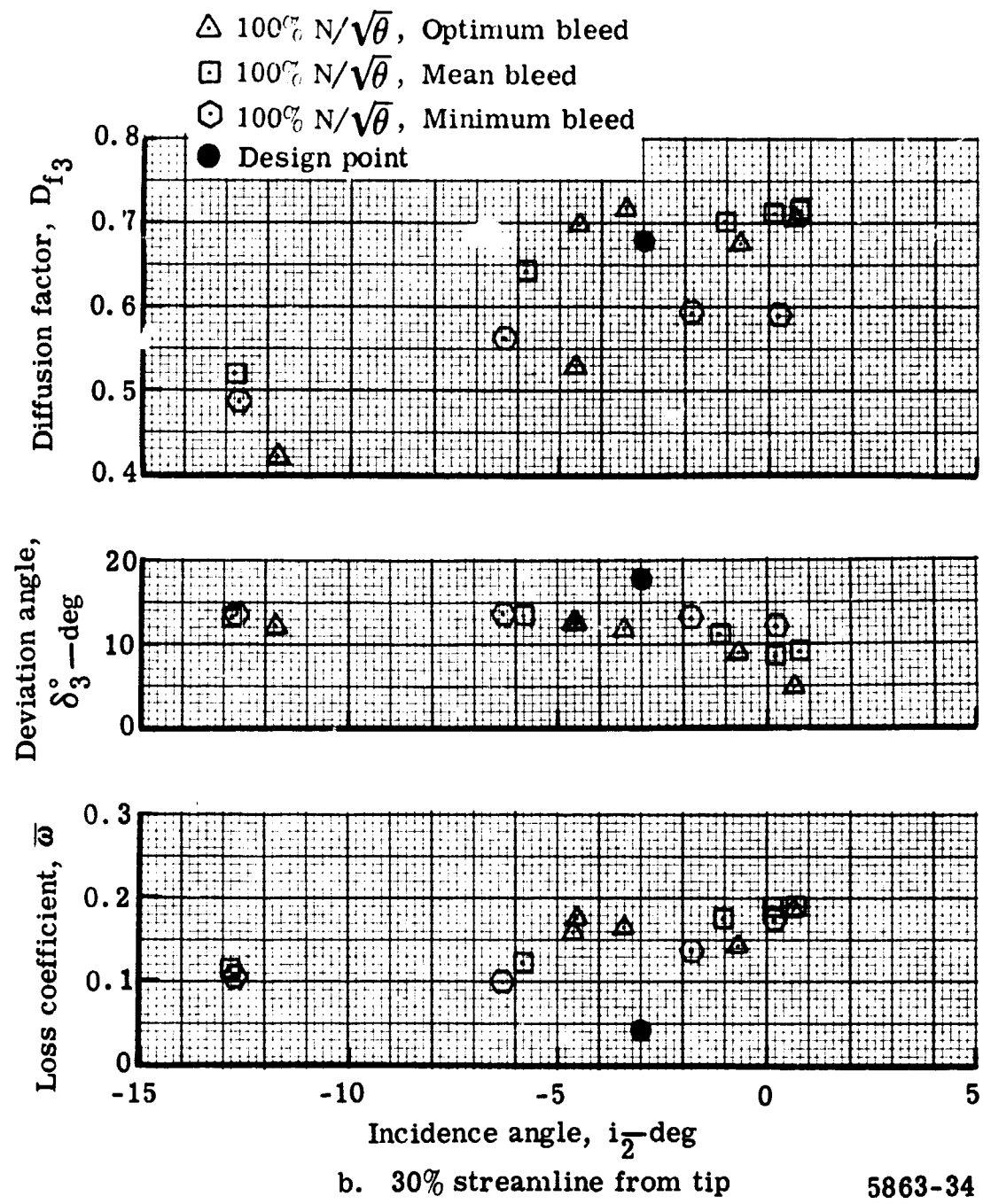
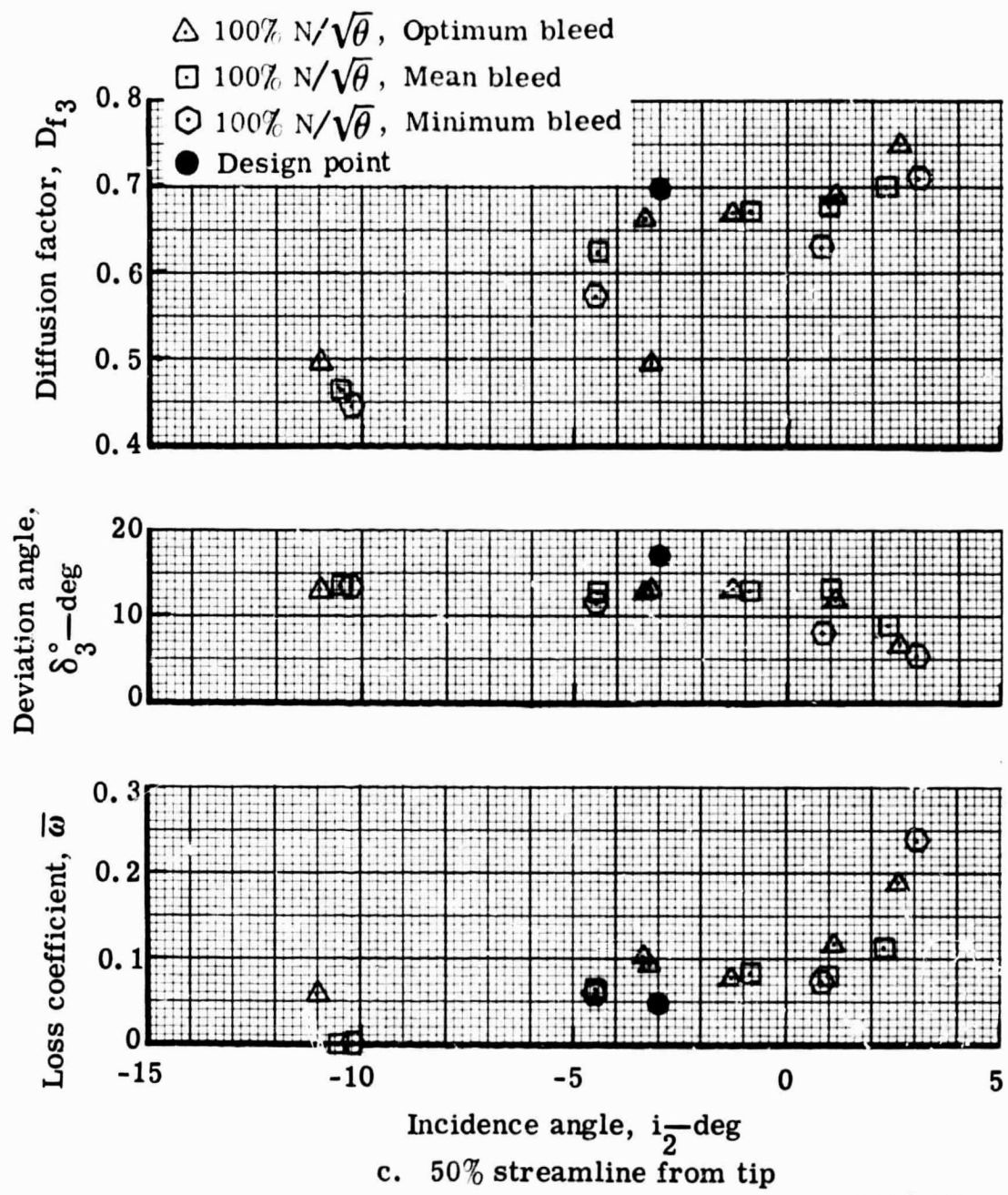
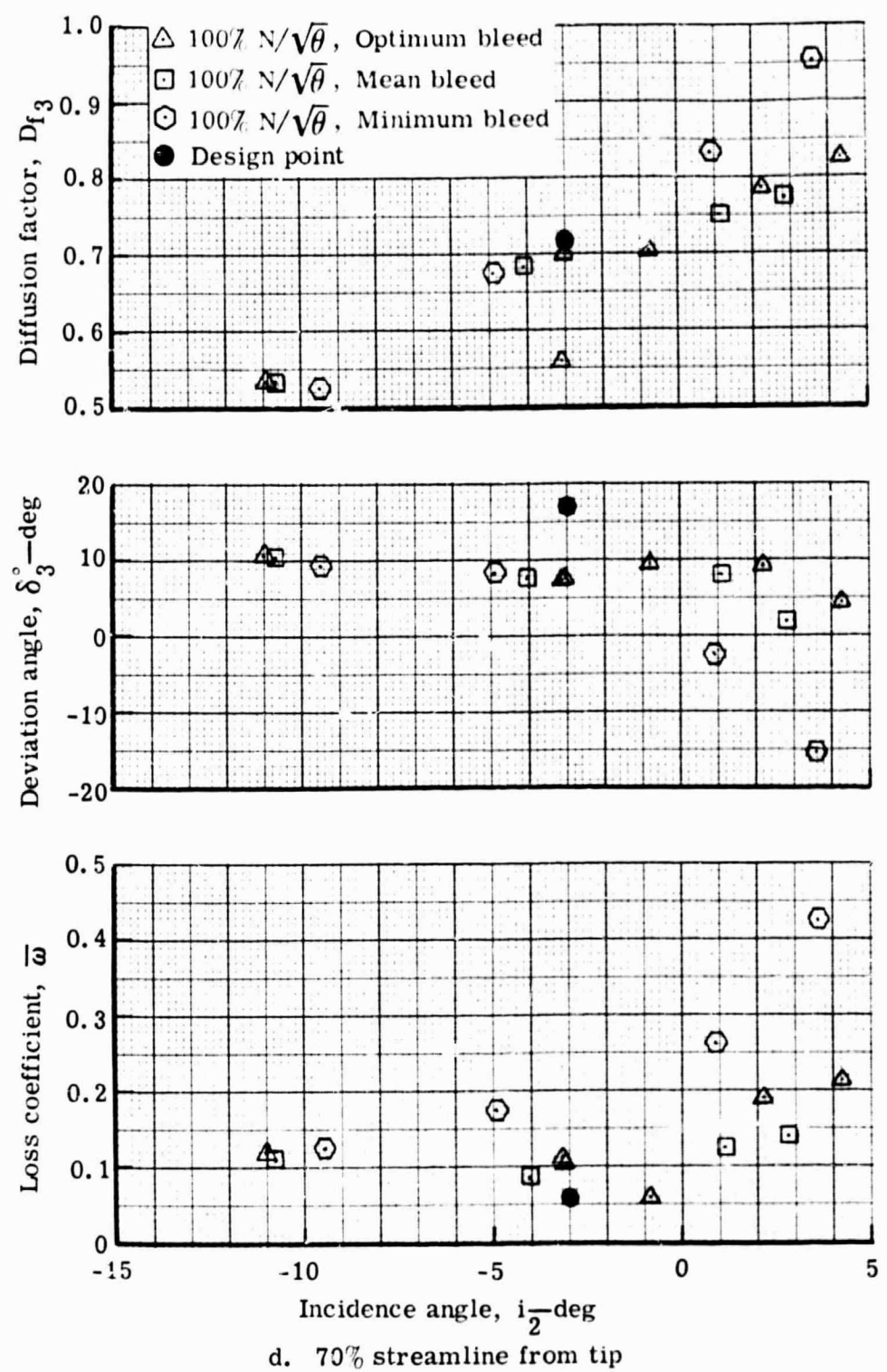


Figure 20. Stator blade element performance for 100% design speed with varying wall bleed rates.



5863-35

Figure 20. Stator blade element performance for 100% design speed
with varying wall bleed rates.



5863-36

Figure 20. Stator blade element performance for 100% design speed with varying wall bleed rates.

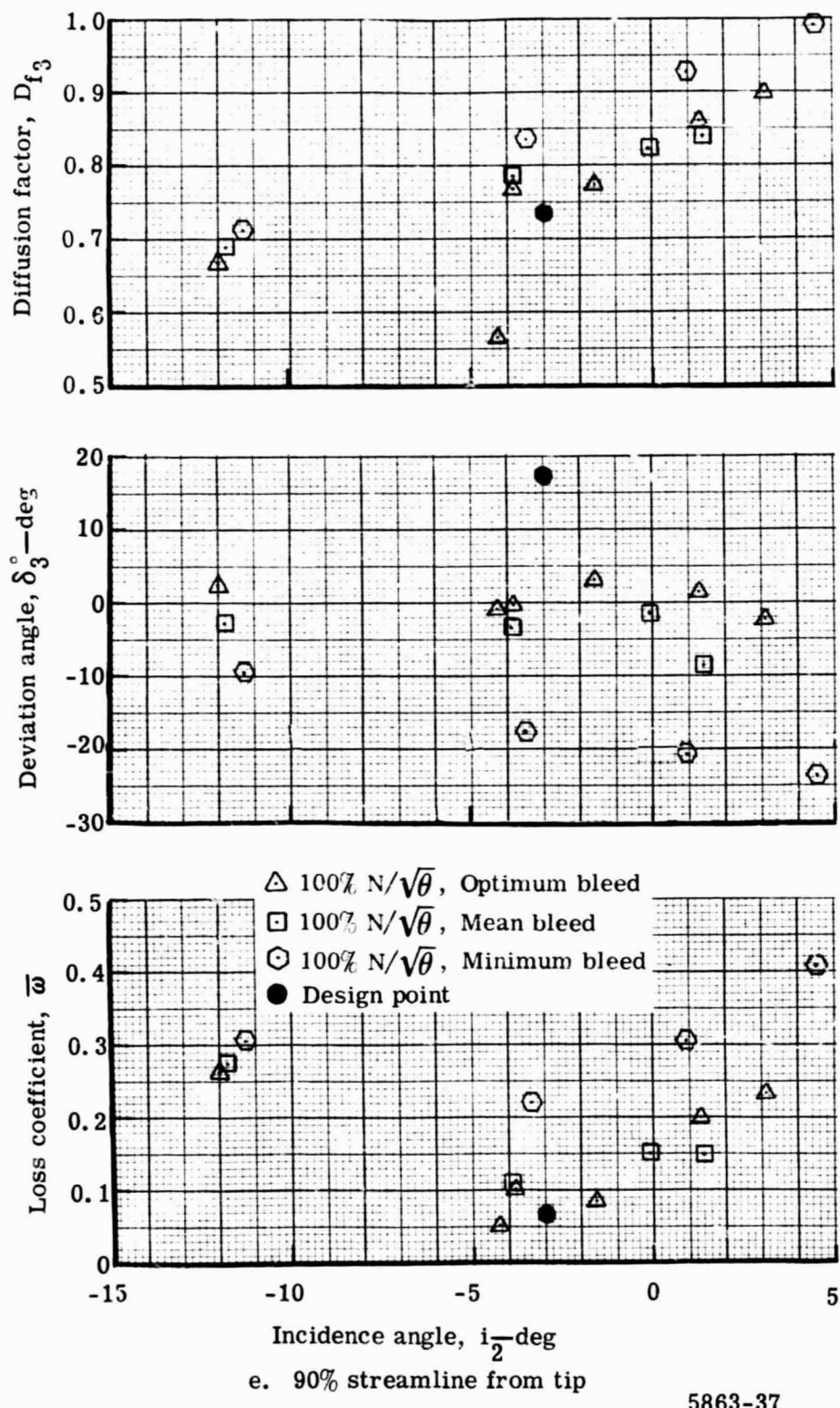


Figure 20. Stator blade element performance for 100% design speed with varying wall bleed rates.

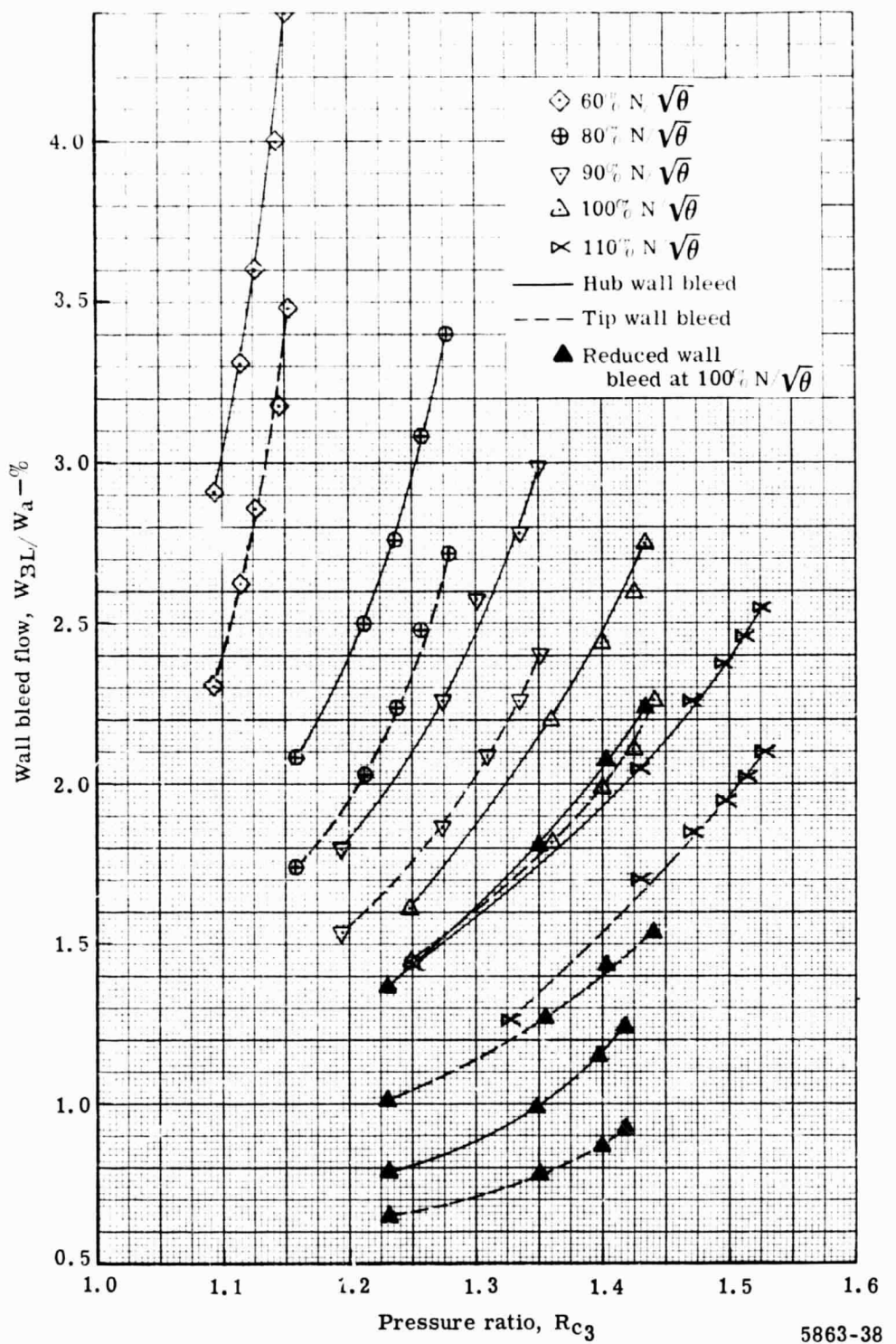
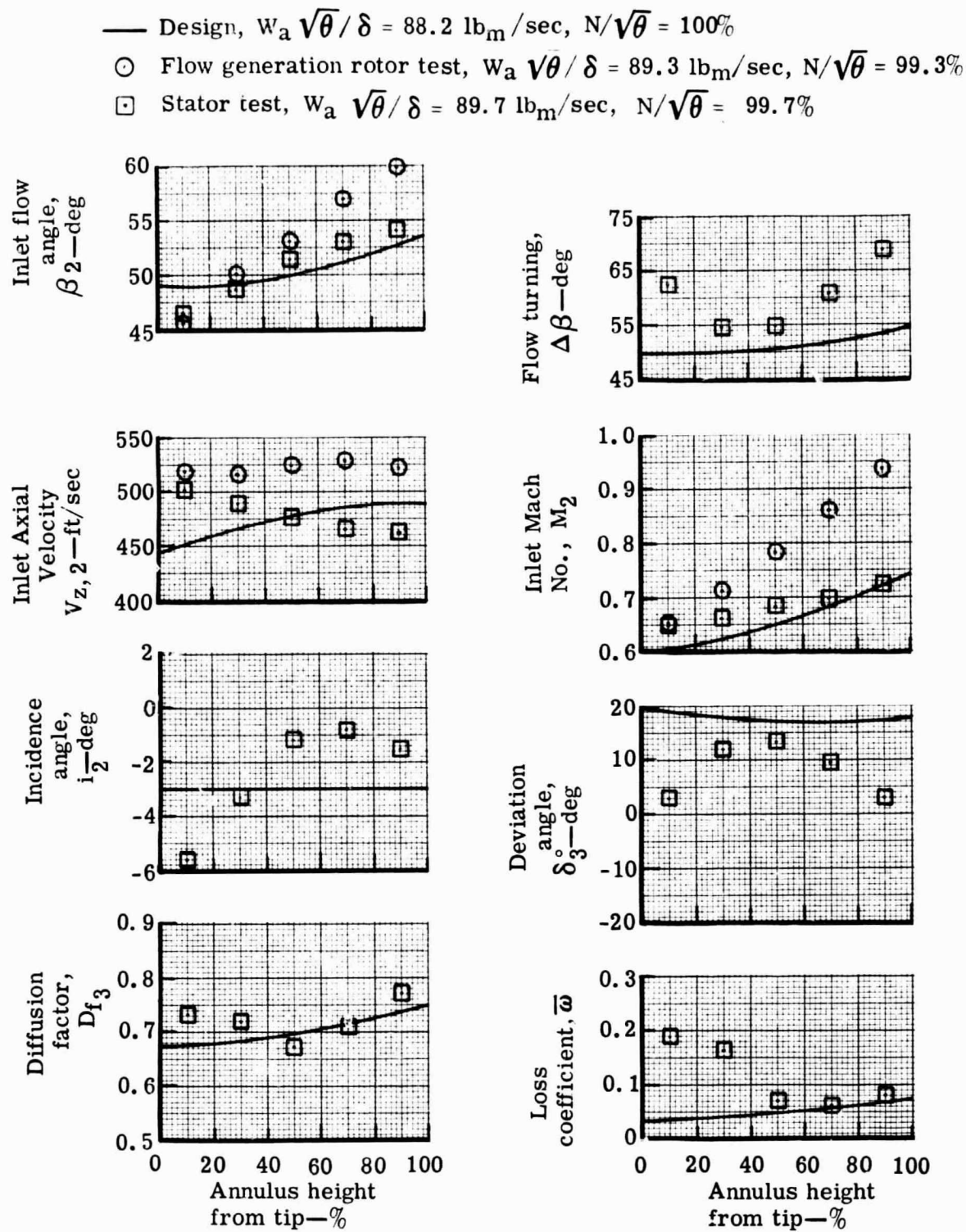
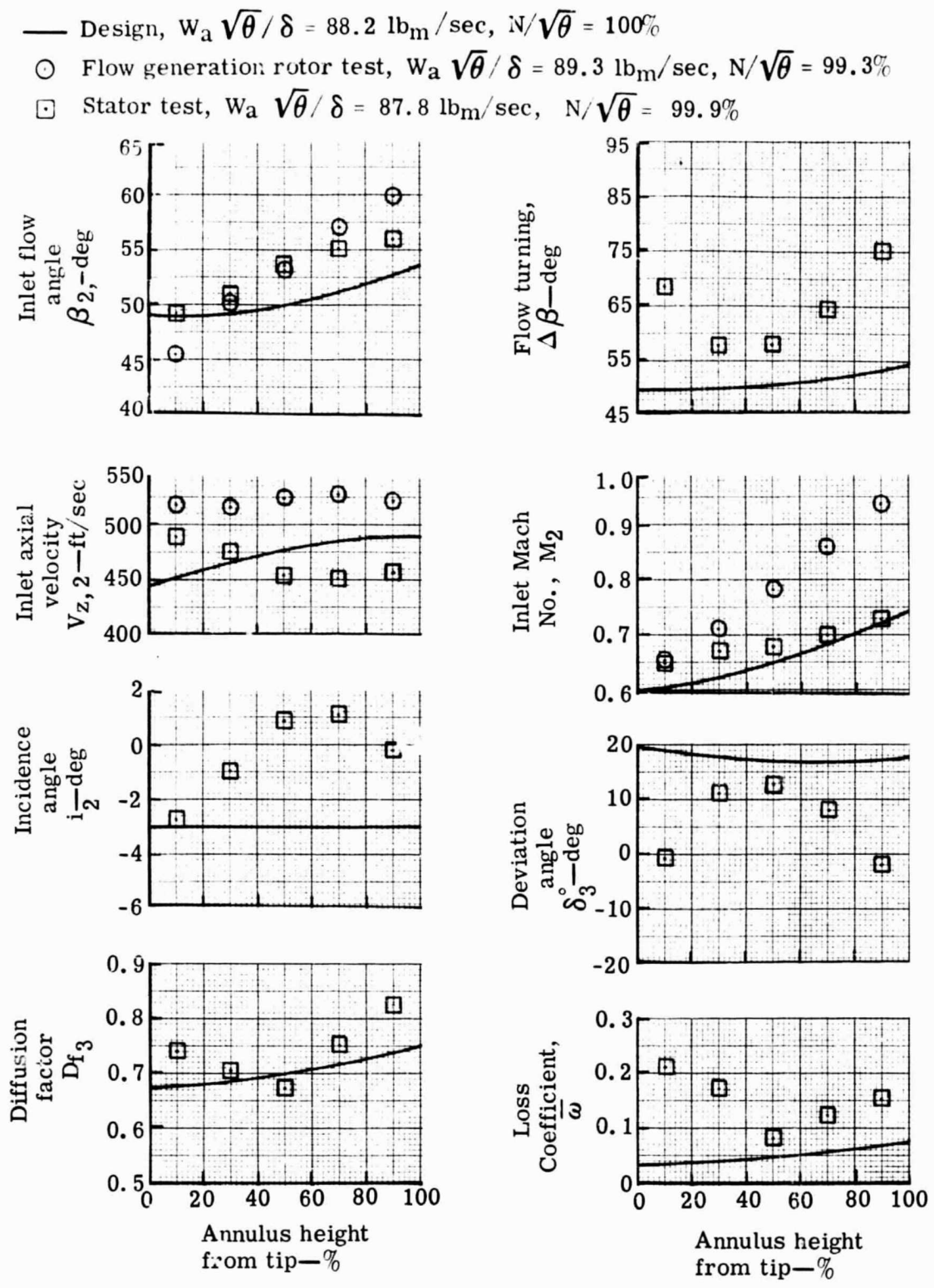


Figure 21. Variation of wall bleed flows with stage pressure ratio.



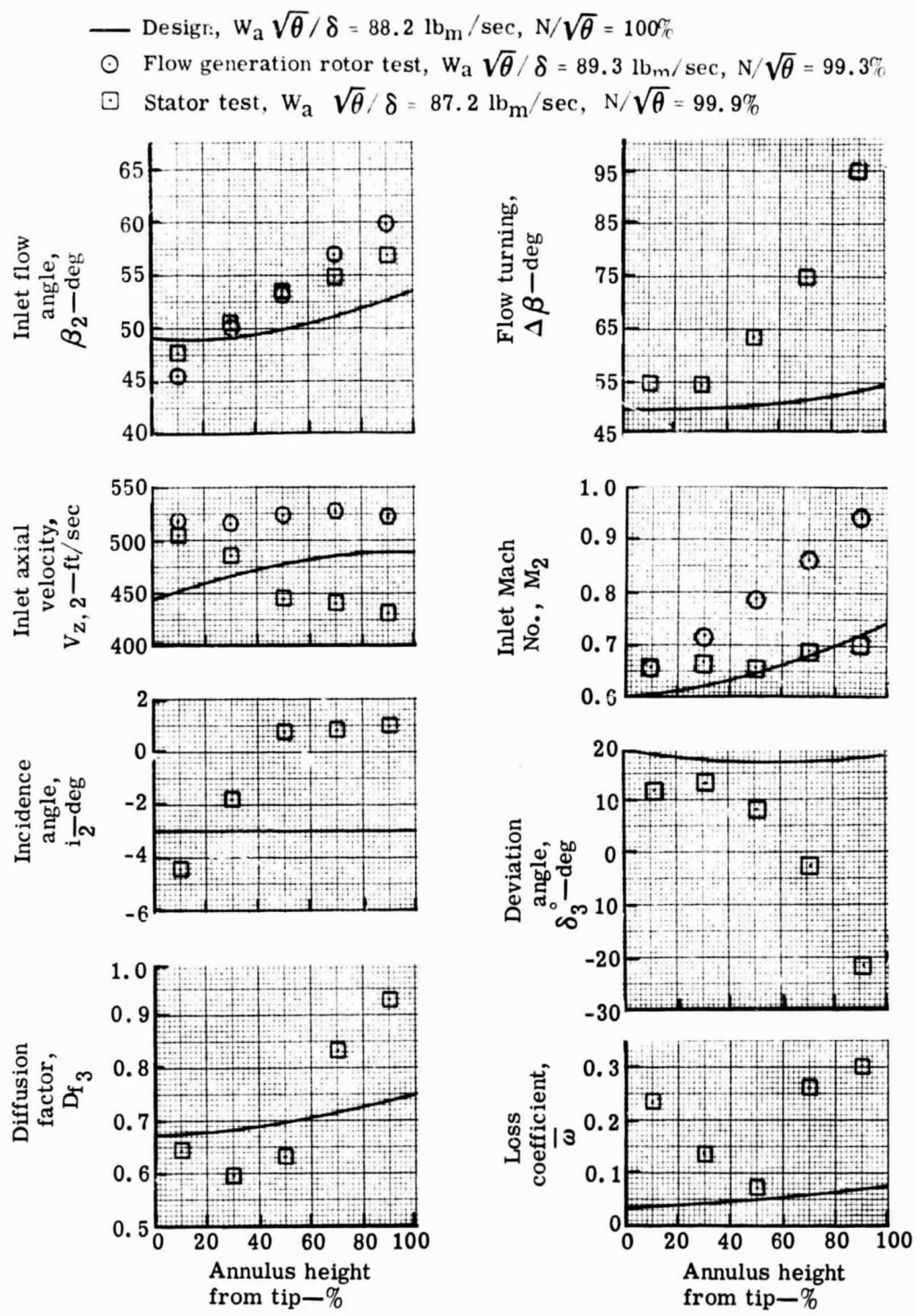
5863-39

Figure 22. Radial variation of 0.75 D_f stator blade element performance with optimum wall bleed.



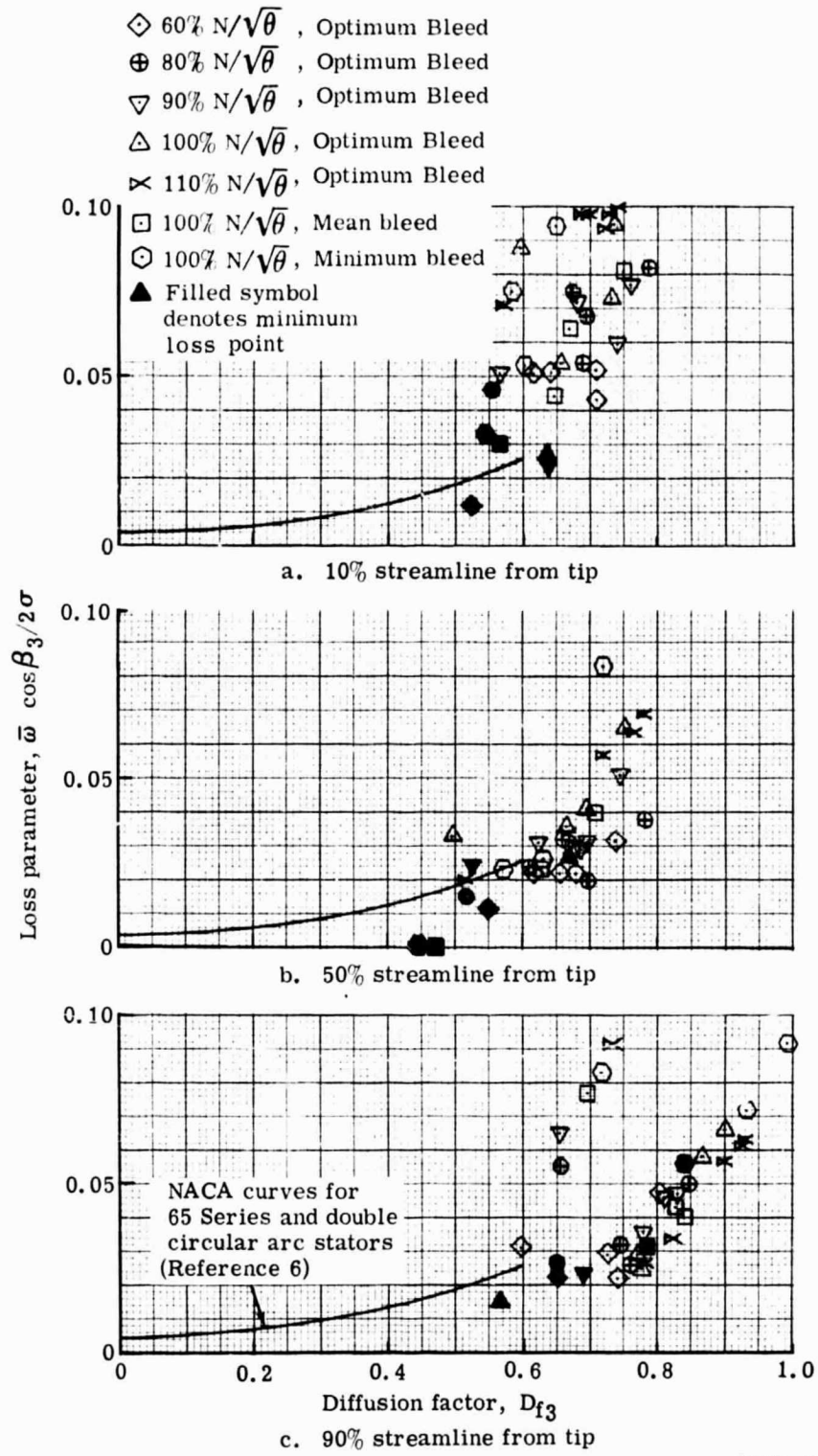
5863-40

Figure 23. Radial variation of $0.75 D_f$ stator blade element performance with mean wall bleed.



5863-41

Figure 24. Radial variation of 0.75 D_f stator blade element performance with minimum wall bleed.



5863-42

Figure 25. Stator loss parameter versus diffusion factor.

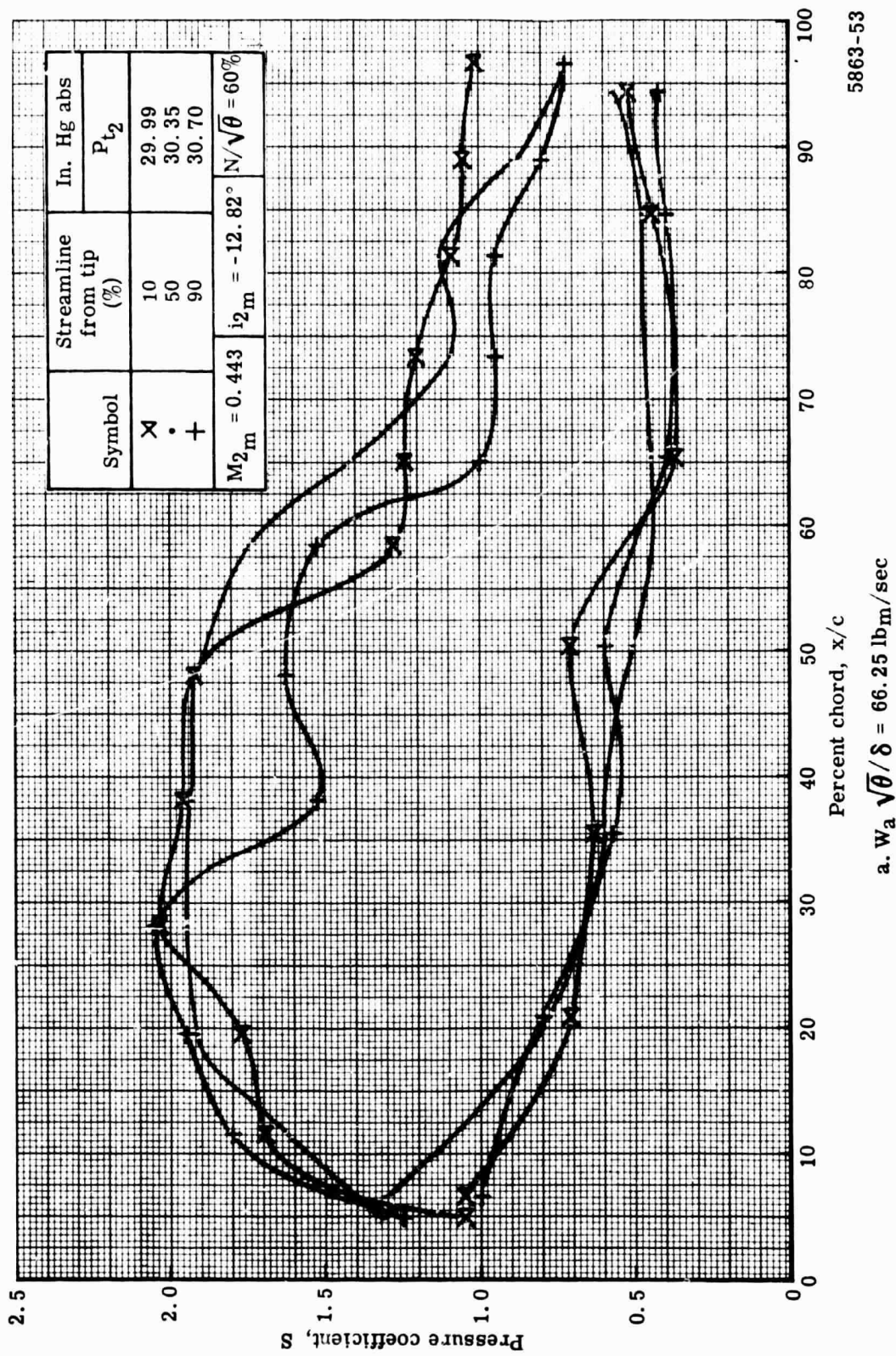


Figure 26. Stator static pressure distribution at 60% speed with optimum wall bleed.

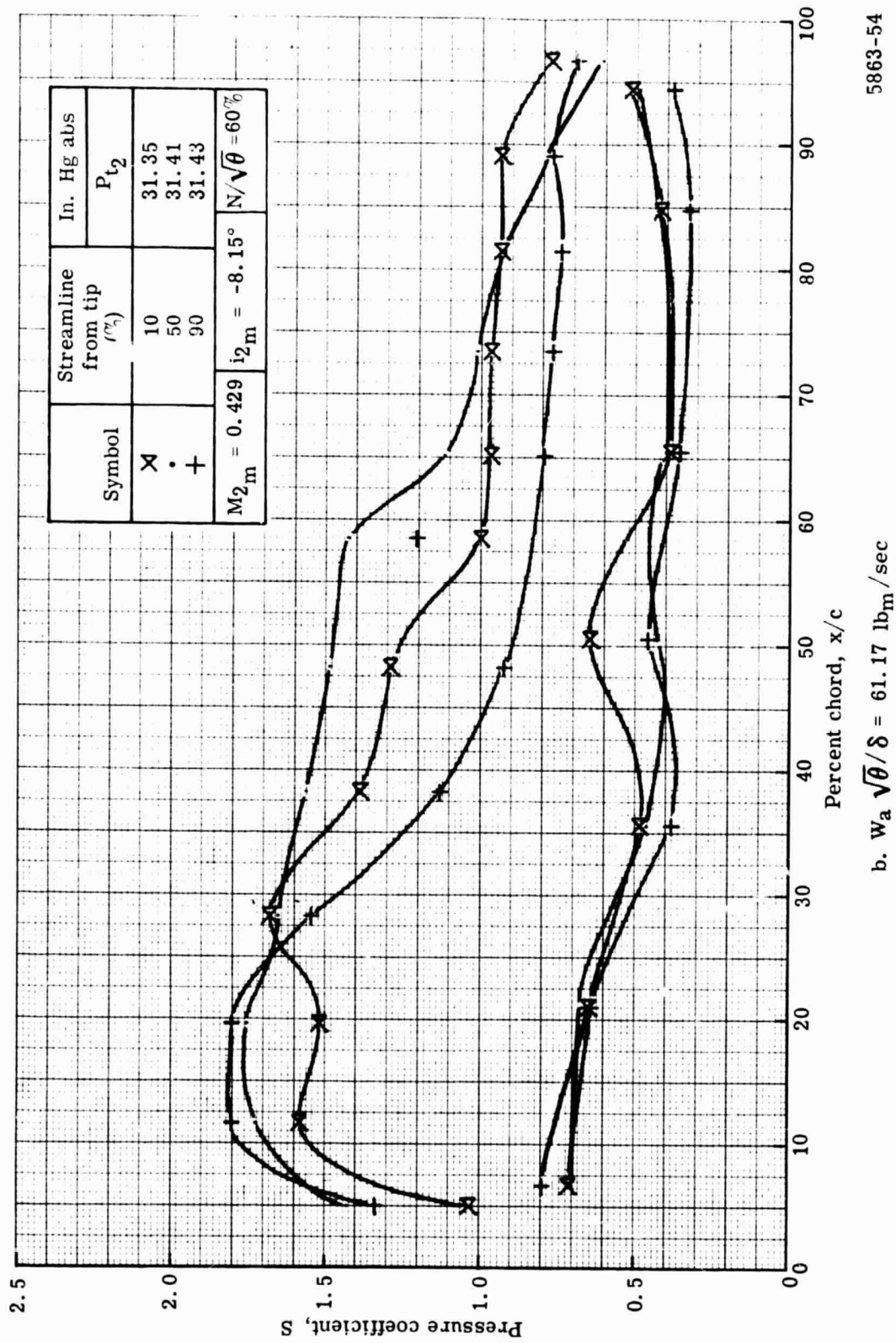


Figure 26. Stator static pressure distribution at 60% speed with optimum wall bleed.

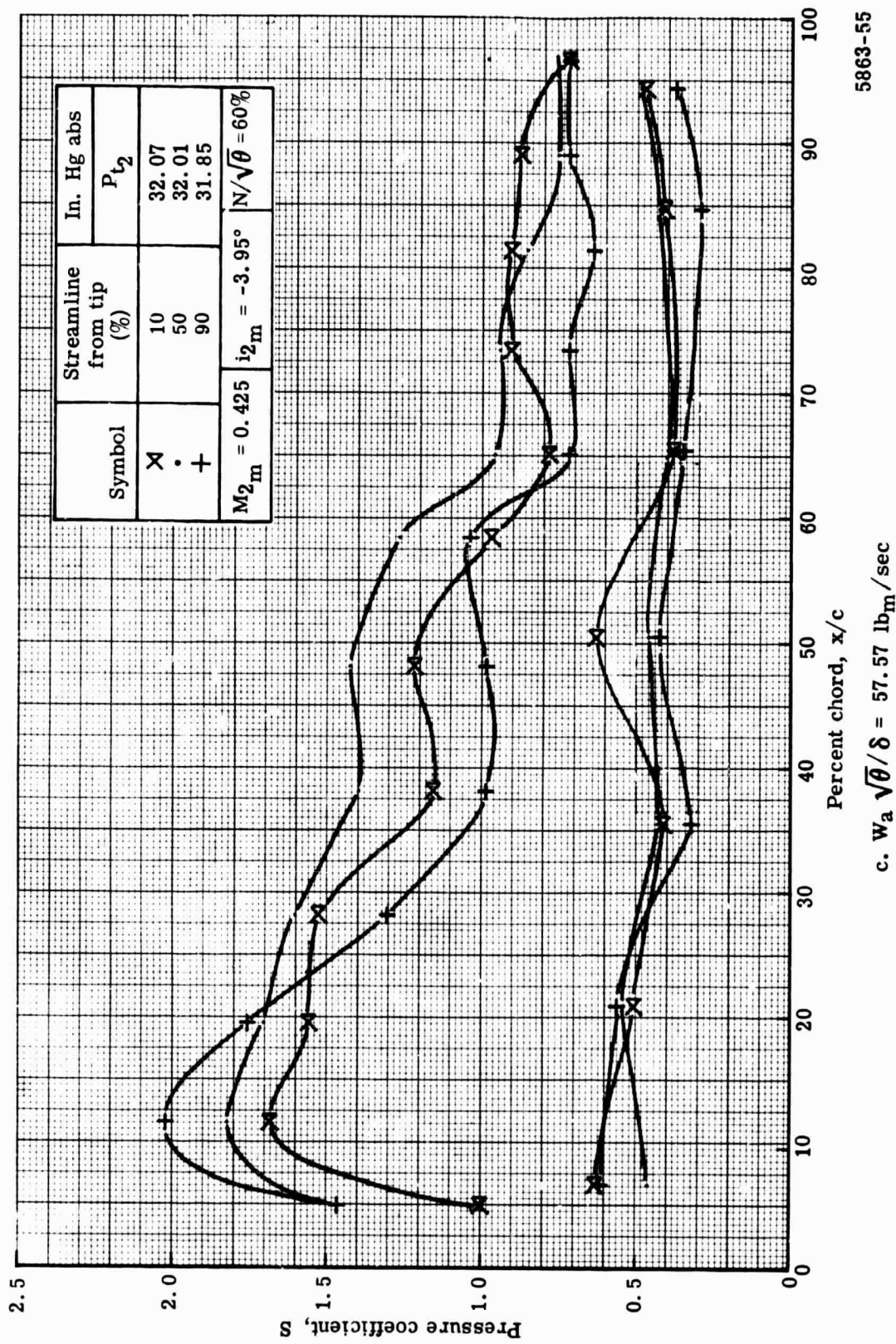


Figure 26. Stator static pressure distribution at 60% speed with optimum wall bleed.

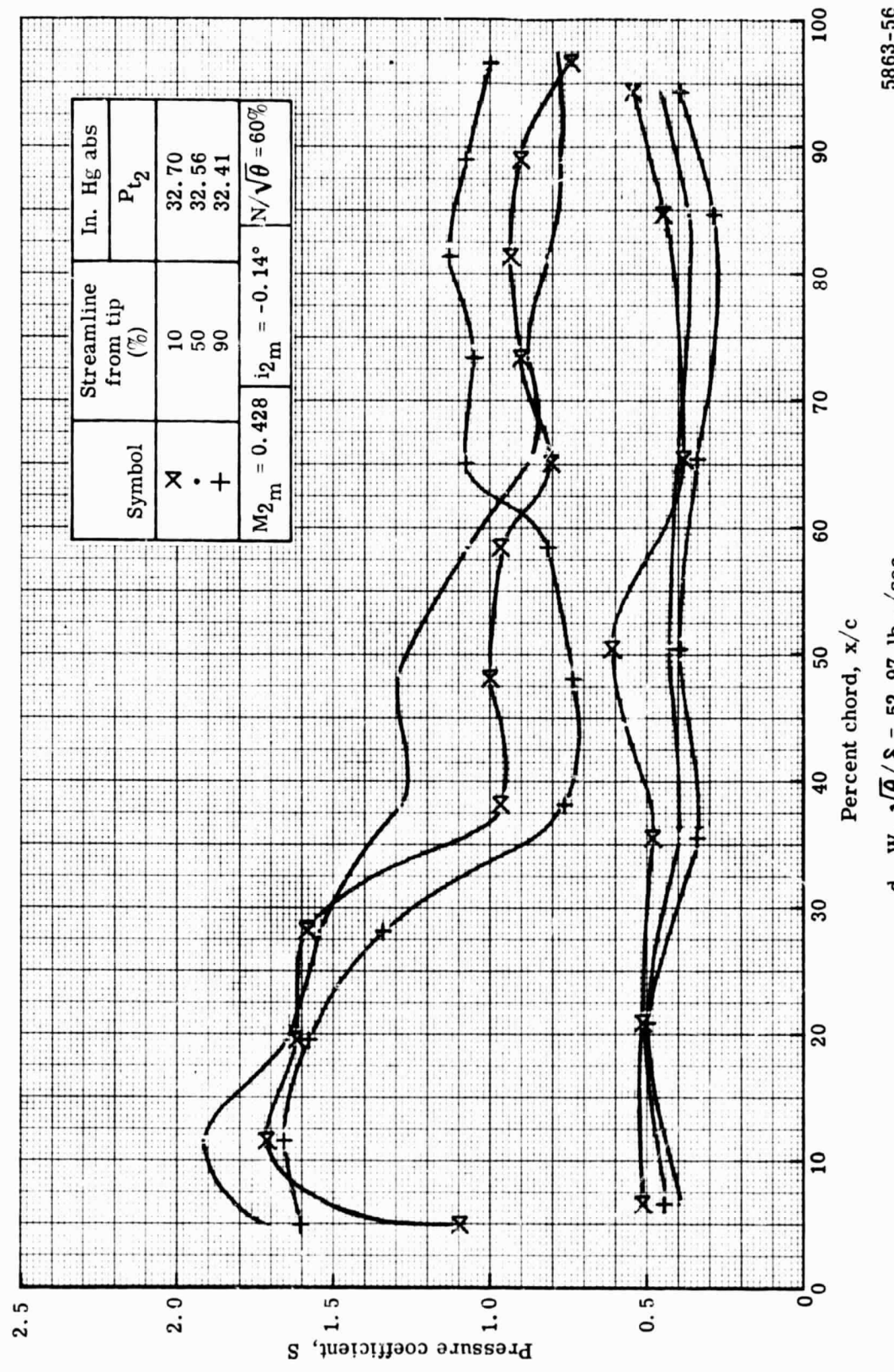


Figure 26. Stator static pressure distribution at 60% speed with optimum wall bleed.

d. $w_a \sqrt{\theta}/\delta = 52.97 \text{ lb}_m/\text{sec}$

5863-56

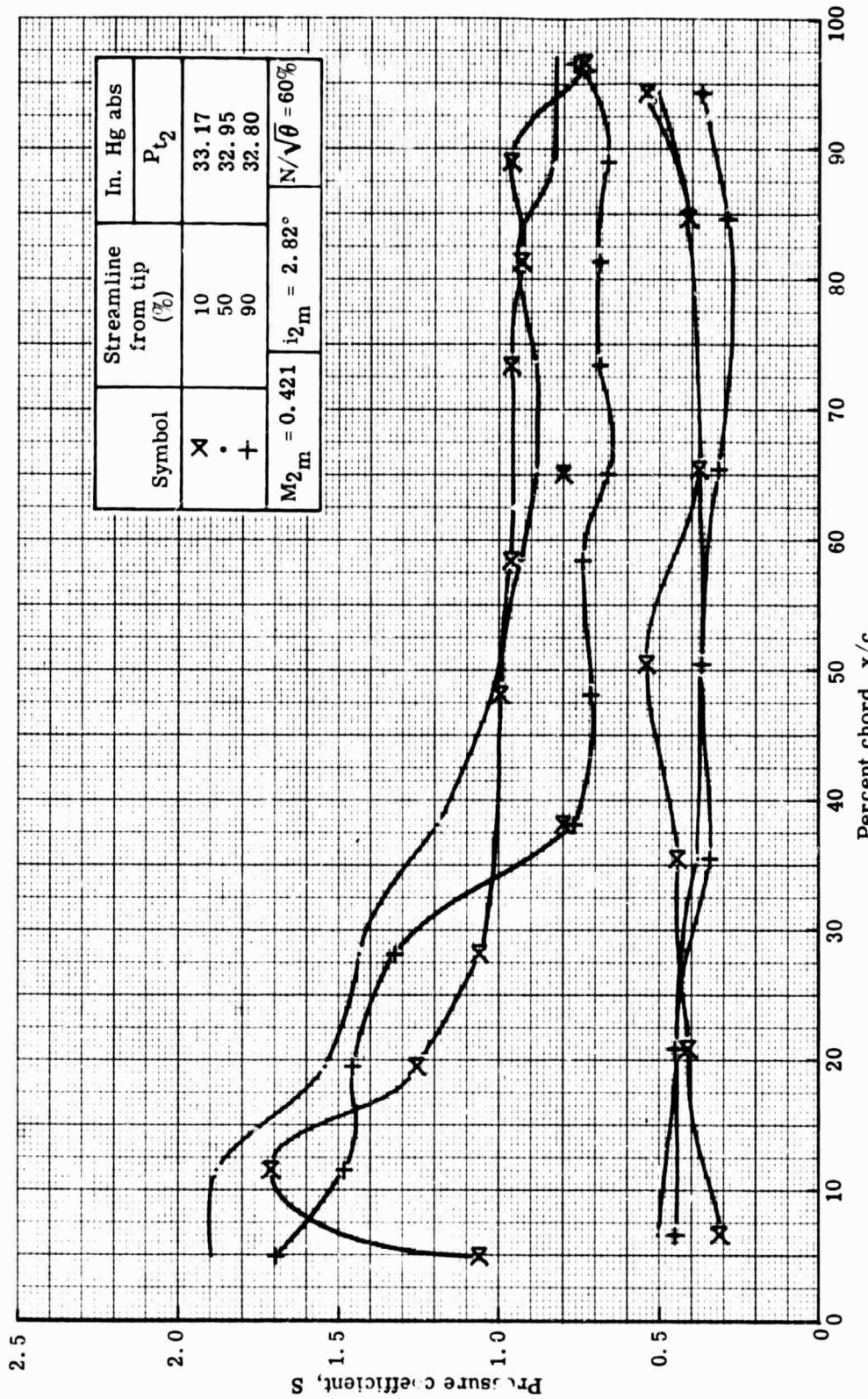


Figure 26. Stator static pressure distribution at 60% speed with optimum wall bleed.

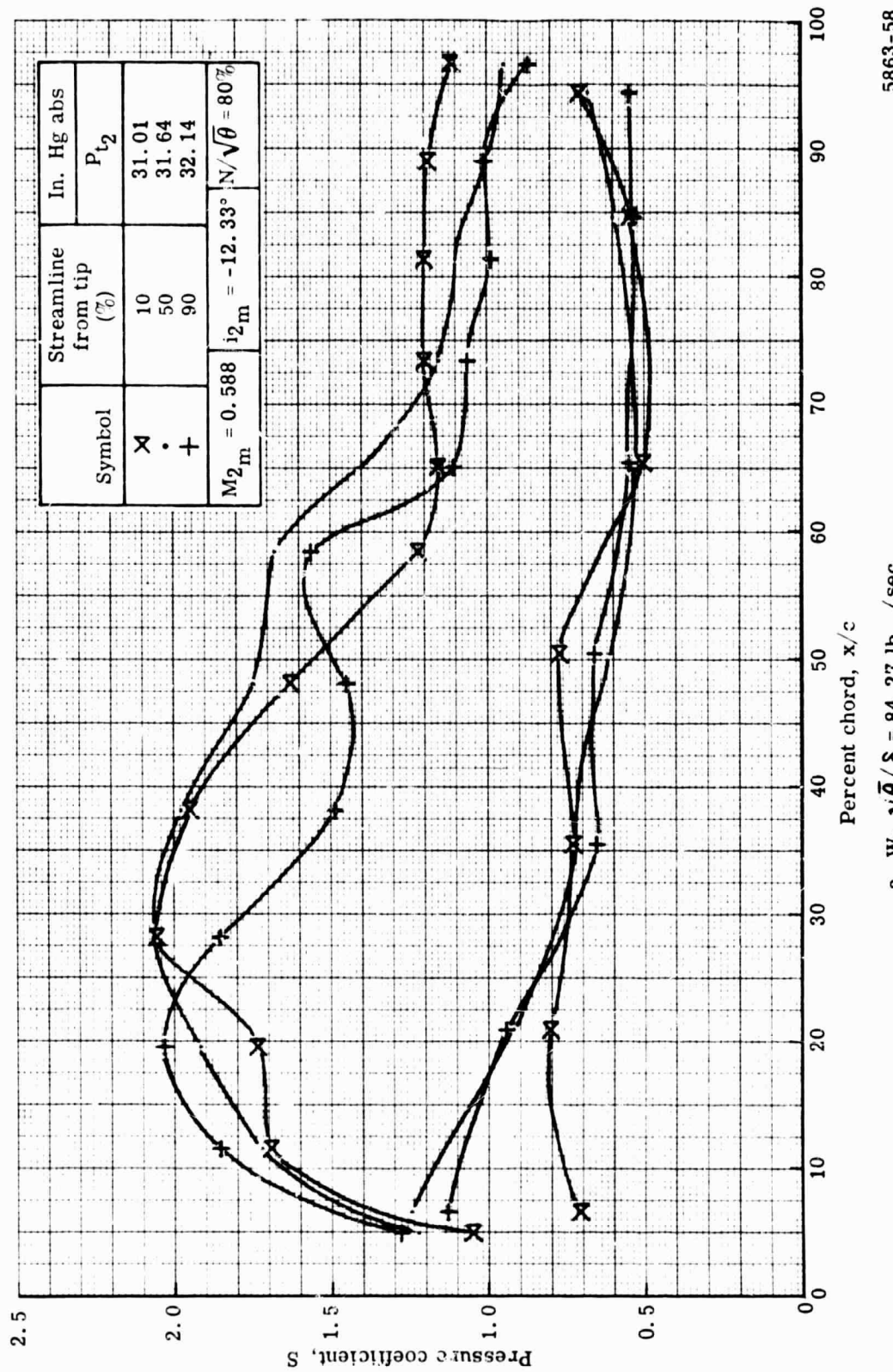


Figure 27. Stator static pressure distribution at 80% speed with optimum wall bleed.

2.5

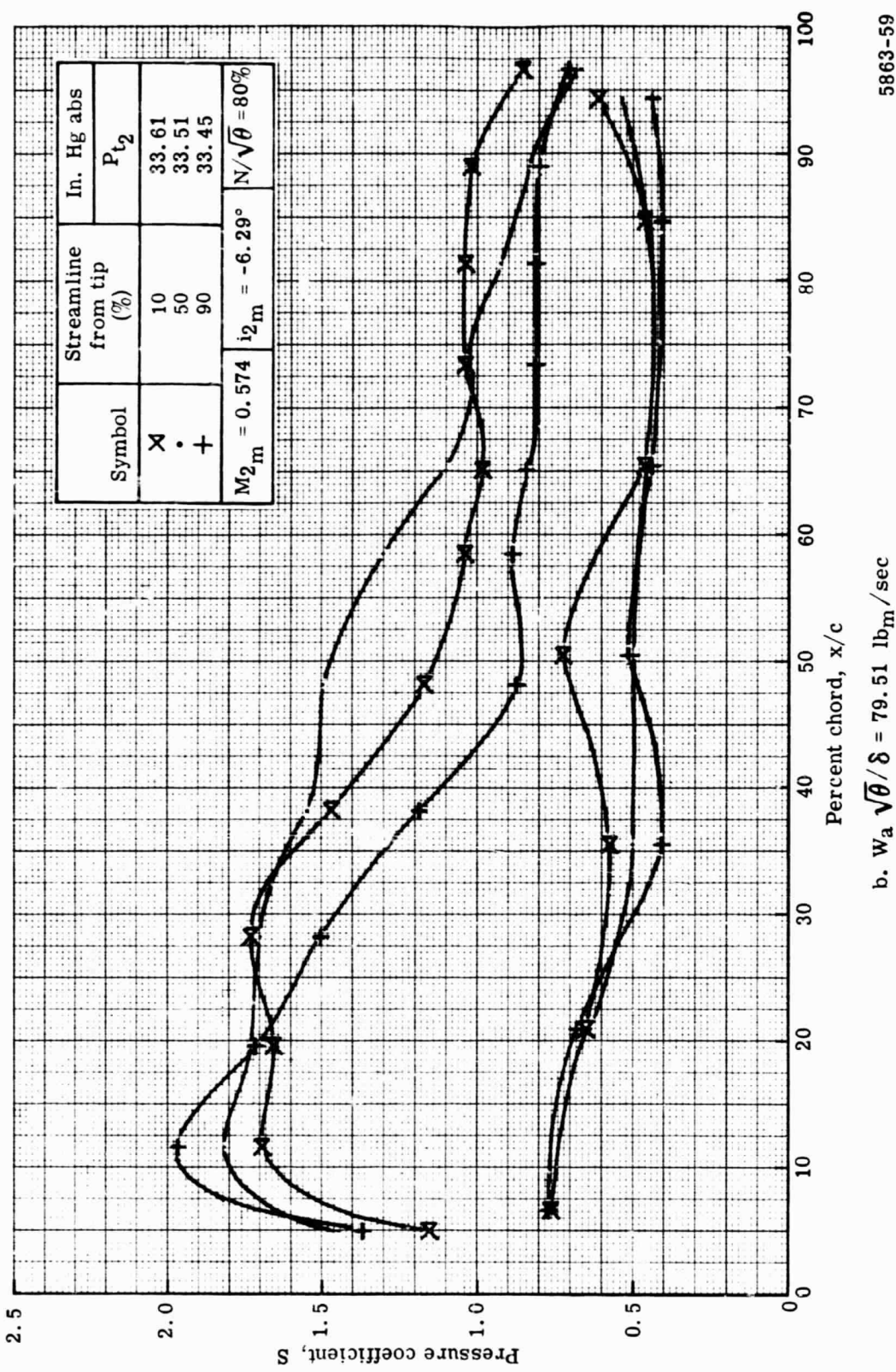


Figure 27. Stator static pressure distribution at 80% speed with optimum wall bleed.

5863-59

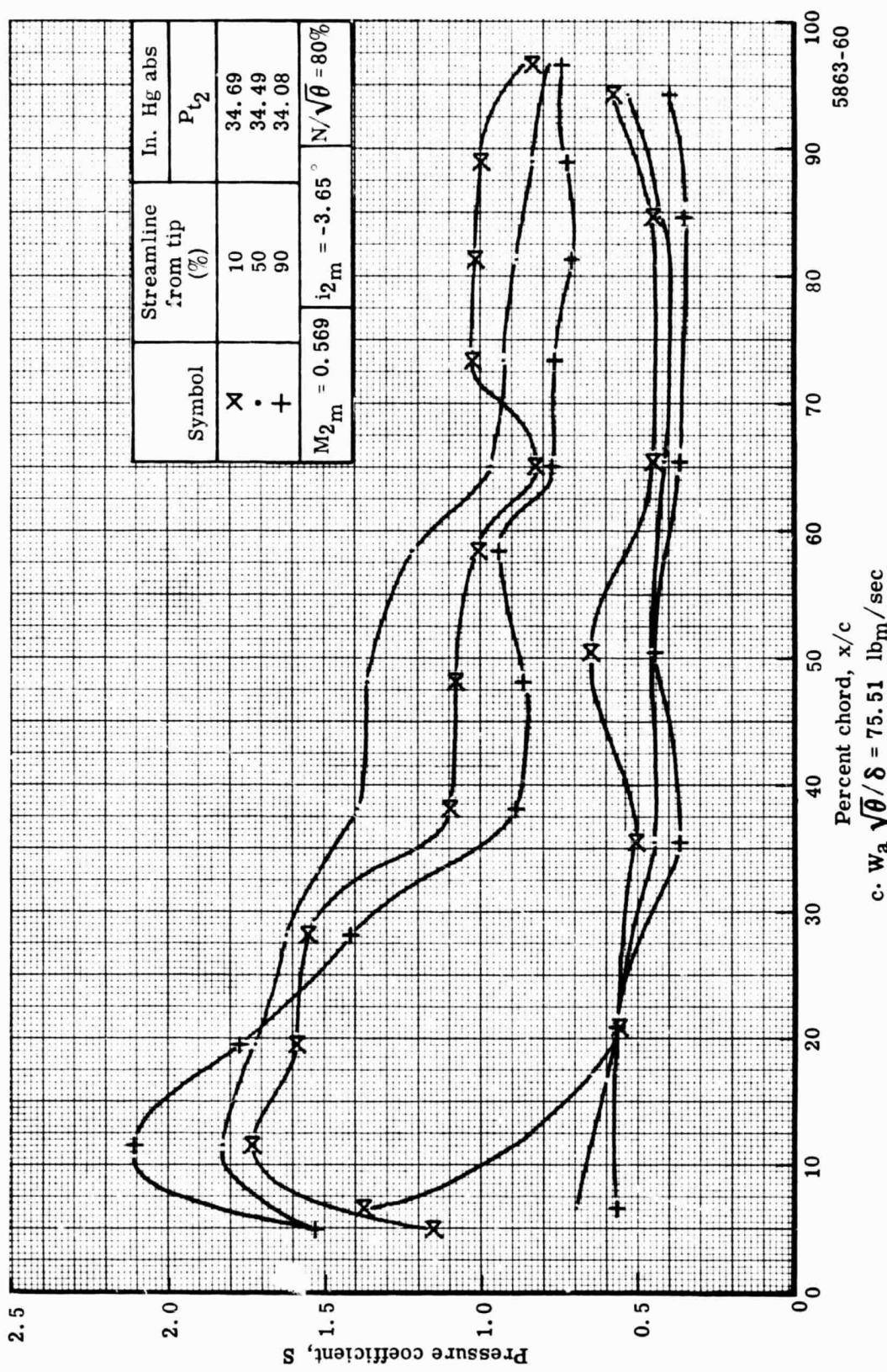


Figure 27. Stator static pressure distribution at 80% speed with optimum wall bleed.

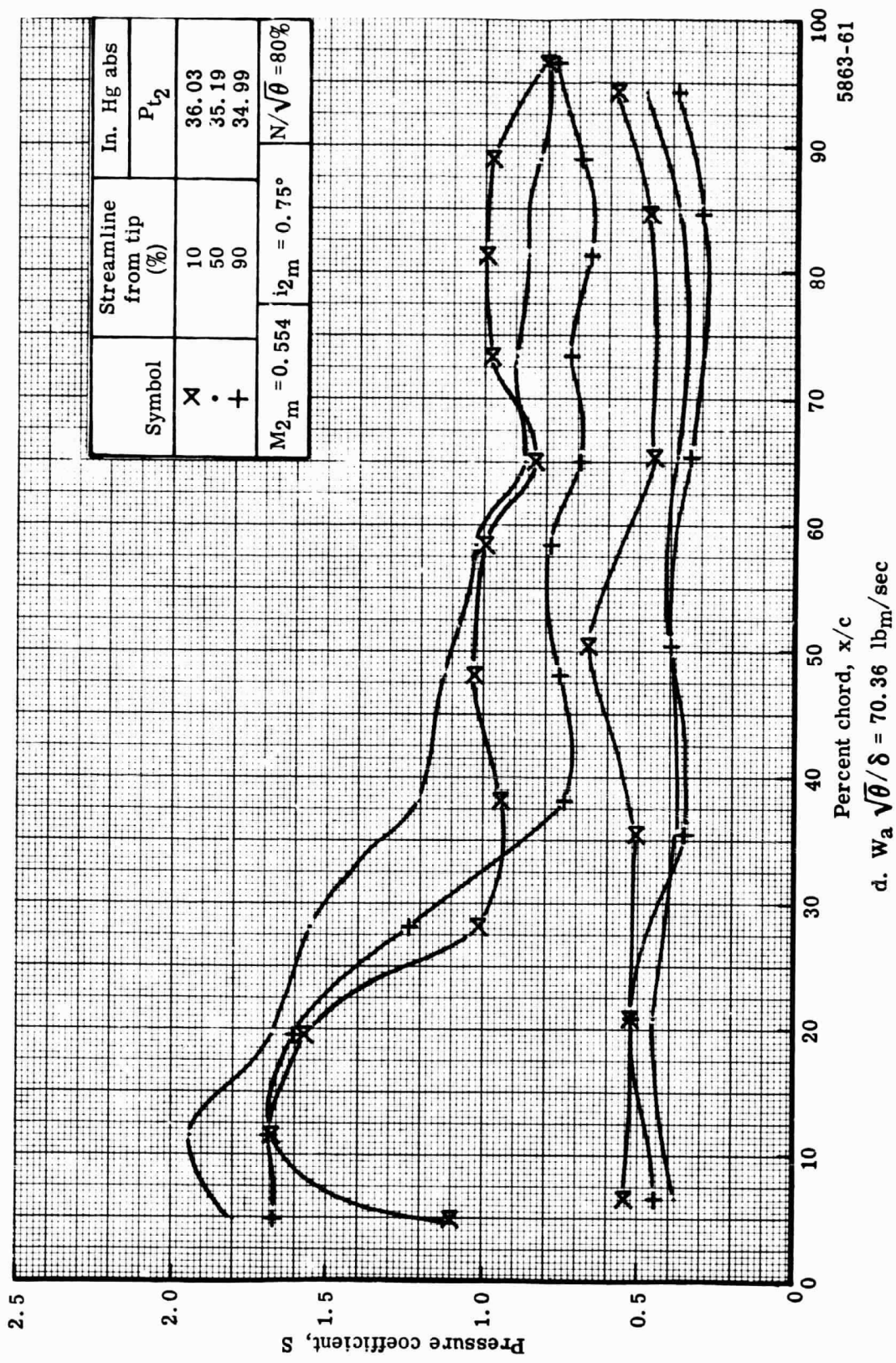


Figure 27. Stator static pressure distribution at 80% speed with optimum wall bleed.

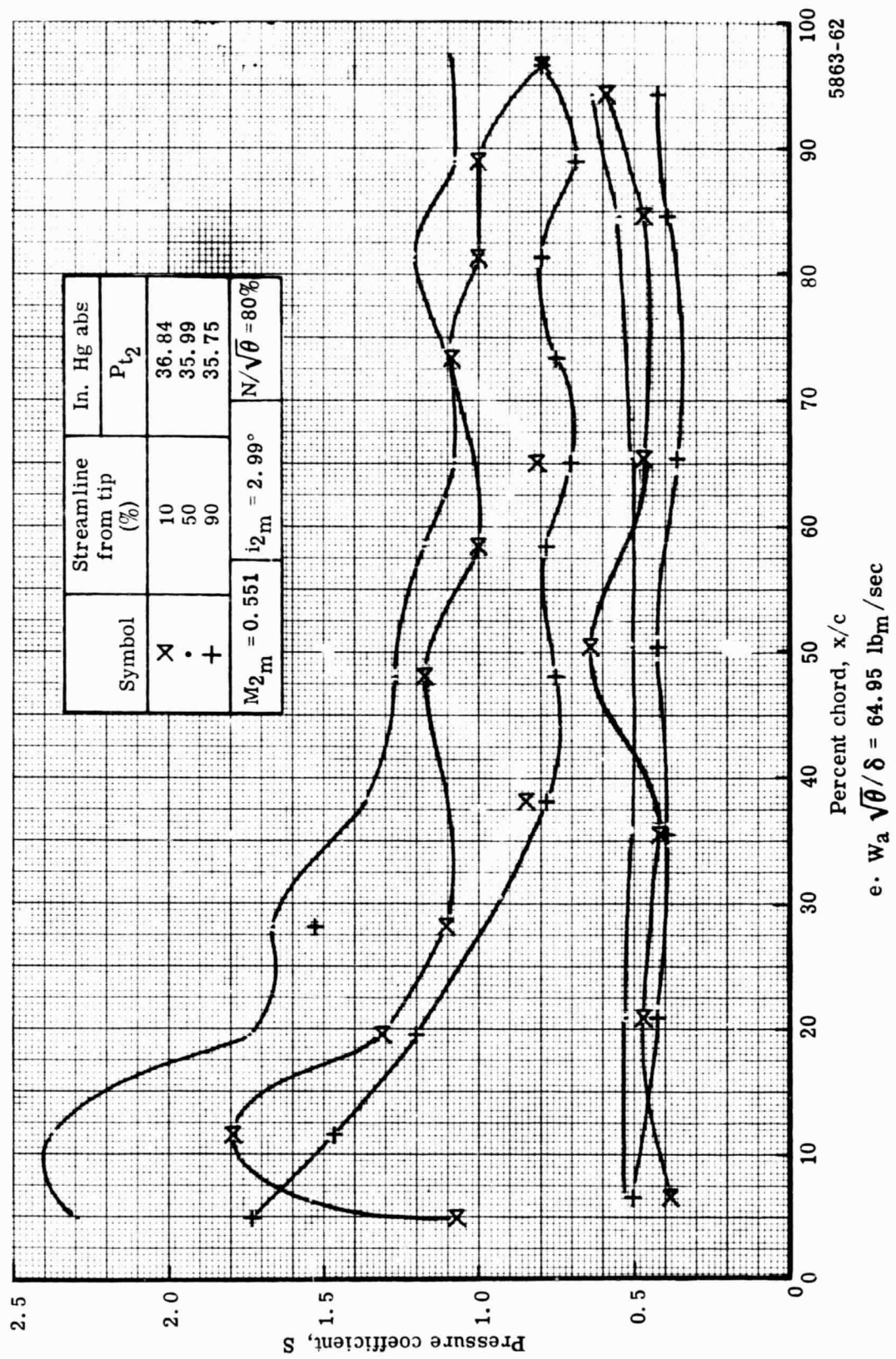


Figure 27. Stator static pressure distribution at 80% speed with optimum wall bleed.

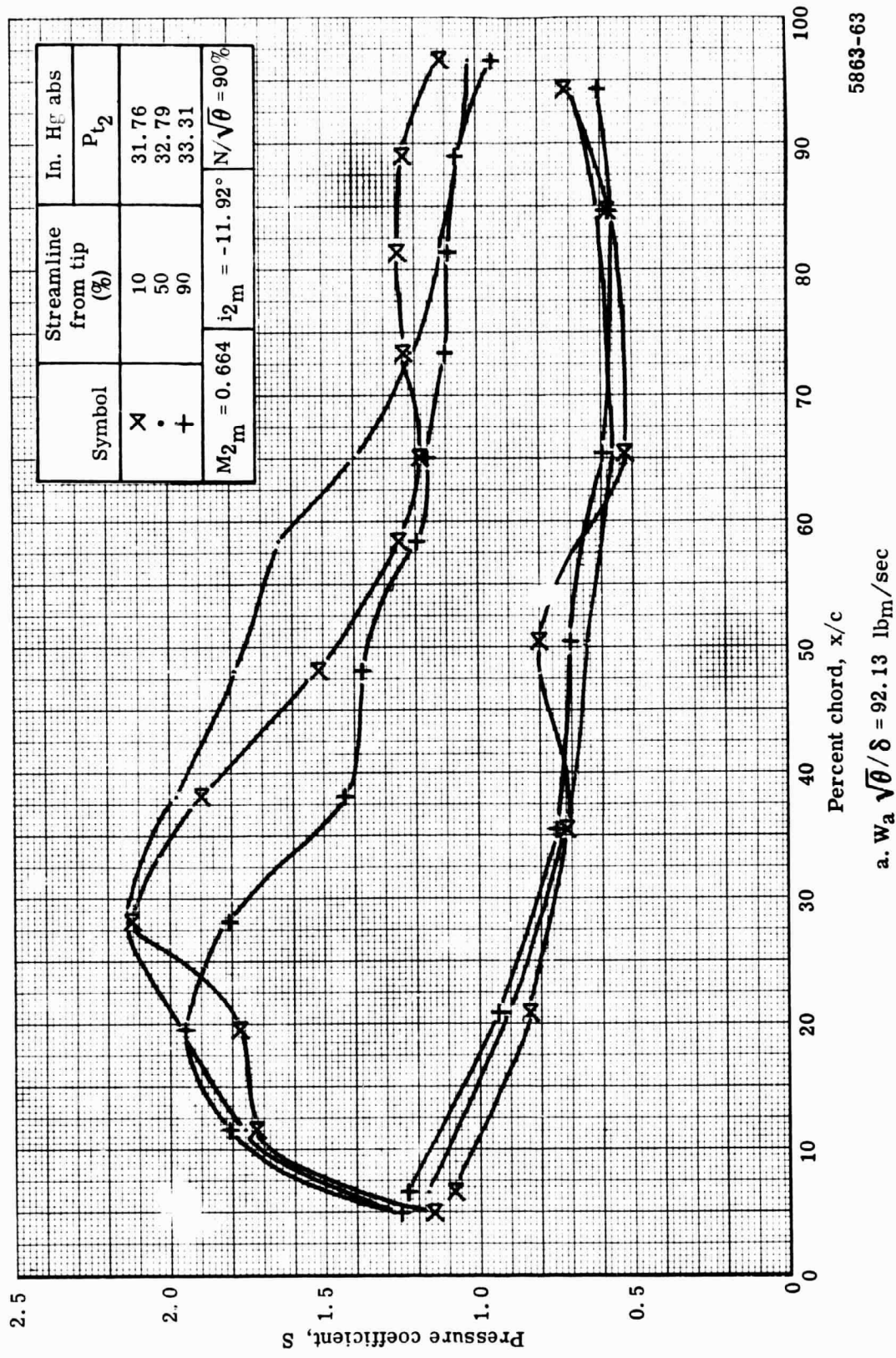


Figure 28. Stator static pressure distribution at 90% speed with optimum wall bleed.

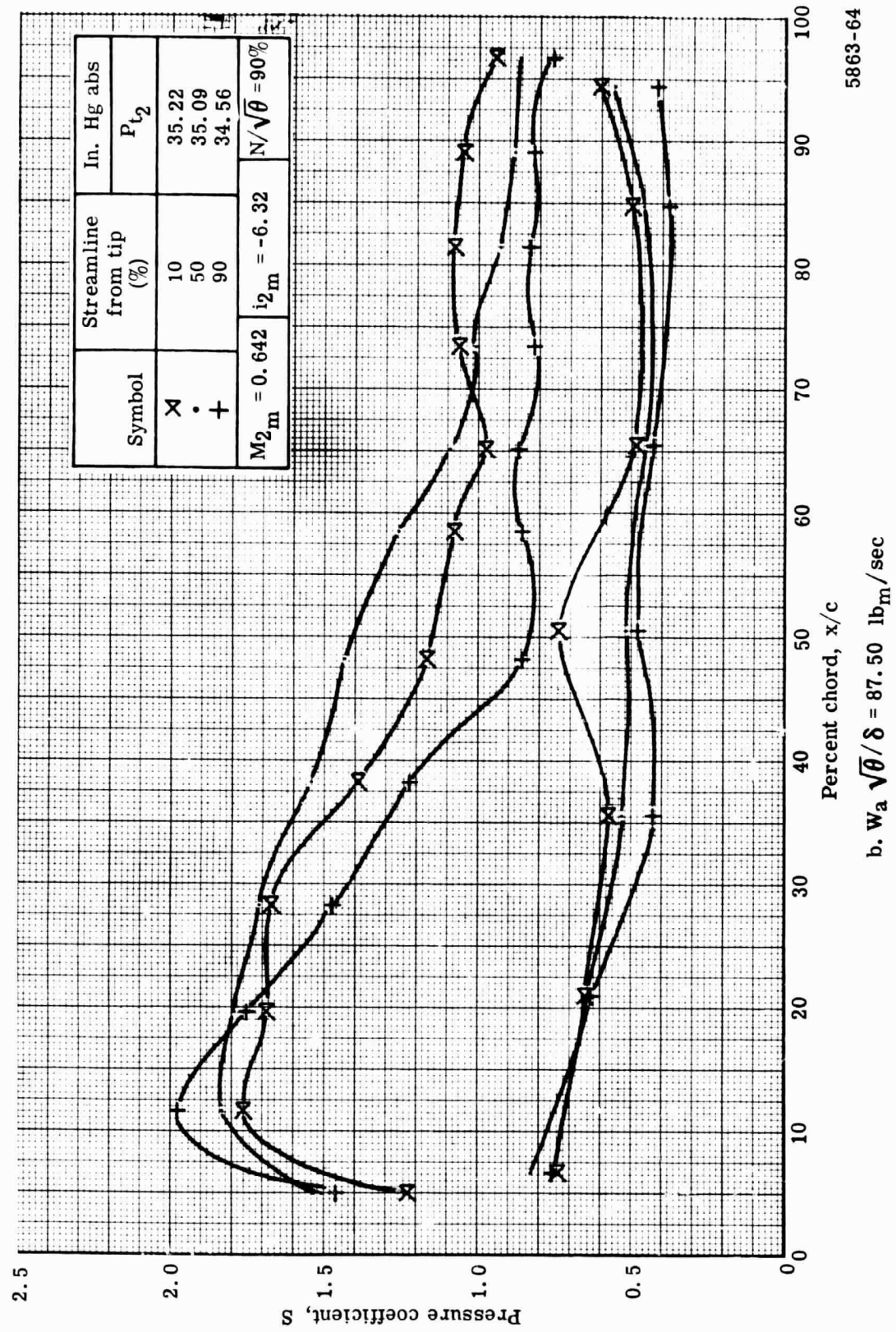


Figure 28. Stator static pressure distribution at 90% speed with optimum wall bleed.

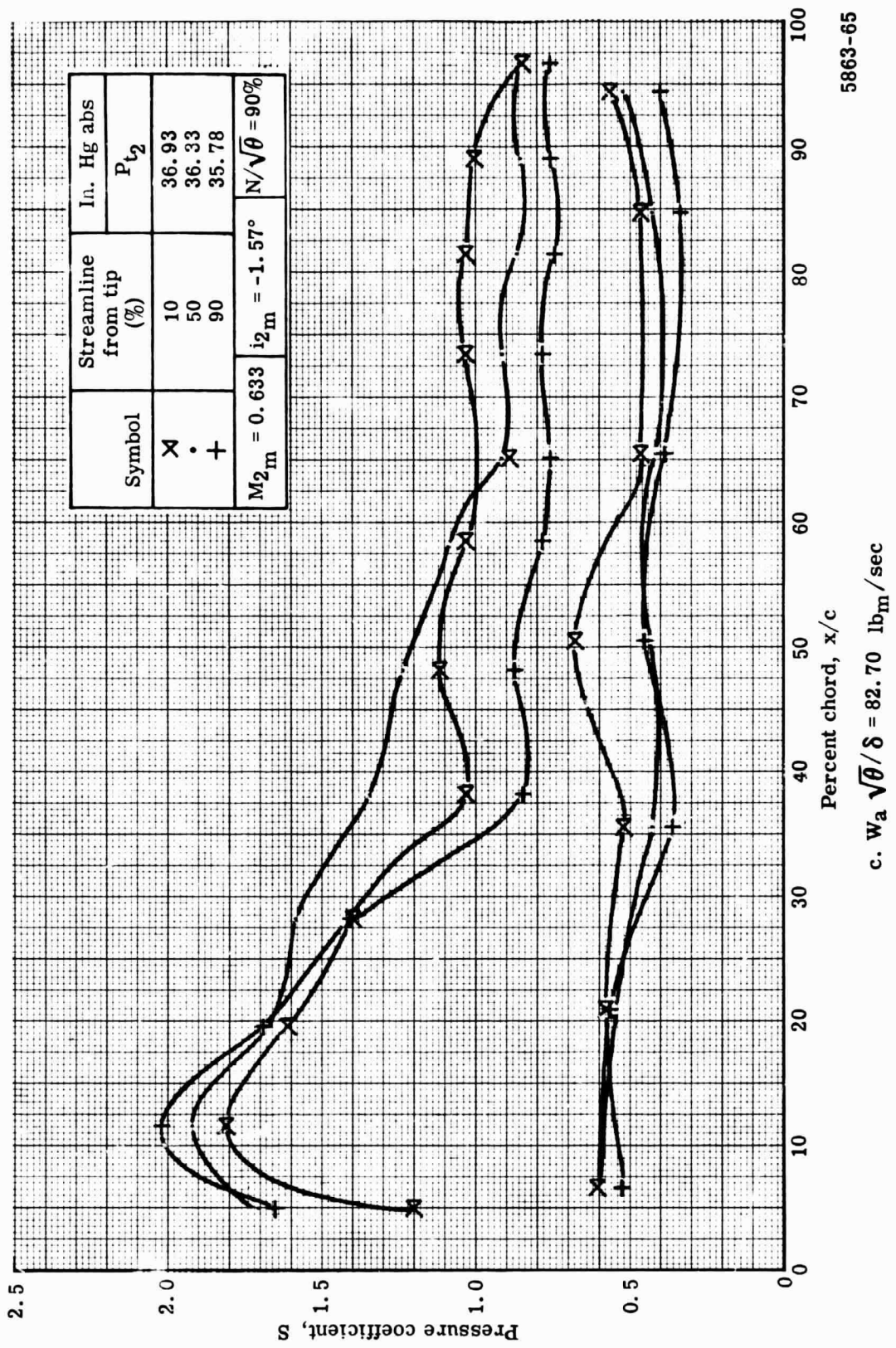


Figure 28. Stator static pressure distribution at 90% speed with optimum wall bleed.

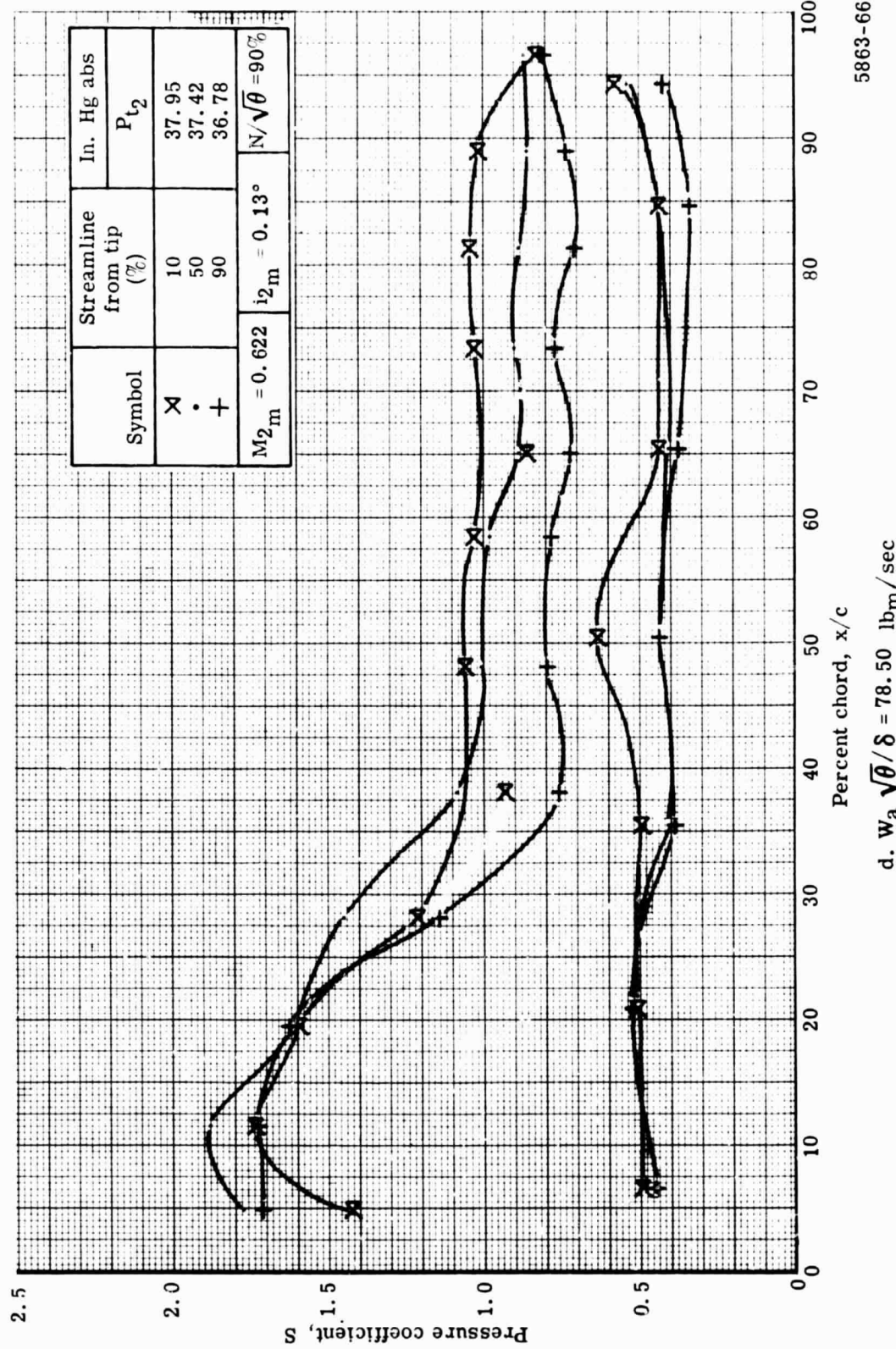


Figure 28. Stator static pressure distribution at 90% speed with optimum wall bleed.

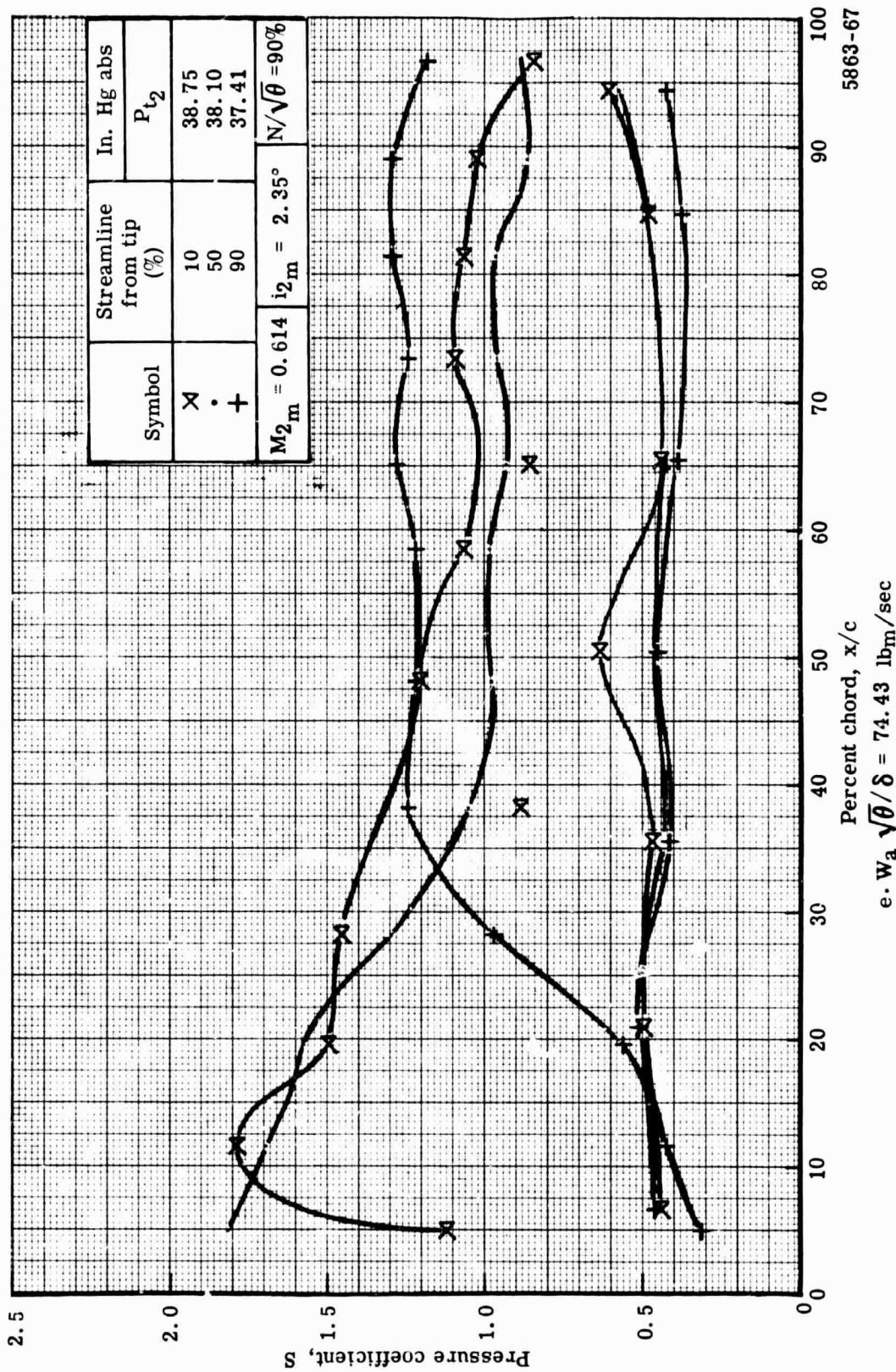


Figure 28. Stator static pressure distribution at 90% speed with optimum wall bleed.

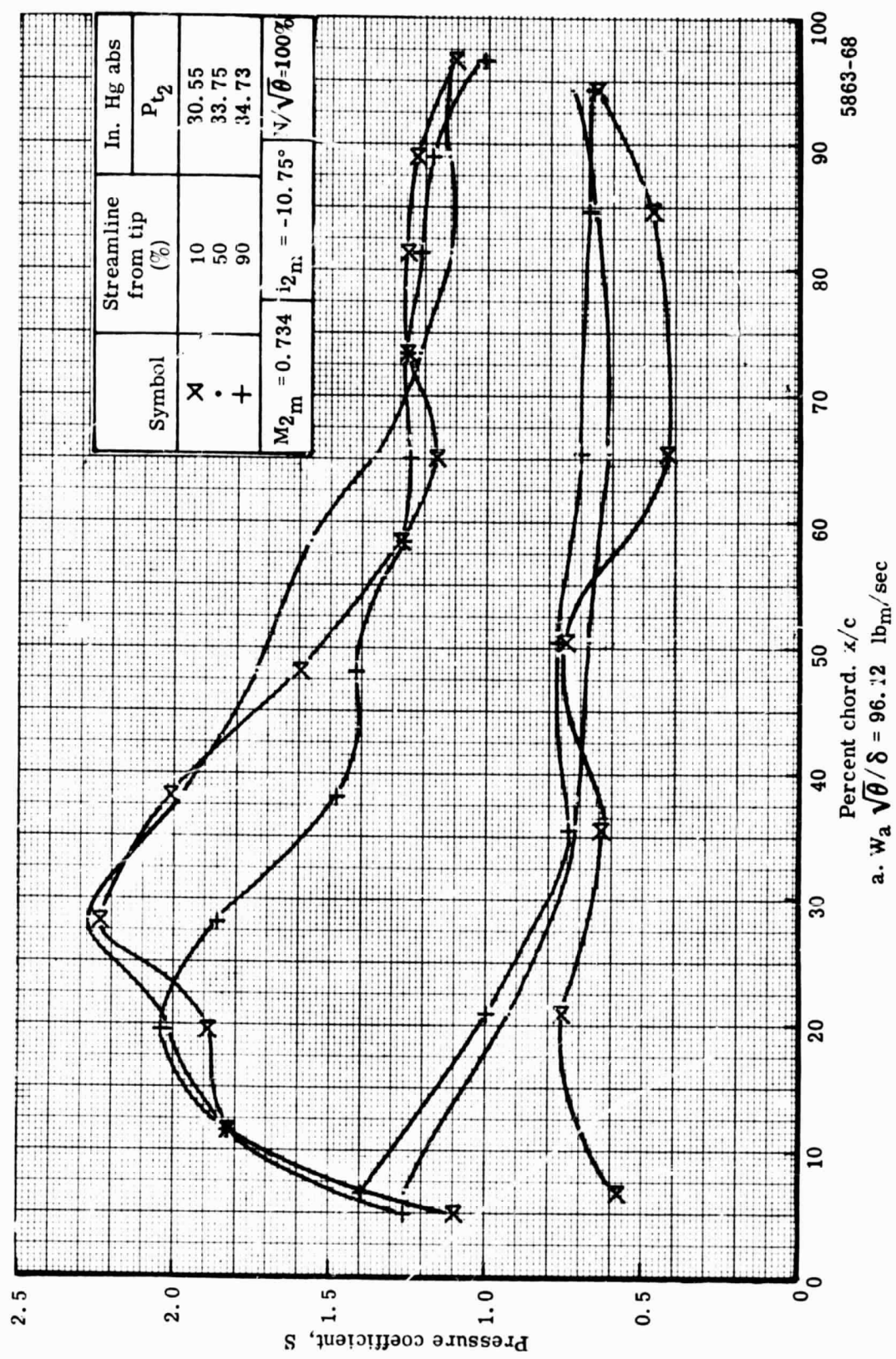


Figure 29. Stator static pressure distribution at 100% speed with optimum wall bleed.

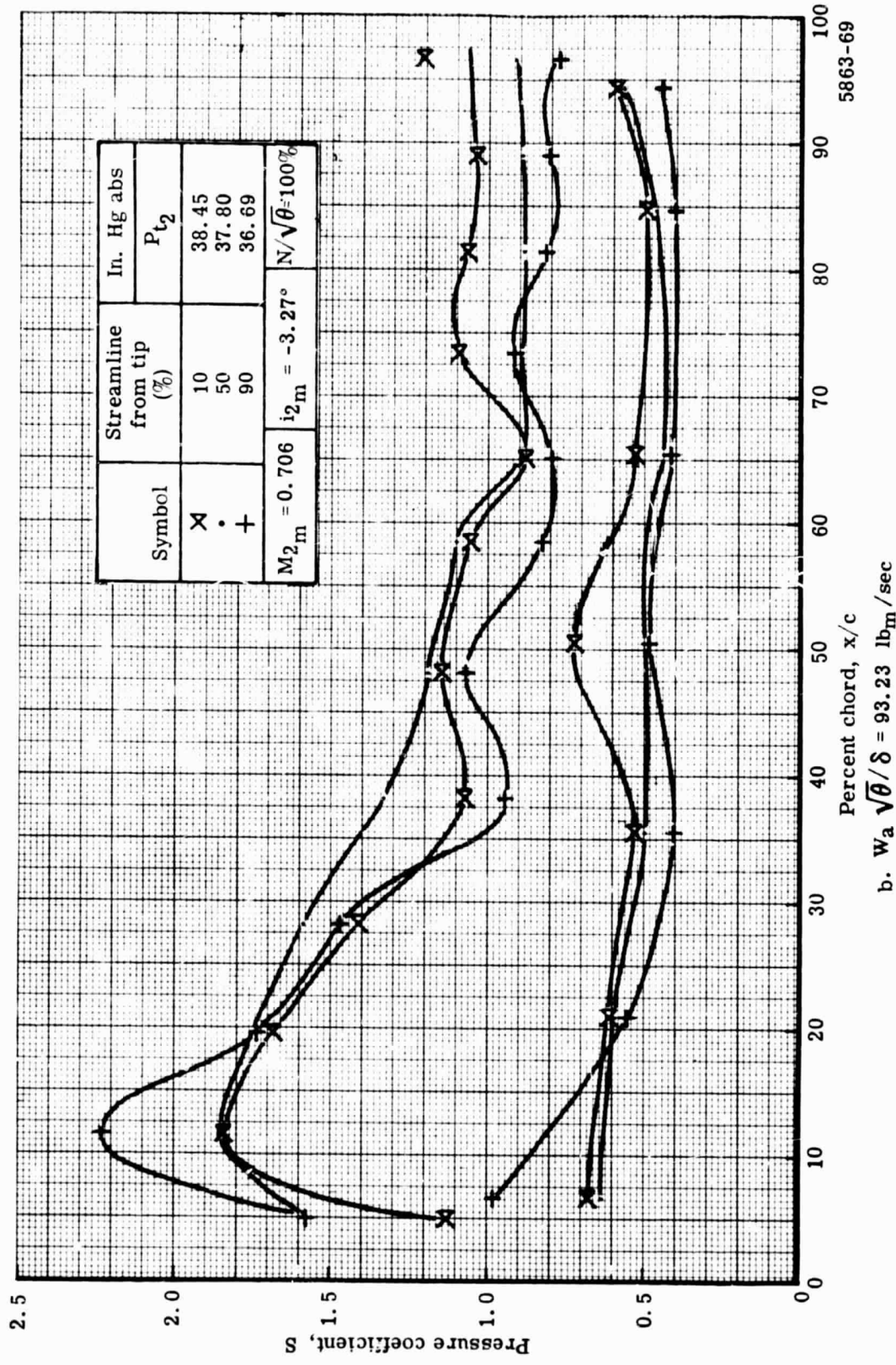


Figure 29. Stator static pressure distribution at 100% speed with optimum wall bleed.

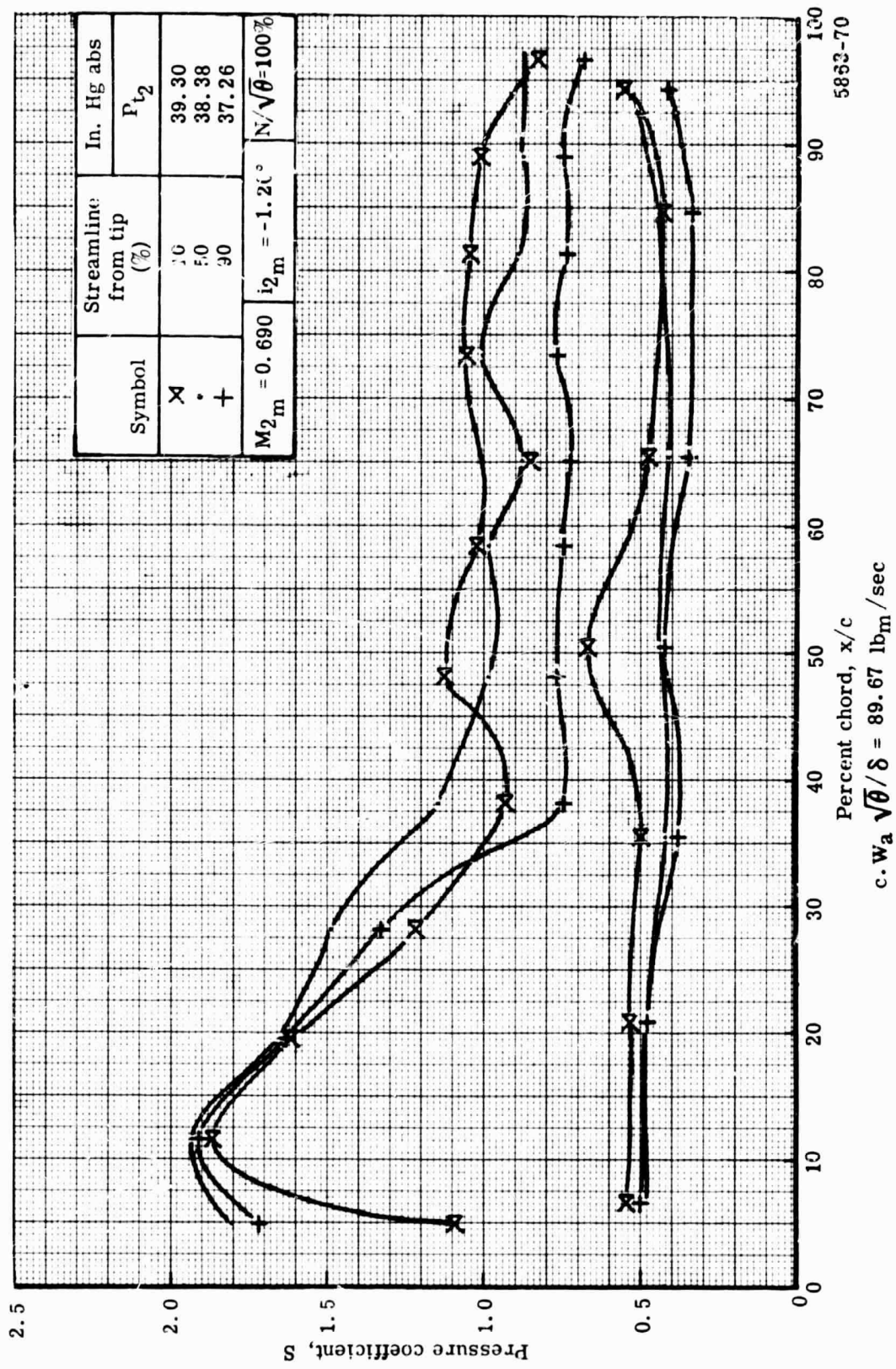


Figure 29. Stator static pressure distribution at 100% speed with optimum wall bleed.

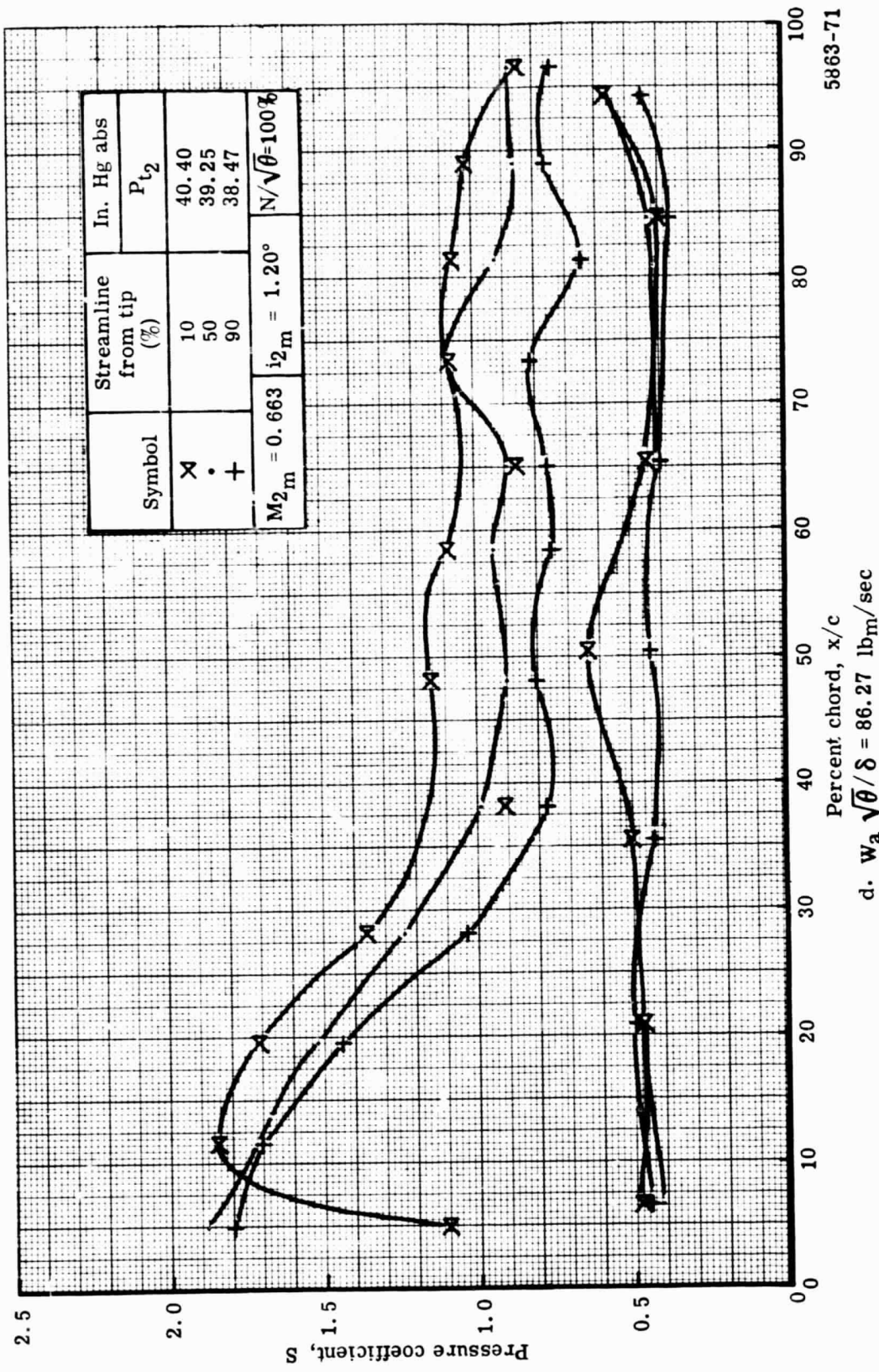
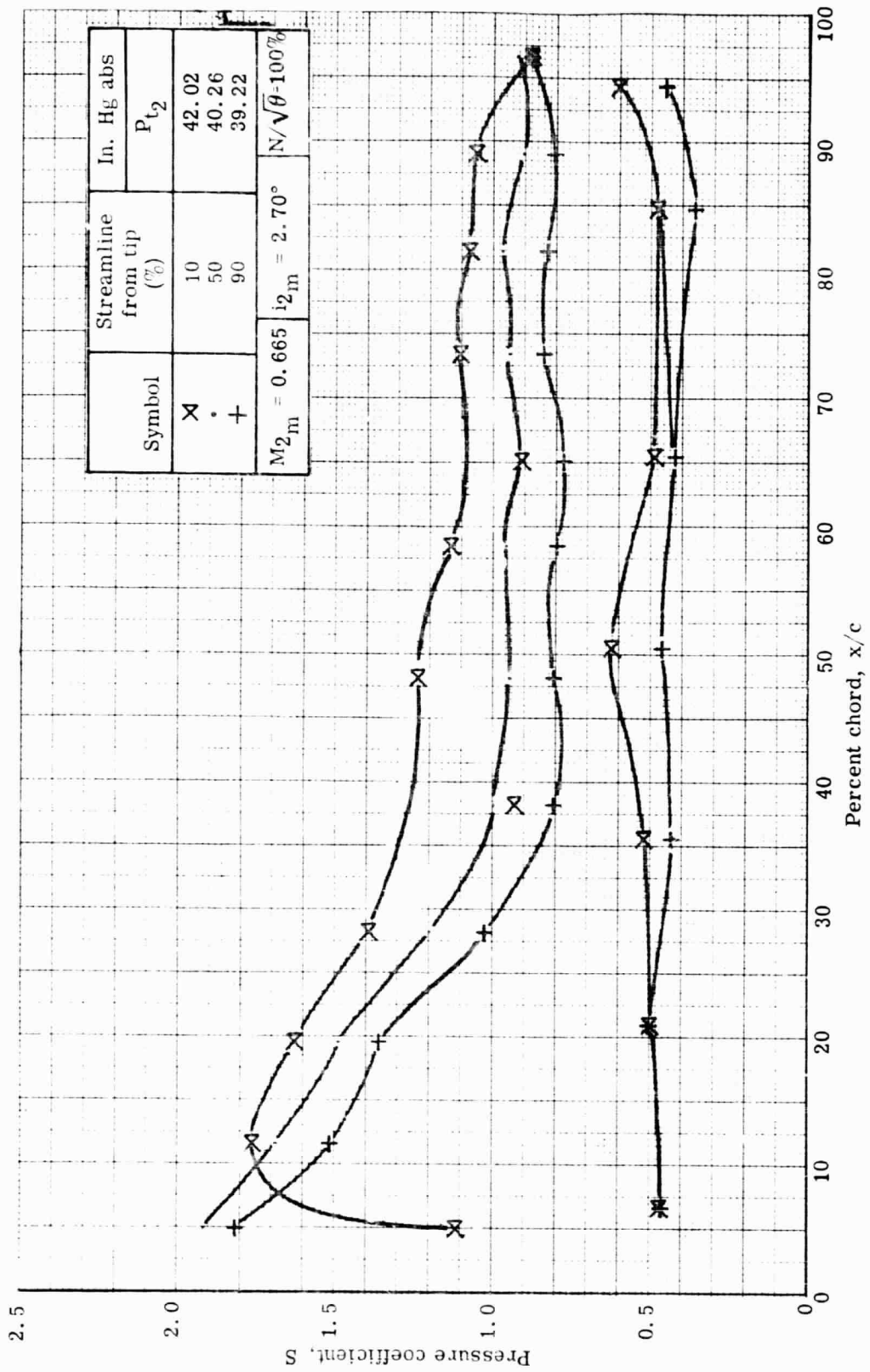


Figure 29. Stator static pressure distribution at 100% speed with optimum wall bleed.



5863-72

e. $W_a \sqrt{\theta}/\delta = 82.61 \text{ lb}_m/\text{sec}$

Figure 29. Stator static pressure distribution at 100% speed with optimum wall bleed.

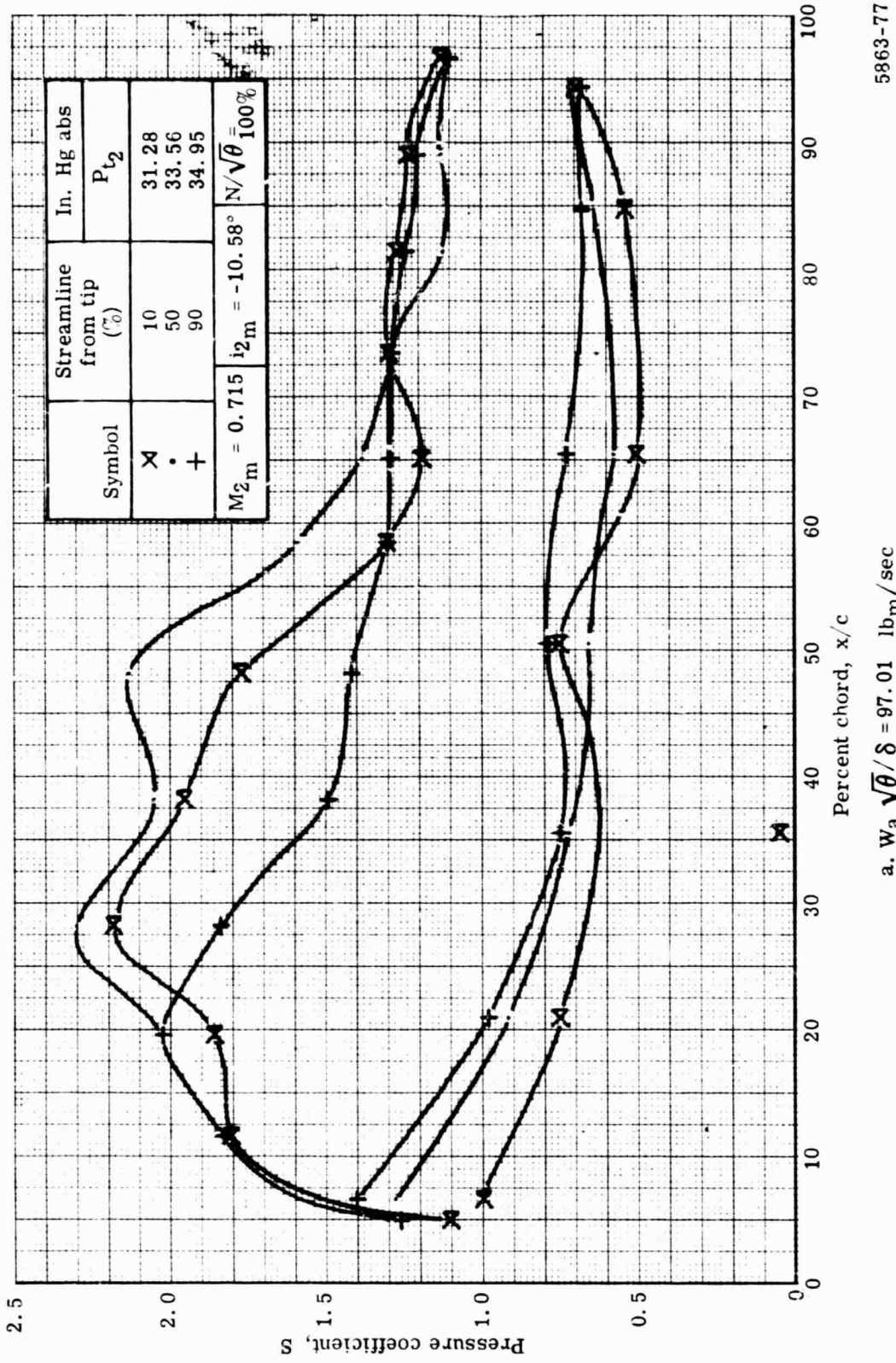


Figure 30. Stator static pressure distribution at 100% speed with mean wall bleed.

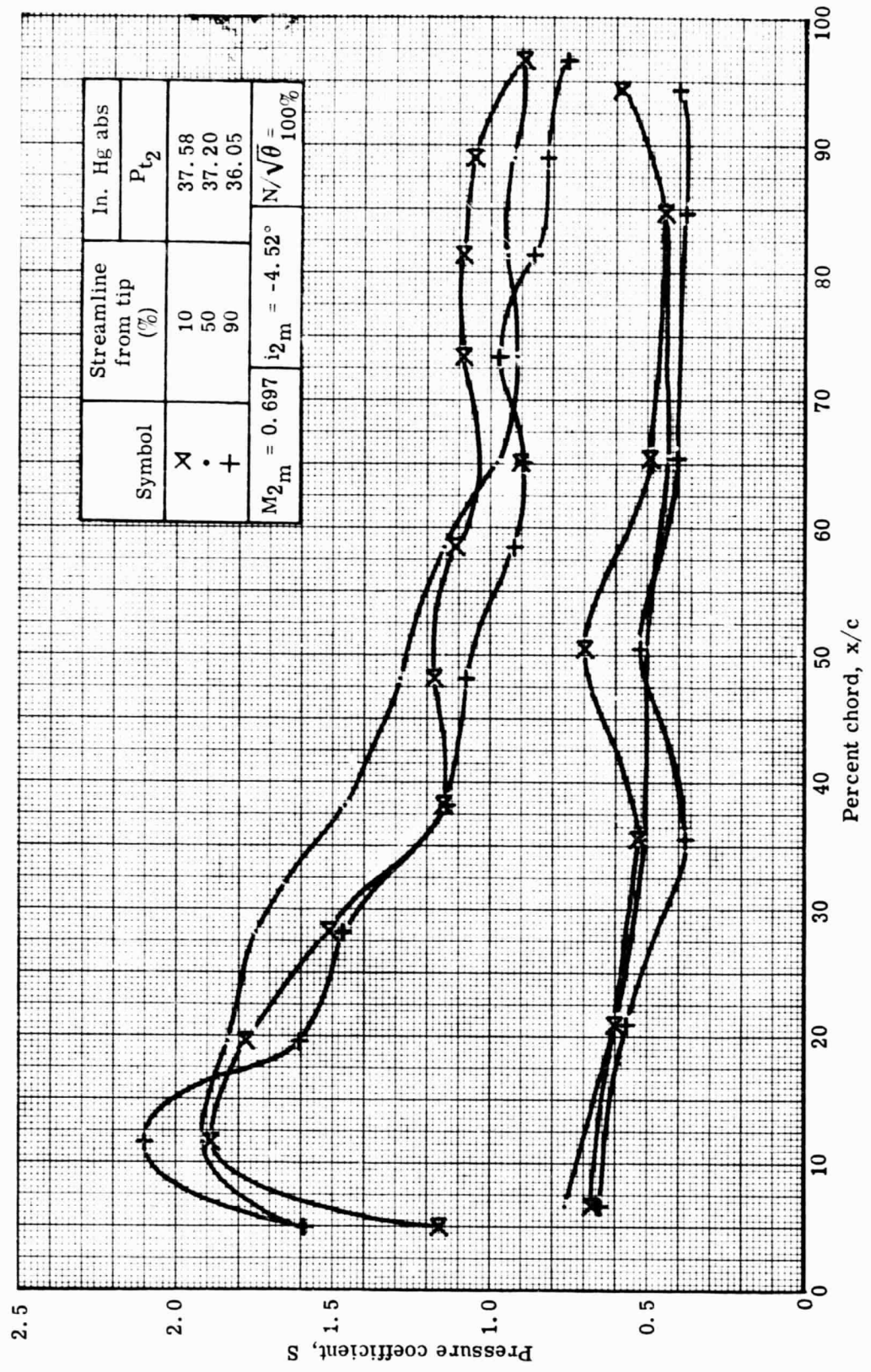


Figure 30. Stator static pressure distribution at 100% speed with mean wall bleed.

5863-78

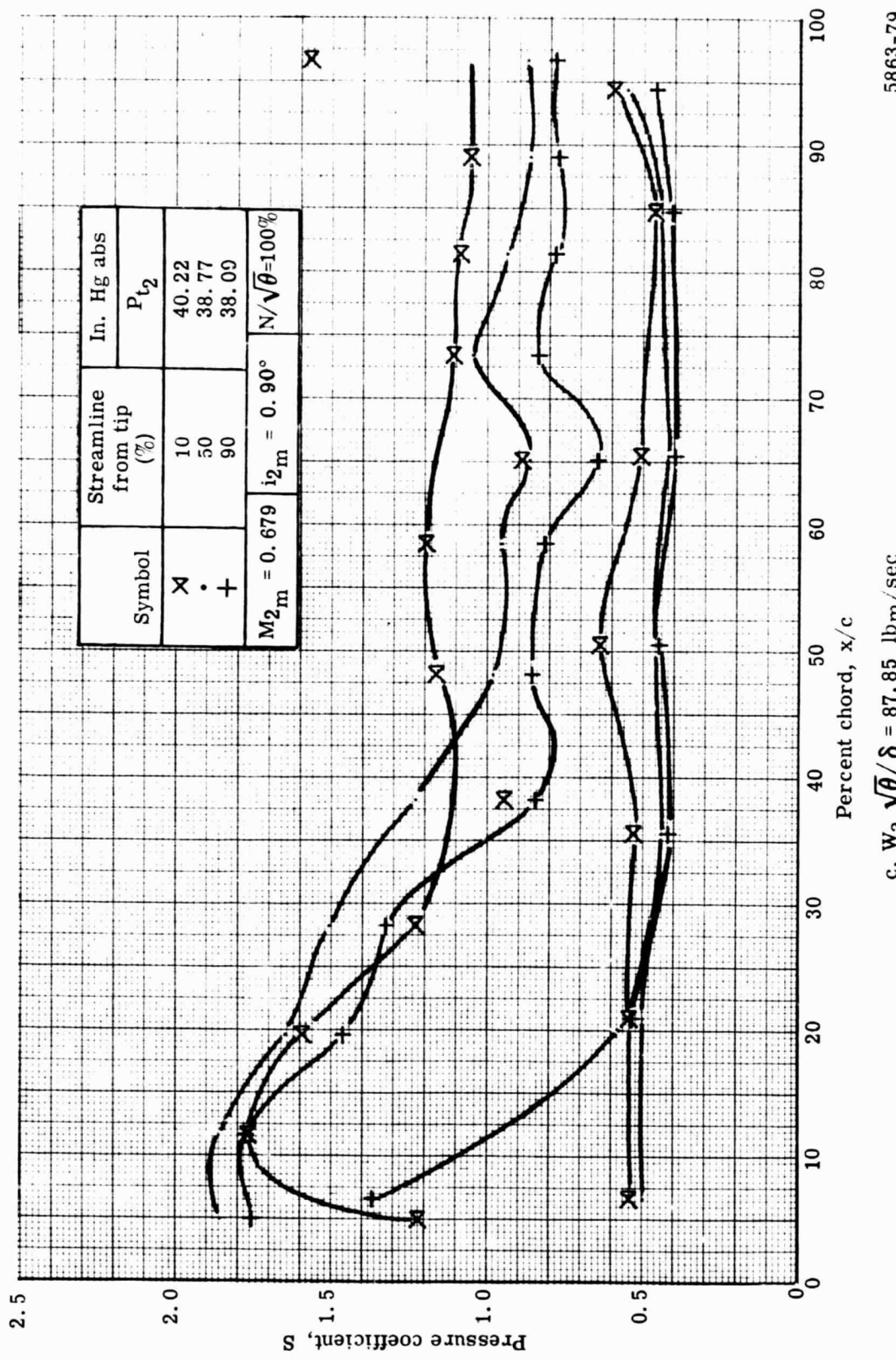


Figure 30. Stator static pressure distribution at 100% speed with mean wall bleed.

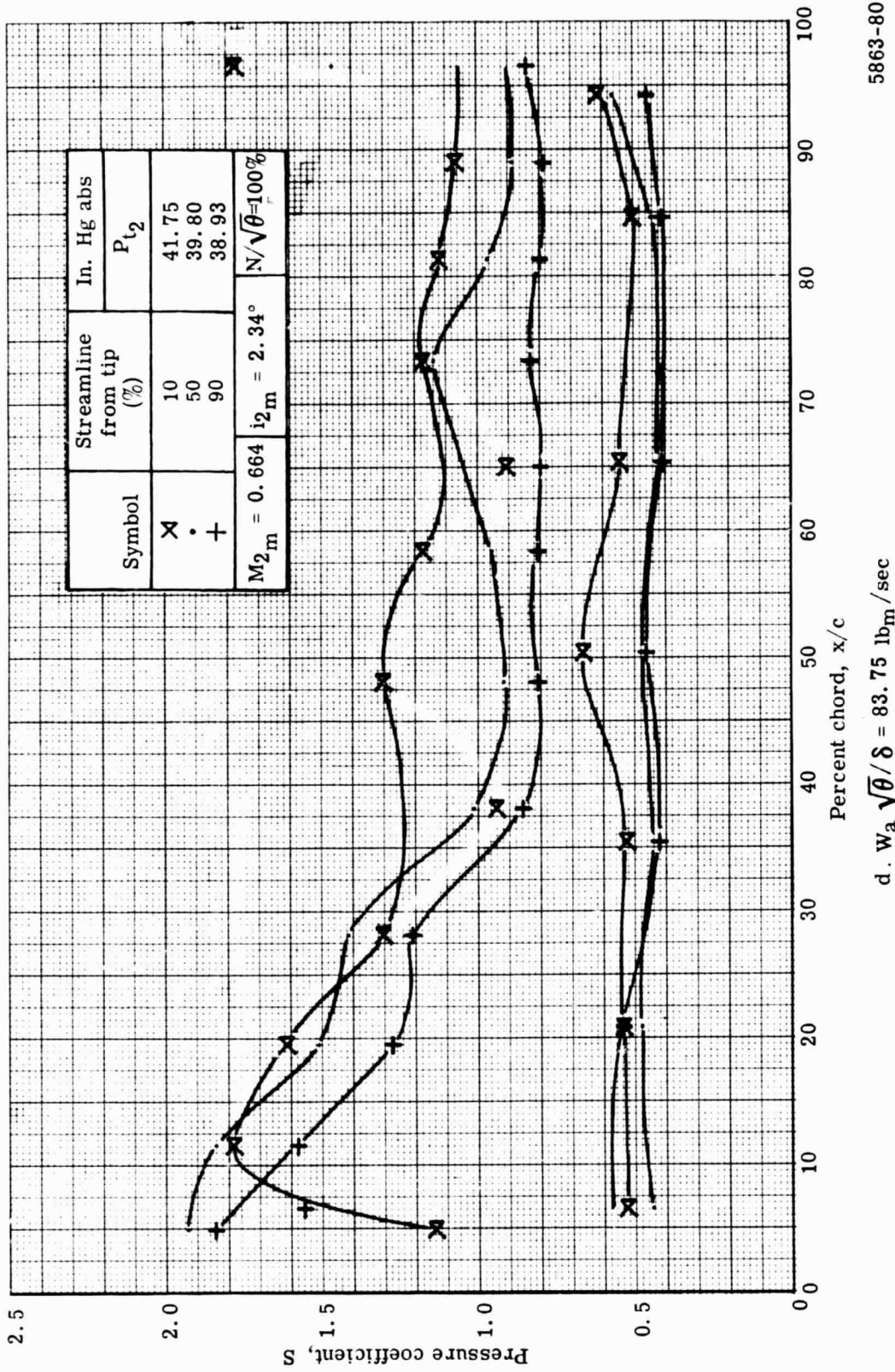


Figure 30. Stator static pressure distribution at 100% speed with mean wall bleed.

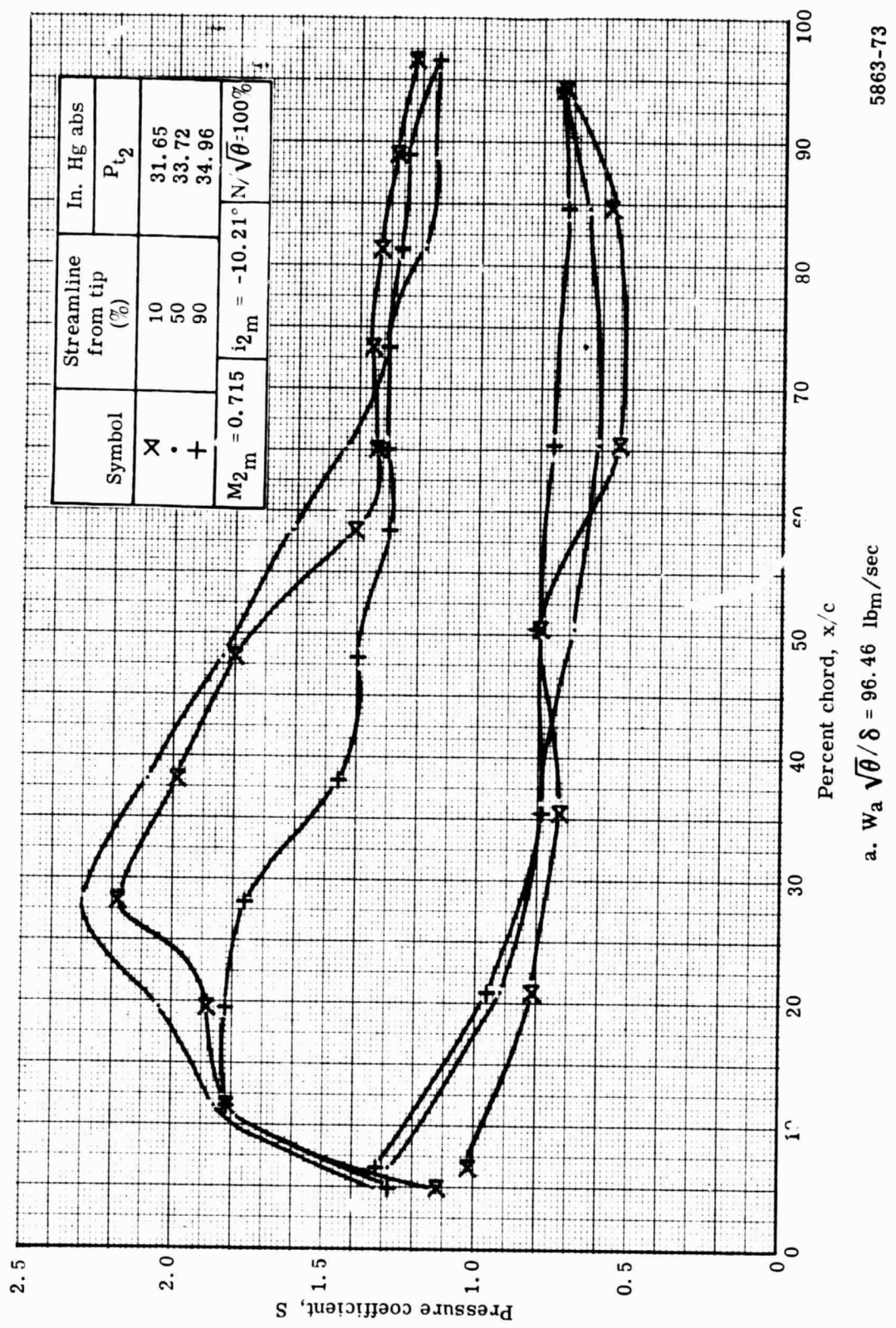


Figure 31. Stator static pressure distribution at 100% speed with minimum wall bleed.

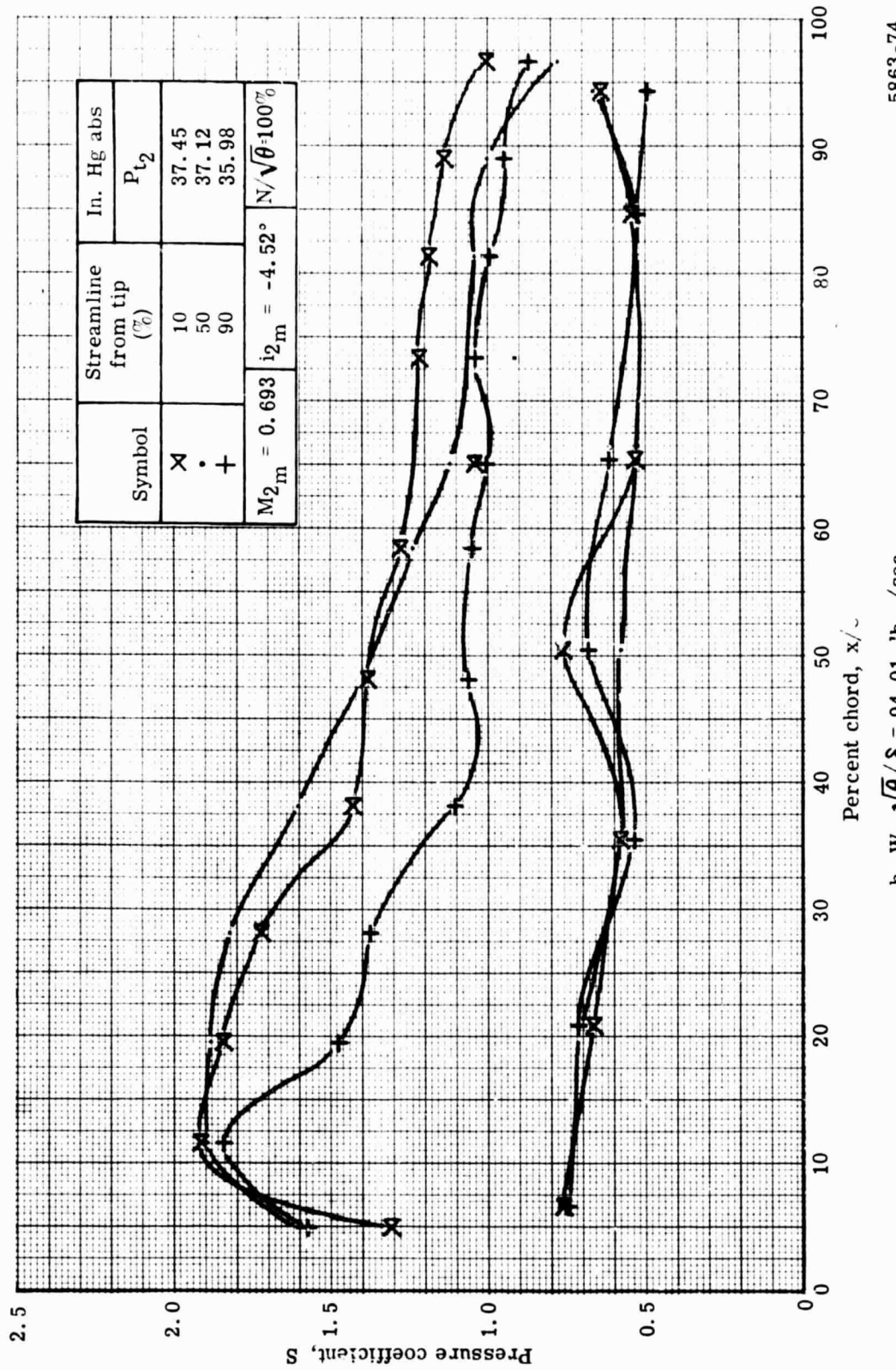


Figure 31. Stator static pressure distribution at 100% speed with minimum wall bleed.

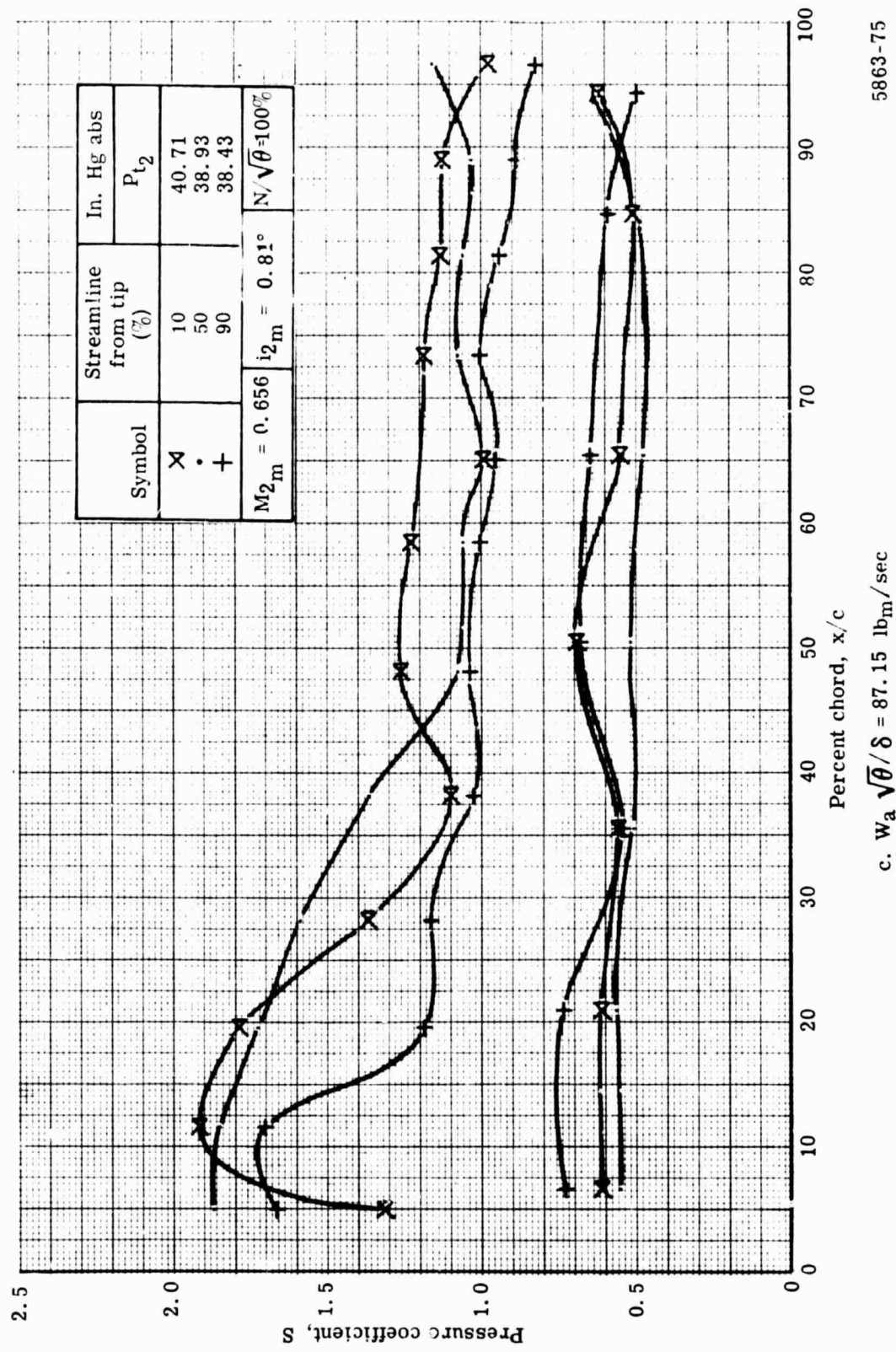


Figure 31. Stator static pressure distribution at 100% speed with minimum wall bleed.

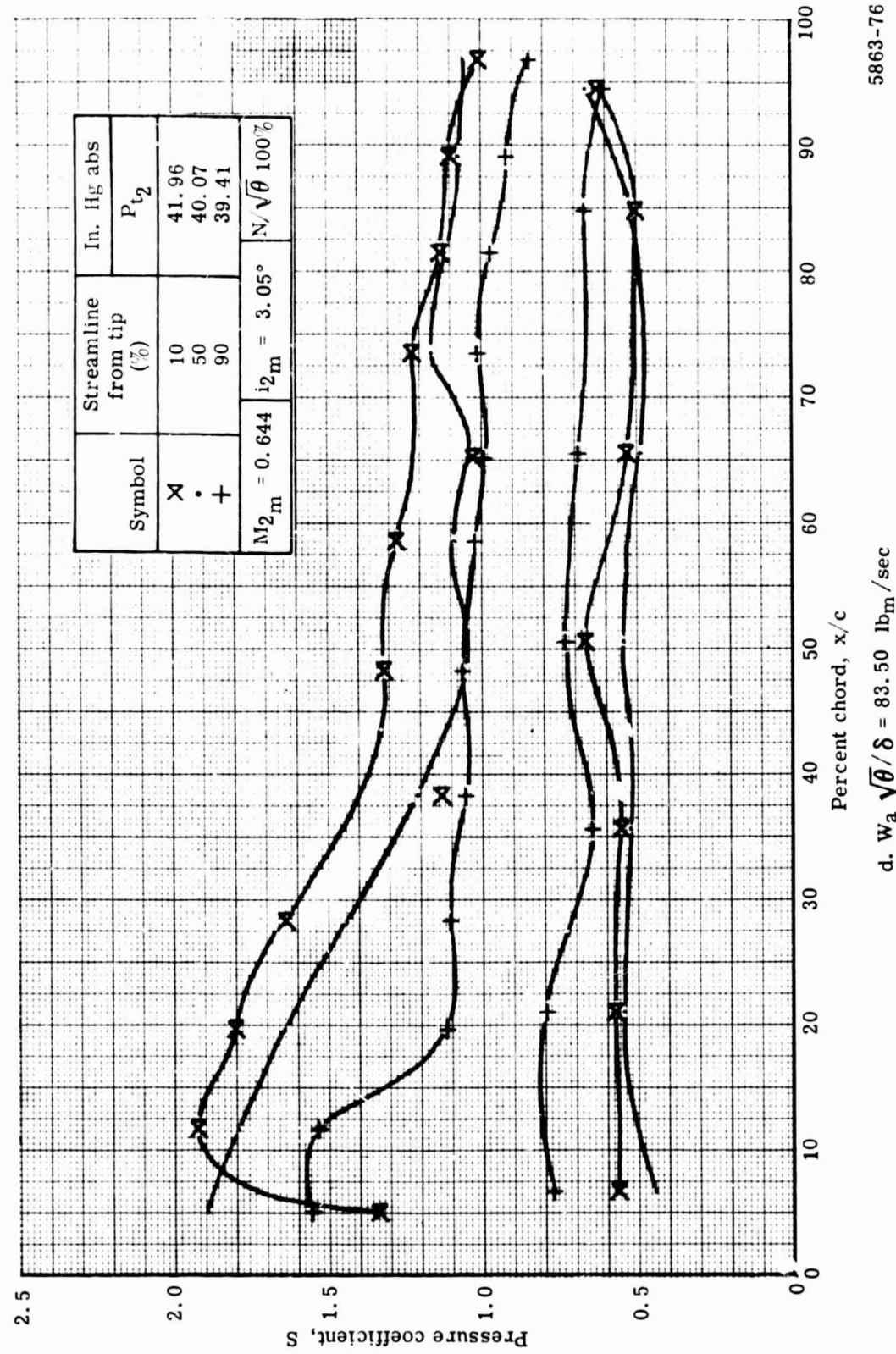


Figure 31. Stator static pressure distribution at 100% speed with minimum wall bleed.

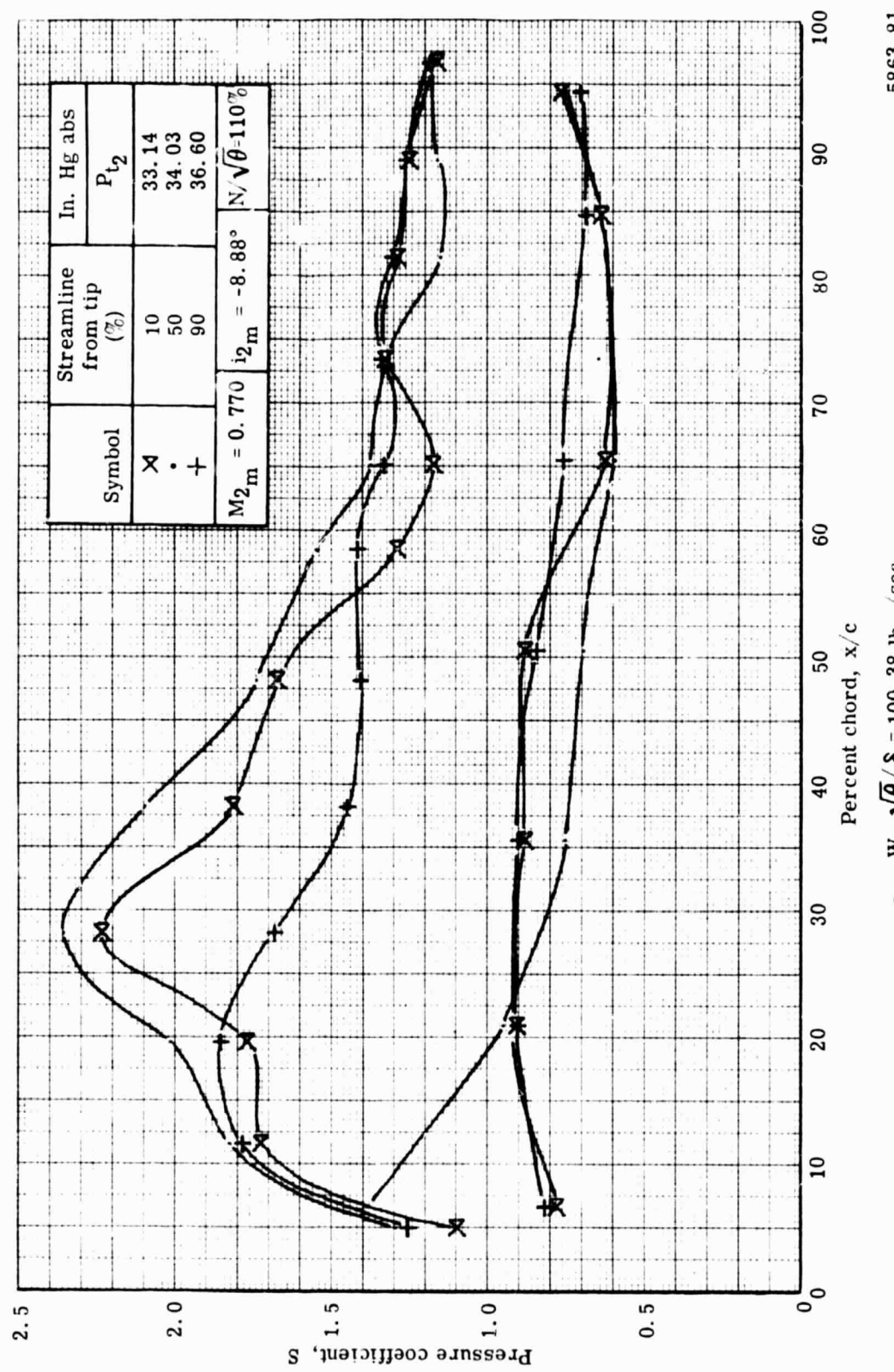


Figure 32. Stator static pressure distribution at 110% speed with optimum wall bleed.

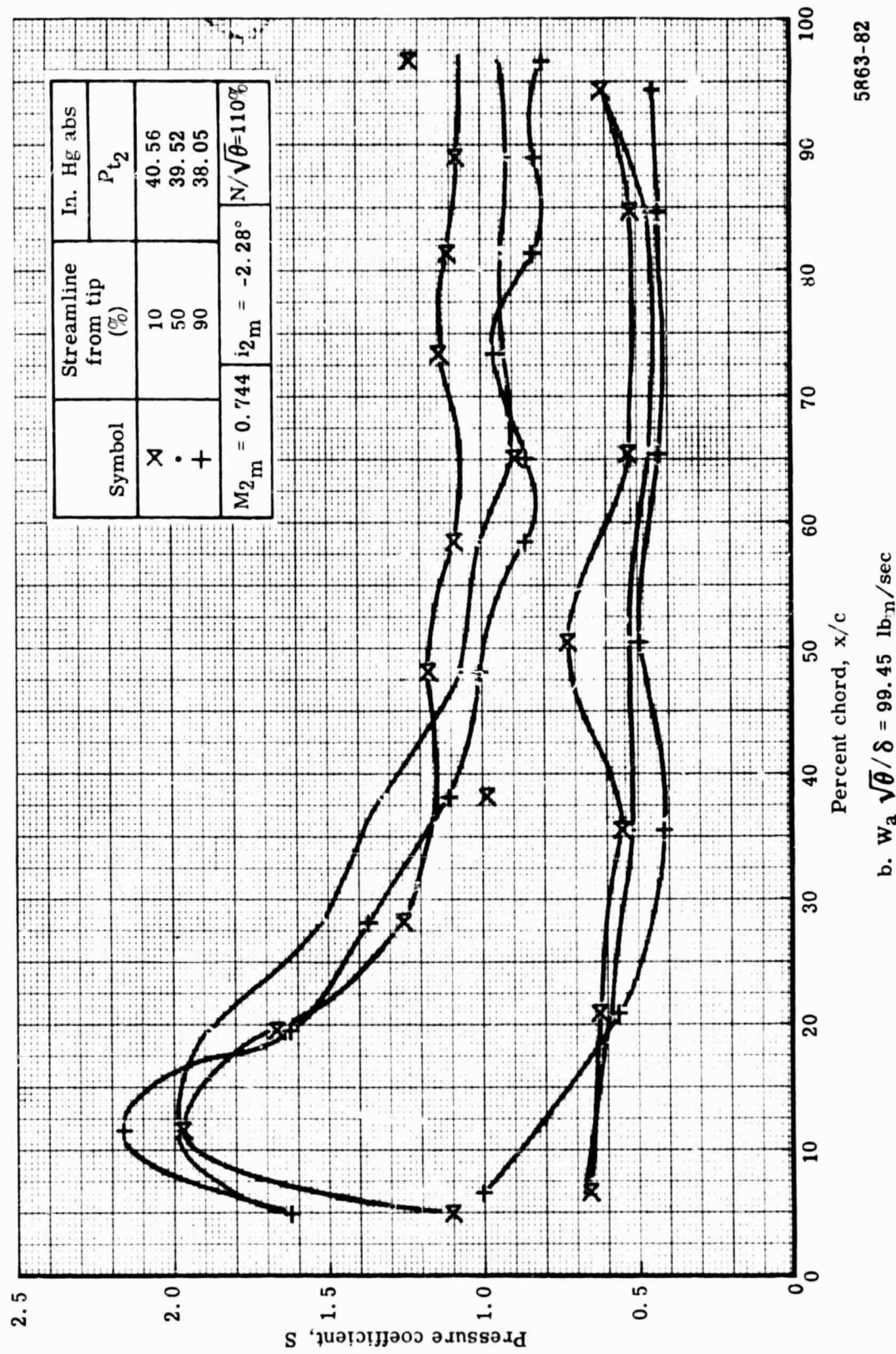


Figure 32. Stator static pressure distribution at 110% speed with optimum wall bleed.

b. $W_a \sqrt{\theta}/\delta = 99.45 \text{ lb}_a \text{in/sec}$

5863-82

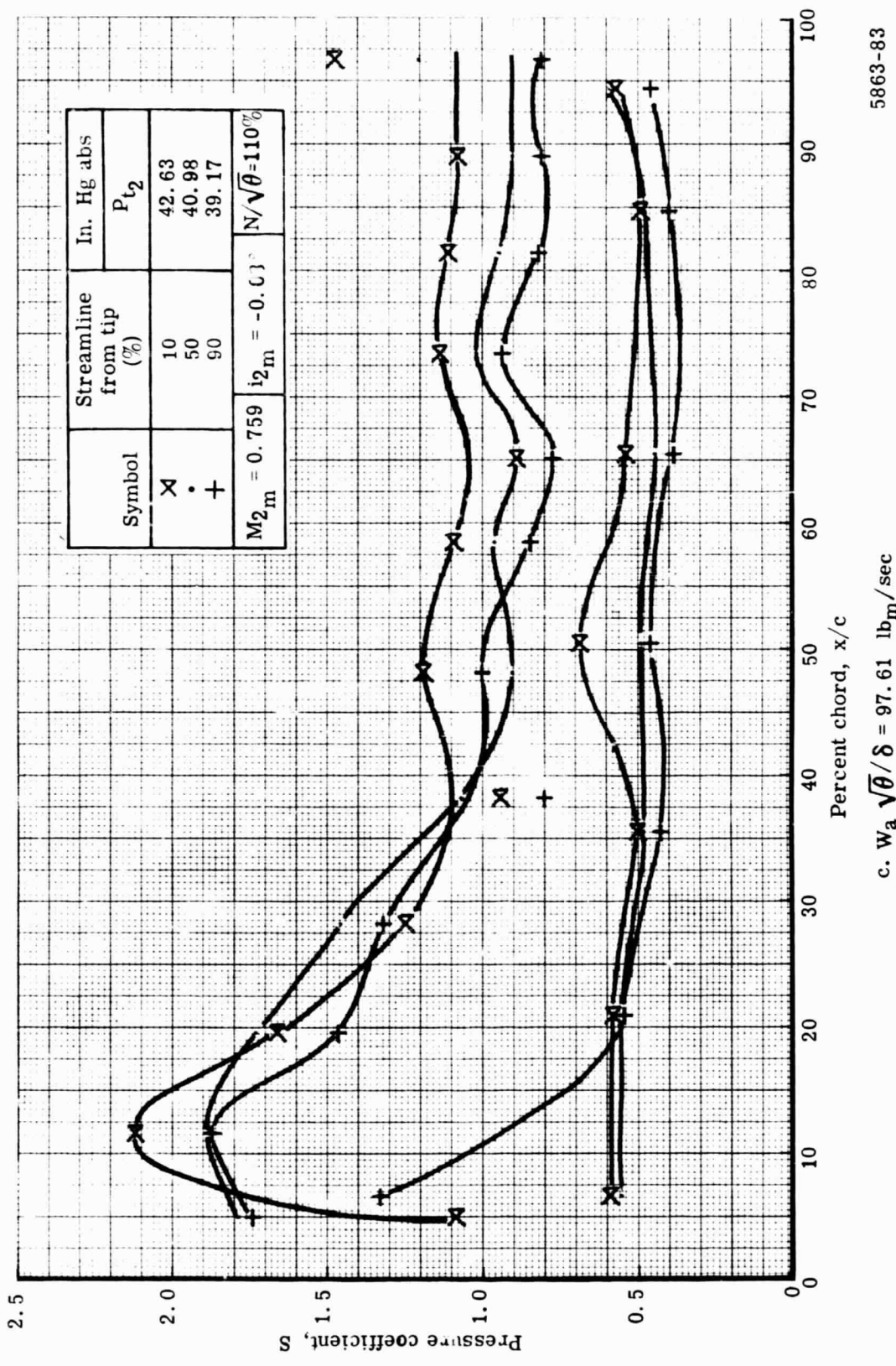


Figure 32. Stator static pressure distribution at 110% speed with optimum wall bleed.

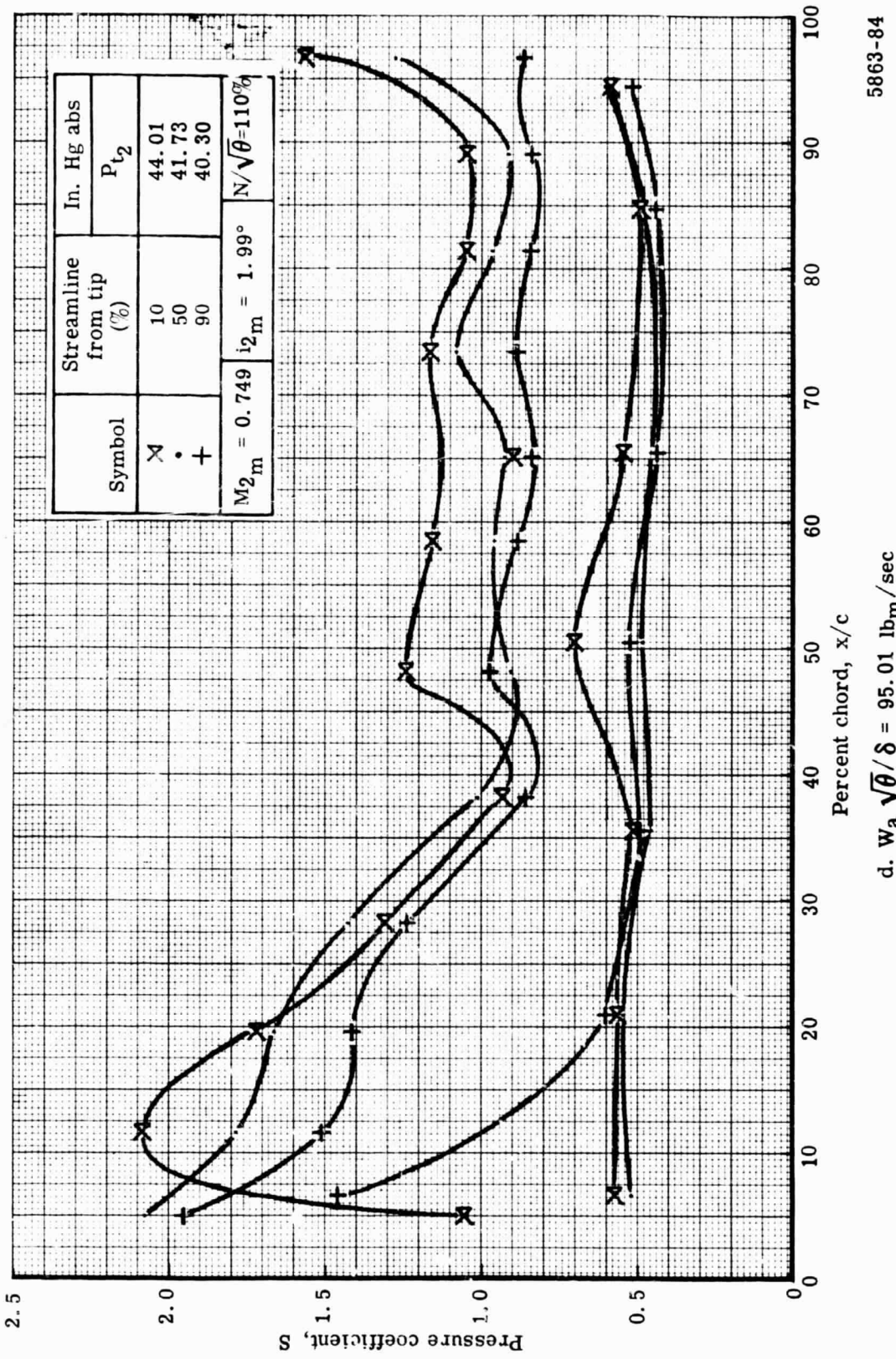


Figure 32. Stator static pressure distribution at 110% speed with optimum wall bleed.

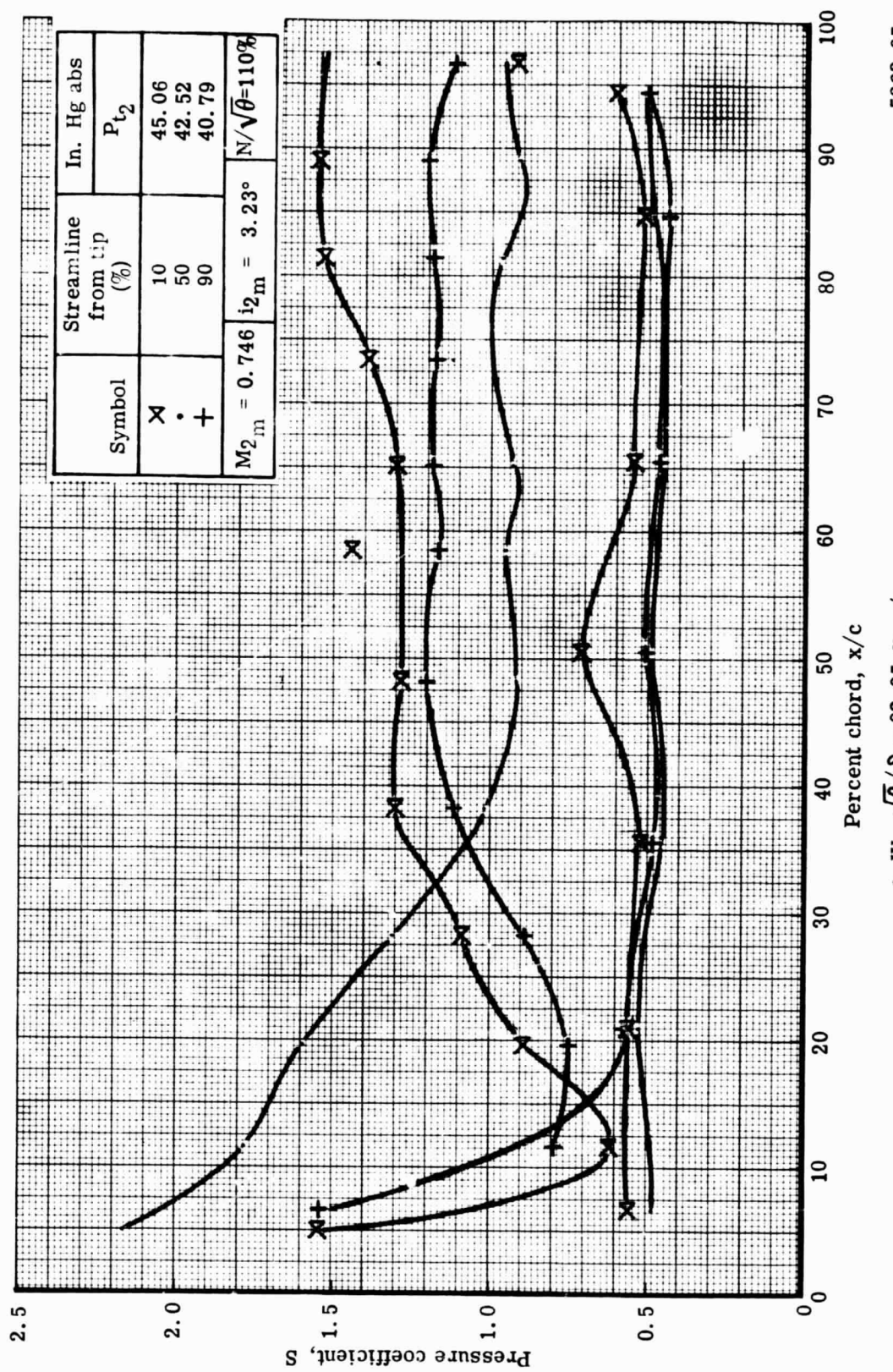


Figure 32. Stator static pressure distribution at 110% speed with optimum wall bleed.

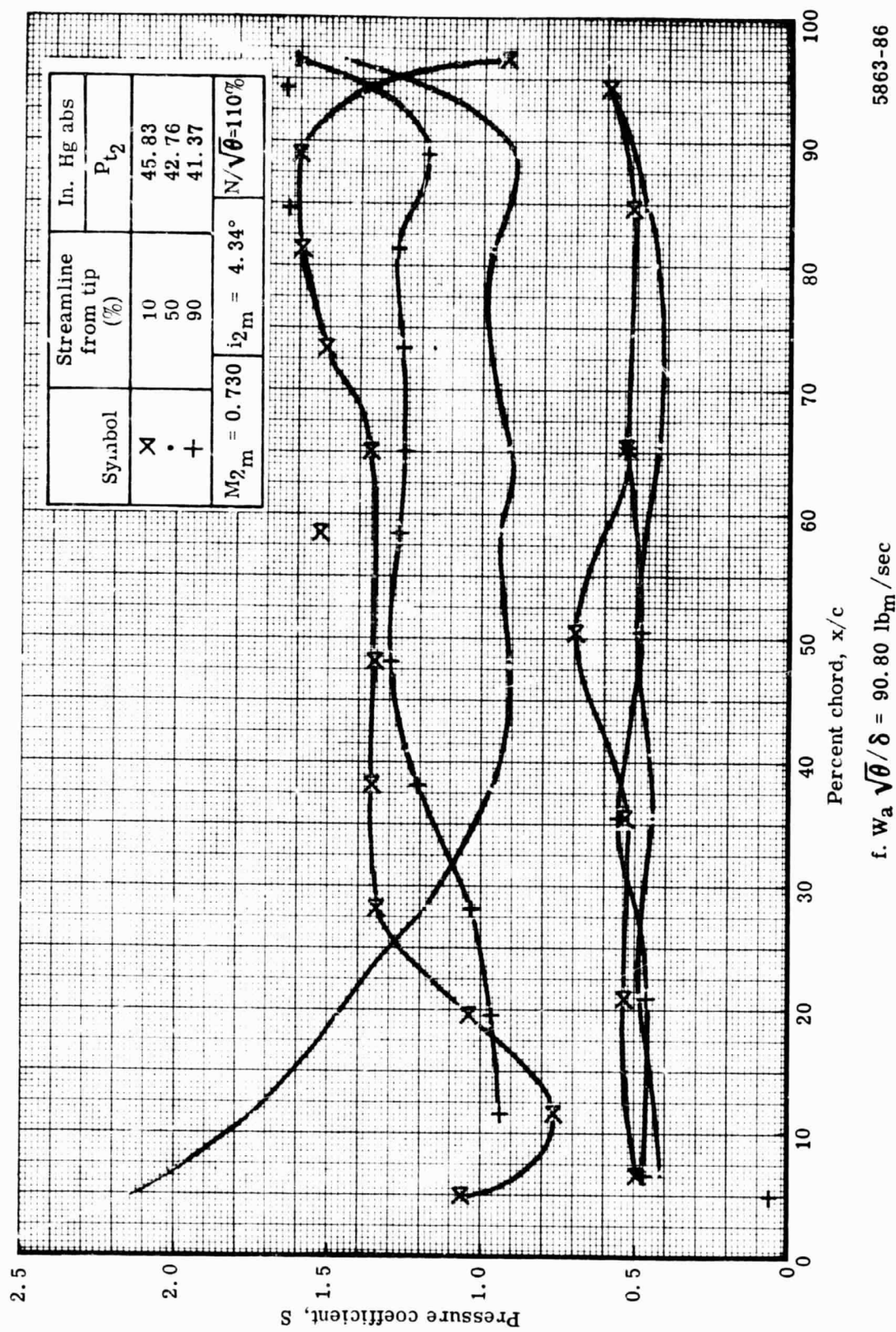
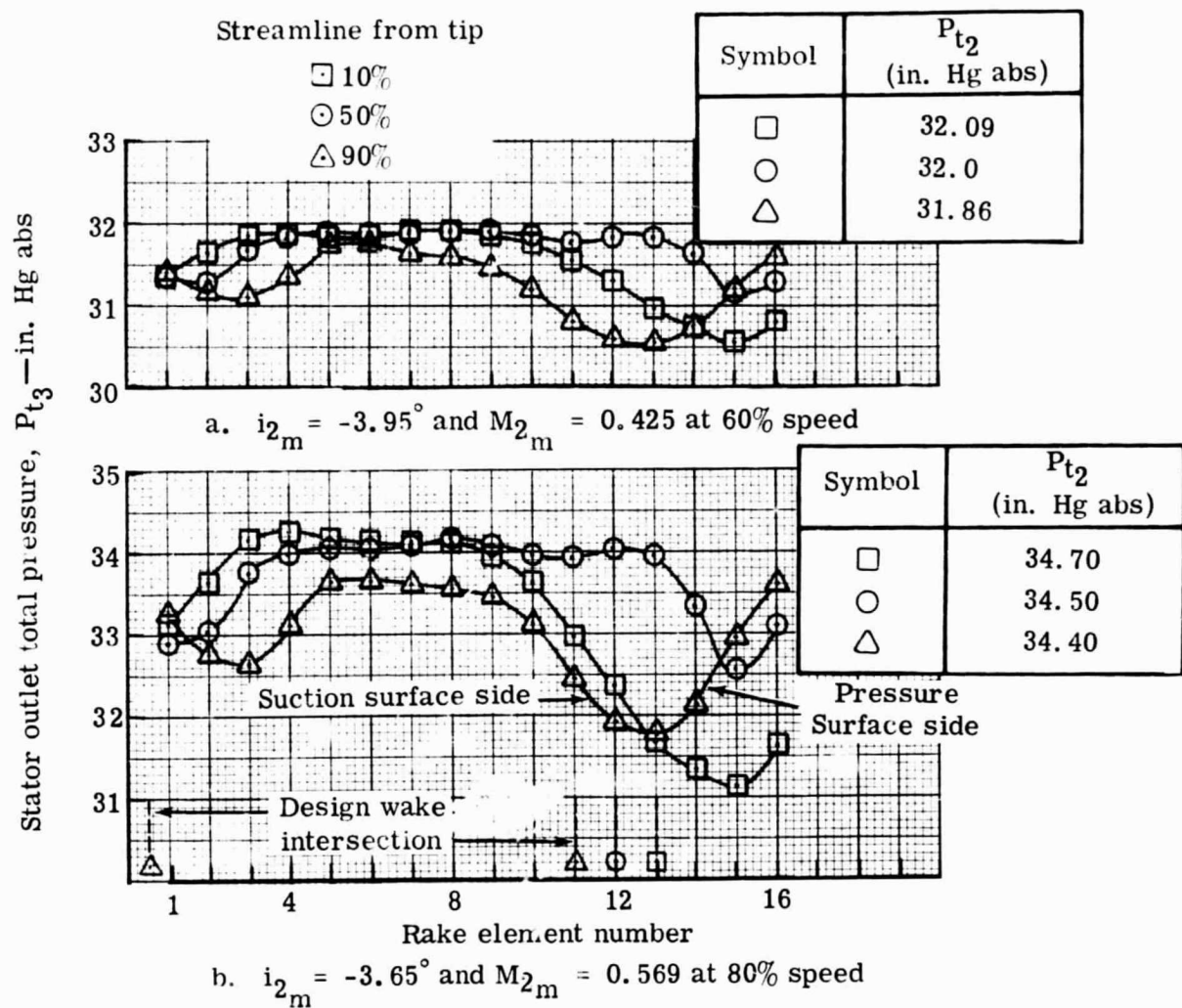
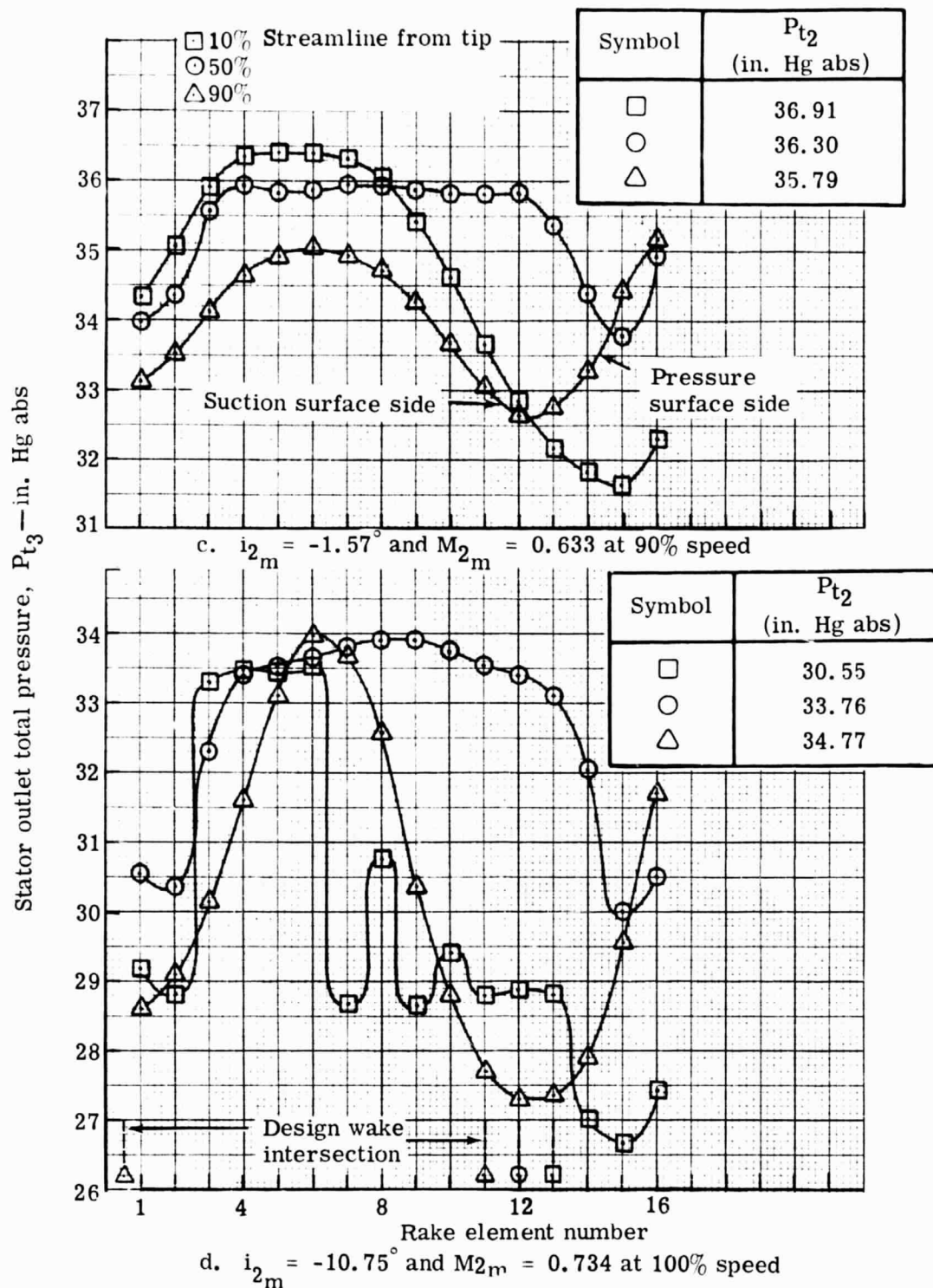


Figure 32. Stator static pressure distribution at 110% speed with optimum wall bleed.



5863-43

Figure 33. Stator wake surveys with optimum wall bleed.



5863-44

Figure 33. Stator wake surveys with optimum wall bleed.

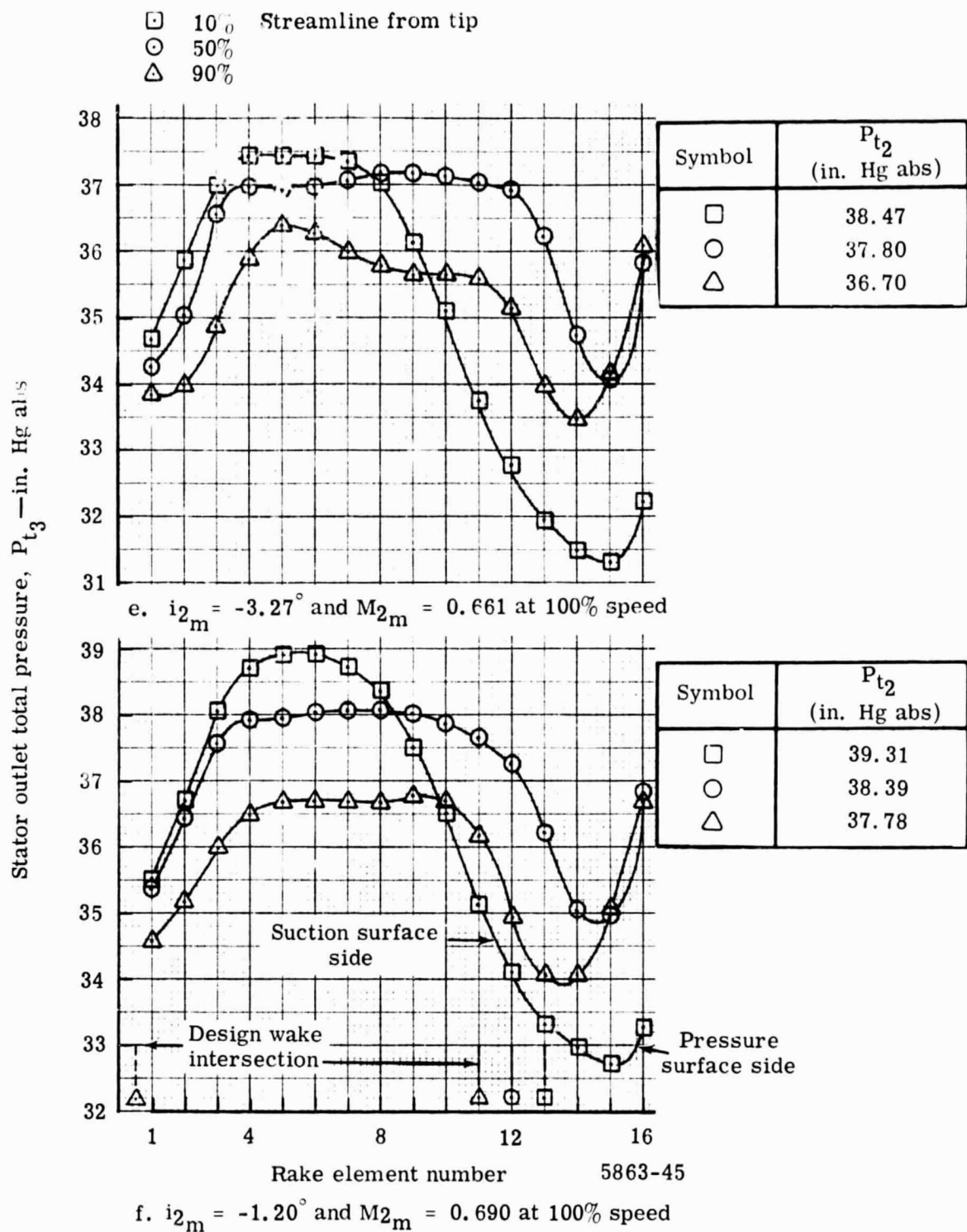


Figure 33. Stator wake surveys with optimum wall bleed.

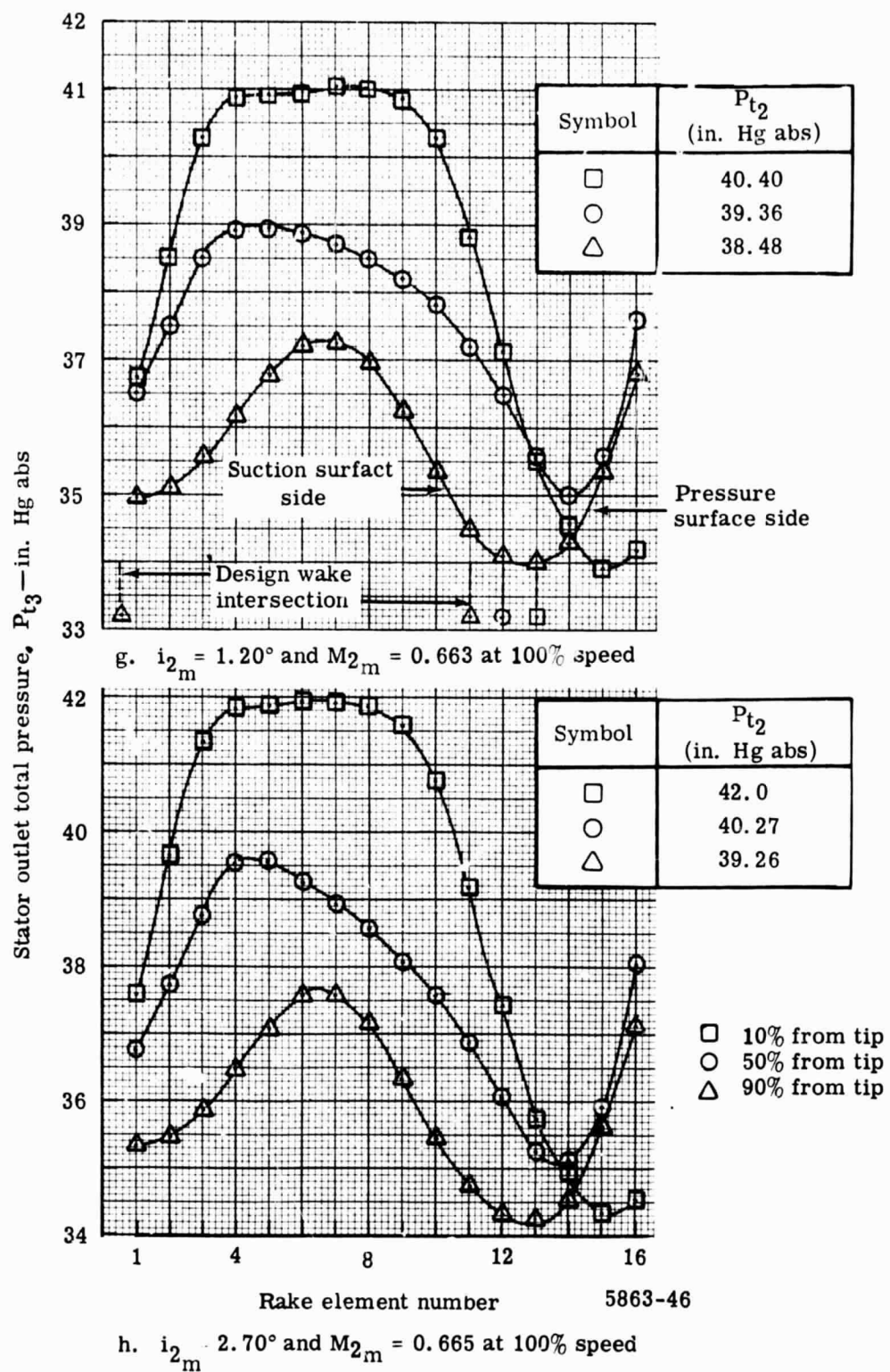
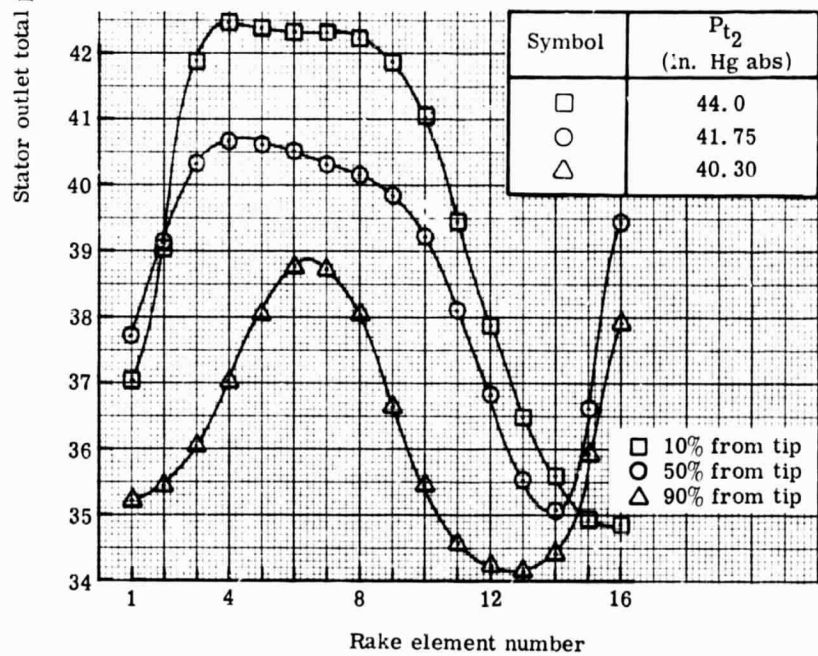
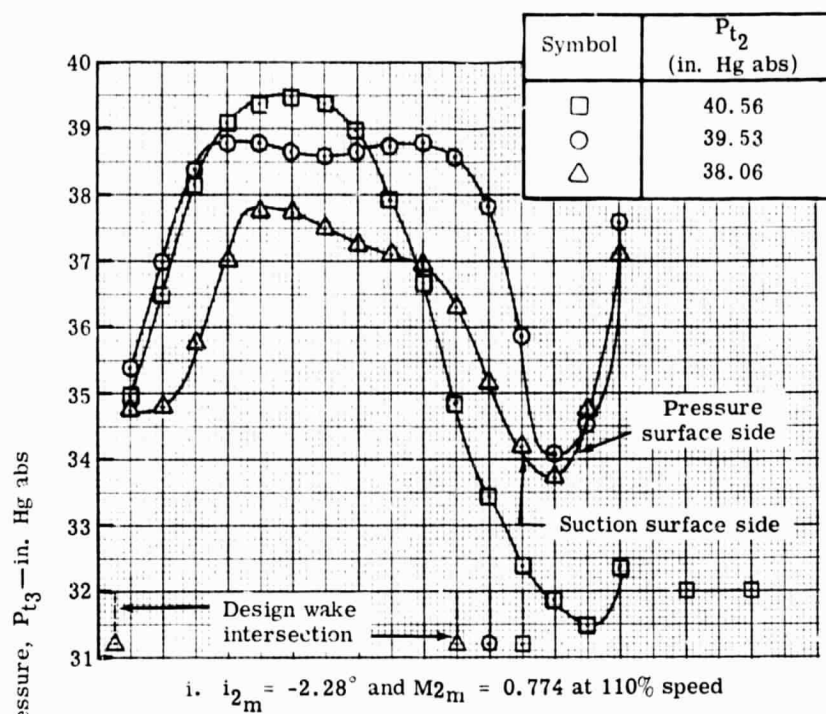


Figure 33. Stator wake surveys with optimum wall bleed.



5863-51

Figure 33. Stator wake surveys with optimum wall bleed

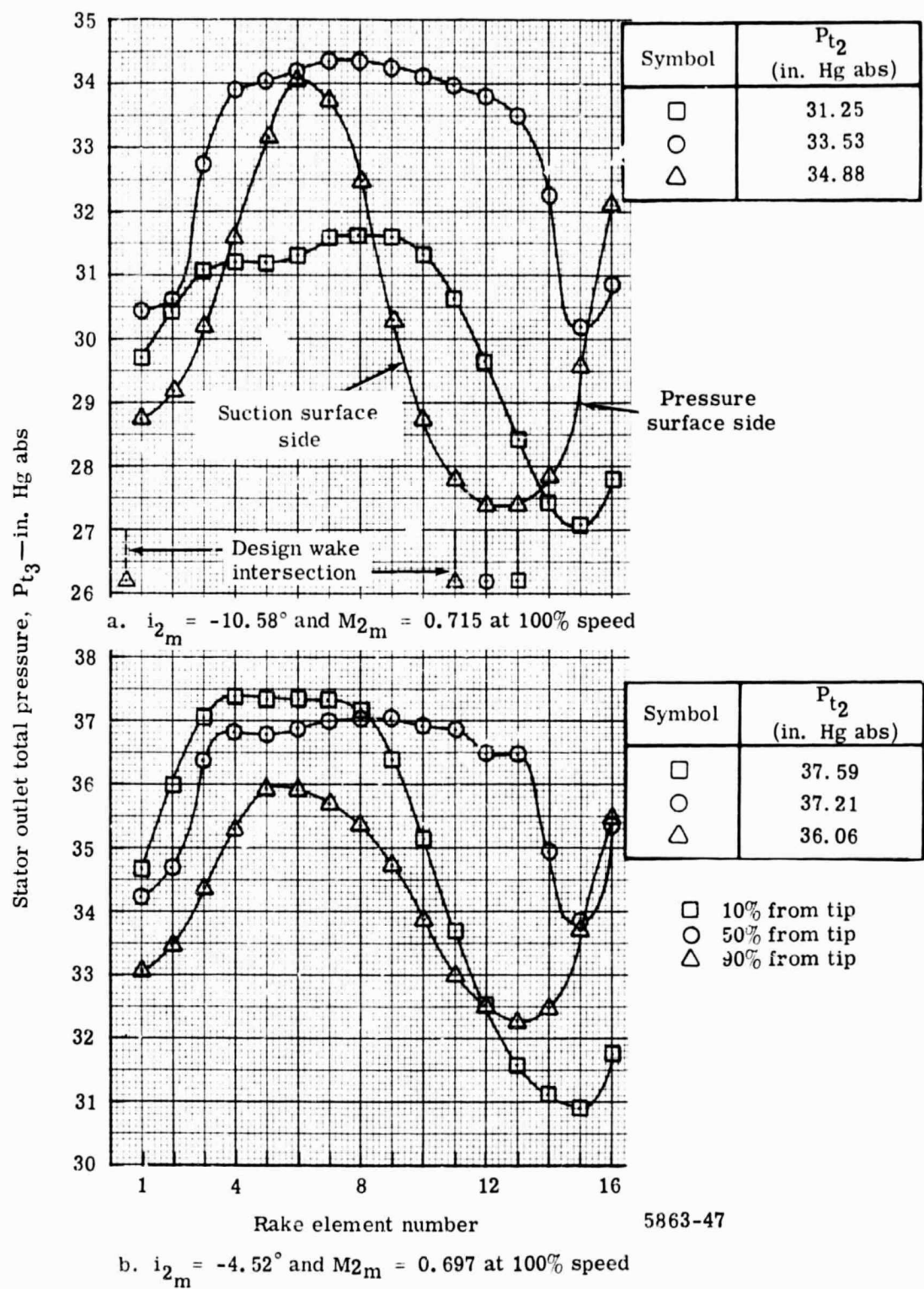


Figure 34. Stator wake surveys with mean wall bleed.

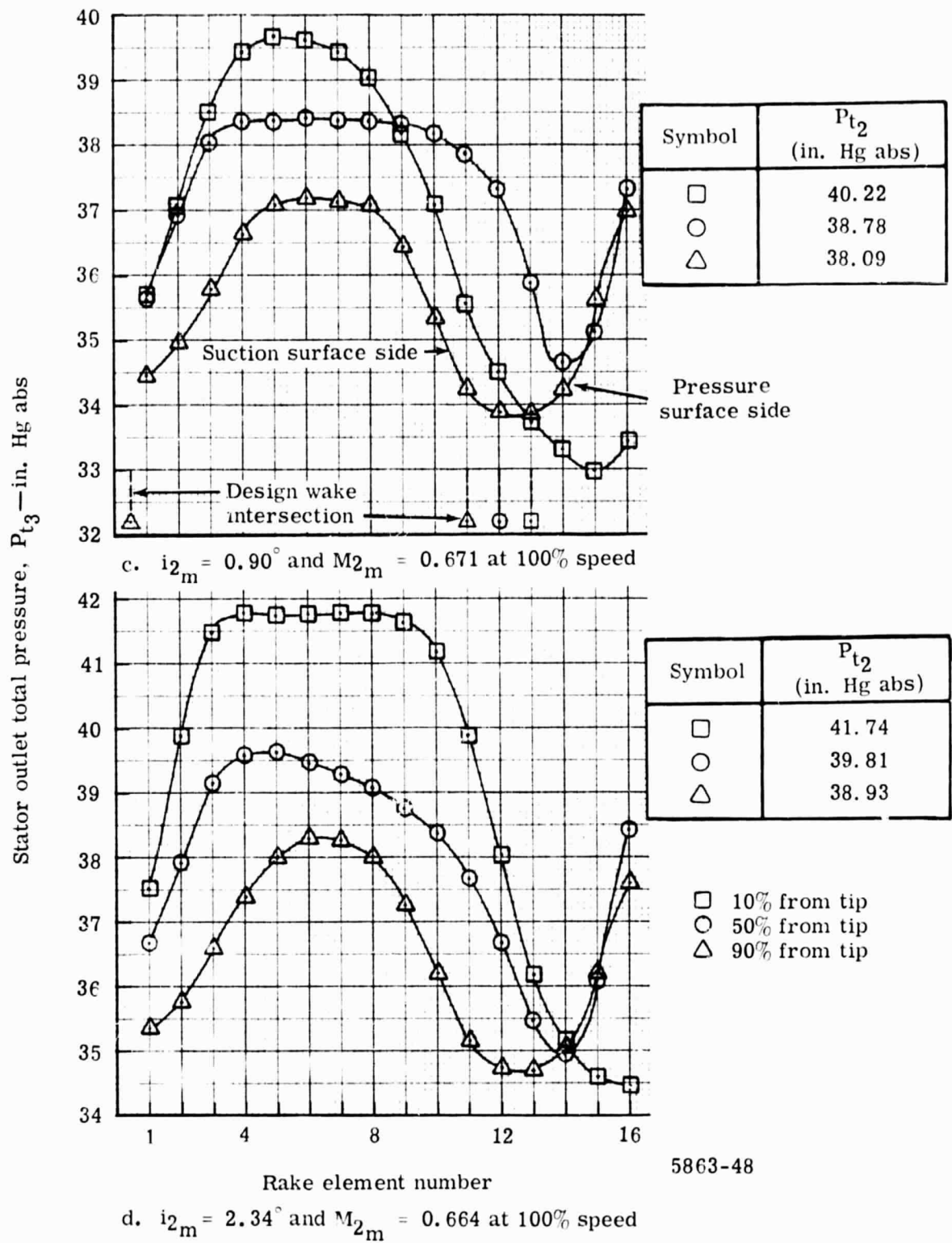


Figure 34. Stator wake surveys with mean wall bleed.

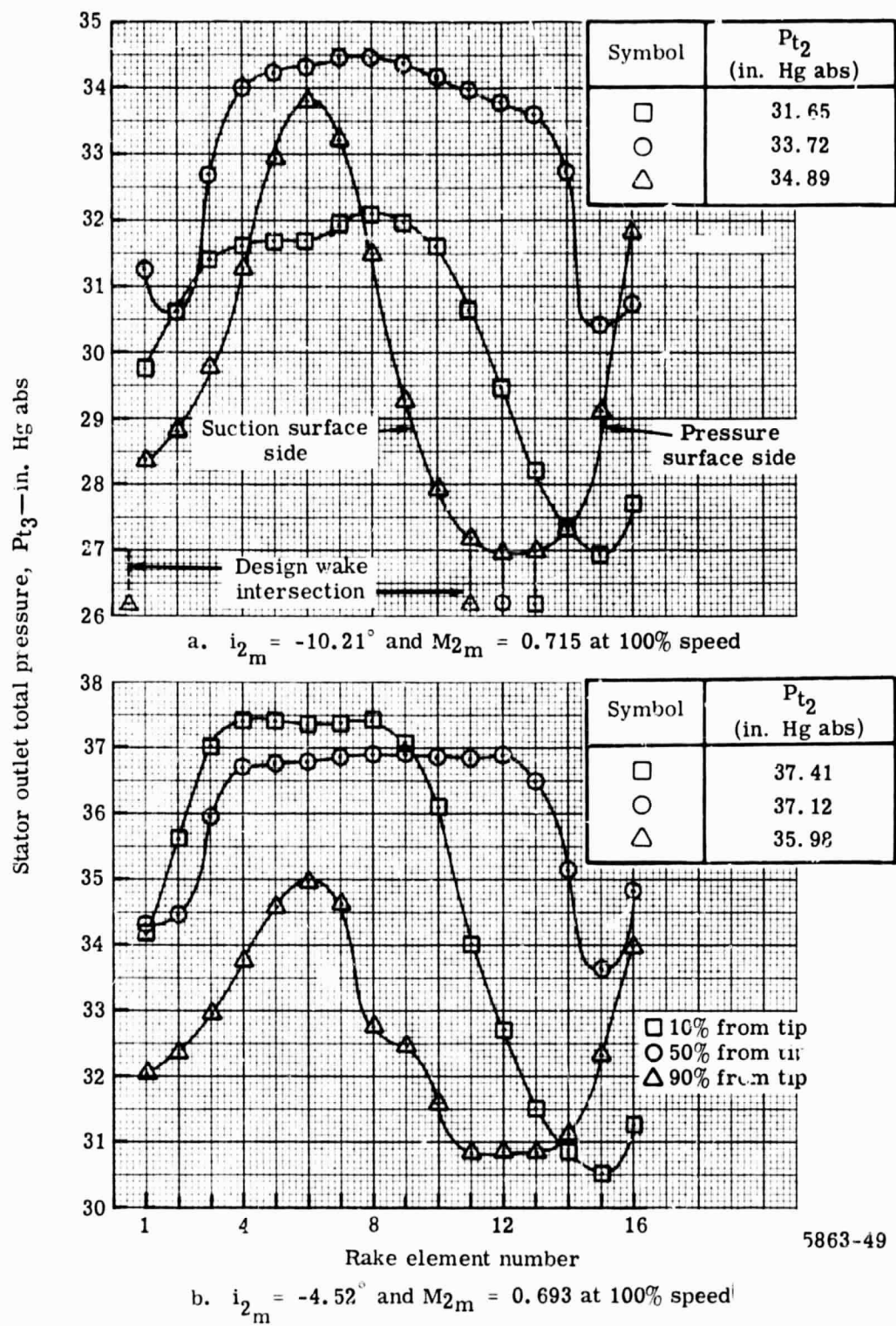


Figure 35. Stator wake surveys with minimum wall bleed.

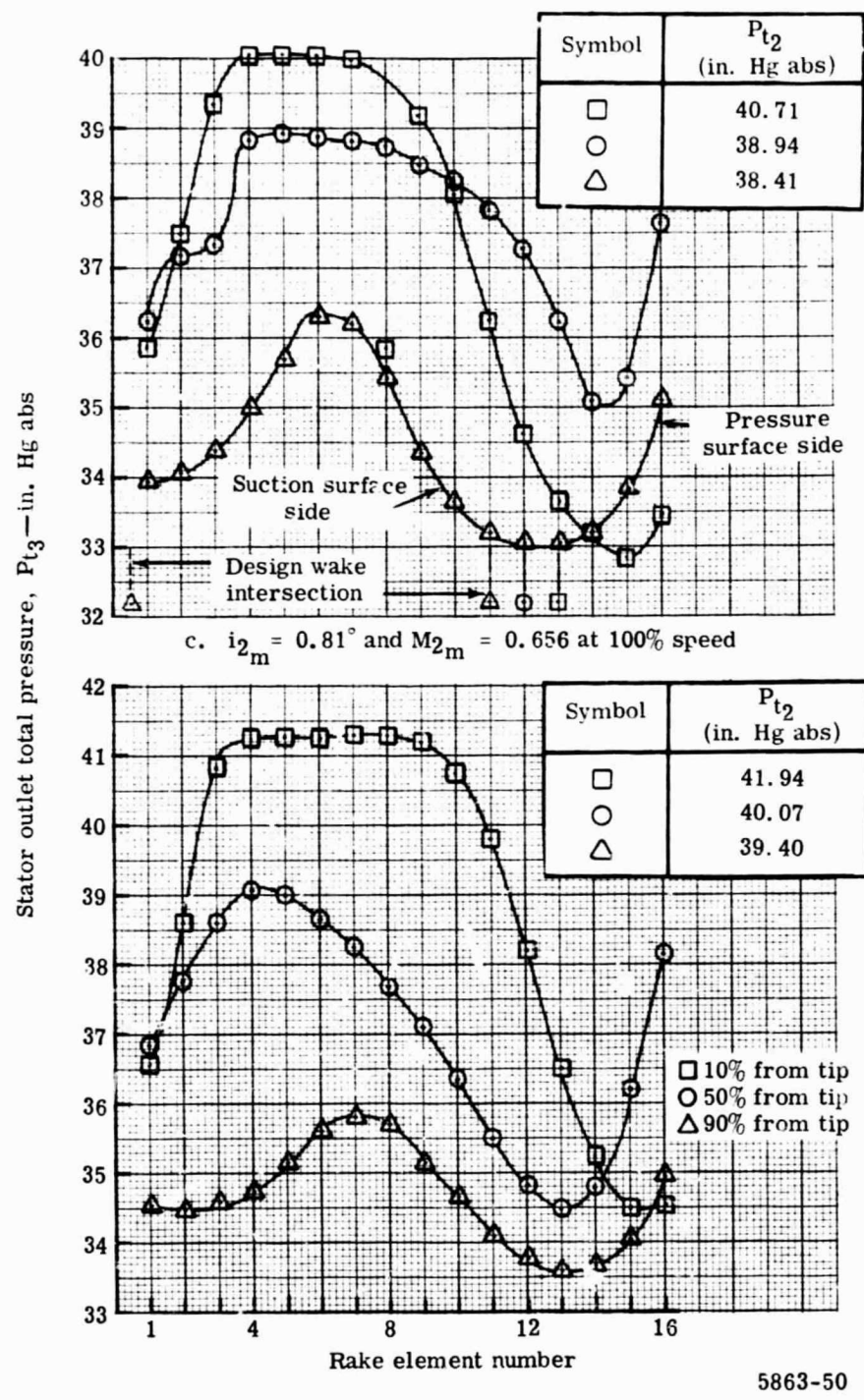


Figure 35. Stator wake surveys with minimum wall bleed.

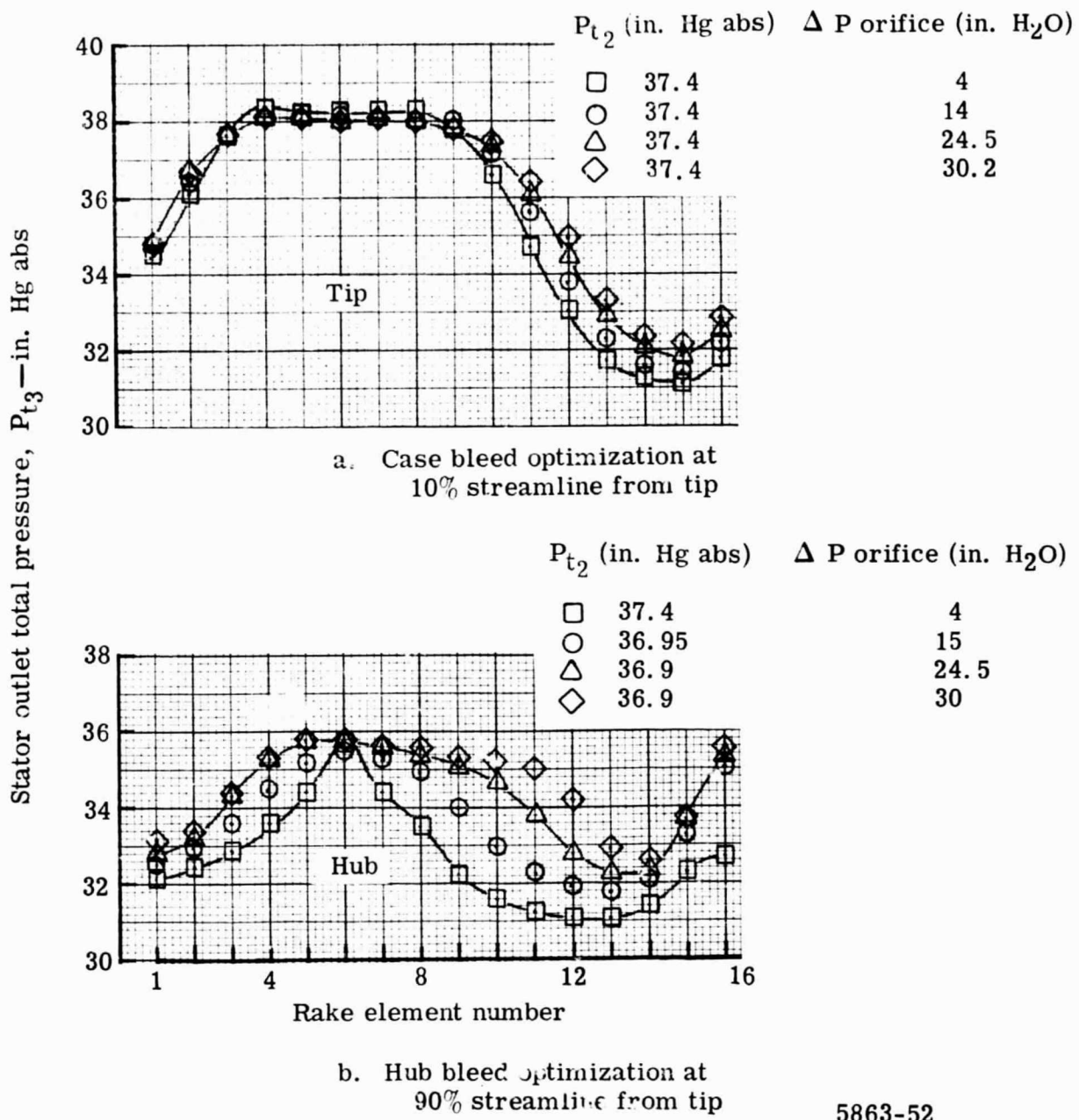


Figure 36. Variation in stator wake at 10 and 90% streamlines from tip during wall bleed optimization.

Table I.

Blade and vane geometry summary.

Blade row	Exit radius (in.)	κ_1 (degrees)	κ_2 (degrees)	ϕ ($\kappa_1 - \kappa_2$)	c (in.)	$\bar{\sigma}$	t/c	δ° (degrees)	i_{des} (degrees)	a_{des} (degrees)	n
Design inlet guide vane (63-006 series)	10.49	—	—	—	2.733	1.41	0.06	—	—	17.80	—
	11.51	—	—	—	2.733	1.26	0.06	—	—	16.25	—
	12.53	—	—	—	2.733	1.18	0.06	—	—	15.16	34
	13.54	—	—	—	2.733	1.09	0.06	—	—	14.36	—
	14.58	—	—	—	2.733	1.02	0.06	—	—	13.30	—
Rotor blade (double circular arc)	10.97	43.1	9.1	34.0	2.875	1.89	0.078	7.81	0	—	—
	11.86	49.2	21.0	28.2	2.875	1.74	0.052	7.38	0	—	—
	12.76	53.4	31.2	22.2	2.875	1.61	0.039	6.34	0	—	45
	13.65	56.7	39.1	17.6	2.875	1.51	0.033	5.52	0	—	—
	14.54	59.6	44.4	15.2	2.875	1.42	0.032	4.85	0	—	—
Stator blade 0.75 D _{HT} (65 series-circular arc meanline)	11.02	56.16	-17.80	73.96	3.0	1.65	0.10	17.82	-3	—	—
	11.94	54.15	-17.70	71.85	3.0	1.52	0.10	17.70	-3	—	—
	12.84	52.74	-17.75	70.49	3.0	1.41	0.10	17.74	-3	—	38
	13.71	52.12	-18.05	70.17	3.0	1.32	0.10	18.06	-3	—	—
	14.58	50.09	-18.96	69.05	3.0	1.24	0.10	19.03	-3	—	—

Table II.

Rotor incidence at minimum and maximum flow for flow generation rotor and complete stage.

Corrected speed (%)	Streamline from tip (%)	Flow generation rotor test		Complete stage test	
		i _{max} (stall) (degrees)	i _{min} (choke) (degrees)	i _{max} (stall) (degrees)	i _{min} (choke) (degrees)
60	10	6.2	-8.0	5.26	-5.40
	50	6.0	-12.0	6.51	-5.02
	90	7.6	-13.0	8.62	-6.25
80	10	5.4	-8.0	5.64	-3.22
	50	5.4	-7.5	6.16	-5.02
	90	8.0	-8.0	7.19	-5.51
100	10	4.0	-3.0	4.16	-5.88
	50	4.0	-4.3	4.20	-3.83
	90	4.7	-5.0	5.34	-1.54

Table III.

Rotating stall results for complete stage test.

Corrected speed (%)	Corrected airflow (lbm/sec)	Number of stall cells at streamline from tip 10% 90%	Rotative cell speed (% rpm)	Stall cell frequency (cps)	Comment
60	47.39	1 1	40	33	Hysteresis points were not dictated by stress considerations
	35.11	1 1	27	22	
	43.82	1 1	31	35.5	
60	43.77	1 1	45	37	Stresses 9.41 cps; stall abrupt, however, there were no high stress problems
80	61.47	1 1	45	52	
		1 1	47	55	Abrupt stall; stresses were above steady-state limit
90	72.08	1 1	44	55	Abrupt stall, stresses were approaching the transient limit
100	79.33	1 1	46	64	Stress limited, abrupt stall; maximum stresses observed were with wall bleed at optimum rate
		1 1	45	62	
100	79.71	5 6	44	300	Stress limited, abrupt stall; stresses were above the steady state limit; wall bleed held at minimum rate
		6 6	42	350	
100	80.81	1 1	46	64	Wall bleed at mean rate; stress limited, abrupt stall
100	83.75	2 2	40	110	Intermittent stall; stresses above steady-state limit, wall bleed at mean rate
110	86.57	1 1	44	67	Abrupt stall observed with stresses of 13,500 psi which were above the steady-state limit

Table IVa.

Blade element performance for complete stage.

OPTIMUM BLEED						
STATION 1 - STATION 2						
	10	30	50	70	90	
DIA 1	29.159	27.080	25.060	23.020	20.932	
DIA 2	29.089	27.302	25.516	23.730	21.544	
BETA 1	19.021	21.559	22.850	24.764	27.244	
BETA 2	34.553	36.462	39.879	40.664	42.485	
BETA(PRI) 1	56.109	52.581	43.986	38.743		
BETA(PRI) 2	47.642	40.981	32.763	24.724	15.669	
V 1	364.63	370.87	378.27	385.30	388.50	
V 2	428.88	457.82	487.40	513.41	539.26	
VZ 1	344.72	346.92	348.58	345.87	345.40	
VZ 2	353.20	368.20	374.03	391.04	397.94	
V-THETA 1	118.84	116.28	116.89	117.39	117.85	
V-THETA 2	243.27	272.08	312.51	337.65	364.23	
V(PRI) 1	618.42	567.7	527.9	485.42	442.9	
V(PRI) 2	526.2	487.7	444.8	431.0	413.0	
V(THETA PRI)	513.2	450.8	396.4	337.7	277.2	
V(THETA PK2)	387.4	319.9	240.7	177.5	111.5	
U 1	632.00	587.12	543.32	495.10	455.04	
U 2	630.66	591.93	553.21	514.49	475.77	
M 1	0.3334	0.3393	0.3462	0.3578	0.3558	
M 2	0.3880	0.4152	0.4429	0.4715	0.4914	
M(PRI) 1	0.5653	0.5193	0.4832	0.4453	0.4056	
M(PRI) 2	0.4742	0.4424	0.4042	0.3922	0.3764	
TURN(PRI)	8.466	11.601	15.912	19.762	23.079	
LOSS CUEF.	0.0881	0.0537	0.0474	0.0608	0.0600	
DFAC	0.2237	0.2170	0.2179	0.2076	0.1648	
EFFP	0.8318	0.8098	0.9329	0.9311	0.9443	
EFF	0.8298	0.9087	0.9320	0.9301	0.9435	
LCS PARA.	0.0209	0.0134	0.0122	0.0157	0.0151	
INC ID	-3.49	-4.32	-5.02	-5.81	-6.25	
DEV	2.542	2.181	1.963	3.524	6.959	
CORRECTED WEIGHT FLOW						
H 2	0.3880	0.4152	0.4429	0.4715	0.4914	UPSTREAM OF ROTOR
H 3	0.2822	0.2922	0.3081	0.3211	0.3036	66.25
TURN	39.864	41.769	45.885	46.321	48.316	UPSTREAM OF STATOR
LOSS COEF.	0.0309	0.0367	0.0302	0.0430	0.1033	66.25
DFAC	0.5228	0.5393	0.5490	0.5471	0.5968	DOWNSTREAM OF STATOR
LOSS PARA.	0.0123	0.0138	0.0106	0.0140	0.0310	62.73
INC ID	-17.52	-15.68	-12.82	-13.34	-13.46	
DEV	13.654	12.734	11.745	12.022	11.969	

Table IVb.

Blade element performance for complete stage.

Optimum Bleed														
PERCENT DESIGN SPEED	=	59.97	CORRECTED WEIGHT FLOW	=	61.17	CORRECTED ROTOR SPEED	=	5017.33	PRESSURE RATIO	=	1.1145	ADIABATIC EFFICIENCY	=	89.7287
ROTOR 1														
STATION 1 - STATION 2														
		10	30	50	70	90								
DIA 1		29.152	27.080	25.060	23.020	20.988								
DIA 2		29.083	27.302	25.516	23.730	21.944								
BETA 1		19.023	23.993	22.652	23.993	25.079								
BETA 2		40.374	42.131	44.552	45.997	47.375								
BETA(PR) 1		58.589	55.012	51.928	48.052	43.244								
BETA(PR) 2		46.982	41.168	33.231	24.588	15.920								
V 1		337.03	344.90	347.34	350.44	356.44								
V 2		430.45	448.39	473.18	495.75	511.84								
VZ 1		318.62	319.85	320.55	320.21	322.97								
VZ 2		327.93	332.53	337.20	344.40	346.61								
V-THETA 1		109.95	126.36	133.77	142.52	151.10								
V-THETA 2		278.83	300.79	331.56	356.59	376.62								
V(PR) 1		611.4	560.6	519.8	479.0	443.2								
V(PR) 2		480.7	441.7	403.1	378.7	360.4								
VTHETA PR1		521.8	460.4	409.2	356.3	303.7								
VTHETA PR2		351.4	290.8	220.9	157.6	98.3								
U 1		631.62	586.77	543.00	498.79	454.77								
U 2		630.27	591.58	552.88	514.18	475.48								
M 1		0.3080	0.3145	0.3177	0.3206	0.3262								
M 2		0.3884	0.4056	0.4286	0.4697	0.4656								
M(PR) 1		0.5585	0.5126	0.4756	0.4882	0.4056								
M(PR) 2		0.4337	0.3996	0.3452	0.3435	0.3274								
TURN(PR)		11.607	14.044	18.697	23.464	27.324								
LOSS COEF.		0.0338	0.0338	0.0407	0.0529	0.0729								
DFAC		0.3123	0.3119	0.3356	0.3712	0.3071								
EFF P		0.9083	0.9550	0.9538	0.9494	0.9390								
EFF		0.9074	0.9542	0.9530	0.9485	0.9340								
LOSS PARA.		0.0164	0.0084	0.0105	0.0137	0.0192								
INCID		-1.01	-1.69	-1.77	-1.75	-1.76								
DEV		1.882	2.364	2.431	3.488	7.220								
CORRECTED WEIGHT FLOW														
STATION 2 - STATION 3														
		10	30	50	70	90								
DIA 3		27.422	25.672	23.874	22.034	20.988								
BETA 2		42.131	44.552	45.997	47.376	49.744								
BETA 3		5.831	-4.956	-5.481	-6.180	-6.005								
V 1		43C.45	448.39	473.18	495.75	511.84								
V 2		289.54	305.38	310.24	312.20	302.92								
V 3		327.93	332.53	337.20	344.40	346.61								
VZ 2		288.04	304.24	308.82	310.39	301.26								
VZ 3		278.93	300.79	331.96	356.59	376.62								
V-THETA 2		-29.41	-26.38	-29.63	-33.61	-31.69								
V-THETA 3		0.3884	0.4056	0.4286	0.4497	0.4650								
M 1		0.2591	0.2739	0.2784	0.2802	0.2715								
M 2		46.204	47.087	50.033	52.177	53.382								
FURN		0.1271	0.0609	0.0616	0.0654	0.0738								
LOSS COEF.		0.61149	0.5939	0.6131	0.6276	0.6492								
DFAC		0.0508	0.0229	0.0216	0.0213	0.0222								
LOSS PARA.		-11.71	-10.04	-8.15	-8.00	-8.00								
INCID		13.129	13.084	12.269	11.500	11.795								
DEV		0.2591	0.2739	0.2784	0.2802	0.2715								
UPSTREAM OF ROTOR														
UPSTREAM OF STATOR														
		10	30	50	70	90								
		10	30	50	70	90								
DOWNSTREAM OF STATOR														
		10	30	50	70	90								

Table IV.C.

Blade element performance for complete stage.

	OPTIMUM BLEED					
PERCENT DESIGN SPEED = 60.02	CORRECTED WEIGHT FLOW = 57.57	CORRECTED ROTOR SPEED = 5021.55	PRESSURE RATIO = 1.1262			
ADIABATIC EFFICIENCY = 87.7723						
ROTOR 1						
STATION 1 - STATION 2						
	10	30	50	70		
DIA 1	29.153	27.080	25.060	23.020		
DIA 2	29.083	27.302	25.514	23.740		
BETA 1	19.965	21.736	22.959	24.957		
BETA 2	44.009	46.114	48.749	50.420		
BETA(PR) 1	63.873	58.632	54.262	45.875		
BETA(PR) 2	46.615	41.500	32.865	24.359		
V 1	312.65	310.11	325.54	324.65		
V 2	433.33	443.89	469.88	485.93		
VZ 1	295.48	288.36	292.75	296.47		
VZ 2	311.41	307.72	309.92	313.03		
V-THETA 1	1C1.62	114.84	126.99	132.31		
V-THETA 2	301.11	319.92	353.27	380.28		
V(PR) 1	607.5	553.4	513.2	471.8		
V(PR) 2	453.9	410.9	368.9	339.9		
VTHETA PR1	530.6	472.5	416.6	367.0		
VTHETA PR2	329.9	272.2	200.2	140.2		
U 1	632.25	587.36	543.54	499.30		
U 2	630.91	592.17	553.43	514.70		
M 1	0.2853	0.2830	0.2973	0.2991		
M 2	0.3893	0.4003	0.4246	0.4525		
M(PR) 1	0.5544	0.5050	0.4687	0.3967		
M(PR) 2	0.4083	0.3705	0.3333	0.2943		
TURN(PR)	14.257	17.132	21.397	31.398		
LOSS COEF.	0.0677	0.0349	0.0420	0.0701		
STATION 2 - STATION 3						
	10	30	50	90		
DIA 3	27.422	23.672	23.874	22.034		
BETA 2	46.114	48.749	50.420	51.196		
BETA 3	-4.255	-4.781	-5.481	-5.306		
V 2	433.39	443.89	469.88	485.93		
V 3	285.15	295.03	296.34	282.17		
VZ 2	311.71	307.72	309.82	313.03		
VZ 3	284.36	292.01	294.98	280.96		
V-THETA 2	319.92	353.27	374.52	389.28		
V-THETA 3	-21.16	-24.42	-28.31	-26.09		
M 2	0.3899	C.4003	0.4246	0.4399		
M 3	0.2544	0.2620	0.2651	0.2523		
TURN	48.264	50.895	54.230	55.726		
LOSS COEF.	0.1284	0.0547	0.0626	0.0791		
DFAC	0.6407	C.6321	0.5549	0.6889		
LOSS PARA.	0.0514	0.0206	0.0219	0.0258		
INC10	-8.37	-6.03	-3.95	-3.58		
DEV	14.705	13.259	12.269	11.271		
CORRECTED WEIGHT FLOW						
			UPSTREAM OF ROTOR	57.57		
			UPSTREAM OF STATOR	57.57		
			DOWNSTREAM OF STATOR	53.84		

Table IVd.

Blade element performance for complete stage.

Optimum Bleed						
	PERCENT DESIGN SPEED = 59.9%	CORRECTED WEIGHT FLOW = 52.97	CORRECTED ROTOR SPEED = 5014.92	PRESSURE RATIO = 1.1438	ADIABATIC EFFICIENCY = 89.8999	ROTOR 1
STATION 1 - STATION 2						
	10	30	50	70	90	
DIA 1	29.150	27.080	25.060	23.020	20.998	
DIA 2	29.098	27.302	25.516	23.730	21.944	
BETA 1	18.979	22.192	24.748	26.570	25.855	
BETA 2	49.574	50.304	52.560	52.480	53.357	
BETA(PR) 1	62.056	60.028	56.927	53.337	49.455	
BETA(PR) 2	45.734	39.308	31.474	23.197	13.341	
V 1	29.127	29.58	30.132	29.665	30.574	
V 2	444.28	457.35	474.29	486.81	503.90	
V 2 1	275.52	279.29	277.98	272.30	275.17	
V 2 2	293.96	288.43	295.48	300.57		
V-THETA 1	34.443	102.71	116.51	125.07	123.33	
V-THETA 2	333.13	350.37	376.59	384.11	404.37	
V(PR) 1	503.3	559.1	509.2	462.6	423.2	
V(PR) 2	418.2	380.4	338.1	323.0	309.3	
VTHETA PR1	531.4	494.3	426.7	373.9	321.6	
VTHETA PR2	297.4	176.5	129.3	71.1		
U 1	631.47	587.00	542.22	490.00	454.05	
U 2	630.53	591.81	553.10	515.39	475.67	
W 1	0.2654	0.2712	0.2746	0.2731	0.2787	
W 2	0.3996	0.4116	0.4276	0.4294	0.4552	
W(PR) 1	0.0502	0.5095	0.4641	0.4216	0.3850	
W(PR) 2	0.3752	0.3423	0.3048	0.2717	0.2792	
STATOR 2 - STATION 3						
	10	30	50	70	90	
DIA 3	27.422	25.672	23.874	22.034	20.640	
BETA 2	50.004	52.480	53.367	0.04930	0.0377	0.0216
BET ^a 3	-10.079	-6.355	-5.306	0.4477	0.4623	0.4525
V 2	44.128	451.35	474.29	0.01013	0.9574	0.9400
V 3	283.00	300.93	291.01	0.9565	0.9560	0.9387
V 2 2	293.58	291.96	288.33	0.0221	0.0105	0.0096
V 2 3	278.63	290.08	290.21	0.0105	0.0099	0.0095
V-THETA 2	333.13	250.37	376.59	3.25	3.13	4.14
V-THETA 3	-49.53	-32.31	-21.59	-24.55	-2.52	4.64
H 2	0.3985	0.4116	0.4276	0.4553	0.4741	0.4944
H 3	0.2516	0.2684	0.2796	0.2367	0.2014	0.1944
TURN	58.465	56.059	5.6	57.786	58.674	
LOSS COEF.	0.1320	C _c 0.006	0.16	0.05040	0.1554	
DFAC	0.7099	C _c 0.581	0.16	0.7206	0.8061	
LOSS PARA.	0.0522	0.0189	0.0219	0.0306	0.0469	
INCID	-2.51	-2.14	-C _c 1.1	-1.52	-2.52	
DEV	8.481	11.585	13.495	12.374	12.494	
CORRECTED WEIGHT FLOW						
UPSTREAM OF ROTOR						
TURN STREAM OF STATOR						52.97
LOSS STREAM OF STATOR						52.97
DOWNSTREAM OF STATOR						49.15

Table IVe.

Blade element performance for complete stage.

Optimum Bleed

PERCENT DESIGN SPEED = 59.9;

CORRECTED WEIGHT FLOW = 48.76

CRECTED ROTOR SPEED = 5012.28

PRESSURE RATIO = 1.1525

ADIABATIC EFFICIENCY = 92.0855

Knotor 1

		STATION 1 - STATION 2						
		10	30	50	70	90		
DIA 1	23.153	27.081	25.060	23.020	20.989			
DIA 2	29.089	27.302	23.516	21.946				
BETA 1	19.024	21.095	22.647	24.757	25.767			
BETA 2	54.803	53.510	55.515	56.517	55.943			
BETA(PR) 1	55.863	53.215	60.207	57.351	53.672			
BETA(PR) 2	46.581	39.960	32.100	27.789	12.227			
V 1	259.24	265.63	271.89	271.56	274.10			
V 2	441.73	454.07	463.57	497.23	500.21			
VZ 1	245.08	247.83	250.84	246.60	247.03			
VZ 2	254.57	270.04	265.30	266.04	270.81			
V-THETA 1	94.50	95.60	106.66	113.72	119.22			
V-THETA 2	350.99	365.07	386.23	417.20	414.55			
V(PRI) 1	599.3	569.3	504.9	457.1	416.5			
V(PRI) 2	170.4	352.3	313.2	288.6	288.2			
VTHETA PR1	546.3	490.9	419.1	394.9	335.4			
VTHETA PR2	263.1	226.3	166.4	111.8	50.6			
U 1	631.35	586.53	542.78	498.55	454.59			
U 2	630.02	591.34	552.45	513.97	475.22			
U 3	0.2354	0.2418	0.2475	0.2472	0.2498			
M 1	0.3947	0.4077	0.4214	0.4246	0.4215			
M 2	0.5453	0.5005	0.4595	0.4162	0.3733			
M 3	0.3403	0.3163	0.2817	0.2601	0.2514			
TURN(PH)	19.279	23.254	29.107	34.563	41.328			
LOSS COEF.	0.1844	1.0747	0.0858	0.0460	0.0114			
DFAC	0.5454	0.5182	0.4477	0.4474	0.4844			
EFFP	0.9258	0.9314	0.9307	0.9543	0.9667			
EFF	0.4218	0.4218	0.4218	0.4218	0.4218			
LOSS PARA.	0.0447	0.0447	0.0447	0.0447	0.0447			
INCID	6.24	6.31	6.51	7.55	8.62			
DEV	1.481	1.481	1.481	1.481	1.481			

		CORRECTED WEIGHT FLOW						
		UPSTREAM OF ROTOR	UPSTREAM OF STATOR	UPSTREAM OF STATOR	DOWNSTREAM OF STATOR	DOWNSTREAM OF STATOR		
DIA 3	29.154	27.422	25.672	23.874	22.034			
BETA 2	54.803	53.510	55.515	56.517	55.988			
BETA 3	-1.515	-13.679	-10.439	-7.634	-7.756			
V 2	441.73	454.09	468.57	482.23	500.23			
V 3	296.61	258.28	275.75	271.06	265.93			
VZ 2	250.57	270.04	265.10	266.04	279.81			
VZ 3	290.64	250.95	271.19	268.46	262.49			
V-THETA 2	366.99	365.07	386.23	402.20	414.65			
V-THETA 3	-59.21	-61.48	-49.96	-37.42	-35.89			
H 2	0.3947	0.4077	0.4214	0.4346	0.4515			
H 3	0.2627	0.2292	0.2452	0.2412	0.2365			
TURN	6.324	6.189	6.593	6.451	6.744			
LOSS COEF.	0.1059	0.0923	0.0747	0.0745	0.0745			
DFAC	0.7106	0.7848	0.7368	0.7360	0.7405			
LOSS PARA.	0.0429	0.0611	0.0319	0.0242	0.0223			
INCID	2.73	1.37	2.42	2.52	2.04			
DEV	7.445	4.361	7.312	9.746	10.044			

Table IVf.

Blade element performance for complete stage.

	Optimum			Bladed		
	10	30	50	70	90	
PERCENT DESIGN SPEED =	79.99					
CORRECTED WEIGHT FLOW =	84.27					
CORRECTED ROTOR SPEED =	4684.70					
PRESSURE RATIO =	1.1575					
ADIABATIC EFFICIENCY =	82.6912					
ROTOR 1						
STATION 1 - STATION 2						
DIA 1	29.153	27.080	25.060	23.020	20.988	
DIA 2	23.088	27.332	25.216	23.730	21.946	
BETA 1	20.707	21.921	23.988	25.012	25.793	
BETA 2	36.145	37.776	40.265	42.249	43.634	
BETA(PRI) 1	56.378	52.777	49.678	39.482	39.482	
BETA(PRI) 2	47.381	40.694	33.013	23.013	14.012	
V 1	499.35	501.90	512.74	524.25	525.97	
V 2	595.79	624.34	659.86	701.50	722.30	
V 2 1	457.74	455.61	468.00	475.35	474.46	
V 2 2	473.03	493.35	515.76	515.27	527.74	
V-THETA 1	173.03	187.37	190.25	221.78	223.29	
V-THETA 2	345.51	342.62	427.36	4.1.65	438.45	
V(PRI) 1	326.7	769.7	708.8	660.4	614.8	
V(PRI) 2	698.5	650.6	599.6	567.8	543.9	
V(THETA PRI)	598.4	612.9	532.3	458.5	390.9	
V(THETA PR2)	514.1	424.2	326.7	229.6	150.1	
U 1	851.41	900.74	740.55	640.27	620.27	
U 2	859.58	906.80	754.02	701.25	649.47	
M 1	0.4412	0.4530	0.4527	0.4743	0.4743	
M 2	0.5185	0.5552	0.5882	0.5276	0.6477	
M(PRI) 1	0.7453	0.6966	0.6402	0.5972	0.5557	
M(PRI) 2	0.6194	0.5785	0.5345	0.5079	0.4977	
TURN(PRI)	4.997	12.047	15.665	20.113	23.477	
LOSS COEF.	0.0815	0.0421	0.0491	0.0246	0.0474	
DIA 2	23.034	22.034	0.2293	0.2356	0.2431	0.2174
BETA 1	42.249	43.638	EFFAC	0.9344	0.9355	0.9553
BETA 2	-5.056	-5.056	EFFP	0.9575	0.9730	0.9730
V 2	624.34	579.86	EFF	0.8544	0.9319	0.9539
V 3	426.70	466.56	LOSS PARA.	0.0195	0.0175	0.0112
V 2 2	473.03	493.35	LNCID	-3.22	-4.12	-5.02
VZ 3	421.44	464.81	DEV	2.291	1.888	2.213
V-THETA 2	345.51	362.62				
V-THETA 3	-66.79	-40.31				
M 2	0.5185	0.5552				
M 3	0.3129	0.4098				
TURN	45.151	42.752				
LOSS COEF.	0.1186	0.0552				
DFAC	0.5542	0.5080				
LOSS PARA.	0.0462	0.0207				
INCLD	-15.93	-14.34				
DEV	13.084	12.269				
CORRECTED WEIGHT FLOW						
UPSTREAM OF ROTOR	96.27					
DOWNSTREAM OF STATOR	84.27					
A1.03						

Table IVg.

Blade element performance for complete stage.

	Optimum Bleed			
	STATION 1 - STATION 2			
PERCENT DESIGN SPEED = 90.00	10	30	50	70
CORRECTED WEIGHT FLOW = 79.51				
CORRECTED ROTOR SPEED = 6693.23				
PRESSURE RATIO = 1.2133				
ADIABATIC EFFICIENCY = 91.2435				
ROTOR 1				
DIA 1	29.150	27.040	25.040	23.020
DIA 2	29.098	27.302	25.516	23.730
BETA 1	19.291	21.647	23.124	24.357
BETA 2	41.702	44.193	46.412	48.700
BETA(PQ) 1	58.572	55.262	51.774	47.745
BETA(PR) 2	45.865	40.270	32.578	23.458
V 1	447.47	458.47	464.64	474.61
V 2	586.67	605.61	633.82	665.20
V 1	424.61	426.09	427.35	429.57
V 2	437.98	434.25	437.70	446.92
V-THETA 1	148.62	169.10	182.49	197.31
V-THETA 2	190.75	422.09	459.09	497.71
V(PRI) 1	816.3	747.7	690.7	617.4
V(PRI) 2	529.0	569.2	511.6	437.2
V(THETA PRI)	694.9	514.5	542.6	469.8
V(THETA PR2)	451.4	367.9	279.2	193.9
U 1	843.47	783.59	725.13	664.10
U 2	861.68	790.00	738.12	686.64
M 1	0.4139	0.4220	0.4279	0.4394
M 2	0.5273	0.5464	0.5735	0.6201
M(PRI) 1	0.7491	0.6891	0.6361	0.5416
M(PRI) 2	0.5654	0.5136	0.4693	0.4282
TURN(PQ)	12.705	14.932	19.200	24.287
LOSS COEF.				
DIFAC	0.3330	0.3476	0.3662	0.3845
EFF P	0.9370	0.9620	0.9664	0.9670
EFF	0.9350	0.9603	0.9653	0.9660
LOSS PARA.	0.0117	0.0080	0.0093	0.0098
INCID	-1.03	-1.64	-1.92	-1.99
VZ 2	437.98	437.00	446.92	454.69
VZ 3	370.92	408.38	419.91	419.76
V-THETA 2	390.26	422.08	459.09	492.71
V-THETA 3	-78.00	-50.52	-40.29	-36.40
H 1	0.2358	0.3661	0.5735	0.6201
H 2	0.5273	0.5464	0.6035	0.6201
H 3	0.6273	0.3758	0.3752	0.3572
TURN	53.577	51.235	51.894	52.746
LOSS COEF.	0.1913	0.0901	0.0657	0.0848
DFAC	0.6765	0.6146	0.6115	0.6518
LOSS PARA.	0.0752	0.0337	0.0230	0.0255
INCID	-10.38	-7.96	-6.29	-7.74
DEV	7.0985	13.988	12.269	12.669
UPSTREAM OF ROTOR				79.51
UPSTREAM OF STATOR				79.51
DOWNSTREAM OF STATOR				75.89

Table IVh.

Blade element performance for complete stage.

	OPTIMUM			BLADE		
	STATION 1	STATION 2	STATION 3	STATION 1	STATION 2	STATION 3
PERCENT DESIGN SPEED	= 79.86					
CORRECTED WEIGHT FLOW	= 75.51					
CORRECTED ROTOR SPEED	= 1682.22					
PRESSURE RATIO	= 1.2350					
ADIABATIC EFFICIENCY	= 90.9349					
DIA 1	29.152	27.080	25.060	23.020	20.094	19.064
DIA 2	29.084	27.302	25.516	23.730	21.964	20.303
BETA 1	19.203	21.106	23.210	24.492	26.303	27.048
BETA 2	44.733	47.013	49.050	50.061	52.084	46.203
BETA(PR) 1	61.014	57.931	54.293	50.566	46.823	
BETA(PR) 2	45.624	39.937	32.178	24.147		
V 1	414.22	423.59	432.89	437.31	442.60	
V 2	587.85	605.77	631.45	648.37	664.39	
V 2 1	391.17	396.94	397.86	397.96	400.14	
V 2 2	417.61	413.03	413.85	411.01	407.48	
V-THETA 1	136.26	153.15	170.60	181.20	189.17	
V-THETA 2	413.73	443.12	476.14	501.44	525.74	
V-(PR) 1	407.2	407.0	681.7	626.5	578.1	
V-(PR) 2	597.1	538.7	489.0	450.4	473.6	
VTHETA PR1	706.1	629.4	553.5	481.9	417.3	
VTHETA PR2	426.9	345.8	260.4	184.7	108.4	
U 1	842.33	782.51	724.14	665.19	606.48	
U 2	840.54	788.93	737.32	685.71	634.17	
M 1	0.3799	0.3976	0.3976	0.4018	0.4064	
M 2	0.5261	0.5444	0.5603	0.5861	0.6035	
M-(PR) 1	0.7404	0.6240	0.6261	0.5774	0.5314	
M-(PR) 2	0.5304	0.4841	0.4408	0.4072	0.3836	
TURN(PR)	15.390	17.054	22.115	26.420	31.380	
STATOR 1						
STATION 2 - STATION 3						
10	30	50	70	90		
DIA 3	29.164	27.422	25.672	23.874	22.034	0.0412
BETA 2	44.733	47.013	49.050	50.661	52.086	DFAC
BETA 3	-9.900	-6.878	-5.131	-5.656	-9.184	EFFP
V 2	587.85	605.77	631.45	648.37	666.39	EFF
V 3	372.53	387.48	390.12	372.40	345.30	LOSS PARA.
V 2 2	417.61	413.03	413.85	411.01	409.48	INCID
V 2 3	366.99	384.69	388.55	370.59	340.87	DEV
V-THETA 2	413.73	443.12	476.92	501.46	525.74	CORRECTED WEIGHT FLOW
V-THETA 3	-64.05	-46.40	-34.89	-36.70	-55.11	
M 2	0.561	0.5444	0.5693	0.5861	0.6035	UPSTREAM OF ROTOR
M 3	0.282	0.3429	0.3297	0.3052	0.2720	UPSTREAM OF STATOR
TURN	54.633	53.890	54.181	56.317	61.270	75.51
LOSS COEF.	0.1725	0.1687	0.0911	0.0904	0.1064	DOWNSHIFT OF STATOR
DFAC	0.6927	0.6648	0.6672	0.6571	0.7452	71.72
LOSS PARA.	0.0682	0.0406	0.0319	0.0294	0.0317	
INCID	-7.35	-5.13	-3.65	-3.34	-3.86	
DEV	9.060	11.162	12.619	12.024	8.616	

Table IVi.

Blade element performance for complete stage.

	Optimum Blade		
	STATION 1 - STATION 2	STATION 1	STATION 2
PERCENT DESIGN SPEED = 70.94			
CORRECTED WEIGHT FLOW = 70.16			
CORRECTED ROTOR SPFED = 5688.98			
PRESSURE RATIO = 1.2574			
ADIABATIC EFFICIENCY = 86.7177			
ROTOR 1			
	10	30	50
DIA 1	29.150	27.040	25.040
DIA 2	29.088	27.302	25.516
BETA 1	19.200	21.436	22.540
BETA 2	49.112	51.016	53.450
RETA 1	62.293	59.808	56.829
RETA 2	44.644	39.773	33.469
V 1	396.64	198.71	402.67
V 2	600.13	607.24	616.79
VZ 1	374.39	371.13	371.58
VZ 2	392.98	392.02	367.31
V-THETA 1	130.39	145.71	155.13
V-THETA 2	453.63	472.02	495.49
V(PRI) 1	805.4	738.0	680.4
V(PRI) 2	552.1	497.0	440.3
VTHETA PR1	713.1	637.9	570.0
VTHETA PR2	348.3	318.0	247.8
U 1	847.47	783.58	171.95
U 2	841.68	790.00	738.22
M 1	0.3631	0.3652	0.3689
M 2	0.5469	0.5433	0.5335
M(PRI) 1	0.7376	0.6759	0.6524
M(PRI) 2	0.4422	0.4447	0.3957
TURN(PRI)	17.055	20.035	23.431
LOSS COEF.	0.0761	0.0747	0.0701
DFAC	0.4663	0.4695	0.5004
EFF P	0.9215	0.9552	0.9546
EFF	0.9415	0.9536	0.9473
LOSS PARA.	0.0191	0.0120	0.0108
INC10	2.73	2.91	2.70
DEV	-0.455	0.973	2.649
CORRECTED WEIGHT FLOW			
	10	30	50
DIA 3	29.164	27.422	25.672
BETA 2	49.112	51.016	53.450
BETA 3	-18.020	-10.438	-4.956
V 2	354.98	373.85	371.08
V 3	392.84	382.02	367.31
VZ 2	337.47	325.66	369.69
VZ 3	453.69	472.02	495.49
V-THETA 2	-105.78	-67.73	-32.06
V-THETA 3	0.5349	0.5433	0.5535
H 2	0.3106	C.3288	0.3268
H 3	67.132	61.453	58.406
TURN	0.2146	0.1120	0.0565
LOSS COEF.	0.7857	0.7193	0.6991
DFAC	0.0820	0.0415	0.0198
LOSS PARA.	-2.97	-1.12	0.75
INC10	7.602	12.794	12.724
DEV	0.940	10.922	10.924
UPSTREAM OF ROTOR			
	10	30	50
TURN	62.648	62.648	62.648
LOSS COEF.	0.1652	0.1652	0.1652
DFAC	0.8649	0.8649	0.8649
LOSS PARA.	1.0496	1.0496	1.0496
INC10	-0.14	-0.14	-0.14
DEV	10.922	10.922	10.922
UPSTREAM OF STATOR			
	10	30	50
TURN	61.157	61.157	61.157
LOSS COEF.	0.0904	0.0904	0.0904
DFAC	0.4795	0.4795	0.4795
LOSS PARA.	0.9414	0.9414	0.9414
INC10	4.543	4.543	4.543
DEV	4.543	4.543	4.543
DOWNSTREAM OF STATOR			
	10	30	50
TURN	61.157	61.157	61.157
LOSS COEF.	0.0904	0.0904	0.0904
DFAC	0.4795	0.4795	0.4795
LOSS PARA.	0.9414	0.9414	0.9414
INC10	4.543	4.543	4.543
DEV	4.543	4.543	4.543

Table IVj.

Blade element performance for complete stage.

		Optimum <i>Beta</i>					
		10	30	50	70	90	
PERCENT DESIGN SPEED	= 79.90	DIA 1	29.151	27.080	25.060	24.020	20.980
CORRECTED WEIGHT FLOW	= 64.95	DIA 2	29.089	27.302	25.516	23.739	21.944
CORRECTED ROTOR SPEED	= 6685.57	BETA 1	19.627	21.914	22.895	25.070	25.669
PRESSURE RATIO	= 1.2774	BETA 2	53.623	53.744	55.691	56.632	56.751
ADIABATIC EFFICIENCY	= 82.91% R	BETA(PR) 1	65.736	62.496	59.865	59.193	
		BETA(PR) 2	45.187	40.325	33.476	23.938	12.751
		V 1	354.336	363.338	366.715	375.112	380.600
		V 2	599.93	603.45	615.90	636.47	660.77
		VZ 1	333.15	337.12	337.96	339.78	343.06
		VZ 2	355.92	356.88	347.16	350.06	362.25
		V-THETA 1	120.79	135.62	142.68	158.95	164.85
		V-THETA 2	481.02	486.61	508.74	531.55	552.54
		V(PR) 1	795.3	730.0	673.0	610.1	559.4
		V(PR) 2	504.3	668.1	416.0	382.7	371.4
		V(THETA) PR1	722.2	647.5	582.0	504.7	442.4
		V(THETA) PR2	358.2	302.9	229.1	154.7	82.0
		U 1	842.96	783.10	724.69	665.70	606.91
		U 2	841.17	789.52	737.87	646.23	574.54
		M 1	0.3237	0.3321	0.3353	0.3431	0.3487
		M 2	0.5309	0.5384	0.5511	0.5712	0.5944
		M(PR) 1	0.6265	0.6672	0.6152	0.5580	0.5120
		M(PR) 2	0.6467	0.6176	0.3722	0.1435	0.3346
		TURN(PR)	20.049	22.171	26.439	32.319	39.424
		LOSS COEFF.	0.1758	0.0587	0.0601	0.0740	0.0796
		DFAC	0.5266	0.5145	0.5427	0.5317	0.5048
		EFP	0.8447	0.9494	0.9547	0.9516	0.9531
		EFF	0.8182	0.9464	0.9506	0.9476	0.9513
		LOSS PARA.	0.0447	0.0148	0.0144	0.0192	0.0260
		INCID	5.64	5.60	5.60	5.36	7.19
		DEV	2.087	1.525	2.626	3.138	4.361
CORRECTED WEIGHT FLOW							
DIA 3	23.164	27.422	25.672	23.874	22.034	UPSTREAM OF ROTOR	64.05
BETA 2	53.623	53.744	55.691	56.632	56.150	UPSTREAM OF STATOR	64.05
BETA 3	-10.376	-10.617	-19.460	-23.960	-11.335	DOWNSTREAM OF STATOR	50.05
V 2	599.93	603.45	615.90	636.47	660.70		
V 3	411.25	338.50	356.32	356.90	345.27		
VZ 2	355.82	356.88	347.16	350.06	362.26		
VZ 3	403.72	232.71	234.07	326.14	336.53		
V-THETA 2	483.02	486.61	508.74	531.55	552.54		
V-THETA 3	-78.30	-62.37	-118.04	-144.94	-61.86		
M 2	0.5308	0.5384	0.5511	0.5712	0.5948		
M 3	0.3588	0.2958	0.3107	0.3135	0.3033		
TURN	64.599	64.361	75.151	80.592	68.045		
LOSS COEFF.	0.1379	0.2092	0.1138	0.0847	0.0887		
DFAC	0.6903	0.7818	0.7826	0.7868	0.7611		
LOSS PARA.	0.0544	0.0775	0.0377	0.0263	0.0263		
INCID	1.54	1.60	2.99	2.63	0.80		
DEV	7.984	7.423	-1.710	-6.280	6.4e5		

Table IVk.

Blade element performance for complete stage.

		Optimum Bleed			
		STATION 1 - STATION 2	STATION 1	STATION 2	STATION 3
		10	30	50	70
DIA 1	29.150	27.080	25.060	23.070	20.930
DIA 2	29.038	27.362	25.516	23.720	21.944
BETA 1	20.407	21.924	23.678	23.383	25.674
BETA 2	30.151	38.169	40.783	42.349	43.393
DETA(PK) 1	55.645	52.236	48.313	44.364	38.152
DETA(PK) 2	47.844	+0.505	32.876	24.621	16.659
V 1	554.09	563.67	572.75	581.42	588.12
V 2	641.87	692.26	730.20	764.35	783.17
VZ 1	519.11	522.91	524.53	533.67	52.5.94
VZ 2	518.29	544.25	552.91	566.10	57.6.31
V-THETA 1	193.75	210.47	230.02	230.75	24.6.31
V-THETA 2	378.05	+27.80	476.96	516.45	54.6.97
V(PK) 1	919.9	953.8	789.0	746.5	693.4
V(PK) 2	772.2	715.8	658.3	622.8	601.5
VTHETA PK1	759.4	675.0	589.4	522.0	431.5
VTHETA PK2	572.5	+64.9	257.4	172.4	
J 1	953.15	d85.47	819.42	752.71	68.5.27
J 2	951.13	892.73	834.33	775.93	71.7.51
M 1	0.5117	0.5117	0.5210	0.5384	0.5443
M 2	0.5775	0.6205	0.6268	0.6639	0.6955
M(PRI) 1	0.8495	0.7893	0.7300	0.6912	0.6332
M(PRI) 2	0.6949	0.6481	0.5986	0.5685	0.5537
TURB(PK)	7.801	11.711	15.457	19.743	22.483
LCLS CDEF.	0.1249	0.0712	0.0492	0.0302	0.0253
UFAC	0.2322	0.2429	0.2558	0.2656	0.2183
EFF P	0.7906	0.8935	0.8957	0.9657	0.9759
LCLS PARA.	0.7851	0.8904	0.9344	0.9645	0.9751
INCLU	-3.96	-4.66	-5.37	-5.44	-5.85
DEV	2.744	1.705	2.076	3.921	7.959
CORRECTED WEIGHT FLOW					
H 1	0.6639	0.6555	0.7261	92.13	
H 2	0.5776	0.6284	0.6555	92.13	
H 3	0.4126	0.4561	0.4777	92.13	
TURN	46.230	43.050	46.439	92.13	
LCLS CDEF.	0.1297	0.0923	0.0699	92.13	
UFAC	0.5617	0.5193	0.5213	92.13	
LCLS PARA.	0.0316	0.0316	0.0301	92.13	
INCLU	-15.41	-12.97	-11.92	92.13	
DEV	8.884	12.559	12.094	92.13	

Table IVI.

Blade element performance for complete stage.

				<i>Optimum</i>	<i>Blown</i>
PERCENT BLISK SPAN =	50.00				
CHAMFERED WINGLET FLOW =	0.70.20				
CHAMFERED FUTTER SPL. ₀ = 75.3<math>\times 10^3					
FREQUENCY RATIO =	1.2723				
AEROSOL EFFICIENCY = 13.5346					
STATION 1 - STATION 2					
		10	30	50	70
DIA 1	20.159	27.040	25.040	23.020	20.984
DIA 2	27.043	27.302	25.216	23.730	21.944
BETA 1	14.649	21.284	23.753	25.205	25.439
BETA 2	42.795	43.569	46.379	44.211	44.897
BETA(PK) 1	53.363	54.971	51.208	47.034	47.459
BETA(PK) 2	47.021	49.625	32.923	24.184	16.524
V 1	510.84	522.96	531.29	546.13	
V 2	650.25	680.58	712.34	742.17	750.21
V 3	431.10	487.29	486.28	447.14	493.23
V 4	444.47	492.29	491.43	494.57	493.41
V-THETA 1	171.77	139.43	214.00	229.20	254.61
V-THETA 2	446.57	459.94	515.68	553.37	573.77
V(PK) 1	317.2	846.9	776.2	714.7	658.5
V(PK) 2	697.7	648.6	585.2	542.2	494.2
V(BETA) PK1	780.3	695.2	605.0	523.0	451.3
V(BETA) PK2	502.1	422.3	318.2	222.1	143.4
U 1	952.64	884.99	818.58	752.31	685.93
U 2	950.57	952.25	833.38	775.51	717.15
M 1	0.4705	0.4822	0.4902	0.4971	0.5049
M 2	0.5835	0.6106	0.6619	0.6714	0.6803
M 3	0.8447	0.7827	0.7162	0.6596	0.6177
M 4	0.4821	0.6229	0.5820	0.5276	0.4572
M 5	0.4822	0.6229	0.5820	0.5276	0.4572
TURN(PK) 1	12.342	14.346	18.265	22.844	25.930
TURN(PK) 2	12.342	14.346	18.265	22.844	25.930
LOSS CUEF.	0.0568	0.0393	0.0255	0.0165	0.0554
JFAC	0.3465	0.3465	0.3591	0.3657	0.3657
EFF	0.9295	0.9541	0.9757	0.9861	0.9549
EFF	0.9295	0.9541	0.9757	0.9861	0.9549
LSS PARA.	0.9257	0.9523	0.9747	0.9855	0.9571
LSS PARA.	0.0139	0.0100	0.0063	0.0043	0.0161
INC 1	-1.24	-1.93	-2.49	-2.77	-2.54
INC 2	0.921	1.825	2.123	3.488	7.824
CUTRECTED WINGLET FLOW					
UPSTREAM OF FUTTOR					
DIA 3	29.164	27.422	25.672	23.034	20.50
BETA 2	42.756	43.065	46.379	49.625	
BETA 3	-1.4950	-6.878	-5.131	-10.258	
V 2	66.0.25	70.58	74.2.34	750.21	
V 3	429.43	447.18	463.90	458.65	
V 2	484.47	492.29	491.43	494.57	
V 2	516.58	443.50	462.04	455.56	
V-THETA 2	446.57	465.54	515.68	533.37	513.70
V-THETA 3	-96.39	-53.55	-41.49	-43.75	-76.41
M 2	0.5855	0.6168	0.6419	0.6714	0.6033
M 3	0.2767	0.2936	0.4693	0.4400	0.3779
TURN	55.753	52.247	51.510	53.592	60.140
LSS CUEF.	0.0575	0.0184	0.0877	0.0558	0.0699
JFAC	0.6803	0.6238	0.6238	0.6459	0.6899
LSS PARA.	0.6724	0.6443	0.0307	0.0303	0.0226
INC 1	-5.28	-6.47	-6.32	-5.79	-6.07
INC 2	11.162	12.615	12.199	12.542	

Table IVm.

Blade element performance for complete stage.

Dominant Bleed

PERCENT DESIGN SPEED = 89.30

CORRECTED WEIGHT FLOW = 82.70

CORRECTED ROTOR SPEED = 7522.33

PRESSURE RATIO = 1.3084

ADIABATIC EFFICIENCY = 88.2594

ROTOR 1

STATION 1 - STATION 2						
	10	30	*	50	70	90
UIA 1	29.150	27.060		25.060	23.020	20.94
UIA 2	29.089	27.392	25.516	23.730	21.944	
BETA 1	13.652	21.469	23.769	25.265	26.048	
BETA 2	40.414	48.869	51.132	51.585	52.622	
BETA(PKA) 1	60.457	57.431	56.028	50.011	45.555	
BETA(PKA) 2	45.115	39.607	32.637	26.304	15.324	
V 1	475.93	484.53	491.26	494.96	505.06	
V 2	659.82	686.38	705.07	730.98	744.24	
VZ 1	448.21	450.96	449.59	451.22	453.57	
VZ 2	461.80	451.69	442.45	454.15	451.41	
V-THETA 1	160.06	177.36	198.00	212.95	227.18	
V-THETA 2	495.18	516.98	543.96	572.75	591.41	
V(PKA) 1	909.0	837.7	765.4	702.1	677.7	
V(PKA) 2	654.4	586.0	525.4	474.5	428.5	
V(THETA) PKA	790.3	706.0	619.4	538.0	462.4	
V(THETA) PAKA	463.7	373.6	283.4	201.2	124.4	
U 1	930.30	883.34	817.45	750.90	644.62	
U 2	918.84	390.59	432.32	774.06	715.31	
STATION 1						
STATION 2 - STATION 3						
	10	30	50	70	90	
UIA 3	27.442	25.672	23.874	22.034	0.426	0.4652
BETA 4	46.414	48.869	51.132	55.586	62.422	62.717
BETA 5	-12.70	-7.40	-4.781	-5.406	0.7042	0.64964
V 2	605.42	cde.38	702.07	730.98	0.5229	0.4221
V 2	442.30	421.55	426.50	413.37	335.41	17.824
VZ 2	461.30	451.45	442.45	456.19	451.81	21.391
VZ 3	387.46	398.20	425.07	411.60	334.11	26.107
V-THETA 2	485.18	516.98	548.96	572.75	591.41	0.4474
V-THETA 3	-116.38	-51.72	-35.55	-38.23	-53.53	0.4474
H 2	0.5935	L.c136	U.6326	C.6583	0.5719	0.4474
H 3	0.2510	C.3238	U.3764	C.3624	0.2528	0.253
H 3	0.2510	C.3238	U.3764	C.3624	0.2528	0.253
TURN	63.174	56.269	55.513	56.892	61.882	0.4482
LOSS CCF	U.2033	C.1556	U.0813	U.0515	J.1527	0.4482
UFAC	C.1272	U.6865	C.7678	J.8111	J.1527	0.4482
LOSS PAKA	J.04770	U.0581	J.02977	J.01670	J.01170	0.4482
INC1C	-5.57	-3.27	-1.57	-2.41	-3.33	0.21
DEV	c-2.00	10.644	12.969	12.374	8.616	4.604
UNRECTIFIED WEIGHT FLOW						
UPSTREAM OF STATION 1						52.70
UPSTREAM OF STATION 2						82.70
UNRECTIFIED OF STATION 3						78.42

Table IVn.

Blade element performance for complete stages.

	<i>Optimum Bleed</i>			
	10	30	50	90
DIA 1	29.150	27.080	25.060	23.020
DIA 2	29.089	27.302	25.516	23.770
BETA 1	19.543	21.748	23.195	25.070
BETA 2	48.872	51.670	52.934	54.115
BETA(PRI) 1	62.505	59.674	56.475	52.655
BETA(PRI) 2	46.332	40.941	33.413	25.298
V 1	441.37	440.20	457.01	462.73
V 2	655.13	674.48	693.37	705.00
VZ 1	415.89	420.26	420.07	420.17
VZ 2	430.91	418.31	418.99	411.01
V-THETA 1	147.79	166.37	190.00	207.61
V-THETA 2	493.47	529.10	552.53	576.58
V(PRI) 1	820.9	826.4	760.6	685.8
V(PRI) 2	524.1	555.5	501.8	454.6
V THETA PQ1	799.1	713.3	634.1	545.2
V THETA PR2	451.4	357.9	276.3	104.2
U 1	946.92	879.68	814.06	747.70
U 2	944.33	886.89	828.97	770.85
M 1	0.4061	0.4135	0.4210	0.4264
M 2	0.5813	0.6022	0.6221	0.6373
M(PRI) 1	0.8288	0.7507	0.7006	0.6319
M(PRI) 2	0.5537	0.4914	0.4502	0.4092
TURN(PRI)	16.173	19.133	23.063	27.355
LOSS COEF.	0.0903	0.0961	0.0202	0.0362
DFAC	0.4433	0.4759	0.4845	0.4224
EFFD	0.9099	0.9580	0.9860	0.9545
EFF	0.9055	0.9660	0.9829	0.9545
LOSS PARA.	0.0221	0.0116	0.0052	0.0093
INC10	2.91	2.77	2.78	2.85
TEV	1.232	1.741	2.613	4.599
CUTRECTED WEIGHT FLOW				
UPSTREAM OF ROTOR	78.50			
UPSTREAM OF STATOR	78.50			
DOWNSSTREAM OF STATOR	74.52			
DIA 3	29.164	27.422	25.874	22.034
BETA 2	48.872	51.670	52.934	56.163
BETA 3	-17.840	-15.128	-5.656	-5.529
V 2	655.13	674.48	693.37	708.09
V 3	42C.49	387.20	419.48	403.59
VZ 2	430.91	418.31	418.89	411.03
VZ 3	400.28	373.79	417.83	401.74
V-THETA 2	493.47	529.10	552.53	576.58
V-THETA 3	-128.82	-101.05	-41.38	-38.55
M 2	0.5913	C.6022	0.6221	0.6313
M 3	0.3660	C.3379	0.3680	0.3561
TURN	66.712	66.798	58.490	59.997
LOSS COEF.	0.1559	0.1735	0.0892	0.0676
DFAC	0.7396	C.7779	0.6956	0.714*
LOSS PARA.	0.0596	C.0312	0.0312	0.0349
INC10	-2.21	-0.47	0.13	0.52
DEV	1.120	2.912	12.094	11.271

Table IVc.

Blade element performance for complete stage.

	Optimum Bleed			
	10	30	50	
PERCENT DESIGN SPEED = 89.90	27.080	25.060	23.020	
CORRECTED WEIGHT FLOW = 74.43	27.372	25.516	23.730	
CORRECTED ROTOR SPEED = 7521.53	21.860	22.895	24.953	
PRESSURE RATIO = 1.3515	53.922	55.050	56.986	
ADIABATIC EFFICIENCY = 82.9921	61.650	58.823	59.736	
ROTOR 1				
STATION 1 - STATION 2				
DIA 1	29.150	42.213	34.079	
DIA 2	29.089	42.052	425.98	
BETA 1	19.292	421.9	432.83	
BETA 2	52.917	660.84	686.79	
BETA(PR) 1	64.013	390.29	392.42	
BETA(PR) 2	47.159	393.59	389.16	
V 1	417.98	393.44	389.16	
V 2	652.74	393.44	389.16	
VZ 1	394.41	393.44	389.16	
VZ 2	393.59	393.44	389.16	
V-THETA 1	138.05	156.57	165.73	
V-THETA 2	520.74	534.10	562.92	
V(PR) 1	900.1	921.9	758.0	
V(PR) 2	578.8	525.4	475.0	
VTHETA PR1	800.1	723.3	649.6	
VTHETA PR2	422.4	357.3	266.2	
U 1	947.17	879.91	814.76	
U 2	945.16	887.13	829.09	
M 1	0.3838	0.3863	0.3914	
M 2	0.5163	0.5479	0.6139	
M(PR) 1	0.8667	0.7550	0.6996	
M(PR) 2	0.5113	0.4674	0.4246	
STATOR 1				
STATION 2 - STATION 3				
10	30	50	70	
DIA 3	27.422	25.672	23.874	22.034
BETA 2	53.922	55.050	56.986	57.632
BETA 3	-12.235	-11.515	-11.875	-16.036
V 2	652.74	686.79	700.63	722.30
V 3	486.85	427.55	401.26	352.36
VZ 2	393.58	389.16	393.44	381.73
VZ 3	475.79	418.23	393.19	344.82
V-THETA 2	520.74	534.10	562.92	587.51
V-THETA 3	-103.18	-90.69	-80.10	-72.51
H 2	0.5763	0.5879	0.6139	0.6284
H 3	0.4232	0.3729	0.3500	0.3069
TURN	65.153	66.157	66.565	68.861
LOSS COEF.	0.0603	0.1186	0.1489	0.1712
DFAC	0.6380	0.7086	0.7450	0.8051
LOSS PARA.	0.0237	0.0437	0.0513	0.0548
INC10	0.84	1.78	2.35	2.99
DEV	6.725	5.805	6.235	5.805
CORRECTED WEIGHT FLOW				
UPSTREAM OF ROTOR				
UPSTREAM OF STATOR				
DOWNSTREAM OF STATOR				

Table IVp.

Blade Element performance for complete stage.

<i>Optimum Beta</i>									
STATION 1 - STATION 2									
STATION 1 - STATION 2									
	10	30	50	70	90				
DIA 1	29.153	27.086	25.060	23.020	20.989				
DIA 2	29.089	27.322	25.516	23.730	21.944				
BETA 1	20.766	22.166	23.478	25.316	25.478				
BETA 2	37.253	40.477	41.954	43.161	44.065				
BETA(PRI) 1	53.716	50.269	49.869	47.832	43.460				
BETA(PRI) 2	53.046	41.520	32.817	24.749	16.276				
V 1	661.91	671.59	622.45	596.97	603.72				
V 2	665.93	763.20	821.67	859.86	896.20				
VZ 1	618.91	521.96	539.64	545.10					
VZ 2	514.16	580.54	611.06	627.21	641.97				
V-THETA 1	234.68	253.38	247.98	255.27	259.32				
V-THETA 2	390.97	495.43	569.31	588.20	673.24				
VIPRI 1	1345.8	972.7	887.5	803.9	751.1				
VIPRI 2	956.1	775.4	727.1	690.6	670.4				
VTHETA PRI 1	843.2	747.8	678.5	595.8	516.5				
VTHETA PRI 2	684.5	514.0	394.1	289.1	188.3				
U 1	1077.72	1001.19	926.51	851.09	775.94				
U 2	1075.43	1009.40	943.37	877.31	811.30				
STATOR 1									
MIPRI 1	0.9582	0.8921	0.8007	0.7315	0.6819				
MIPRI 2	0.7498	0.6884	0.6442	0.6196	0.6045				
TURN(PRI)	0.6229	0.870	1.052	2.038	2.183				
LOSS COEF.	0.3495	0.2320	0.1028	-0.0027	-0.0473				
DFAC	0.2343	0.2822	0.2492	0.2208	0.2208				
EFF	0.4016	0.6510	0.8764	1.0032	1.0432				
EFFP	0.4016	0.6510	0.8764	1.0032	1.0432				
LOSS PARA.	0.0743	0.0573	0.0265	1.0033	1.0451				
INC10	-5.88	-6.65	-3.83	-0.0006	-0.0120				
DEV	7.985	2.720	2.017	4.049	7.574				
CORRECTED WEIGHT FLOW									
STATION 2 - STATION 3									
	10	30	50	70	90				
DIA 3	29.164	27.422	25.672	23.874	22.034				
BETA 1	40.477	41.954	43.161	44.065	45.477				
BETA 2	-5.481	-6.080	-6.180	-5.128	-4.962				
BETA 3	-10.258	763.20	721.67	659.86	607.27				
V 2	645.93	656.98	621.59	580.54	543.9				
V 3	496.39	514.16	580.54	611.06	627.21				
VZ 2	488.46	553.97	620.01	503.74	506.12				
VZ 3	390.97	495.43	549.31	588.20	623.28				
V THETA 2	-88.40	-62.75	-66.22	-65.37	-136.83				
V THETA 3	0.5658	0.6776	0.7236	0.7714	0.8077				
H 2	0.4296	0.5771	0.5420	0.5291	0.4529				
H 3	47.508	45.558	46.031	49.342	59.192				
TURN	-0.0765	-0.1465	0.0662	0.1219	0.2566				
LOSS COEF.	0.5226	0.4147	0.4975	0.5423	0.6712				
DFAC	-0.0302	-0.0550	0.0211	0.0396	0.0749				
LOSS PARA.	-14.83	-11.66	-10.75	-10.84	-11.89				
INC10	12.559	13.670	11.500	2.672					
DEV	8.702								

Table IVq.

Blade element performance for complete stage.

Constant Beta

PERCENT DESIGN SPEED = 99.96

CALCULATED WEIGHT FLUX = 93.23

CALCULATED FLOW SPEED = 9363.01

PRESSURE RATIO = 1.3594

EVALUATED EFFICIENCY = 97.1155

Station 1

STATION 1 - STATION 2

	10	30	50	70	90
OMA 1	29.159	27.049	25.340	23.420	20.939
OMA 2	23.034	27.302	25.516	23.730	21.946
BETA 1	20.405	22.420	26.397	25.804	25.943
BETA 2	45.752	47.638	49.633	50.024	52.176
BETALPR 1	58.326	55.091	51.583	47.486	43.644
BETALPR 2	45.191	39.255	32.666	24.351	16.553
V 1	570.00	579.71	586.83	533.15	501.11
V 2	749.79	756.19	792.02	811.44	424.33
V 2.1	536.73	535.89	534.49	534.00	531.35
V 4.2	522.64	516.27	515.04	514.53	505.84
V-TRBL 1	195.73	221.03	254.14	284.36	
V-TRBL 2	536.37	556.13	601.62	636.16	651.19
V(P4) 1	101.44	93b.4	860.2	760.3	734.5
V(P4) 2	741.46	672.5	611.9	565.6	527.4
V(B7A) P81	36.34	767.9	673.6	582.5	507.4
V(B7A) P42	226.62	431.0	330.02	23.05	150.1
V 1	1054.81	169.01	915.24	840.74	766.52
V 2	1052.35	971.12	931.49	855.67	401.44
A 1	0.5243	0.5337	0.5402	0.5464	0.5445
W 2	0.5607	0.6801	0.7064	0.7134	0.7331
W(P4) 1	0.4929	0.8621	0.7654	0.6724	0.6771
W(P4) 2	0.6541	0.5970	0.5457	0.5064	0.4732
TURBINE	13.4192	15.235	13.417	23.412	27.414
LSS CUF	2.0545	0.0357	0.0316	0.0373	0.0391
DFAC	3.3841	3.4095	0.4112	0.4104	0.4043
CFP	0.9462	0.9640	0.9716	0.9824	0.9347
CF	0.9327	0.9621	0.9702	0.9705	0.9335
LSS P444	0.0145	0.0091	0.0062	0.0123	0.0125
INC1D	-1.27	-1.81	-2.12	-2.31	-1.41
JEV	3.001	1.755	1.386	3.354	7.484

DIRECTED FLOW

	STATION 1	STATION 2	STATION 3	STATION 4	STATION 5	STATION 6	STATION 7	STATION 8	STATION 9	STATION 10	STATION 11	STATION 12	STATION 13	STATION 14	STATION 15	STATION 16	STATION 17	STATION 18	STATION 19	STATION 20	STATION 21	STATION 22	STATION 23	
OMA 1	47.444	25.672	23.676	22.036																				
BETA 2	45.152	47.936	49.433	50.524	52.175																			
BETA 3	-11.515	-5.306	-4.781	-4.721	-4.620																			
V 4	746.78	766.15	792.02	619.44	624.39																			
V 3	624.23	586.31	450.71	475.62	426.66																			
V 2	524.93	516.27	515.06	516.53	505.59																			
V 4.3	44.10	456.34	489.30	488.79	492.44																			
V-BETA 2	52.37	56.15	60.65	636.14	651.18																			
V-BETA 3	-96.27	-46.38	-40.93	-80.31	-131.42																			
N 2	0.4667	0.7664	0.7336	0.7337	0.7337																			
N 3	0.2985	0.3561	0.5621	0.6129	0.6651																			
FLN	51.267	52.944	54.414	60.445	70.195																			
LSS CUF	0.1666	0.1767	0.1632	0.1665	0.1667																			
DFAC	0.2342	0.2711	0.2657	0.2755	0.2757																			
LSS FAN	0.0924	0.0923	0.0362	0.0343	0.0759																			
INC1C	7.645	1.6734	1.6460	7.6559	-0.220																			
JEV																								

Table IVr.

Blade element performance for complete stage.

Optimum Beta

PERCENT DESIGN SPEED = 99.71
 CORRECTED WEIGHT FLUX = 09.67
 CORRECTED ROTOR SPEED = 4342.53
 PRESSURE RATIO = 1.3982
 AERODYNAMIC EFFICIENCY = 07.7467

ROTOR 1

STATION 1 - STATION 2

	10	30	50	70	90
U1A 1	29.150	27.080	25.060	23.020	20.942
U1A 2	29.088	27.302	25.516	23.730	21.944
delta 1	23.240	22.366	24.366	25.301	25.147
delta 2	46.472	46.771	51.497	53.186	54.439
delta(PK) 1	57.282	56.983	53.752	44.557	45.315
delta(PK) 2	45.824	40.749	33.687	26.143	16.776
V 1	544.04	519.36	544.12	552.64	554.73
V 2	720.95	743.24	755.41	779.91	787.47
VZ 1	510.29	498.71	495.69	497.55	502.14
VZ 2	512.96	489.85	476.63	466.70	464.44
V-THETA 1	144.62	205.42	224.40	240.54	255.52
V-THETA 2	328.52	526.98	599.14	623.67	649.76
V(PK) 1	399.0	915.4	838.3	759.2	721.3
V(PK) 2	720.4	666.6	572.8	517.0	484.5
V(MLTA PK)	558.39	767.0	676.1	544.6	518.5
V(MLTA PK2)	516.7	422.1	317.7	227.1	149.4
U 1	1047.44	173.06	900.47	927.17	754.16
U 2	105.21	311.03	915.86	852.65	769.51
A 1	0.0534	0.5013	0.5065	0.144	0.5159
A 2	0.0593	0.6664	0.6995	0.7046	0.7240
M(PK) 1	0.6294	0.7817	0.7804	0.7166	0.6724
M(PK) 2	0.6427	0.5797	0.5458	0.4704	0.4373
TURB(PK)	13.458	15.241	20.065	23.554	28.144
LGS C.E.F.	0.0477	0.0173	0.0173	0.0173	0.0173
DFAC	0.4796	0.4143	0.4474	0.4656	0.4867
CFPP	0.9502	0.9807	0.9559	0.9711	0.9725
LFF	0.4750	0.4974	0.4952	0.4946	0.4915
LSS PAA	0.0474	0.0117	0.0052	0.0044	0.0044
INC1U	-0.32	0.03	0.05	-0.10	-0.11
DEV	0.724	1.947	2.847	3.443	3.776

CUMULATIVE WEIGHT FLUX

	ROTOR 1	STATION 1 + STATION 2	STATION 1 + STATION 2 + STATION 3	CUMULATIVE WEIGHT FLUX
U1A 3	29.154	25.674	23.074	9.0
delta 2	46.472	51.497	53.186	34.0
beta 2	-12.036	-9.035	-7.050	-1.0
V 2	728.96	743.24	765.61	778.91
V 3	458.22	455.56	474.30	450.33
VZ 2	502.04	485.85	476.03	466.10
VZ 3	440.71	433.16	472.34	445.81
V-THETA 4	526.52	559.14	523.82	486.66
H 2	-145.57	-35.57	-30.75	-10.213
H 3	0.653	0.685	0.704	0.7467
TUR	0.377c	0.415c	0.3547	0.3547
LGS CUF*	02.209	54.77c	55.527	0.5414
DFAC	0.1865	0.1055	0.0714	0.0694
LGS PAA	0.6728	0.6240	0.0271	0.0247
INC1U	-5.91	-2.37	-1.20	-0.52
DEV	2.924	1.332	1.3216	1.3216

Table IVs.

Blade element performance for complete stage.

Optimum Bleed

PERCENT DESIGN SPEDD = 99.49
 CORRECTED WEIGHT FLCW = 86.27
 CORRECTED Rotor SPEED = 9357.45
 PRESSURE RATIO = 1.4239
 AERODYNAMIC EFFICIENCY = 84.4486

ROTOR 1

	STATION 1 - STATION 2			STATION 1 - STATION 3			
	10	30	50	70	90	100	
DIA 1	29.150	27.090	25.050	23.020	20.993	20.993	
DIA 2	29.098	27.302	25.516	23.730	21.944	21.944	
BETA 1	20.465	22.472	23.115	25.043	26.043	26.043	
BETA 2	49.435	51.500	53.879	56.195	57.314	57.314	
BETA(PK) 1	61.798	59.155	55.874	52.059	48.076	48.076	
BETA(PK) 2	47.642	41.774	36.267	26.767	16.319	16.319	
V 1	500.33	505.07	514.28	520.02	574.71	574.71	
V 2	710.75	733.99	740.40	764.35	784.95	784.95	
VZ 1	458.75	466.72	470.49	467.22	471.45	471.45	
VZ 2	462.21	456.92	436.26	427.47	423.57	423.57	
V-THETA 1	174.94	193.05	207.66	221.32	230.35	230.35	
V-THETA 2	539.94	574.42	591.23	635.45	660.75	660.75	
V(PK) 1	991.9	910.3	838.6	750.5	705.5	705.5	
V(PK) 2	986.0	612.7	541.1	478.4	442.8	442.8	
VTHETA PR1	974.2	781.5	694.2	600.2	575.0	575.0	
VTHETA PR2	506.9	406.2	320.1	215.6	129.1	129.1	
U 1	1049.09	974.59	901.89	828.45	755.75	755.75	
U 2	1046.86	982.53	918.31	856.03	784.75	784.75	
M 1	0.4640	0.4630	0.4775	0.4831	0.4877	0.4877	
M 2	0.6304	0.6551	0.6633	0.6922	0.7049	0.7049	
M(PK) 1	0.9199	0.8445	0.7767	0.7046	0.6554	0.6554	
M(PK) 2	0.6044	0.5409	0.4848	0.4313	0.4070	0.4070	
TURN(PK)	14.150	17.391	12.607	25.338	31.137	31.137	
LUSS COEF.	0.0502	0.0131	0.0216	0.0040	0.0531	0.0531	
DFAC	0.4389	0.4623	0.4917	0.5142	0.5186	0.5186	
EFFP	0.9514	0.9891	0.9762	0.9980	0.9859	0.9859	
EFF	0.9445	0.9884	0.9749	0.9979	0.9631	0.9631	
LCSS PARA.	0.0119	0.0032	0.0073	0.0010	0.0132	0.0132	
INCID	2.20	2.26	2.17	2.30	3.08	3.08	
DEV	2.542	2.974	5.467	6.062	9.239	9.239	
CORRECTED WEIGHT FLOW							
UPSTREAM OF ROTOR							86.27
UPSTREAM OF STATOR							86.27
DCWNSTREAM CF STATOR							82.15
INCID FARA.							
INCID	-2.64	-0.24	1.20	2.20	1.39	1.582	
DEV	4.376	9.213	12.094	9.746	1.582		

Table IVt.

Blade element performance for complete stage.

Centrifugal flow

PERFECT DESIGN SPEED = 99.12
 CORRECTED WEIGHT FLOW = 86.61
 CORRECTED ROTOR SPEED = 3360.14
 PRESSURE RATIO = 1.4135
 ADIABATIC EFFICIENCY = 84.676

ROTUR 1

	STATION 1 - STATION 2			
	10	30	50	70
OIA 1	28.150	27.080	25.660	23.020
OIA 2	29.083	27.302	25.518	21.944
BETA 1	19.739	22.113	23.042	25.340
BETA 2	52.914	52.832	55.403	52.151
BETA(PRI) 1	63.760	61.105	57.818	59.471
BETA(PRI) 2	40.143	41.135	35.812	27.431
V 1	471.48	478.96	489.01	492.55
V 2	741.76	749.20	751.62	757.70
V 2 1	443.77	443.73	446.91	441.42
V 2 2	447.29	452.63	426.77	403.67
V-THETA 1	159.24	140.50	138.50	219.55
V-THETA 2	591.73	597.02	613.71	653.00
V(PRI) 1	1003.7	913.3	940.9	759.6
V(PRI) 2	645.5	601.0	526.7	451.6
V(THETA) PRI 1	900.3	804.0	712.4	614.2
V(THETA) PR2	465.5	395.3	309.7	205.5
U 1	1055.53	934.29	910.86	816.72
U 2	1057.27	932.36	927.44	862.52
M 1	0.4319	0.4390	0.4486	0.4520
M 2	0.6478	0.6596	0.6650	0.6723
M(PRI) 1	0.9194	0.8417	0.7714	0.6970
M(PRI) 2	0.5637	0.5291	0.4610	0.4342
STATOR 1				
STATION 2 - STATION 3	10	30	50	90
OIA 3	27.442	25.672	23.874	22.034
BETA 2	52.832	55.403	58.226	59.151
BETA 3	-13.860	-12.956	-10.976	-12.776
BETA 4	741.76	749.20	751.62	767.70
V 2	544.91	484.83	432.63	369.01
V 2 1	447.29	452.63	426.77	403.67
V 2 2	525.05	472.49	424.72	359.88
V-THETA 2	591.73	557.42	618.71	653.00
V-THETA 3	-130.53	-108.70	-82.37	-108.24
H 2	0.6476	0.6596	0.6650	0.6823
H 3	0.4662	0.4160	0.3718	0.3182
TURN	66.774	65.789	66.379	71.052
LOSS COEF.	0.1396	0.1865	0.1886	0.2171
DFAC	0.6564	0.7078	0.7524	0.8322
LOSS PARA.	0.0564	0.6685	0.6651	0.6633
INCID	Q.83	0.69	2.70	4.28
DEV	5.100	5.084	6.774	4.904
CORRECTED WEIGHT FLOW				
				82.61
				92.61
				78.46

Table IVu.

Blade element performance for complete stage.

Minimum Buoy

PERCENT DESIGN SPEED = 79.93
 CONNECTED WEIGHT FLOW = 96.45
 CORRECTED FACTOR SPEED = 5361.12
 PRESSURE RATIO = 1.2299
 ADIABATIC EFFICIENCY = 53.4738

STATION 1 - STATION 2							STATION 1 - STATION 3							CORRECTED WEIGHT FLOW									
			10			30			50			70			30			10			30		
DIA 1	29.150	27.080	25.060	23.020	20.944																		
DIA 2	29.034	27.302	25.516	23.730	21.944																		
BETA 1	20.405	22.172	24.473	25.744	27.438																		
BETA 2	36.702	39.452	42.489	44.474	44.658																		
BETA(PK) 1	55.792	53.533	49.791	45.430	40.854																		
BETA(PK) 2	51.326	+1.527	34.220	24.752	16.752																		
V 1	589.33	598.25	605.50	614.76	624.59																		
V 2	855.19	745.53	780.99	830.25	862.04																		
V 2 1	552.57	554.02	551.10	553.75	564.03																		
V 2 2	525.23	575.67	575.91	592.47	613.22																		
V-THETA 1	205.60	225.78	250.83	267.04	264.23																		
V-THETA 2	391.60	+73.74	527.52	591.70	605.94																		
V(PR) 1	1009.3	932.2	853.7	792.2	745.7																		
V(PR) 2	940.6	769.0	696.5	652.4	640.4																		
V(THETA) PR1	844.4	749.8	651.9	562.2	487.4																		
V(THETA) PR2	656.2	509.8	391.7	277.2	184.5																		
U 1	1050.11	975.54	902.77	829.24	765.08																		
U 2	1047.93	943.54	913.20	854.86	761.52																		
W 1	5.551.8	0.5597	0.5669	0.5742	0.5860																		
W 2	0.5922	0.6797	0.7148	0.7639	0.7962																		
4(PR) 1	0.9435	0.8722	0.7993	0.7396	0.5945																		
4(PR) 2	0.7539	0.7010	0.6374	0.6002	0.5915																		
TURB(PR)	5.450	12.011	15.571	20.583	24.192																		
LSS COEF.	0.1791	0.1049	0.0980	0.0624	0.0496																		
DFAC	0.2323	0.2601	0.2774	0.2774	0.2471																		
DIA 3	27.422	25.672	23.674	22.634	21.624																		
BETA 2	42.489	44.658	44.658	44.658	44.658																		
BETA 3	-4.606	-7.534	-7.534	-7.534	-7.534																		
V 2	745.53	830.99	862.04	862.04	862.04																		
V 3	505.95	533.80	512.42	497.97	497.97																		
V 4	525.28	575.91	592.47	613.22	613.22																		
VZ 3	49C.05	574.65	632.19	662.19	662.19																		
V-THETA 2	391.60	472.74	527.52	581.70	605.94																		
V-THETA 3	-125.65	-46.25	-42.05	-38.54	-229.01																		
H 2	0.5922	0.7148	0.7339	0.7562	0.7662																		
H 3	0.4492	0.5680	0.5485	0.4402	0.4402																		
TURB	51.104	44.058	46.268	52.4C9	72.038																		
LSS COEF.	0.1091	0.0622	0.1244	0.3087	0.7150																		
DFAC	0.5470	0.4855	0.4463	0.5248	0.6365																		
LSS PARA.	0.C339	0.0410	0.0022	C.04C3	0.0828																		
INCID	-15.38	-12.65	-10.21	-9.53	-11.29																		
DEV	4.557	13.434	13.670	9.146	-9.580																		

Table IVv.

Blade element performance for complete stage.

Minimun Gasto

Table IVw.
Blade element performance for complete stage.

Minimum Beta									
ROTOR 1									
STATION 1 - STATION 2									
	10	30	50	70	90				
DIA 1	29.150	27.081	25.050	23.070	20.980				
DIA 2	29.083	27.302	25.516	23.730	21.944				
BETA 1	20.047	22.115	23.757	25.406	25.743				
BETA 2	47.673	50.300	53.507	54.868	56.869				
BETA(PK) 1	61.518	55.301	51.961	48.051					
BETA(PK) 2	45.569	41.059	37.235	29.137	18.494				
V 1	51.72	51.64	535.75	536.11	538.26				
V 2	751.39	758.64	748.47	757.80	752.37				
V 2 1	436.36	492.53	490.35	482.65	484.93				
V 2 2	505.76	484.60	445.14	441.13	433.04				
V-THETA 1	177.47	200.15	215.84	233.38	233.78				
V-THETA 2	555.51	543.70	601.72	627.63	663.57				
V(PK) 1	1019.9	937.3	860.7	761.5	725.3				
V(PK) 2	722.7	642.7	559.1	505.8	456.7				
V(THETA) PR1	556.4	797.5	707.4	611.7	539.4				
V(THETA) PR2	516.1	422.1	338.3	246.3	144.9				
V 1	1073.90	977.64	923.23	843.07	773.21				
V 2	1071.52	1005.82	940.02	874.23	808.43				
M 1	0.4695	0.4827	0.4866	0.4870	0.4890				
M 2	0.6517	0.6619	0.6558	0.6754	0.6991				
M(PK) 1	0.5249	0.5810	0.7818	0.7049	0.6543				
M(PK) 2	0.6269	0.5807	0.4899	0.4450	0.4029				
TURB(PK)	15.349	17.242	18.036	22.124	25.554				
STATOR 1									
STATION 2 - STATION 3									
	10	30	50	70	90				
DIA 3	27.422	25.672	23.674	22.034					
BETA 2	56.300	53.507	54.868	56.869					
BETA 3	-7.226	-4.430	-4.721	-20.360	-34.720				
V 4	751.39	758.64	761.80	792.39					
V 3	514.62	539.72	517.82	315.80					
V 2 2	505.96	484.60	445.14	441.83	433.08				
V 2 3	510.57	538.11	510.39	351.39	246.28				
V-THETA 2	555.51	583.70	611.72	627.53	663.57				
V-THETA 3	-6.074	-4.165	-6.743	-130.40	-137.45				
M 2	0.6517	0.6558	0.6554	0.6591	0.6631				
M 3	0.4964	0.4956	0.4950	0.4967	0.4980				
TURN	54.839	54.730	53.226	95.589					
LLSS CJEF*	0.2343	0.1376	0.0759	0.3054	0.7155				
UFAC	0.6946	0.6249	0.8316	0.9259	0.9534				
LLSS PARA*	0.6930	0.6517	0.6262	0.0720	0.0104				
INCID	-6.41	-1.64	0.81	0.87	0.52				
DEV	11.734	12.019	8.029	-2.080	-2.050				
UPSTREAM OF ROTOR									
									97.15
UPSTREAM OF STATOR									
									87.15
DOWNSTREAM OF STATOR									
									95.34

Table IVx.

Blade element performance for complete stage.

		Minimum Beta					
		Station 1 - Station 2					
		Rotor 1					
		10	30	50	70	90	
PERCENT DESIGN SPEED =	100.04						
CORRECTED WEIGHT FLOW =	83.50						
CORRECTED ROTOR SPEED =	3370.58						
PRESSURE RATIO =	1.4159						
AULABATIC EFFICIENCY =	78.2605						
STATION 1 - STATION 3							
STATOR 1							
10	30	50	70	90			
OIA 3	29.164	27.422	25.672	23.874	22.034		
BETA 2	50.242	52.383	55.053	57.632	60.492		
BETA 3	-7.440	-5.831	-12.055	-32.560	-41.780		
V2	751.02	755.62	758.442	758.03	757.91		
V3	576.24	556.67	457.31	299.10	260.13		
V2-2	480.31	461.22	416.11	405.81	381.16		
V2-3	571.44	553.20	447.22	250.96	194.43		
V-TH-ETA 2	-74.22	-56.49	-55.51	-162.72	-173.72		
M2	0.6472	0.6558	0.6442	0.6322	0.6202		
M3	0.6877	0.6736	0.3981	0.2519	0.2198		
TURN	57.642	58.214	67.808	50.552	102.272	UPSTREAM OF STATOR	83.50
LCSS COEF.	0.1865	0.1746	0.2406	0.4280	0.4097	UPSTREAM OF STATOR	93.50
DFAC	0.5811	0.5557	0.7176	0.9518	0.5538	DOWNSTREAM OF STATOR	81.65
LOSS PARA.	0.6751	0.6555	0.0327	0.1174	0.0923		
INCID	-1.84	-0.24	-3.05	3.63	4.54		
DEV	11.560	12.205	5.695	-15.280	-23.980		
CORRECTED WEIGHT FLOW							

Table IVy.

Blade element performance for complete stage.

STATION 1 - STATION 2										COPPER	
	10	30	50	70	90		10	30	50	70	90
U _{IA} 1	29.150	27.080	25.040	23.020	20.990						
U _{IA} 2	29.083	27.302	25.516	23.730	21.964						
U _{ET} 1	20.227	22.172	24.056	25.325	25.443						
U _{ET} 2	36.974	39.279	42.122	43.298	44.107						
B _{ETA(PX)} 1	56.886	53.548	49.553	45.257	40.863						
B _{ETA(PX)} 2	58.040	41.666	25.156	16.655	10.225						
V 1	589.6*	595.26	610.09	620.17	625.25						
V 2	665.93	745.44	782.83	835.52	869.47						
VZ 1	523.28	544.95	547.10	540.57	544.97						
VZ 2	516.69	577.03	580.63	606.53	624.10						
V-THETA 1	203.97	226.16	248.69	265.26	268.79						
V-THETA 2	387.63	471.94	525.06	571.62	605.17						
V(PX) 1	1012.8	934.0	860.5	794.4	747.0						
V(PX) 2	940.0	772.4	702.8	670.2	651.7						
V(THETA PR1)	148.3	751.3	655.8	565.6	498.9						
V(THETA PR2)	562.3	513.5	399.9	244.4	186.3						
U 1	1052.15	977.43	904.52	830.89	757.54						
U 2	1049.91	985.44	920.98	856.51	792.05						
W 1	0.5501	0.5596	0.5704	0.5804	0.5859						
W 2	0.5825	0.6784	0.7152	0.760.0	0.8022						
M(PR1) 1	0.9448	0.8722	0.8045	0.7453	0.6936						
M(PR1) 2	2.7575	2.7575	2.7575	2.7575	2.7575						
TURN(PR)	4.846	11.881	15.364	20.101	24.198						
LSS COEF.	0.1918	0.1128	0.1151	0.1266	0.1464						
DFAC	0.2354	0.2570	0.2760	0.2585	0.2329						
EFP	0.6650	0.8383	0.8383	0.8383	0.9531						
EFF	0.6565	0.8335	0.8335	0.8335	0.9245						
TURN	4.846	11.881	15.364	20.101	24.198						
LSS PARA.	0.0416	0.0278	0.0292	0.0179	0.0116						
INC U	-2.71	-3.35	-4.05	-4.54	-4.14						
JEV	5.940	2.866	3.4F9	4.456	7.965						
STATION 2 - STATION 3										COPPER	
	10	30	50	70	90		10	30	50	70	90
U _{IA} 3	27.422	25.672	23.874	22.034							
U _{IA} 4	37.429	42.122	44.109	47.154							
B _{ETA} 2	-11.695	-4.781	-7.226	-20.540							
B _{ETA} 3	645.93	745.44	762.83	833.52	839.47						
V 2	471.80	551.50	516.0	599.48	503.98						
V 3	516.69	577.03	560.63	506.93	624.30						
VZ 2	461.88	549.58	614.63	594.72	471.94						
VZ 3	387.63	471.54	525.06	571.62	605.17						
V-THETA 2	-56.85	-45.57	-43.84	-75.40	-176.83						
V-THETA 3	0.5825	0.6784	0.7152	0.7660	0.8022						
M 2	0.4230	0.4915	0.5505	0.4454	0.4454						
M 3	0.4230	0.4915	0.5505	0.4454	0.4454						
TURN	43.513	44.660	46.202	50.524	54.649						
LSS COEF.	0.1755	0.1162	0.0506	0.1117	0.2716						
DFAC	0.5615	0.5220	0.4684	0.5346	0.6921						
LSS PARA.	0.4257	0.4436	0.0502	0.0362	0.0768						
INC U	-15.20	-14.86	-10.58	-10.70	-11.84						
Dev	7.265	13.259	13.670	10.454	-2.740						
COPPER										COPPER	
UPSTREAM OF ROTOR										COPPER	
UPSTREAM OF STATOR										COPPER	
DOWNSTREAM OF STATOR										COPPER	

Table IVz.

Blade element performance for complete stage.

Mean Beta

PERCENT DESIGN SPEED = 99.38
 CORRECTED WEIGHT FLUX = 93.74
 CORRECTED FLOW SPL = 0.956.00
 PRESSURE RATIO = 1.3554
 ADIABATIC EFFICIENCY = 95.9958

POINT 1

STATION 1 - STATION 2

	10	30	50	70	90
DIA 1	29.150	27.080	25.060	23.020	20.990
DIA 2	29.080	27.302	25.516	23.730	21.944
BETA 1	19.821	22.292	24.352	25.464	25.805
BETA 2	43.494	46.250	48.182	49.886	52.030
BETA(PK) 1	53.314	55.093	51.434	47.378	42.153
BETA(PK) 2	45.793	40.933	33.895	25.510	17.900
V 1	554.15	572.51	581.14	587.96	591.56
V 2	716.34	744.63	771.20	798.05	801.65
V 3	530.73	529.72	529.66	530.40	532.57
V 4	520.40	514.55	514.21	514.20	493.22
V-T-HETA 1	191.37	217.17	239.63	253.71	257.51
V-T-HETA 2	494.21	538.25	574.75	610.32	631.94
V(PK) 1	1010.4	925.8	849.2	783.3	730.0
V(PK) 2	760.9	681.1	619.4	569.7	518.3
V(HETA PK1	859.8	759.3	664.0	576.4	499.3
V(HETA PK2)	534.7	446.2	345.3	245.4	159.3
J 1	1051.13	976.48	903.65	830.08	76.81
J 2	1045.89	984.49	920.09	855.69	791.28
J 3	1045.89	984.49	920.09	855.69	791.28
STATION 1					
STATION 2 - STATION 3					
10	20	50	70	90	
DIA 3	27.422	25.672	23.874	22.034	
BETA 2	46.490	45.182	43.886	52.030	
BETA 3	-11.515	-4.636	-10.079	-21.440	
V 2	718.04	771.20	798.05	301.66	
V 3	476.95	502.53	481.52	410.17	
V 4	526.90	514.21	514.20	493.22	
V 5	467.25	466.09	503.80	474.09	
V-T-HETA 2	496.21	528.25	574.75	610.32	
V-T-HETA 3	-55.19	-36.84	-42.14	-64.27	
N 2	0.6420	0.6761	0.6751	0.7242	0.7291
N 3	0.4129	0.4240	0.4450	0.4233	0.4538
TURN	55.009	50.855	52.963	59.555	73.470
LSS CUEF.	0.1t38	0.1t55	0.0664	0.0774	0.1t97
UFAC	0.6520	0.6525	0.6527	0.6512	0.6530
LSS PARA.	0.0430	0.0431	0.0432	0.0433	0.0434
INCIC	-t.59	-5.85	-4.52	-4.11	-3.52
DEV	7.443	1.4434	1.4434	7.4431	-1.4430
CORRECTED WELIGHT FLOW					
UPSTREAM OF ROTUR					
UPSTREAM OF STATOR					
DOWNSTREAM CF STATOR					
DOWNSTREAM CF STATOR					

Table IVaa.

Blade element performance for complete stage.

	MEAN BEAM			
	10	30	50	70
STATION 1 - STATION 2				
OIA 1	29.150	27.080	25.060	24.120
OIA 2	25.084	27.302	25.516	25.720
BETA 1	21.048	22.964	24.357	25.745
BETA 2	49.368	51.131	53.596	55.103
BETA(P-E) 1	69.847	76.993	54.728	56.958
BETA(P-E) 2	42.417	40.301	34.260	25.835
V 1	524.15	533.36	539.29	545.20
V 2	749.72	762.15	768.31	771.42
V 2 1	495.22	411.39	491.79	441.09
V 2 2	498.41	478.28	458.56	452.77
V-TETRA 1	198.27	296.13	222.41	235.92
V-TETRA 2	598.81	593.40	619.18	649.11
V(PK) 1	105.4	92.4	850.8	776.6
V(PK) 2	995.8	527.1	554.4	503.0
VLTheta PK1	495.5	782.8	594.6	605.5
VLTheta PK2	495.5	605.6	314.5	452.57
U 1	105.65	99.91	91.99	84.234
U 2	105.4	99.03	93.0	767.39
M 1	0.4784	0.4775	0.4732	0.4757
M 2	0.6542	0.6701	0.6762	0.6720
M(PK) 1	0.9162	0.8847	0.7741	0.7134
M(PK) 2	0.6073	0.5514	0.4895	0.4472
TURBINE(EF)	1.2467	1.7597	20.167	25.123
LUGS CLEF.	0.0523	0.0377	0.0448	0.0446
UFAC	0.4422	0.4421	0.4454	0.4455
UFP	0.9379	0.9665	0.9634	0.9575
ERT	0.9341	0.9667	0.9614	0.9557
LUGS PAWA.	0.0102	0.0095	0.0113	0.0114
LUGS ID	1.00	1.03	1.16	2.12
DEV	0.317	1.561	3.760	5.135
CORRECTED AT TIC-T FLW				
STATION 2 - STATION 3				
10	-20	50	70	90
OIA 3	29.164	27.422	25.672	23.834
BETA 4	49.348	51.124	53.296	55.162
BETA 5	-19.290	-30.876	-4.606	-9.542
V 2	749.72	769.72	791.42	817.15
V 3	432.23	465.30	481.63	432.70
V 2 2	468.44	476.20	466.50	452.77
V 2 3	455.23	465.52	480.27	426.71
V-TETRA 4	568.00	593.40	619.18	649.11
V-TETRA 5	-159.24	-56.40	-38.69	-71.73
M 2	0.6549	0.6701	0.6762	0.6720
M 3	0.4108	0.4015	0.4144	0.4165
LUGS CLEF.	0.0228	0.0209	0.0202	0.0202
UFAC	0.2124	0.1743	0.0840	0.1233
LUGS PAWA.	0.0107	0.0105	0.0104	0.0104
ANGLU	-2.13	-1.61	0.90	1.10
OLV	-0.320	11.12	1.134	0.138

Table IVbb.

Blade element performance for complete stage.

MEAN BREEZE		STATION 1 - STATION 2						CORRECTED LIGHT FLOW	
		10	30	50	70	90			
PERCENT DESIGN SPTRU =	94.93								
CORRECTED WEIGHT FLOW =	43.75								
CORRELATED MOTOR SPEED =	1331.24								
PRESSURE RATIO =	1.4376								
ADIABATIC EFFICIENCY =	53.0526								
STATION 1		STATION 1 - STATION 2						CORRECTED LIGHT FLOW	
M 1		10	30	50	70	90			
DIA 1	29.150	27.080	25.060	23.020	21.040				
DIA 2	29.035	27.302	25.516	23.730	21.940				
BETA 1	20.434	22.503	24.206	25.742	26.100				
BETA 2	51.583	52.944	55.043	56.009	57.300				
BETA(P) 1	62.774	50.046	57.166	53.535	49.730				
BETA(P) 2	43.495	+1.129	35.977	16.239	16.740				
V 1	49.024	49.802	50.143	50.856	51.040				
V 2	75.039	75.206	75.407	77.474	79.780				
VZ 1	45.076	46.010	45.760	45.909	45.800				
VZ 2	46.628	45.371	43.206	42.412	42.930				
V-THETA 1	178.32	150.61	205.80	220.88	225.00				
V-THETA 2	287.34	500.92	618.02	648.34	672.10				
V-PR1 1	1004.9	921.5	946.3	776.8	709.8				
V-PR1 2	265.2	602.4	536.0	477.0	448.0				
VTHETA PR1	d93.6	798.4	709.4	619.9	541.0				
VTHETA PR2	474.4	396.2	318.9	218.8	129.0				
U 1	1055.51	989.01	915.24	840.74	766.00				
U 2	1062.35	997.12	931.89	866.67	801.40				
STATOR 1		STATION 2 - STATION 3						CORRECTED LIGHT FLOW	
M 1		10	30	50	70	90			
M 2	0.5532	0.6607	0.6645	0.6856	0.7056				
M(P) 1	0.9175	0.8418	0.7716	0.7048	0.6448				
M(P) 2	0.5790	0.5285	0.4406	0.4221	0.3921				
TUR(VPR)	174.279	18.917	21.169	26.296	32.970				
LCSS CCEF.	0.01079	0.0547	0.0590	0.0676	0.0967				
UFAC	0.4851	0.4904	0.5112	0.5291	0.5180				
EFFP	0.0047	0.9539	0.9540	0.9469	0.9360				
EFF	0.9986	0.9512	0.9514	0.9440	0.9360				
LCSS PARA.	0.0267	0.0136	0.0146	0.0194	0.0224				
INCID	3.17	3.15	3.47	3.73	4.00				
DEV	0.395	2.329	5.197	6.539	8.000				
STATION 2		UPSTREAM OF ROTOR						UPSTREAM OF STATOR	
M 1		10	30	50	70	90			
M 2	0.5532	0.6607	0.6645	0.6856	0.7056				
M 3	0.4772	0.4050	0.3627	0.3274	0.2970				
TUR	66.167	62.577	62.669	62.481	63.878				
LCSS COEF.	0.1140	0.1900	0.1353	0.1453	0.1553				
DFAC	0.6650	0.7110	0.7117	0.8352	0.8352				
LCSS PARA.	0.0433	0.0433	0.0433	0.0433	0.0433				
INCID	-C.543	C.81	2.81	1.45	1.45				
DEV	4.376	8.523	2.007	-8.680	-8.680				

Table IVcc.

Blade element performance for complete stage.

Optimum Bleed

PERCENT DESIGN SPEED = 109.96
 CORRECTED RELATIVE FLOW = 105.38
 CORRECTED ROTOR SPEED = 9201.16
 PRESSURE RATIO = 1.2506
 AERODYNAMIC EFFICIENCY = 0.22502

NOTE 1

STATION 1 - STATION 2

	10	30	50	70	90	99
DIA 1	29.150	27.040	25.460	23.020	21.919	21.044
DIA 2	29.048	27.302	25.216	23.730	23.730	21.044
BETA 1	21.805	22.584	24.360	25.690	25.855	25.855
BETA 2	37.040	39.134	43.423	45.028	45.467	45.467
DETA(PRI) 1	57.413	54.234	50.572	46.707	47.307	47.307
DETA(PRI) 2	46.613	44.043	35.453	24.523	1.5.323	1.5.323
V 1	633.33	643.31	646.47	656.38	662.74	662.74
V 2	761.14	783.37	941.08	911.11	941.11	941.11
V 2.1	588.07	592.33	588.91	591.50	566.40	566.40
V 2.2	657.25	607.60	606.83	644.50	574.25	574.25
V-THETA 1	235.825	250.99	286.65	244.54	243.02	243.02
V-THETA 2	458.92	494.46	532.29	545.13	444.71	444.71
V(PRI) 1	1091.9	1013.4	935.3	962.6	906.4	906.4
V(PRI) 2	922.1	945.3	743.1	709.0	639.1	639.1
V(THETA) PRI	920.1	822.3	726.6	627.8	542.3	542.3
V(THETA) PRI 2	694.3	587.6	428.9	295.4	194.8	194.8
U 1	1155.34	1073.79	993.23	912.38	831.84	831.84
U 2	1152.98	1082.06	1011.21	940.52	879.73	879.73
M 1	0.5950	0.6050	0.6082	0.6183	0.6247	0.6247
M 2	0.6836	0.7147	0.7700	0.8404	0.8911	0.8911
M(PRI) 1	1.0258	0.9531	0.8799	0.8125	0.7602	0.7602
M(PRI) 2	0.8342	0.7712	0.6803	0.6534	0.6482	0.6482
TURN(PRI)	9.605	10.190	15.721	22.084	27.979	27.979
LESS COEF.	0.2043	0.1642	0.1343	0.1245	0.1083	0.0873
UFAC	0.2285	0.2423	0.3031	0.2876	0.2437	0.2437
EFF	0.6929	0.7717	0.8024	0.8737	0.9270	0.9270
EFF.	0.4984	0.7640	0.7948	0.8680	0.9234	0.9234
LLSS PARA.	0.0474	0.0365	0.0413	0.0334	0.0219	0.0219
INC10	-2.18	-2.67	-2.73	-3.09	-2.59	-2.59
DEV	3.713	5.243	4.453	3.923	6.629	6.629
CORRECTED WEIGHT FLOW						
UPSTREAM OF ROTOR						
TURN	46.443	47.304	53.655	55.769	UPSTREAM CF STATION	100.38
LESS COEF.	0.0582	0.1638	0.3325	0.73C7	DOWNSTREAM CF STATOR	97.56
UFAC	0.5187	0.5152	0.5700	0.73C7		
LESS PARA.	0.0701	0.0294	0.0529	0.0515		
INC10	-13.00	-8.88	-8.97	-10.50		
DEV	12.734	12.269	6.653	-6.520		

Table IVdd.

Blade element performance for complete stage.

Optimum Beta

PERCENT DESIGN SPEED = 109.95
 CORRECTED WEIGHT FLOW = 99.45
 CORRECTED ACTOR SPEED = 1199.41
 PRESSURE RATIO = 1.4298
 ADIABATIC EFFICIENCY = 82.4708

		STATION 1 - STATION 2						STATION 1 - STATION 2						
		ROTOR 1			ROTOR 2			ROTOR 1			ROTOR 2			
		10	30	50	70	90	10	30	50	70	90	10	30	50
BETA 1	29.150	27.080	25.060	23.020	20.948									
BETA 2	27.081	27.302	25.516	23.710	21.944									
BETA 1	21.214	23.384	24.970	26.164	26.428									
BETA 2	47.102	49.075	50.416	51.726	53.625									
BETA(PRI) 1	58.479	55.060	51.369	47.217	43.121									
BETA(PRI) 2	44.627	39.271	32.653	23.910	16.377									
V 1	622.23	635.93	647.18	655.62	656.93									
V 2	632.17	649.61	669.55	900.87	900.26									
VZ 1	579.77	583.68	587.17	588.44	588.27									
VZ 2	566.47	556.55	556.08	558.02	513.92									
V-THETA 1	225.91	252.44	272.18	289.09	262.39									
V-THETA 2	609.62	641.93	670.15	707.23	724.85									
VIPR 1	1109.0	1019.3	940.5	866.4	806.3									
VIPR 2	795.9	716.9	658.1	609.5	556.5									
VTHETA PRI 1	945.3	835.6	734.7	635.6	550.9									
VTHETA PRI 2	559.1	455.1	355.1	246.2	156.9									
U 1	117.26	1068.07	1008.91	924.94	943.29									
U 2	110.675	1098.99	1025.23	953.47	981.71									
M 1	0.5752	0.5887	0.5999	0.6083	0.6096									
M 2	0.7297	0.7512	0.7740	0.8073	0.8092									
M(PRI) 1	1.0252	0.9437	0.8718	0.8036	0.7477									
STATION 1														
STATION 2 - STATION 3														
10	30	50	70	90										
LIA 3	27.422	25.672	23.674	22.034	LSS COEF.	0.1146	0.0877	0.0752	0.0508	0.0516				
BETA 4	47.102	50.416	51.726	53.625	ERFP	0.4051	0.4179	0.4241	0.4237	0.4269				
BETA 3	-8.4693	-9.005	-10.041	-21.530	EFF	0.9740	0.9420	0.9171	0.9340	0.9600	0.9318			
V 2	835.17	869.61	869.25	900.26	LSS PARA.	0.0297	0.0224	0.0194	0.0132	0.0229	0.0293			
V 3	505.39	503.56	504.50	517.92	INC10	-1.12	-1.63	-2.31	-2.58	-1.88				
VZ 2	504.46	505.56	504.04	538.02	INC10	-0.473	0.471	1.453	3.1110	7.672				
VZ 3	495.66	501.85	501.21	502.45	436.04									
V-THETA 2	605.02	641.53	670.15	707.23	724.85	CORRECTED WEIGHT FLW								
V-THETA 3	-74.44	-41.20	-56.97	-125.65	-172.81	UPSTREAM OF ROTOR	99.45							
M 2	0.7257	0.7512	0.7740	0.8073	0.8052	UPSTREAM OF STATOR	99.45							
M 3	0.4535	0.4311	0.4696	0.4465	0.4548	DOWNSTREAM OF STATOR	99.45							
TURN	55.271	51.768	56.421	55.167	75.155									
LSS COEF.	0.4265	0.1544	0.0985	0.1224	0.0536									
DFAC	0.7228	0.7102	0.6678	0.7274	0.7782									
LSS PARA.	0.979	0.730	0.0364	0.0388	0.0263									
INCL	-0.58	-3.67	-2.28	-2.27	-2.32									
DEV	10.491	13.347	11.745	3.639	-3.730									

Table IVee.

Blade element performance for complete stage.

<i>Optimum Curve</i>									
ROTOR 1									
STATION 1 - STATION 2									
	10	30	50	70					
DIA 1	29.150	27.080	25.060	23.020	20.989				
DIA 2	24.093	27.302	25.516	23.730	21.944				
BETA 1	21.495	23.147	25.111	26.383	27.940				
BETA 2	49.165	50.354	52.617	54.217	55.487				
BETA (PR) 1	69.181	56.166	52.623	48.591	43.822				
BETA (PR) 2	44.552	39.237	33.495	25.943	17.207				
V 1	647.44	615.65	628.84	631.20	641.72				
V 2	633.72	446.76	466.01	870.25	846.22				
V 2 1	505.19	566.27	565.79	551.07	571.47				
V 2 2	345.15	541.54	519.72	518.85	499.29				
V-THETA 1	222.54	242.99	267.17	255.46	251.56				
V-THETA 2	510.74	533.55	680.14	701.98	721.13				
V(PR) 1	1103.2	1017.3	912.0	851.3	765.4				
V(PR) 2	705.04	599.2	523.2	505.4	422.7				
VTHETA PR1	347.44	644.4	740.6	593.5	650.7				
VTHETA PR2	536.7	346.2	343.9	346.5	346.5				
V 1	1149.97	1046.93	1046.81	922.93	842.38				
V 2	1167.48	1045.84	1044.11	952.43	880.75				
M 1	0.5610	1.5671	0.5742	0.5645	0.5649				
M 2	0.7242	0.7461	0.7549	0.7753	0.7879				
M (PR) 1	1.0199	0.9402	0.9624	0.7483	0.7375				
M (PR) 2	0.6642	0.6163	0.5525	0.5037	0.4673				
STATOR 1									
STATION 2 - STATION 3									
	10	30	50	70	90				
DIA 3	27.6424	25.672	23.034	19.829	16.979	22.746			
BETA 2	52.017	54.217	55.467	52.432	49.432	0.4946	0.1130		
BETA 3	-16.470	-16.468	-24.860	0.9112	0.926	0.7635	0.9213		
V 2	833.72	840.76	856.01	0.9050	0.9600	0.9650	0.9153		
V 3	516.50	511.76	461.64	430.72	400.00	0.0124	0.0121		
V 2 1	545.15	541.54	519.72	508.85	499.29	-0.42	-1.07		
V 2 2	523.71	523.07	442.86	390.81	726.13	-0.43	-0.43		
V-THETA 2	631.77	630.18	705.54	-130.34	-161.08	0.4041	0.4041		
V-THETA 3	-114.62	-42.05	-75.65	-130.34	-161.08	JPS1 INLET UF QGT M			
M 2	0.7282	0.7585	0.7753	0.7879	0.7879				
M 3	0.4377	0.4372	0.4551	0.4556	0.4556	JPS2 INLET UF QGT M			
TURN	01.74	52.135	51.267	50.617	49.347	JPS1 REAUF UF STATOR	47.61		
LUSS CURF.	0.2562	0.2045	0.1177	0.1223	0.1223	JPS1 REAUF UF STATOR	47.61		
DFAC	0.1394	0.1141	0.0533	0.0538	0.0538	JPS1 REAUF UF STATOR	47.61		
LUSS FARFA.	0.0403	0.0755	0.0407	0.0462	0.0462	JPS1 REAUF UF STATOR	47.61		
INC10	-1.91	-1.75	-0.08	0.22	-0.46	JPS1 REAUF UF STATOR	47.61		
Dev	0.194	13.253	5.102	1.280	-7.646	JPS1 REAUF UF STATOR	47.61		

Table IVff.

Blade element performance for complete stage.

<i>Optimum Bleed</i>									
ROTOR 1									
STATION 1 - STATION 2									
	10	30	50	70					
Ω_{1a} 1	29.150	27.380	25.360	23.020					
Ω_{1a} 2	23.089	27.302	25.516	21.730					
β_{ETA} 1	21.003	25.547	24.395	27.047					
β_{ETA} 2	51.635	51.580	54.691	55.327					
$\beta_{T(PI)}$ 1	61.223	51.346	54.115	50.342					
$\beta_{T(PI)}$ 2	44.185	39.274	34.128	46.453					
V_1	536.71	594.79	600.34	54.127					
V_2	840.49	846.33	647.93	841.49					
$V_{\bar{Z}} 1$	544.74	549.32	544.02	545.42					
$V_{\bar{Z}} 2$	530.13	527.20	490.09	470.11					
$V-\theta_{ETA}$ 1	217.91	228.07	253.96	272.55					
$V-\theta_{ETA}$ 2	652.22	554.69	691.95	721.50					
$V_{(PI)}$ 1	1096.9	1019.5	928.1	109.3					
$V_{(PI)}$ 2	739.3	681.0	592.1	523.6					
$V\theta_{ETA} PR_1$	952.1	859.8	751.9	651.0					
$V\theta_{ETA} PR_2$	515.3	527.20	490.09	470.11					
ψ_1	1169.97	1046.63	1005.81	923.93					
ψ_2	1157.48	1095.80	1024.11	952.43					
ψ_3	0.5405	0.5484	0.5539	0.5632					
ψ_4	0.7316	0.7457	0.7489	0.7650					
$\psi_{(PI)} 1$	1.0106	0.940	0.9562	0.7843					
$\psi_{(PI)} 2$	0.6435	0.5986	0.5229	0.4354					
$TUR(N) PR_1$	16.038	18.122	19.987	23.920					
LCS5 COEF.	0.0935	0.0298	0.0392	0.0485					
JFAC	0.4066	0.4704	0.5008	0.5241					
EFP	0.9121	0.9752	0.9675	0.9551					
EFP	0.9121	0.9752	0.9675	0.9551					
LCS5 PARA.	0.0236	0.0076	0.0130	0.0174					
INCID	0.42	0.50	0.41	0.24					
DEV	-0.915	0.474	3.32H	1.47					
CORRECTED WEIGHT FLOW									
Ω_{1a} 3	27.422	25.672	23.874	22.034					
β_{ETA} 2	51.560	54.631	56.527	57.921					
β_{ETA} 3	-5.481	-5.721	-21.080	-33.010					
V_1	840.49	847.93	861.48	886.49					
V_2	56C.66	510.39	414.60	372.04					
V_3	53C.13	527.72	450.09	470.11					
V_2	531.64	558.10	5G3.06	386.85					
V_3	651.95	651.95	721.50	721.50					
$V\theta_{ETA} 2$	651.22	651.22	751.14	751.14					
$V\theta_{ETA} 3$	-165.33	-53.55	-86.18	-186.47					
ψ_1	0.7316	0.7457	0.7489	0.7914					
ψ_2	0.4774	0.4791	0.4366	0.3530					
ψ_3	0.4375	57.061	64.412	78.007					
TURN	0.2441	0.1812	0.1552	0.2226					
LCS5 COEF.	0.7219	0.708	0.6454	0.6599					
DFAC	0.6561	0.6579	0.6572	0.6677					
LCS5 PARA.	0.6935	1.18	1.99	2.53					
INCID	-C.56	-C.56	1.99	1.97					
DEV	1.480	12.559	8.029	-3.400	-12.280				

Table IVgg.

Blade element performance for complete stage.

		Optimum Case			
		10	30	50	70
PERCENT DESIGN SPECIE	= 109.48				
CORRECTED WEIGHT FLOW	= 92.95				
CORRECTED ROTOR SPEC = 193.41					
PRESSURE RATIO	= 1.5125				
AERODYNAMIC EFFICIENCY	= 97.3659				
ROTOR 1		STATION 1 - STATION 2			
DIA 1	29.150	27.080	25.060	23.070	20.970
DIA 2	29.086	27.302	25.316	23.730	21.944
BETA 1	21.024	23.495	25.044	26.255	27.398
BETA 2	51.730	52.857	55.277	54.275	56.075
BETA(PR) 1	61.038	58.303	55.138	51.343	47.711
BETA(PR) 2	43.813	39.519	34.181	26.127	15.785
V 1	572.30	576.99	582.48	593.60	589.34
V 2	846.41	946.04	847.22	859.21	877.32
V 2.1	513.94	529.15	527.72	525.95	527.44
V 2.2	524.24	510.84	474.66	451.80	450.91
V-THETA 1	205.24	230.03	246.57	266.38	262.32
V-THETA 2	664.52	674.41	701.77	730.83	753.24
V(PR) 1	1102.7	1007.1	926.6	842.1	794.5
V(PR) 2	726.5	662.2	573.8	503.2	468.6
VTHETA PR1	964.7	856.9	759.2	657.6	540.4
VTHETA PR2	503.0	421.4	322.3	221.6	127.5
U 1	1169.97	1066.89	1009.81	923.93	842.34
U 2	1167.48	1095.90	1024.11	952.43	890.75
M 1	0.5264	0.5312	0.5365	0.5435	0.5442
M 2	0.7344	0.7416	0.7473	0.7610	0.7809
M(PR) 1	1.0146	0.9271	0.8917	0.7762	0.7231
M(PR) 2	0.6303	0.5805	0.5504	0.4457	0.4154
TURN(PR)	0.6303	0.6003	0.5703	0.5403	0.5103
LCS COEF.	0.1115	0.0392	0.0470	0.0541	0.0752
STATOR 1		STATION 2 - STATION 3			
DIA 3	27.422	23.674	22.034	20.4452	0.5244
51.730	55.527	58.275	53.095	0.9453	0.6330
BETA 2	-6.529	-13.137	-24.680	0.4053	0.9632
BETA 3	-14.584	-846.41	847.22	0.4995	0.9648
V 2	846.41	847.22	859.21	0.0284	0.9624
V 3	581.25	482.67	376.37	0.0100	0.9606
V 2.2	524.24	510.84	451.80	1.44	1.50
V 2.3	565.52	470.04	341.99	295.13	207.11
V-THETA 2	664.52	674.41	701.77	753.28	805.55
V-THETA 3	-146.36	-65.13	-109.70	-157.15	-173.43
H 2	0.7344	0.7446	0.7610	0.7809	0.8000
H 3	0.4907	0.4882	0.4105	0.2698	0.1300
TURN	66.314	59.384	69.064	62.555	89.535
LCS COEF.	0.2512	0.1759	0.2166	0.2784	0.2457
DFAC	0.6980	0.6523	0.7671	0.8559	0.9290
LCS FARAD	0.6976	0.6558	0.0742	0.0627	0.0640
INCID	-C.35	C.772	3.23	4.28	2.15
DEV	4.376	11.511	4.613	-7.000	-12.640
CORRECTED WEIGHT FLOW				92.95	
UPSTREAM OF ROTOR				86.76	
DOWNSTREAM OF STATOR				92.95	

Table IVhh.

Blade element performance for complete stage.

Optimum Base

PERCENT DESIGN SPEED = 109.93
 CORRECTED WEIGHT FLOW = 90.80
 CORRECTED FUTTER SPEED = 197.78
 PRESSURE RATIO = 1.5276
 ADIABATIC EFFICIENCY = 78.3808

ROTOR 1

		STATION 1 - STATION 2			STATION 1 - STATION 2		
		10	30	50	70	90	
DIA 1	29.150	27.060	25.060	23.020	20.994		
DIA 2	24.088	27.302	25.516	23.730	21.944		
DETA 1	21.020	23.401	25.044	23.456	26.750		
DETA 2	53.921	23.410	58.473	56.883	56.562		
DETA (PR) 1	62.510	59.516	56.478	52.775	46.103		
DETA (PR) 2	4.00.231	40.427	35.370	25.765	16.246		
V 1	5.00.51	55.385	55.160	50.921	5.64.45		
V 2	845.03	836.13	930.57	852.02	871.36		
V 2 1	50.7.34	508.30	508.80	506.63	50.7.75		
V 2 2	497.67	497.23	452.05	440.64	441.59		
V-T-META 1	194.95	219.97	237.74	255.03			
V-T-META 2	0.02.99	672.21	697.25	730.16	751.71		
V (PR) 1	1.00.1	1.00.4	1.921.3	4.35.0	775.6		
V (PR) 2	5.00.0	5.00.2	5.07.8	4.03.5	4.00.2		
V-META PR1	975.0	666.9	768.1	667.2	546.3		
V-META PR2	484.5	425.6	326.9	222.3	129.1		
U 1	1167.97	1086.87	1035.81	923.73	422.34		
U 2	1167.43	1095.80	1024.11	930.75			
A (PR) 1	4.00.92	4.00.92	4.00.92	4.00.92	4.00.92		
A (PR) 2	0.00.92	0.00.92	0.00.92	0.00.92	0.00.92		
STATION 1							
STATION 2 - STATION 3							
10	30	50	70	90			
DIA 3	27.0422	25.672	22.036				
DETA 2	53.510	57.063	58.689				
DETA 3	-12.035	-16.218	53.562				
V 4	0.05.00	0.30.97	0.52.00				
V 5	398.07	565.44	474.77				
V 2	457.67	497.23	452.05				
V 2 3	514.71	500.03	422.08				
V-T-META 4	682.39	672.21	697.25				
V-T-META 3	-124.63	-78.05	-132.60				
H 2	0.7304	0.7314	0.7301				
H 3	0.4047	0.4054	0.4029				
TURN	0.01.52	0.1.44	0.1.44				
LLSS CCF	0.02.07	0.17.00	0.20.52				
DFAC	0.00.77	0.00.77	0.00.77				
LLSS FAF	0.00.54	0.00.54	0.00.54				
INC10	10.10.0	10.10.0	10.10.0				
DEV	0.72.23	1.00.87	1.00.87				
CORRECTED WEIGHT FLOW							
JETS STREAM OF FLOW							
TURN							
LLSS CCF							
DFAC							
LLSS FAF							
INC10							
DEV							